UNIVERSITEIT GENT

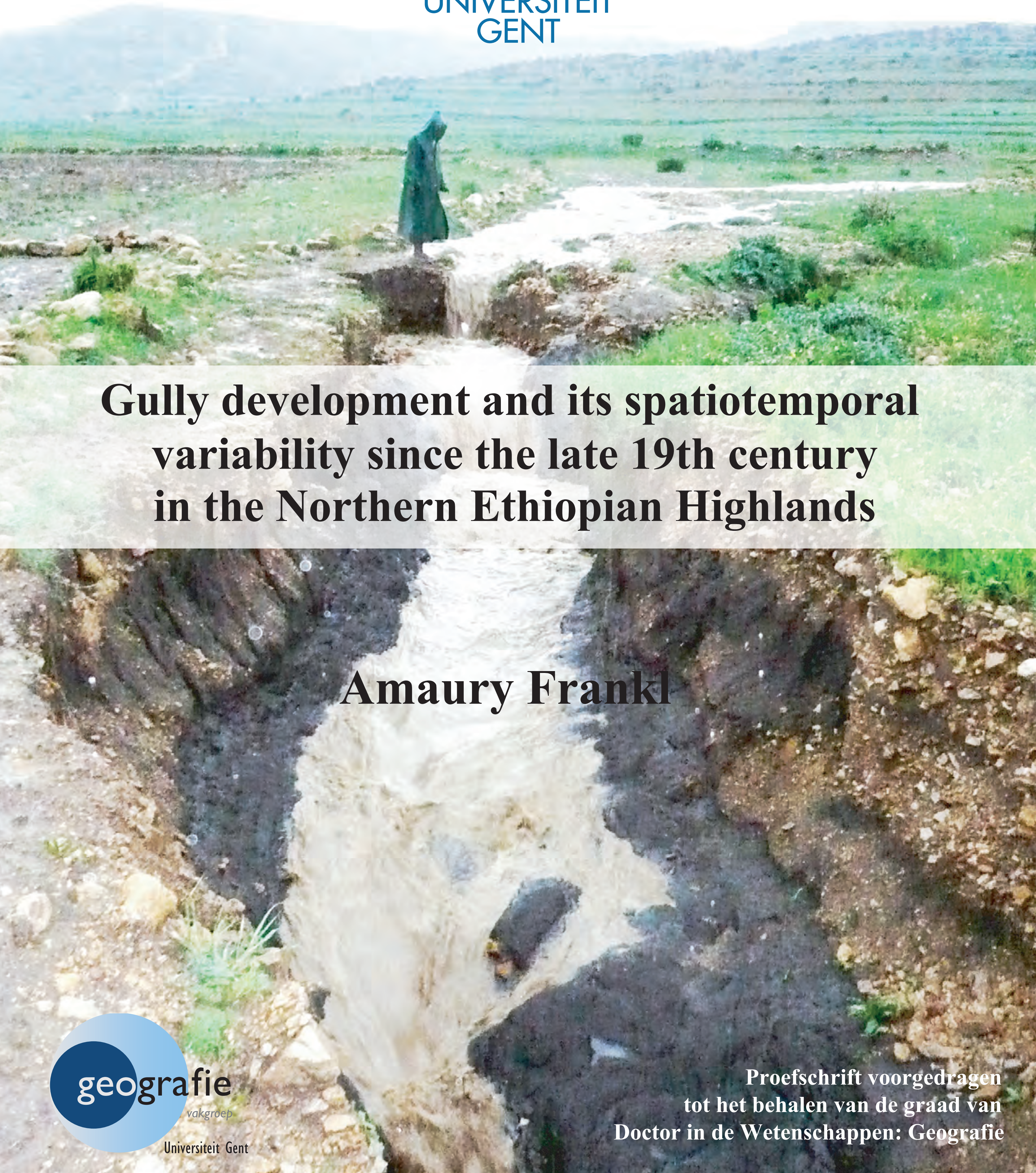

Gully development and its spatiotemporal variability since the late 19th century in the Northern Ethiopian Highlands

Amaury Frankl

geografie
vakgroep
Universiteit Gent

Proefschrift voorgedragen
tot het behalen van de graad van
Doctor in de Wetenschappen: Geografie

Published by:
Department of Geography - Ghent University
Krijgslaan 281 (S8), 9000 Gent (Belgium)
ISBN:

UNIVERSITEIT GENT

Faculteit Wetenschappen

Amaury Frankl

Gully development and its spatio-temporal variability since the late 19th century in the Northern Ethiopian Highlands

Promotoren
Prof. Dr. Jan Nyssen (UGent)
Prof. Dr. Jean Poesen (KU Leuven)

Leden van de examencommissie
Prof. Dr. Paolo Billi (U. Ferrara)
Prof. Dr. Morgan De Dapper (UGent)
Prof. Dr. Alain De Wulf (UGent)
Prof. Dr. Rudi Goossens (UGent)
Dr. Jan Moeyersons (Kon. Museum voor Midden-Afrika)
Dr. Dirk Rieke-Zapp (U. Bern)
Prof. Dr. Eric Van Ranst (UGent)

Proefschrift voorgedragen tot het behalen van de graad van Doctor in de Wetenschappen: Geografie
2012

Cover: An active gully head in the valley bottom of May Mekdan. On top of the black Vertisol a debris fan has been deposited at the lower margin of a hillslope gully. Incision now occurs by an active headcut. Photograph taken by Amaury Frankl on 12-08-2010. Standing at the gully head is Gebrekidan Mesfin.

In his description of 19th century researchers, Graf (1988) concluded that contributors to the field of geomorphology, which investigate on vast areas in difficult conditions, needed to be 'enquiring of mind and adventurous of spirit'. The qualitative descriptions of that time have at present largely been replaced by quantitative work, but the investigative mind and spirit of adventure have certainly remained.

Amaury Frankl

Graf, W.L.,1988. Fluvial processes in dryland environments. The Blackburn Press.Caldwell, USA.

Acknowledgements

The research that led to the preparation of this thesis could only be done with the help of many persons and institutions.

Sincere thanks all researchers whom, in one way or another, contributed to the development of ideas and the writing down of it. Key was of course the support of Prof. Dr. Jan Nyssen, my main promoter. He gave me the unique opportunity to specialize on gully erosion in Northern Ethiopia. Truly motivated, Jan shared many ideas, taught me a lot about geomorphology and gave me an *sensu lato* introduction to Northern Ethiopia. Special thanks also to Prof. Dr. Jean Poesen (my second promoter), who as an expert on gully erosion could give proper direction to this thesis. In facilitating the research, the help of Prof. Dr. Morgan De Dapper was appreciated. Researchers that are involved in the MU-IUC Program are also warmly thanked. Among others, these include Prof. Dr. Seppe Deckers, Prof. Dr. Mitiku Haile and Dr. Hans Bauer. The many field-interactions with them were thought of as very valuable. Thanks also to Prof. Dr. Paolo Billi, who shared his views on dryland rivers while working at Ghent University in 2010-2011; and to Neil Munro, who is familiar with Northern Ethiopia since the 1970s. Help and support by colleagues from the Geography Department of Ghent University, and in particular, Prof. Dr. Alain De Wulf, Prof. Dr. Rudi Goossens, Drs. Ruben Maddens, Dr. Ruben Vandekerckhove and Dr. Tony Vanderstraeten was also much appreciated. Thanks also to all the members of the examination committee for accepting to be a jury member of the thesis defense and for giving valuable comments on the preliminary draft of this thesis: Prof. Dr. Paolo Billi, Prof. Dr. Morgan De Dapper, Prof. Dr. Alain De Wulf, Prof. Dr. Rudi Goossens, Dr. Jan Moeyersons, Prof. Dr. Jan Nyssen, Prof. Dr. Jean Poesen, Dr. Dirk Rieke-Zapp, Prof. Dr. Eric Van Ranst. The interactions with colleagues at national and international conferences or workshops (IAG 2011, Cordoba workshop 2011, etc.) was very fruitful for developing ideas.

I want to express my thanks to the MSc. students whom contributed to this thesis: Stephanie de Mûelenaere, Ellen Meire, Miró Jacob, Nelles Scholiers, Simon Stock, Martin

Schumacher and Lys Moulaert. Spending long periods living and working together in Ethiopia was motivating, pleasant and unforgettable.

Working on gully erosion in Ethiopia can hardly be done alone. Research spots may be difficult to reach and investigating on meter-deep gullies can prove to be difficult. Field assistance was provided by Gebrekidan Mesfin, an engineering student at Mekelle University. His contribution to the fieldwork was huge. Special thanks also to Yohannes Gebrezehir and Samuel Zeslassie for field assistance, and to the members of the MU-IUC Program whom provided logistic support. Local residents are thanked for their hospitality and for sharing their views on past environmental change.

Many of the results presented in this thesis are based on the analysis of historical terrestrial photographs portraying the Northern Ethiopian landscape. Accessing these photographs was not always easy, and in that regard, I was blessed with the help of Jan Nyssen. Thanks also to all the persons and institutions that provided copies of the original photographs: the former Hunting Technical Services team members in Tigray (Neil Munro in special), IAO (Firenze), Peter Donnelly (The Kings Own Regiment Museum at Lancaster, U.K.), Jean Poesen, Dick Grove, Ruth Trummer, André Crismer and Francesco Dramis.

Thanks are expressed to the funding bodies and providers of research equipment: Ghent University, Research Foundation Flanders (FWO), Royal Academy of Overseas Sciences (Yola Verhasselt in special), Couderé Geomatic Engineering bvba, Flemish Interuniversity Council - University Development Cooperation (VLIR-UOS), Geology and Soil Science Department at Ghent University (sedimentological laboratory - Danielle Schram in special).

Last but not least, I want to thank my family and friends. They have endured and supported me during periods of hard work, but above all, they added quite some fun to my life. Special thanks to Ilke Werbrouck, Ann Zwertvaegher and Sofie Vanmaele! Warm thanks also to Michel and Sonja Frankl-Van Lerberge, Magali, Dries and Marjolein Frankl-Declercq, whom backed me since the early beginning and welcomed me in their home as it was mine. Dinners with Roel, Eline and Rosanne Vanderbeuren-Shmidt were also much appreciated, as were the resto-lunches with Anneke during the last months of the thesis writing. To Govinda-das Hugo Liénart, the ‘Manama’, Bee Acholi vzw members, the ‘Geo’s’, the ‘Sport@Gent Weerwolven’, Miró Jacob, Katrien Plasschaert, Tesfa’alem Asfaha and all other friends, I’d like express my gratitude for their support which, in one way or another, motivated me further.

To everyone: thanks for all the good times, and I look forward to many more!

Table of Contents

Chapter 1 General introduction.......1
1.1 Problem statement.......1
1.2 Defining gully erosion.......3
1.3 Objectives.......5
1.4 Choice of the study area.......6
1.5 Thesis outline.......9
1.6 Thesis inputs.......10
1.7 Publication list.......11

Part 1.......15

Chapter 2 Assessing gully development patterns since 1868 from repeat photography.......17
Abstract.......19
2.1 Introduction.......20
2.2 Materials and methods.......21
2.2.1 Study area.......21
2.2.2 Repeat photography.......23
2.2.3 Analysis of gully and river-channel development.......25
2.3 Results.......30
2.3.1 General trends of gully and river channel cross-sectional development.......30
2.3.2 Gully development around Atsela and Lake Ashenge.......34
2.4 Discussion: use of repeat photography.......41
2.5 Conclusions.......42
2.6 References.......42

Chapter 3 Quantifying gully development patterns since 1963 from small-scale aerial photographs and high-resolution satellite images.......47

Abstract……. 49
3.1 Introduction 51
3.2 Materials and Methods 54
3.2.1 Study area 54
3.2.2 Fieldwork and laboratory analysis 56
3.2.3 Creating time-series of aerial photographs and satellite images 58
3.2.4 Quantifying gully network development patterns 59
3.2.5 Factors controlling gully cross-sections 60
3.2.6 Quantifying the evolution of gully volume 61
3.3 Results 62
3.3.1 Horizontal positional accuracy of the small-scale aerial photographs and high-resolution satellite images 62
3.3.2 Factors controlling gully cross-sectional shape 63
3.3.3 Gully network development since 1963 69
3.3.4 $V - L$ and $V - A$ relations 74
3.3.5 Evolution of gully volume 77
3.4 Discussion 78
3.4.1 Using small-scale aerial photographs and Google® Earth 78
3.4.2 Gully cross-sectional shape 79
3.4.3 $V - L$ and $V - A$ relations 81
3.4.4 Gully network and volume development 86
3.5 Conclusions 89
3.6 References 91

Chapter 4 Gully head retreat rates 97

Abstract……. 99
4.1 Introduction 100
4.2 Materials and methods 104
4.2.1 Study area 104
4.2.2 Monitoring short-term gully headcut retreat 105
4.2.3 Medium- to long-term (1-47 years) gully headcut retreat rates 107
4.2.4 Gully head erosion after road construction 109
4.3 Results 109
4.3.1 Short-term gully headcut retreat rates 109
4.3.2 Medium- to long-term (1-47 years) gully headcut retreat rates 113
4.3.3 Gully headcut retreat after a recent road construction 119
4.4 Discussion 120
4.4.1 The use of repeat terrestrial photography for assessing gully head retreat rates 120
4.4.2 Gully headcut retreat rates in Ethiopia compared to other semi-arid regions of the world 120
4.4.3 The effect of soil piping (especially in Vertisols) on gully head retreat rates 122
4.5 Conclusions 125
4.6 References 126

Part 2 ... *131*

Chapter 5 Land use and cover changes since the 19th century as evidenced by terrestrial photographs ... **133**

Abstract ... 135
5.1 Introduction ... 136
5.2 Materials and Methods ... 137
5.2.1 Study area ... 137
5.2.2 Repeat photography ... 141
5.2.3 LUC classification ... 142
5.2.4 GPS measurements ... 146
5.2.5 Preparation of othophotographs ... 146
5.2.6 Warping land use and cover interpretations to the horizontal plane of the map ... 146
5.2.7 Delineation of the mapping boundaries ... 148
5.2.8 From interpreted terrestrial photograph to LUC map ... 149
5.3 Results ... 154
5.3.1 Land use and cover changes in Bolago (1868-2008) ... 154
5.3.2 Land use and cover changes in Ayba (1942-2008) ... 156
5.3.3 Land use and cover changes in Sinkata (1868-2008) ... 158
5.3.4 Land use and cover changes in North Ethiopia (1868-2008) ... 161
5.4 Discussion ... 162
5.4.1 Land use and cover trends in Northern Ethiopia (1868-2008) ... 162
5.4.2 Quantifying land use and land cover from repeat photography ... 163
5.5 Conclusions ... 164
5.6 References ... 164

Chapter 6 Land use and land cover changes since 1973 as quantified from Landsat imagery ... **169**

Abstract ... 171
6.1 Introduction ... 172
6.2 Study area ... 173
6.2.1 Geographical Context ... 173
6.2.2 Climate ... 174
6.2.3 Vegetation ... 175
6.2.4 Socio-economic Environment ... 175
6.2.5 Land Degradation ... 176
6.3 Materials and Methods ... 177
6.3.1 Data Collection ... 177
6.3.2 Image classification ... 179
6.3.3 Accuracy Assessment ... 180
6.3.4 Analysis of Land Use and Cover Change (1972/1984–1986/2000) ... 181
6.4 Results ... 181
6.4.1 Image Classification ... 181
6.4.2 Accuracy Assessment ... 185
6.4.3 Analysis of Land Use and Cover Change from 1972 until 2000 ... 186

6.5 Discussion ... 192
6.5.1 Methodology ... 192
6.5.2 Land Use and Cover Change and Explaining ... 193
6.6 Conclusions ... 195
6.7 References ... 196

Chapter 7 Spatiotemporal covariability in rainfall, cropping systems, land cover by crops and gully dynamism ... 201
Abstract ... 203
7.1 Introduction ... 204
7.2 Materials and Methods ... 205
7.2.1 Study area ... 205
7.2.2 Fieldwork ... 208
7.2.3 Spatiotemporal rainfall variability maps ... 208
7.2.4 Defining the cropping systems ... 208
7.2.5 Upscaling the cropping system patterns to the regional scale ... 209
7.3 Results ... 210
7.3.1 Variability in cropping systems as related to rainfall ... 210
7.3.2 Regional cropping system maps (1996-2009) ... 215
7.4 Discussion: duration of land cover by crops and implications for land degradation and gully erosion ... 219
7.5 Conclusions ... 220
7.6 References ... 221

Chapter 8 General discussion ... 227
Abstract ... 229
8.1 Hydrogeomorphic model ... 230
8.2 Hydrogeomorphic interpretation ... 231
8.3 Pre-1868 erosion cycle ... 240
8.4 References ... 242

Chapter 9 General conclusions ... 247
Scope for feature research ... 251
Recommendations for land managers ... 253

Nederlandse samenvatting ... 255

Appendix A ... Cd-rom

Appendix B ... Cd-rom

Appendix C ... Cd-rom

List of acronyms and symbols

A	catchment area (m^2 or km^2)
ANOVA	analysis of variance
BW	gully bottom width (m)
CSA	gully cross-sectional area (m^2)
D	gully maximum depth (m)
DEM	digital elevation model
D_{total}	total gully drainage density (km km^{-2})
$D_{high\text{-}active}$	drainage density of high-active gullies (km km^{-2})
GCP	ground control point
GIS	geographic information system
GPS	global positioning system
L	gully length (km)
LC	long crop cycle
L_d	daily linear headcut retreat rate (m d^{-1})
$L_{high\text{-}active}$	length of the high-active gullies (km)
$L_{low\text{-}active}$	length of the low-active gullies (km)
LNC	long normal crop cycle
Log	logarthim
LTC	long two crop cycle
LUC	land use and land cover
NDVI	normalized difference vegetation index
PCP	photograph control point
R_a	annual areal headcut retreat rate (m^2 y^{-1})
R_l	annual linear headcut retreat rate (m y^{-1})
RMSE	root mean square error
SC	short crop cycle
S_c	catchment average slope gradient (m m^{-1})
S_l	local slope gradient of the soil surface (m m^{-1})
SLg	soil loss by gully erosion (ton ha^{-1} y^{-1})
SNC	short normal crop cycle
SWC	soil and water conservation
TD	transformed divergence
V	gully volume (m^3 or 10^3 m^3)
V_a	area-specific gully volume (10^3 m^3 km^{-2})

V_e	annual volumetric headcut retreat rate ($m^3\ y^{-1}$)

Chapter 1
General introduction

1.1 Problem statement

Drylands are areas where evapotranspiration exceeds precipitation during part of, or during, the whole year (Kassas, 1995). They cover 40% of the Earth's surface and house about 2.1 billion people in nearly 100 countries, including Ethiopia (UNEP-DDD, 2012). In terms of aridity, drylands are defined as regions where the ratio between long-term annual precipitation and potential evapotranspiration is in-between 0.05 and 0.65, and include hyper-arid, arid, semi-arid and dry sub-humid zones (Thornthwaite, 1948; UNEP, 1994). For these zones, water availability and biomass production are restricted and mostly confined to a short rainy season. As a result, the carrying capacity of the ecosystems is rapidly exceeded by the human exploitation of natural resources, especially in poor countries with fast demographic expansion and deficient exploitation techniques (Kassas, 1995). Furthermore, the resilience of drylands is often reduced by the occurrence of recurring droughts and severe desertification, which threatens sustainable development in these fragile environments.

For the sub-Saharan region, the devastating effects of drought and desertification were brought to a global audience with the famine that stroke the western Sahel the years that precede 1973. World-wide concern was also triggered by the drought that stroke Northern Ethiopia in 1984-1985. In a context of civil war, region-wide crop failures led to massive famine and starvation. The Tigray Rural Development Study which investigated on the state of the environment in the 1970s concluded that land degradation was severe in Northern Ethiopia and that natural resources were put to their limits (Virgo and Munro, 1978). The 1984-1985 drought, which until today remains a text-book example of what drought and desertification can cause in poor and politically unstable dryland countries, was certainly an eye-opener for many policy makers and scientist worldwide. In many dictionaries, Ethiopia is still being used as a prime reference for famine and drought (to the regret of many).

As a response to the deterioration of dryland environments, environmental protection and development cooperation initiatives were launched globally. Key was the initiation of the UN Convention to Combat Desertification (UNCCD) on the UN Conference on Environment and Development in 1994. The main objective of the UNCCD was to combat desertification, defined as “land degradation in arid, semi-arid and dry sub-humid areas resulting from various factors, including climatic variations and human activities” (UNEP, 1994). The focus thereby exclusively lies on land degradation in dryland environments. Land degradation was defined as the “reduction or loss of the biological or economic productivity and complexity of rainfed cropland, irrigated cropland, or range, pasture, forest and woodlands. It may result from processes such as: soil erosion caused by wind and/or water, deterioration of the physical, chemical and biological or economic properties of soil and long-term loss of natural vegetation” (UNEP, 1994).

Almost two decades after the establishment of the UNCCD, land degradation in dryland environments remains high on the international agenda. For example, in 2007, the DESIRE project (framing within the 6th EU Framework Programme) was launched to establish alternative land use and management conservation strategies for 18 degradation and desertification hotspots around the world. In 2010, the United Nations Decade for Deserts and Fight Against Desertification (UNDDD) was launched to promote worldwide actions that will protect drylands from degrading. A year later, in 2011, the UN General Assembly stressed that “unless desertification, land degradation and drought are addressed urgently wherever they occur, sustainable development would be corroded”. In the precedence of Rio+20 (to be held in June 2012), many countries called for a land degradation neutral world, as for many areas worldwide, land degradation may hinder sustainable development and the achievement of the UN Millennium Goals.

Gully erosion is acknowledged as a key erosion process whereby land degradation in dryland environments occurs. In a review, Poesen et al. (2002) conclude that gully erosion contributes to 50% to 80% of the overall sediment production in drylands. Sediment yields are locally very variable, but may be as high as 12.1 ton ha^{-1} y^{-1} in Ethiopia, 3.4 ton ha^{-1} y^{-1} in Kenya, 32 ton ha^{-1} y^{-1} in Niger, 16.1 ton ha^{-1} y^{-1} in Portugal, 64.9 ton ha^{-1} y^{-1} in Spain and 36.8 ton ha^{-1} y^{-1} in the USA (Poesen et al., 2003).

Understanding historical and present-day gully erosion is therefore essential when addressing the consequences of future land use and climate change scenarios (Poesen et al., 2003; Valentin et al., 2005). For instance, land managers need to foresee the effects of land use changes, infrastructure construction or urbanization on gully development. Without such projections, future developments may be unsustainable and yield much higher costs than originally budgeted. In addition, soil losses may strongly increase, jeopardising in-situ and downstream agricultural production (Poesen et al., 2003). Furthermore, the rapid expansion of gullies is related to shifts in the hydrological regime of landscapes (Knighton, 1998), by which runoff and soil water rapidly converges to gullies (Muhindo Sahani, 2011). This often results in flash floods of polluted water which threaten human health.

Relatively few studies investigate the importance of gully erosion on land degradation, especially when considering sub-Saharan Africa. Reports on gully erosion are known for Burkina Faso (Marzolff and Ries, 2007), the Democratic Republic of the Congo (Ndona and Truong, 2011), Kenya (Oostwoud Wijdenes and Bryan, 2001; Katsurada, 2007), Lesotho (Showers, 1996); Namibia (Eitel et al., 2002), Niger (Leblanc et al., 2008), Nigeria (Gobin et al., 1999), Rwanda (Moeyersons, 1989, 1991), Senegal (Poesen et al., 2003), South Africa (Boardman et al., 2003), Swaziland (Felix-Henningsen et al., 1997) and Zimbabwe (Stocking, 1980). Regarding Ethiopia, several studies reported significant gully erosion (Virgo and Munro, 1978; Nyssen et al., 2000, 2002, 2004a, 2006; Billi and Dramis, 2003; Daba et al., 2003; Moges and Holden, 2008; Munro et al., 2008; Reubens et al., 2009), but there is insufficient data on gully characterisitcs, headcut retreat rates, network and volumes development patterns or the importance of controlling factors.

1.2 Defining gully erosion

In the Oxford Dictionary of Earth Sciences (2008), a gully is defined as a “feature of water erosion that develops from the runoff of a violent torrent that bites deeply into topsoil and soft sediments”. Gully erosion can thus be associated with the rapid incision of valley-sides or valley-floors by the erosive action of flash floods. This is also apparent from the definition of Poesen et al. (2003), whom conclude on gully erosion as the “erosion process whereby runoff water accumulates and often recurs in narrow channels and, over short periods, removes the soil from this narrow area to considerable depths”; a definition that is widely used in scientific literature. Gully erosion is the result of disruptions in a previous stage of equilibrium that cases alternations in the amounts of water and sediment delivered to a certain place in the landscape (Graf, 1988; Knighton, 1998). Causes of incision are numerous and can be grouped in six categories (Schumm, 2005): geologic, geomorphic, climatic and hydrologic, animal and human causes. Examples which are most relevant for the case of Northern Ethiopia are uplifting, baselevel lowering, mass movements, increased aridity or humidity, increased mean discharge and/or peak discharge, decreased sediment load, animal grazing and tracking, flow diversion, urbanization and infrastructure construction (for a more complete overview see Schumm, 2005). As the geomorphic development of gullies is related to alternating conditions, they are also referred to as non-regime channels (Schumm, 2005). Depending on the specific setting, gullies are also reported as ‘arroyos’, ‘wadis’ or other regional terms.

With the purpose to efficiently transfer water and sediment downslope, the shape and size of gullies mainly adjusts to (mean, peak) discharge properties (Knighton, 1998). Usually, a gully is perceived as a freshly incised U- or V-shaped channel with depths ranging between 0.5 m and 10 m, and top widths ranging between 0.3 m and 15 m. However, shape and size may be spatially and temporally very variable, depending on local environmental characteristics (e.g., soil, vegetation), and the time that is needed to accommodate changes in discharge and sediment load, i.e. reaction and relaxation times (Knighton, 1998). Regarding the gully size, a lower limit was proposed by Hauge (1977), which defines gullies as channels with a minimal cross-section of 929 cm^2 (one square foot). This corresponds to a channel that is not easily erased by agricultural activities. As gully erosion is commonly associated to soil loss from agricultural land, this criteria is widely accepted. Regarding the upper limit of channel size, no clear definitions exist. When gully networks fully develop and link to ephemeral river systems, it is indeed difficult to clearly distinguish both, and gullies may only refer to low-order channels. In this study, gullies up to 25 m wide and 12 m deep were considered.

In terms of typology, a distinction can be made between ephemeral and permanent gullies. The former are shallow channels with are larger than rills, but do not grow subsequently but are erased after tillage (Poesen, 1996). The latter, which are the subject of this thesis, develop as permanent features of the landscape. In terms of process and development, three kind of permanent gullies can be distinguished: continuous, discontinuous and bank gullies (Bull, 1997; Poesen et al., 2003). Discontinuous gullies do not link to an ephemeral drainage system, and can thus be found isolated on hillslopes and in thalwegs. Degradation and aggradation are confined within a closed system: sediment production in the upper part of the gully, as the result of headcut erosion and channel degradation, sediment accumulation in debris fans at the lower gully margin. Often, discontinuous gullies, while expanding upslope and downslope, will eventually connect to the drainage network. Gullies connected to ephemeral drainage networks are called continuous gullies, also referred to as stream gullies (Billi and Dramis, 2003). Here, sediment produced by degradation along the channel margins is exported to the ephemeral stream network. Bank gullies (Poesen, 1993) develop along over-steepened gradients along roadcuts, terrace banks, rivers, larger gullies, or any other earth bank. They may in a later stage develop as discontinuous or continuous gullies.

1.3 Objectives

The main objective of this thesis is to better understand gully erosion development since the late 19th century at a regional scale in the Northern Ethiopian Highlands. The overall aims are:

- to understand spatiotemporal variations in gully morphology and morphomerty,
- to assess spatiotemporal variations in gully development patterns,
- to understand spatiotemporal variations in factors controlling gully erosion development,
- to propose a hydrogeomorphic model for gully erosion development and environmental control.

It is aimed that this will contribute to the improved understanding of the causes and consequences of the historical and present-day land degradation in Northern Ethiopia, and to a futher extent, enhance the understanding of land degradation processes in dryland environments.

In order to achieve the main objectives, specific objectives and action points are:

- to assemble a large dataset of terrestrial photographs, aerial photographs and satellite images suitable to study gully erosion and environmental control,
- to refine and to develop methods which allow to quantify gully erosion and environmental control from the assembled dataset,
- to characterize and quantify gully morphology, morphometry, networks and volumes,
- to quantify gully network and volume development patterns,
- to quantify gully head erosion rates,
- to relate gully network and volume development patterns and gully head erosion rates to gully and environmental characteristics,

- to quantify land use and land cover changes,
- to understand the effect of rainfall variability on land use and land cover changes,
- to develop a hydrogeomorphic model for gully erosion development that include the major controlling factors.

1.4 Choice of the study area

This study examines an area of 10^4 km² in the Northern Ethiopian Highlands. Main focus was laid on eight catchments within the Tigray Region. These areas reflect the regional variability in environmental characteristics, i.e. variations in climate, topography, lithology, soil and land use/cover. From north to south, these are the catchments of Ablo (15.2 km²), May Mekdan (44.7 km²), May Ba'ati (4 km²), May Tsimble (8.1 km²), Atsela (4.9 km²), Ayba (37 km²), Seytan (8.2 km²) and Lake Ashenge (1.1 km²); and in total they cover an area of 123 km² (**Figure 1.1**). Furthermore, numerous point observations were made outside of the main study areas.

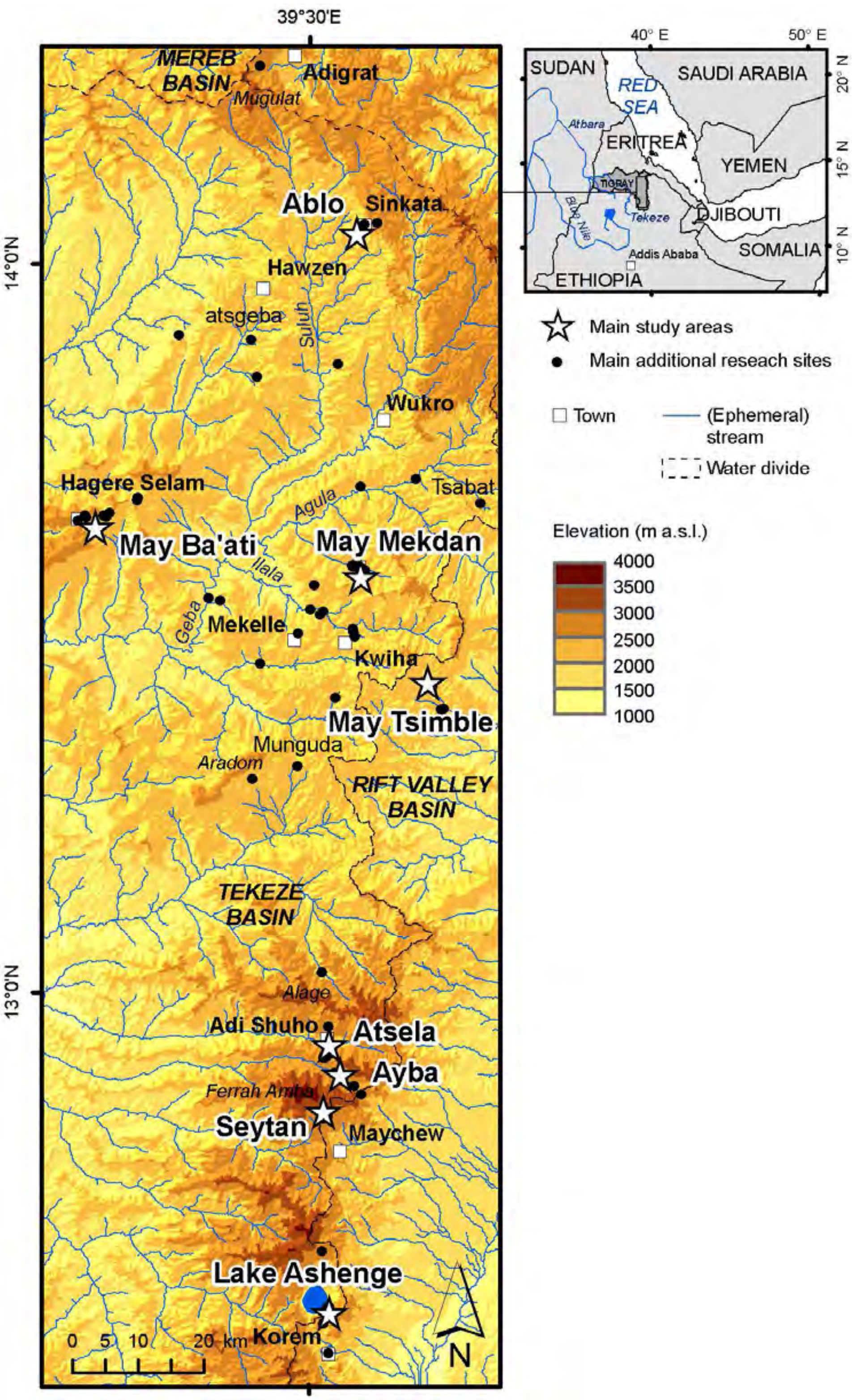

Figure 1.1 Main study areas and main additional reseach sites considered by this thesis, reflecting regional variations in environmental characteristics.

Selecting the study areas was to some extent based on the availability of terrestrial photographs, aerial photographs and satellite images, which allow to study historical gully erosion or environmental change on a specific spatial and temporal scale (**Figure 1.2**).

Low-resolution satellite images permit region-wide analyses as from the 1970s, when the first commercial remote sensing programs where launched. However, the spatial resolutions presented by these first sensors remain in the order of decameters. For this study, Landsat images (30-60 m resolution) and NOAA's Rainfall Estimates (8 km resolution, derived from satellite images) were used.

Aerial photographs of the period 1963-1994 were available from the Ethiopian Mapping Authority. With scales ranging between 1 : 35 000 and 1 : 60 000, these permit to investigate the Northern Ethiopian landscape at resolutions of ~1-2 m. Similar resolutions are given by high-resolution satellite images like IKONOS-2 or images accessed from Google® Earth, and complete the time-series or aerial photographs for the present. Aerial photographs that were taken by the Italian military in the 1930s and that were initially targeted as data-inputs were not considered in this study. This because accessing them prove to be very difficult, as the first copy of an Italian aerial photograph could only be viewed in April 2012.

Historical terrestrial photographs of the period 1868-1994 permited to investigate specific locations in Northern Ethiopia. Especially the following three datasets were key to this study:

- 1868 photographs taken by the Royal Engineers during the British military expedition to Abyssinia,
- 1930s photographs taken during the Italian occupation of Ethiopia,
- 1970s photographs taken during the Tigray Rural Development Study.

The study area and materials will be presented with the relevant details in every chapter of this thesis.

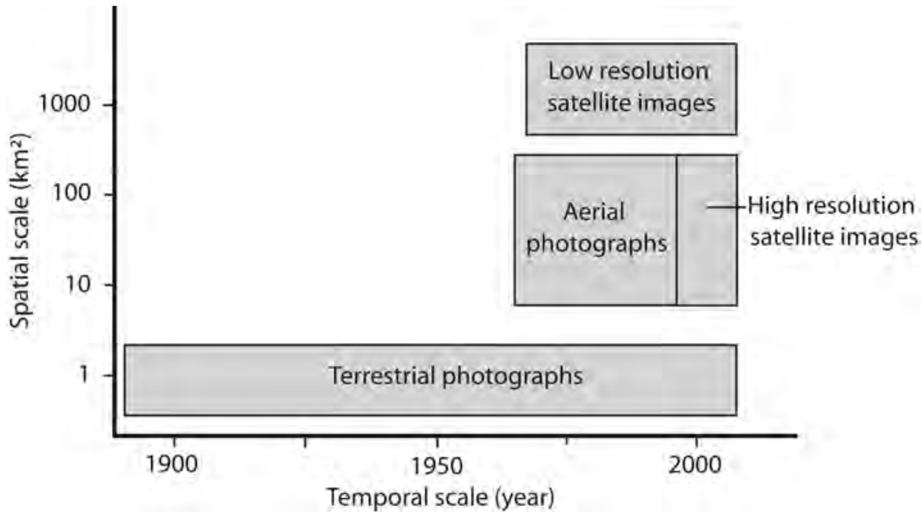

Figure 1.2 Spatiotemporal scale of different datasets used in the thesis.

1.5 Thesis outline

This thesis includes two main parts (**Figure 1.3**). Part 1 is subdivided in three chapters which investigate on gully erosion development since the late 19th century and its present-day importance. Chapter 2 approaches gully erosion from the use of terrestrial photographs and establishes trends in gully erosion development since 1868. Chapter 3 elaborates the use of aerial photographs and high-resolution satellite images to quantify gully erosion development. It presents gully network and volume development patterns since 1963. Furthermore, this chapter provides data on the present-day morphology and morphometry of gullies, in relation to their controls. Chapter 4 investigates on gully head retreat rates. Part 2 addresses land use/cover changes and the relation with rainfall variability in the Northern Ethiopian Highlands. In Chapter 5, terrestrial photographs are used to asses land use/cover changes over a period of 140 years. Chapter 6 focuses on the use of low-resolution satellite images to quantify region-wide changes in land use/cover since 1972. Concerning the effects of rainfall variability on cropping systems and the land cover by crops, development patterns since 1996 are proposed in Chapter 7. The general discussion (Chapter 8) combines findings from Part 1 and Part 2 in a hydrogeomorphic model. General conclusions are presented in Chapter 9. Appendix A and B support the findings of this work.

References from this chapter are listed in the Reference Section of Chapter 8.

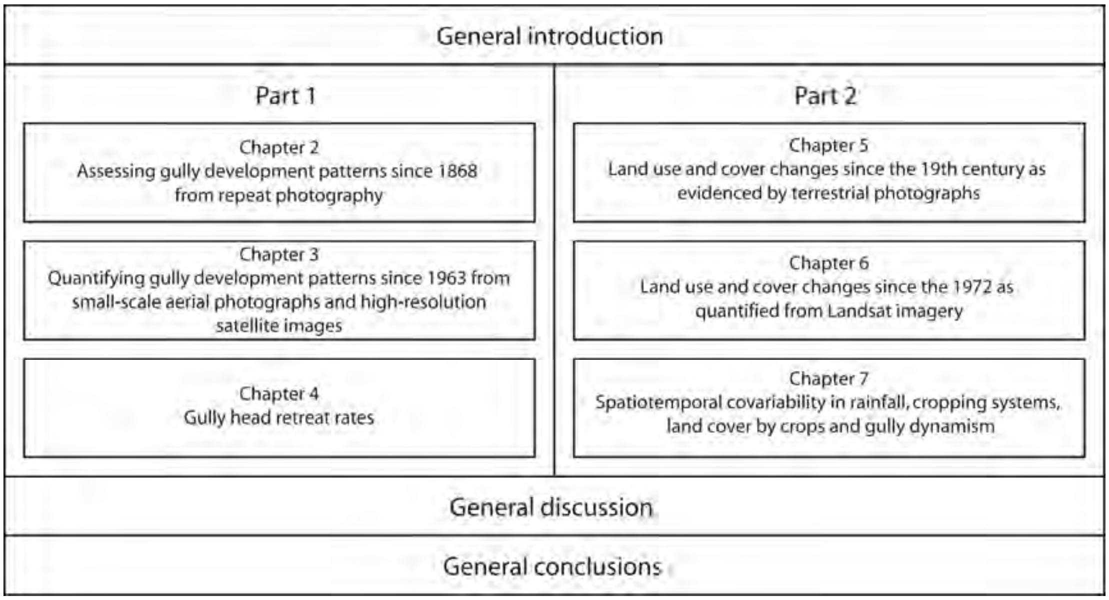

Figure 1.3 Thesis outline.

1.6 Thesis inputs

This thesis incorporates many inputs from own international or national publications, book contributions or conference contributions. A complete publication list can be found in the next section. Some sections or chapters are based on the inputs of MSc. theses (listed here-below) or subsequent publications that were developed in the framework of the PhD. research.

Master dissertations framing within the PhD. research

Moulaert, L., 2012. The use of subsurface plastic dams to stabilize and rehabilitate gullies in Vertisol areas (Northern Ethiopia). Unpub. Master Thesis. Department of Geography, Ghent University.

Schumacher, M., 2012. Recent trends in gully erosion as evidenced by repeat photography around Hagere Selam (Northern Ethiopia). Unpub. Master Thesis. Institute for Geography, Technical University of Dresden.

Stock, S., 2011. Land use/land cover and population dynamics in North-Ethiopia as derived from aerial photographs. Unpub. Master Thesis. Department of Geography, Ghent University.

Scholiers, N., 2010. Development of gully networks and volumes since 1965 in the May Mekdan catchment (North Ethiopian highlands). Unpub. Master Thesis. Department of Geography, Ghent University.

Jacob, M., 2010. Cropping systems in the Tigray highlands (North Ethiopia) as related to spatiotemporal variability of rainfall. Unpub. Master Thesis. Department of Geography, Ghent University.

Meire, E., 2009. Mapping of land use and cover in the North Ethiopian highlands since 1868 using warped terrestrial photographs. Unpub. Master Thesis. Department of Geography, Ghent University.

de Mûelenaere, S., 2009. Land use and cover changes in the Ethiopian highlands; Landsat data analysis using contemporaneous ground photographs for calibration. Unpub. Master Thesis. Department of Geography, Ghent University.

1.7 Publication list

This list was last updated on August 1, 2012.

(a1) – international publications in journals indexed in the ISI Web of Science

Frankl, **A**., Poesen, J., De Dapper, M., Deckers, J., Mitiku Haile, Nyssen, J., 2012. Gully head retreat rates in the semiarid Highlands of North Ethiopia. Geomorphology, online early view: DOI: 10.1016/j.geomorph.2012.06.011. (IF 2.352)

Nyssen, J., Van den Branden, J., Spalević, V., **Frankl**, **A**., Vandevelde, L., Čurović, M., Billi, P., 2012. Twentieth century land resilience in Montenegro and hydrological response. Land Degradation & Development, in press. (IF 1.326)

de Mûelenaere, S., **Frankl**, **A**., Mitiku Haile, Poesen, J., Deckers, J., Munro, N., Veraverbeke, S., Nyssen, J., 2012. Historical landscape photographs for calibration of LANDSAT land use/cover in the Northern Ethiopian Highlands. Land Degradation & Development, online early view: DOI: 10.1002/ldr.2142. (IF 1.326)

Frankl, **A**., Nyssen, J., De Dapper, M., Mitiku Haile, Billi, P., Munro, R. N., Deckers, J., Poesen, J., 2011. Linking long-term gully and river channel dynamics to environmental change using repeat photography (Northern Ethiopia). Geomorphology 129, 238-251. (IF 2.352)

Nyssen, J., **Frankl**, **A**., Munro, R.N., Billi, P. Mitiku Haile, 2010. Digital photographic archives for environmental and historical studies: an example from Ethiopia. Scottish Geographical Journal 126, 185-207. (IF 0.459)

Frankl, **A**., Nyssen, J., Calvet, M., Heyse, I., 2010. Use of Digital Elevation Models to understand and map glacial landforms – the case of the Canigou massif (Eastern Pyrenees, France). Geomorphology 115, 78-89. (IF 2.339)

Nyssen, J., Mitiku Haile, Naudts, J., Munro, N., Poesen, J., Moeyersons, J., **Frankl**, **A**., Deckers, J., Pankhurst, R., 2009. Desertification? Northern Ethiopia re-photographed after 140 years. Science of the Total Environment 407, 8, 2749-2755. (IF 2.579)

Nyssen, J., Poesen, J., Descheemaeker, K., Nigussie Haregeweyn, Mitiku Haile, Moeyersons, J., **Frankl**, **A**., Govers, G., Munro, R.N., Deckers, J., 2008. Effects of region-wide soil and water conservation in semi-arid areas: the case of northern Ethiopia. Zeitschrift für Geomorphologie 52, 291 - 315. (IF 0.614)

(a1) – in review

Frankl, **A**., Zwertvaegher, A., Poesen, J., De Dapper, M., Nyssen, J., Transferring Google Earth observations to ArcGIS: an example for the study of gully erosion. International Journal of Digital Earth, submitted. (IF 1.453)

Frankl, **A**., Poesen, J., Scholiers, N., Jacob, M., Mitiku Haile, Deckers, J., De Dapper, M., Nyssen, J., Assessment of decadal gully network and volume development in Northern Ethiopia using small-scale aerial photographs and high resolution satellite images. Earth Surface Processes and Landforms, submitted. (IF 2.111)

Frankl, **A**., Jacob, M., Mitiku Haile, Poesen, J., Deckers, J., Nyssen, J., Spatiotemporal covariability in rainfall, cropping systems and land cover by crops in the Northern Ethiopian Highlands. Soil Use & Management, submitted.

Meire, E., **Frankl**, **A**., De Wulf, A., Mitiku Haile, Deckers, J., Nyssen, J., Mapping the 19th century landscape in Africa – warped terrestrial photographs of North Ethiopia. Regional Environmental Change, accepted for publication. (IF 1.325)

De Visscher, M., Nyssen, J., Pontzeele, J., Billi, P., **Frankl**, **A**., Spatio-temporal sedimentation patterns in beaver ponds along the Chevral River, Ardennes, Belgium. Journal of Hydrology, accepted for publication. (IF 2.514)

(a2) – international publications with peer-review not indexed in the ISI Web of Science

Frankl, **A**., Nyssen, J., De Dapper, M., Mitiku Haile, Deckers, J., Poesen, J., 2011. Trends in gully erosion as evidenced from repeat photography (North Ethiopia). Landform Analysis 17, 47-49.

(a4) – publications in national journals

Frankl, **A**., Nyssen, J., De Dapper, M., Deckers, J., Poesen, J. 2010. Dynamics of gully and river channel erosion in Northern Ethiopia: Diachronic analysis of terrestrial photographs. Meded. Zitt. K. Acad. Overzeese Wet. Bull. Séanc. Acad. R. Sci. Outre-Mer 56, 265-276.

Frankl, **A**., Heyse, I., 2007. Sporen van glaciale morfologie in het massief van de Canigou (oostelijke Pyreneeën) aan de hand van een detailstudie in de Coumeladevallei. De Aardrijkskunde 2-3, 3-14.

(b) – book chapters (contributions as co-author not listed)

Frankl, **A**., Nyssen, J., De Dapper, M., Mitiku Haile, Billi, P., Munro, N., Deckers, J., Poesen, J., 2011. Long-term gully and river channel dynamics in Tigray. Excursion guide of the post-conference excursion: IAG/AIG regional conference, Ethiopian Association of Geomorphologists (EAG), 39-44.

Frankl, **A**., Poesen, J., De Dapper, M., Deckers, J., Mitiku Haile, Nyssen, J., 2011. Monitoring gully headcut retreat rates in May Ba'ati. Excursion guide of the post-conference excursion IAG/AIG regional conference, Ethiopian Association of Geomorphologists (EAG), 134-135.

(c) – international conference contributions (contributions as co-author not listed)

Frankl, **A**., Poesen, J., De Dapper, M., Mitiku Haile, Deckers, J., Nyssen, J., 2011. Measures to tackle downstream water pollution by urban development in a mountainous semi-arid landscape dominated by gullies (North Ethiopia). Poster presented at the fifth symposium of the Gents Afrika Platform GAPSYM5: (r)Urban Africa multidisciplinary approaches to the African city. <u>Ghent (Belgium)</u>, December 2, Book of Abstracts, 65-65.

Frankl, **A**., de Mûelenaere, S., Jacob, M., Poesen, J., Mitiku Haile, De Dapper, M., Deckers, J., Nyssen, J., 2011. Understanding gully erosion dynamics since 1965 in May Ba'ati, Northern Ethiopia. Paper presented at the Water 2011 conference: integrated water resources management in tropical and subtropical drylands, <u>Mekelle (Ethiopia)</u>, September 19-26, Book of Abstracts, 40.

Frankl, **A**., Poesen, J., De Dapper, M., Deckers, J., Mitiku Haile, Nyssen, J., 2011. Assessing gully headcut retreat rates in the semi-arid highlands of northern Ethiopia. Paper presented at the IAG/AIG regional conference 2011: geomorphology for human adaptation to changing tropical environments, <u>Addis Ababa (Ethiopia)</u>, February 18-22, Book of Abstracts, 65.

Frankl, **A**., Nyssen, J., Poesen, J., de Mûelenaere, S., Meire, E., De Dapper, M., Deckers, J., Mitiku Haile, 2010. Gully development in North Ethiopia's mountains. Poster presented at the European Geosciences Union (EGU), <u>Vienna (Austria)</u>, May 2-7, Book of Abstracts, 12, 1.

Frankl, **A**., Nyssen, J., De Dapper, M., Mitiku Haile, Deckers, J., Poesen, J., 2010. Trends in gully erosion as evidenced from repeat photography (north Ethiopia). Paper presented at the 5th International Symposium on Gully Erosion, <u>Lublin (Poland)</u>, April 19-24, Book of Abstracts, 33.

Frankl, **A**., de Mûelenaere, S., Meire, E., Poesen, J., De Dapper, M., Mitiku Haile, De Wulf, A., Deckers, J., Nyssen, J., 2009. Analyzing Long-Term Gully Erosion Evolution and Environmental Change in North Ethiopia's Semi-Arid Mountains. Poster presented at the AGU Chapman Conference on Examining Ecohydrological Feedbacks of Landscape Change Along Elevation Gradients in Semiarid Regions. Boise and Sun Valley, <u>Idaho (USA)</u>, October 4-8, Book of Abstracts, 29-30.

Frankl, **A**., Meire, E., de Mûelenaere, S., De Dapper, M., Poesen, J., Mitiku Haile, De Wulf, A., Deckers, J., Nyssen, J., 2009. Time-lapsed photography for analyzing gully erosion in its relation with land use changes in the north Ethiopian highlands. Paper presented at the conference Framing Time and Space – Repeats & Returns in Photography, <u>Plymouth (UK)</u>, April 15-17, Book of Abstracts, 5.

(c) – national conference contributions (contributions as co-author not listed)

Frankl, **A**., Poesen, J., De Dapper, M., Deckers, J., Mitiku Haile, Nyssen, J., 2012. Historical gully erosion development in Northern Ethiopia and implications for development projects. Paper presented at Doctoraats-symposium Faculteit Wetenschappen, Ghent, March 22, Book of Abstracts, 19.

Frankl, A., Meire, E., de Mûelenaere, S., Jacob, M., Scholiers, N., De Dapper, M., Mitiku Haile, Billi, P., Deckers, J., Poesen, J., Nyssen, J., 2010. Analyzing historical and present-day gully erosion and its drivers in the highlands of North Ethiopia. Paper presented at the Day of Young Soil Scientists, Royal Academies of Belgium for Science and the Arts, Brussels, February 23, Book of Abstracts, 9.

Frankl, A., Meire, E., de Mûelenaere, S., De Dapper, M., Poesen, J., Mitiku Haile, De Wulf, A., Deckers, J., Nyssen, J., 2009. Analyzing gully erosion and controlling factors since 1868 in north Ethiopia. Poster presented at Doctoraats-symposium Faculteit Wetenschappen, Ghent, April 28, Book of Abstracts, 4.

Frankl, **A**., Meire, E., de Mûelenaere, S., De Dapper, M., Poesen, J., Mitiku Haile, De Wulf, A., Deckers, J., Nyssen, J., 2008. Analyzing gully erosion in its relation to land use changes in the northern Ethiopian highlands using terrestrial photographs, aerial photographs and satellite images. Poster presented at the second symposium of the Gents Afrika Platform (GAPSYM2), Ghent, December 16, Book of Abstracts.

Frankl, **A**., De Dapper, M., Poesen, J., Mitiku Haile, De Wulf, A., Deckers, J., Nyssen, J., 2008. Gully networks and volumes from IKONOS imagery and digital elevation models in northern Ethiopia. Poster presented at the Dag van de Jonge Onderzoeker, Belgische vereniging voor Afrikanisten, Antwerp, December 12, Book of Abstracts.

Frankl, **A**., Nyssen, J., De Dapper, M., Poesen, J., 2008. Semi-automated gully volume quantification from digital elevation models: a new technique tested in the May Zeg Zeg catchment, northern Ethiopia. Paper presented at the third Belgian Geography Days, Brussels, October 24-25, Book of Abstracts.

Part 1

Chapter 2
Assessing gully development patterns since 1868 from repeat photography

This chapter is modified from:

Frankl, A., Nyssen, J., De Dapper, M., Mitiku Haile, Billi, P., Munro, R. N., Deckers, J., Poesen, J., 2011. Linking long-term gully and river channel dynamics to environmental change using repeat photography (Northern Ethiopia). Geomorphology 129, 238-251.

Frankl, A., Nyssen, J., De Dapper, M., Mitiku Haile, Deckers, J., Poesen, J., 2011. Trends in gully erosion as evidenced from repeat photography (North Ethiopia). Landform Analysis 17, 47-49.

Frankl, A., Nyssen, J., De Dapper, M., Deckers, J., Poesen, J. 2010. Dynamics of gully and river channel erosion in Northern Ethiopia: Diachronic analysis of terrestrial photographs. Meded. Zitt. K. Acad. Overzeese Wet. Bull. Séanc. Acad. R. Sci. Outre-Mer 56, 265-276.

Abstract

In the Highlands of Northern Ethiopia gully occurrence is linked to poverty-driven unsustainable use of the land in a vulnerable semi-arid and mountainous environment, where intensive rainfall challenges the physical integrity of the landscape. Trends in gully and river channel erosion, and their relation to triggering environmental changes can proffer valuable insights into sustainable development in Northern Ethiopia. In order to assess the region-wide change in gully and river channel morphology over 140 years, a set of 57 historical photographs taken in Tigray, and, clearly displaying gully cross-sections, were precisely repeated from 2006 till 2009. Ninety-two percent of the gully and river sections (n = 38) increased in cross-sectional area during the studied period, especially after 1975. The average incision rate of the quantified cross-sections was 0.04 m y^{-1}. Maximum incision rates of 0.13 m y^{-1} were observed in Vertisol areas. Two repeatedly photographed catchments of Lake Ashenge and Atsela allowed a detailed study of gully development from 1936 till 2009, including the analysis of aerial photographs. This chapter validates previous research indicating severe land degradation in the second half of the 20th century. It demonstrates that the recent erosive cycle started around 1965, with the increase in highly dynamic gullies and drainage densities. At present, improved land management caused stabilization of headwater streams. Twenty-three percent of the studied gully and river channel were stabilizing in 2009. This Chapter validates previous research indicating severe land degradation in the second half of the 20th century. Additionally, it demonstrates that the recent erosive cycle started around 1965 and, that at the present time, improved land management stabilizes headwater streams.

Keywords: Cross-section, Gully, erosion, Northern Ethiopia, Repeat photography.

2.1 Introduction

The Northern Ethiopian Highlands suffer from severe land degradation, evident in several geomorphic features, including dense gully and river networks. The latter are linked to a poverty-driven unsustainable use of the land in a vulnerable semi-arid and mountainous environment where intense rainfall accelerates the sculpturing of the landscape. Over the past 140 years – since the time that photography provided the first unequivocal evidence of gullying – gullies became widespread. Today, they constitute a serious problem for humans and the environment. Stream network expansion and channel widening are accompanied by mass wasting, which acts on the gully sidewalls and is potentially life-threatening. Gullies are an obstacle to agriculture, while the water tables depressed by their incision (Muhindo Sahani, 2011) reduce agricultural production. Severe landscape dissection leads to the disconnection of rural areas and to the destruction of infrastructure. In the valley bottoms, runoff concentration and gully erosion cause river channel erosion, flooding and water pollution by sediment (Valentin et al., 2005), endangering human life and health.

Improved insights into gully and river channel development and their relation to triggering factors can contribute to sustainable development in Northern Ethiopia, where most Ethiopians rely on the land for their livelihood (Beyene et al., 2006), and live in a subsistence economy where food security is low (FAO, 2009) and regularly threatened by drought.

Dependent on the spatial and temporal scale, several techniques were developed for analyzing the evolution of gully and river channel erosion (Poesen et al., 2003). In the context of Ethiopia, most of the common techniques are not suitable for large spatial and long temporal scale analysis. The most appropriate techniques are based on aerial photography (e.g., Vandaele et al., 1997; Betts and Derose, 1999; Nachtergaele and Poesen, 1999; Martinez-Casasnovas, 2003), ensuring high spatial coverage going back to the onset of land surveying campaigns. Such surveys produced aerial photographs with scales typically ranging between 1:30 000 and 1:60 000 that are too small to precisely determine gullies (or small rivers) and their morphology. The usefulness of aerial photography is therefore limited. With regard to the time scale, interview techniques allowed detailed reconstructions of historical gully erosion (e.g. Showers, 1996; Nyssen et al., 2006; Moges and Holden, 2008). Because these are time-consuming, they were only applied in small areas.

On the contrary, repeated historical terrestrial photographs offer a valuable tool for analyzing long-term changes in environmental features. Repeat photography has been used for studying dynamics in vegetation cover (Roush et al., 2007) and the climatic implications of it (Munroe, 2003), dune field organization (Wilkins and Ford, 2007), glacial extent (Molina et al., 2004), landforms (Webb and Boyer, 2004), landscapes (Dervieux and Picon, 1997; Fjellstad and Dramstad, 1999), and desertification (Munro et al., 2008; Nyssen et al., 2008a, 2009). Repeat photography has seldom been used to study gully erosion. However, Williams (1978), Graf (1982) and Trimble and Lund (1982) studied gully formation and recovery qualitatively through repeat photography, while Trimble (1998) used the presence of a car near to a gully on a 1940 photograph to calculate past gully dimensions. More recently, Webb and Leake (2006) used repeated photographs dated back to 1863 to assess dynamics in riparian vegetation and gullying in the United States. As to the study of river channels, repeat photography is more often applied, as their larger dimensions are easier to analyze (e.g., Preciso et al., 2010.).

The objectives of this study are (1) to develop a methodology that uses repeat photography to assess gully erosion rates over the past 140 years, before aerial photography and beyond living memory; (2) to refine the assessment of gully erosion rates by means of aerial photography and interview techniques; (3) to study long-term (> 100 y) change in gully erosion; (4) to correlate trends of gully erosion to changing environmental characteristics; (5) to demonstrate that the fast environmental degradation started in the second half of the 20th century in the Northern Ethiopian Highlands and finally, (6) to illustrate that recent efforts for soil and water conservation are having positive effects on channel dynamics.

2.2 Materials and methods

2.2.1 Study area

The study examines an area of 10^4 km² in the Northern Ethiopian Highlands, which mainly drains to the Tekeze-Nile basin and partially to the Rift Valley (**Figure 2.1**). The Highlands border the Rift Valley on the west and are mainly composed of Mesozoic limestone and sandstone covered by Tertiary volcanics (Merla et al., 1979). The uplift of these lithological units over the past 25 million years (Williams and Williams, 1980) and their differential resistance to erosion gave the Highlands their typical relief of stepped, flat topped mountains (*ambas*), dissected by canyon-like valleys. Elevations range between 1500 and 4000 m a.s.l.

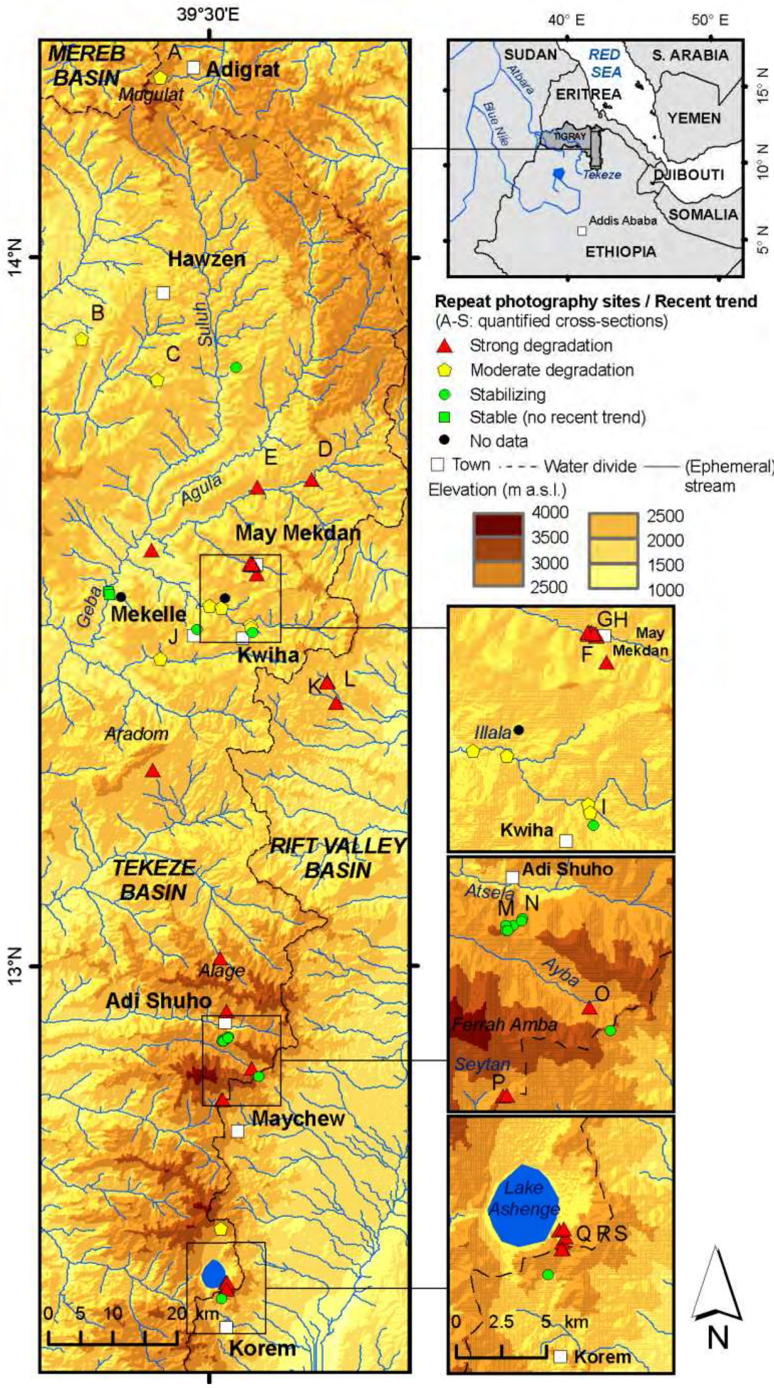

Figure 2.1 Study area, historical camera locations and recent (2009) developments in gully and river channel dynamics based on field observations.

Young soils prevail in the study area (HTS, 1976; Nyssen et al., 2008b; Van de Wauw et al., 2008). Leptosols are found in high landscape positions while Regosols or Cambisols occur on steep slopes. In footslope positions, more developed fine-textured soils are found with Vertisols on basalt and Calcisols on limestone. Under remnant forest Phaeozems occur (Descheemaeker et al., 2006).

Located in the sub-Saharan semi-arid belt, the Northern Ethiopian Highlands region is one of the world's most drought-prone zones. The ustic rainfall regime is driven by the position of the Inter Tropical Convergence Zone (Robinson and Henderson-Sellers, 1999). Its passage over the Highlands from March until May announces the beginning of the monsoon type rainy season, intensifying from June until September. Precipitation occurs as intense rainstorms with large rain-drop sizes (Nyssen et al., 2005). Annual precipitation increases from north to south, ranging between 500 and 900 mm y^{-1}. The inter-annual variability, however, differs considerably.

The natural environment of the Northern Ethiopian Highlands is highly degraded (Virgo and Munro, 1978). Original Afromontane forests have long been reduced to small patches around the churches, and shrub and tree cover on cultivated land and pastures are very rare (HTS, 1976; Wilson, 1977; Nyssen et al., 2004a). Furthermore, high livestock densities reduce the development of grasses and herbs. As a result, flash floods often occur and soil erosion, including gullying, severely affects the land. Since the 1980s, huge efforts have been made to tackle environmental degradation (Nyssen et al., 2004a). Biophysical conservation structures were implemented, such as the closure of steep slopes for vegetation recovery (Descheemaeker et al., 2006), the establishment of stone bunds on farmland (Nyssen et al., 2008a) and the construction of check dams in gullies (Nyssen et al., 2004b).

The catchments of Lake Ashenge (1.1 km^2) and Atsela (4.1 km^2) (**Figure 2.1**) are formed in the deeply weathered Ashengi basalts with tuffs (Merla et al., 1979). In both catchments, steep slopes have gradients ranging between 0.5 and 1.2 m m^{-1} and are well distinguished from the flat valley floors with slope gradients of 0.1 m m^{-1}. Colluvial soils on the steep valley slopes are shallow, while thick alluvial-colluvial deposits occur on the valley bottom. Annual precipitation for the nearby station of Maychew is 900 mm y^{-1} (calculated over the period 1999–2006; NMA, 2010).

2.2.2 Repeat photography

For this study, 57 historical photographs, dated from 1868 until 1994, were selected (**Table 2.1**, **Figure 2.1**). They were originally taken by scientists, tourists and soldiers who were documenting the Northern Ethiopian landscapes on their itinerary. Often the photographers did not mean to capture gully or river channel dynamics, because they were primarily attracted by other landscape elements. Photographs from the Tigray Rural Development Study (TRDS) team (HTS, 1976), however, were taken usually because they did show spectacular examples of, for example erosion, and these were being monitored. Prior to 1974, it can be stated that the photographs do provide us with a random sample of the state of the gullies and river channels in Tigray at various time intervals. In order to compare the previous and current situations, the second set of photographs were taken between 2006 and 2009 according to the technique of repeat photography by Hall (2001, pp. 27): “Repeat photography means retaking photographs from the same spot and of the same subject several times. It requires the accurate replacement of the camera and composition of the subject”. The relocation of the camera position of the photographs was based on (1) text descriptions on some of them, (2) detailed maps of the route of the Abyssinian expedition (obtained from the Kings Own Museum at Lancaster; http:// www.kingsownmuseum.plus.com/contact.htm), (3) knowledge of landforms induced by various lithologies, and (4) a dozen-year long geomorphologic research experience in the study area (Nyssen et al., 2009). The camera position was inferred by identifying unique landscape features such as mountain peaks and drainage ways including their relative position. Finally, the exact camera position and orientation were obtained by lining up near and distant objects in a triangulation system (Nyssen et al., 2009). Several photographs were taken at and near the relocated camera position and the best fitting repeat photograph was selected on-screen. The complete dataset of analyzed historical and repeated photographs (photo-couples 1–57) is available as supplementary data in Appendix A of the thesis.

Table 2.1 Historical photographs used in the analysis (n = 57)

	Authors (and source of the photographs)	Quantitative	Qualitative
1868	Royal Engineers (KingsOwn Museum, Lancaster, U.K.)	1	4
1895	Unknown photographer (Publifoto – Olycom)		1
1935	Unknown photographer (Corbis)		1
1936	Unkown Italian photographer	1	
1939	Maugini (Istituto Agronomico per l'Oltremare, Firenze, I)		5
1942	Unknown photographer (Getty Images)	1	
1944	David Buxton (Cambridge University)		2
1961	Dick Grove (private collection)		1
1970-1	Ernesto Abbate (Merla et al., 1979)		2
1972-4	Ruth Trummer (private collection)		1
1974-5	Tigray Rural Development Study group (Neil Munro, Graham Edgeley, Vernon Robertson, Keith Virgo, Rita Ions)	16	14
1994	André Crismer (private collection)	1	
1994	Francesco Dramis (private collection)	3	3
	TOTAL	**23**	**34**

The quantitative analysis of gully cross-sections (see Section 2.2.3.2) required that the historical and repeat photographs were geometrically almost identical. Therefore, the contours of stable landscape features such as the skyline, cliffs, large rocks, old trees and churches were digitized on the historical photographs with Adobe® Illustrator. These digitized features were then used to slightly rotate, rescale and crop the repeated photographs to the format of the historical photograph (**Figure 2.2**). Under the assumption that both historical and repeated photographs were taken with the same normal lens, deformation properties were identical for the time-lapsed photographs. Each match was checked visually on-screen by layering the repeated photograph on the historical photograph, with gradually increasing its transparency.

2.2.3 Analysis of gully and river-channel development

Channel cross-sectional development was analyzed quantitatively for 19 gully/river reaches, and portrayed perpendicularly on 23 paired photographs. These included the quantification of 30 historical cross-sections which are displayed clearly on the paired photographs, and for which the orientation of the camera allowed measurement of the cross-sectional properties of gullies and river channels. In addition, some reference points (e.g., rocks, trees, and lynchets) were utilized to precisely locate the cross-sections on the paired photographs and in the field. Twenty-three cross-sections (on 23 gully and river reaches), for which repeat photography did not allow derivation of accurate morphometric data, were analyzed qualitatively. Whenever possible, changes in network extension and configuration were also recorded. Results derived from repeat photography were supported by evidence from interviews of local informants and by geomorphic observations in the field. In addition for the two case studies of the Atsela and Lake Ashenge catchments, aerial photographs and satellite images were used to assess gully and river network development patterns.

2.2.3.1 Qualitative analysis

For the qualitative analysis, channel dynamics of the gullies and rivers were assessed visually, making a distinction between low- and high-active channels. This was based on the cross-sectional shape of the channel, the presence of vegetation in the channel, the occurrence of mobile bed material, bank gullying, and tension cracks or mass failure in the channel banks. Low-active gullies or rivers typically have a narrow active channel, smooth cross-sectional profiles, and walls overgrown by vegetation; and mobile bed material is absent or restricted to small grain sizes.

High-active gullies or rivers are characterized by an active channel width equal to the total width of the channel bottom; the channel has a rectangular cross-sectional shape with steep, well-delineated walls subject to mass failure; there is no vegetation on the channel floor and on the lower section of the walls; and mobile bed material is present, especially in the lower sections of the gullies or rivers where sediment deposition becomes more important. Flooding severity can furthermore be assessed by the size of the entrained bed particles and by flood marks in the channel.

In order to understand gully and river-channel dynamics, repeat photographs were scrutinized for environmental parameters affecting runoff volume and sediment load. Important factors that could be observed were the surface morphology and slope, overall vegetation cover, soil and water conservation practices and urbanization. Where a road or track was near a studied gully or river reach, attention was given to the configuration of any road ditch outlets.

2.2.3.2 Quantitative analysis

By layering the best-fitting repeat photograph on top of the historical photograph and by gradually decreasing its transparency, 30 cross-sections visible on the historical photographs could be identified on the repeat photographs. For the previous and current situations, the observable top width, maximum depth and bottom width of the cross-sections were approximated by dimensionless white lines using Adobe® Illustrator (**Figure 2.2**). In the current situation, these lines were calibrated by measuring the cross-sectional properties in the field. Consequently, the cross-sectional properties displayed on the historical photographs could be calculated as well. Field measurements were done between July and September 2009. Possible changes in cross-sectional properties between the dates of the cross-sectional measurements and the repetition of the historical photographs were not taken into consideration, because field verification showed them to be negligible.

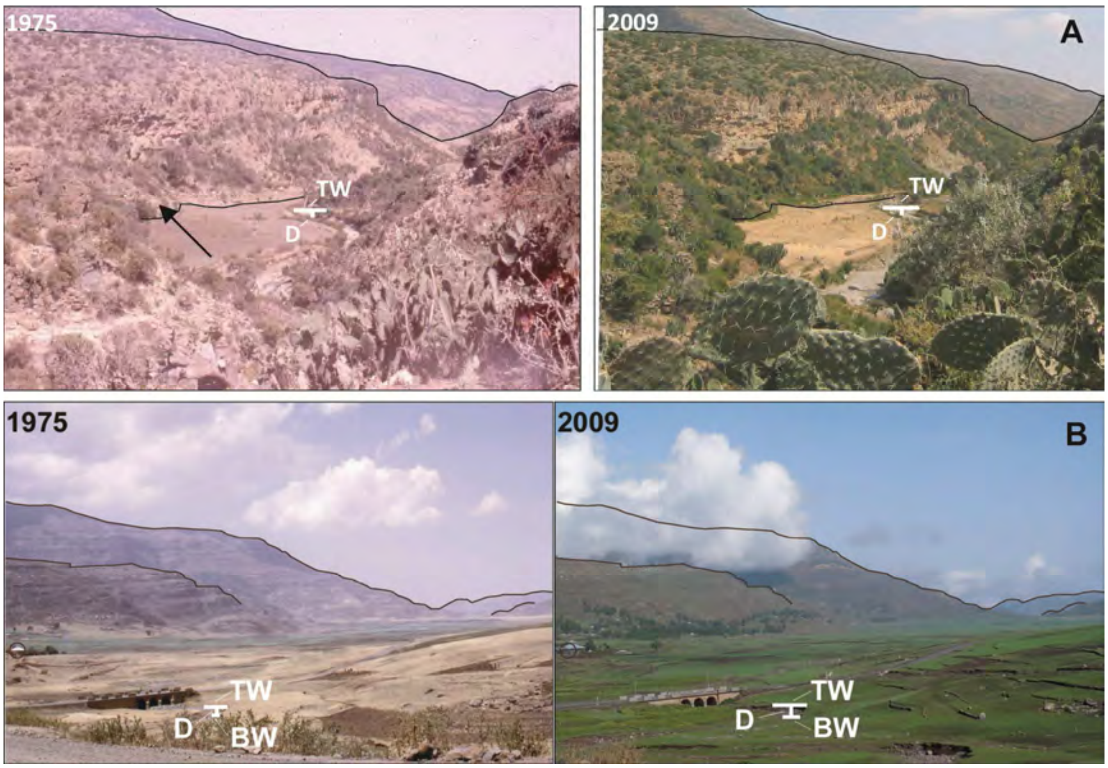

Figure 2.2 Examples of geometrically nearly identical photo-couple. The repeat photographs (right) were fitted to the historical photographs (left) by using contours of stable landscape features (black lines) to rotate, rescale and crop the repeat photographs. This created the white strip at the left side of the repeat photograph at photo-couple A. **A**: Location: Lahama, 12°23’15” N, 39°40’57” E. The arrow on the original photograph indicates a terrace which was irrigated with the base flow of the river up to 1981. Some 100 m upstream, at the beginning of the irrigation channel, the river has been incised by 2.60 m. Landscapes portrayed on photo-couples 31 and 32 drain to this place (Thesis Appendix A). Cross-section properties: historical photograph: *TW* = 13.67 m, *D* = 1.62 m, *CSA* = 19.89 m²; repeat photograph: *TW* = 19.14 m, *D* = 2.90 m (Cross-section L, **Table 2.2**). (historical photograph: Neil Munro; repeat photograph: Amaury Frankl). **B**: Location: Ayba, 12° 52’ 16’’N, 39° 33’ 33’’ E. Note the construction of soil bunds for slope stabilization in the cropland. Cross-section properties: historical photograph: *TW* = 6.55 m, *D* = 1.41 m, *BW* = 1.20 m; repeat photograph: *TW* = 13.60 m, *D* = 2.15 m, *BW* = 2.50 m. (Cross-section O, **Table 2.2**) (historical photograph: Keith Virgo; repeat photograph: Amaury Frankl). *TW* = top width, *D* = maximum depth, *BW* = bottom width.

The accuracy of these calculations was verified after the repetition of this procedure for three cross-sections (L1974, L1994, F, **Table 2.2**) by five experienced geomorphologists. The average relative difference between the five evaluations and the values obtained in this paper was 10% and 16% for top width and maximum depth, respectively. These error terms are to be interpreted as maximum values, as the evaluators completed the procedure rather quickly, without visiting the specific measuring sites, and consequently, without fully understanding the local situation. As bottom width was only obtained for one cross-section, the accuracy of the calculation could not be assessed. Errors due to differences in the precise geometrical properties of the paired photographs were estimated to be rather insignificant, as the time-lapsed photographs match very closely. In addition, the identification of terrace levels and their approximate dating through repeat photography and interviews, supported the measurements of the repeat photography. On cross-section Q (**Table 2.2**), the field measurement of the depth of the 1936 terrace was 3.53 m (Cross-section Q) which corresponds rather well to the 4.84 m for the maximum gully depth then calculated by repeat photography, as the middle of the gully was clearly deeper than its sides in 1936. Lower on the same gully, the field measurement of 2.10 m also corresponds well to 1.73 m calculated by repeat photography (Cross-section R, **Table 2.2**).

The historical quantification of five cross-sections was not based on the measurements on the historical and repeat photographs. Three of them could be quantified through a detailed analysis of the stratification of the deposits displayed on the gully wall and field measurements. The remaining two were quantified by assessing the body length of a photographed person standing on the gully shoulder, and by comparing this to the maximum gully depth.

The calculation of the 2009 area of the cross-sections was performed with field measurements of channel top width, bottom width and maximum depth. Because data on bottom width were not available for most of the historical cross-sections, the cross-sectional area was derived from top width and maximum depth alone. So as not to overestimate the historical cross-sectional area and, under the assumption that the cross-sectional shape did not change much over the studied period, the product of top width and maximum depth was multiplied by a correction factor, corresponding to the ratio between the 2009 cross-sectional area and the 2009 top width and maximum depth product. The underlying assumption for the calculation of the historical cross-sectional area is valid whenever the top width/maximum depth ratio remained approximately the same over time (change $< 20\%$).

Changes in top width, maximum depth and cross-sectional area of the channels over the considered period were calculated. Of the 30 cross-sectional measurements, 11 cross-sections were measured near to one another on the same gully and in the same year. Change in cross-sectional properties was averaged for these measurements. As a result, the cross-sections of 19 gully or river-channel reaches could be quantified.

2.2.3.3 Lake Ashenge and Atsela case studies

With the aim of better defining and understanding the important phases in gully and river-channel development, cross-sectional and network development were studied more in detail in the two catchments of Lake Ashenge and Atsela, which were repeatedly photographed between 1936 and 2009 (**Figure 2.1**). Findings from the qualitative and quantitative analysis were combined with the interpretation of time series of aerial photographs (ground resolution of ca. 1.9 m) dated from 1965, 1986 and 1994, and of very high resolution GeoEye®-1 images (ground resolution 0.50 m) accessible on Google® Earth.

In order to quantify the gully networks and erosion rates displayed on the terrestrial and aerial photographs, an orthophotograph was produced for each catchment in which each pixel in the digital image was tied to its true location (Miller, 2004). Digital image processing of the scanned aerial photographs (at 1200 dpi) with Supersoft® Inc VirtuoZo 2.2 produced the orthophotographs. The geometric rectification was based on a digital elevation model (DEM) devised for the same area. The DEMs were produced through digital photogrammetric restitution and included inner and exterior orientations. The relative orientation was based on > 300 tie points per stereo pair, and the exterior orientation was on seven ground control points. For the orthophotograph of the Lake Ashenge catchment the Root Mean Square Error $(RMSE)_{x,\ y}$ is 0.3 m and for the orthophotograph of the Atsela catchment the RMSE in X is 0.5 m and RMSE in Y is 1.5 m. These errors are less than what ground resolution of the actual aerial photographs would allow.

Subsequently, the orthophotographs were used to calculate the catchment area and to map the gully networks with ArcGIS® 9 through repeat and aerial photography, resulting in a distinction between low- and high-active gullies. Another distinction was made between minor and major gully networks, where the latter includes those gullies clearly recognizable on aerial photographs and on very high resolution satellite images with a good delineation of both gully banks, in contrast to the former, which includes smaller gullies or gullies that are discontinuous and not well-delineated, with a top width varying between ca. 2–6 m.

Next, gully length and drainage density were calculated. By combining gully length with field measurements of cross-sections and by identifying terrace levels, incision rates and volumetric erosion rates were calculated over the period 1965–2009 for the Lake Ashenge catchment.

2.3 Results

2.3.1 General trends of gully and river channel cross-sectional development

The analyzed gully and river channel changes revealed that, during the studied period, 92.7% (*n* = 38) of the sections increased in cross-sectional area, either in maximum depth, width or both. This increase could be quantified for 10 gully or river channel cross-sections and an increase in maximum depth or width was measured for another 9 cross-sections (**Table 2.2**). The average annual incision rate for all the quantified cross-sections was 0.04 m y^{-1}, with a maximum average annual incision rate of 0.13 m y^{-1}. Such extreme values were recorded in the Vertisols west of the town of May Mekdan, draining an area of 44 km^2, where the maximum gully depth of a 600 m long section increased on average by 4.49 m between 1974 and 2009 (Cross-section F, **Table 2.2**, **Figure 2.3**). At the analyzed site, 1.32 m of gully bottom degradation could be attributed to the period 1994–2009, corresponding to an incision rate of 0.09 m y^{-1}. Decrease in maximum depth, recorded for three cross-sections, occurred together with a larger increase in top width that was not quantifiable, however. This is well-evidenced by the three photo-couples portraying the Agula River (Photo-couples 5–7, Thesis Appendix A; **Figure 2.4**) where the river morphology and morphologic development are the result of a strong flash flood regime, and high amounts of sediment supplied to the channel. The high values of 0.09 m y^{-1} for channel aggradation of cross-section E (**Table 2.2**) is linked to the passage of a sediment wave, which, in turn, is the result of the degrading river reach below the diversion dam higher on the river.

Table 2.2 Gully cross-section properties and change (n = 30)

Cross-section	Historical photograph				Repeat photograph				% of present situation that came into existence before the historical			
	Date	*TW* (m)	*D* (m)	*CSA* (m^2)	Date	*TW* (m)	*D* (m)	*CSA* (m^2)	*TW*	*D*	*CSA*	Trend
A	1975	0	0	0	2009	6.9	3,00	10.35	0	0	0	W, D increased
B	1974		6.25		2007		7.12			87.76		D increased
C	1975	5.75			2009	6.8			84.51			W increased
D	1974		3.59		2009		3.53			101.77		D dereased
E	1975		6.13		2009		2.93			209.09		D dereased
F	1974	9.98	4.44	35.12	2008	19.2	9.1	138.32	49.03	47.64	23.79	W, D increased
F	1974	8.55	4.07	25.6	2008	18.6	8.55	116.92				
F	1975		3.73		2009		8.06					
F	1994		8.46		2009		9.09			85.15		D increased
F	1994		8.19		2009		9.52					
F	1994		6.05		2009		8.05					
G	1975	13.91			2009	17.12			80.84			W increased
H	1975	3.53	1.85	6.54	2009	4.45	4.2	18.69	79.33	44.09	34.99	D, W increased
I	1975		2.11		2009		1.38			119.2		D decreased
I	1975		1.74		2009		1.85					
J	1975	33.00			2009	33,00			100.00			W stable
J	1975		5.97		2009		7.37			71.84		D increased
J	1975		0.52		2009		1.67					
K	1975		7.6		2009		11.6			65.52		D increased
L	1975	13.67	1.62	22.21	2009	19.14	2.9	55.51	71.42	56.02	40.01	W, D increased
M	1942	10.94			2009	14.82			73.91			W increased
M	1942	8.81			2009	11.9						
N	1975	6.35			2008	8.2			77.41			W increased
O	1975	6.55	1.41	9.21	2009	13.6	2.15	29.24	48.15	65.38	31.5	W, D increased
P	1868	13.3	1.6	13.97	2009	16,00	2.3	24.15	83.15	69.57	57.85	W, D increased
Q	1936	14.42	4.84	43.69	2009	19,00	6.8	80.92	75.88	71.16	54.00	W, D increased
R	1936	0	0	0	2009	11.6	3.8	29.07		0	0	W, D increased
R	1975	5,00	1.73	5.7	2008	11.6	3.8	29.07	43.12	45.47	19.61	W, D increased
S	1936	0	0	0	2009	12.5			0	0	0	W, D increased
S	1994	10.27			2009	12.5			82.17			W increased

TW : top width, *D* : depth, *CSA* : cross-section area. Historical bottom width not shown (n = 1). Cross-sections A-S: nearby cross-sections on a gully section where the change in cross-sectional properties for a specific period was averaged over the different measurements.

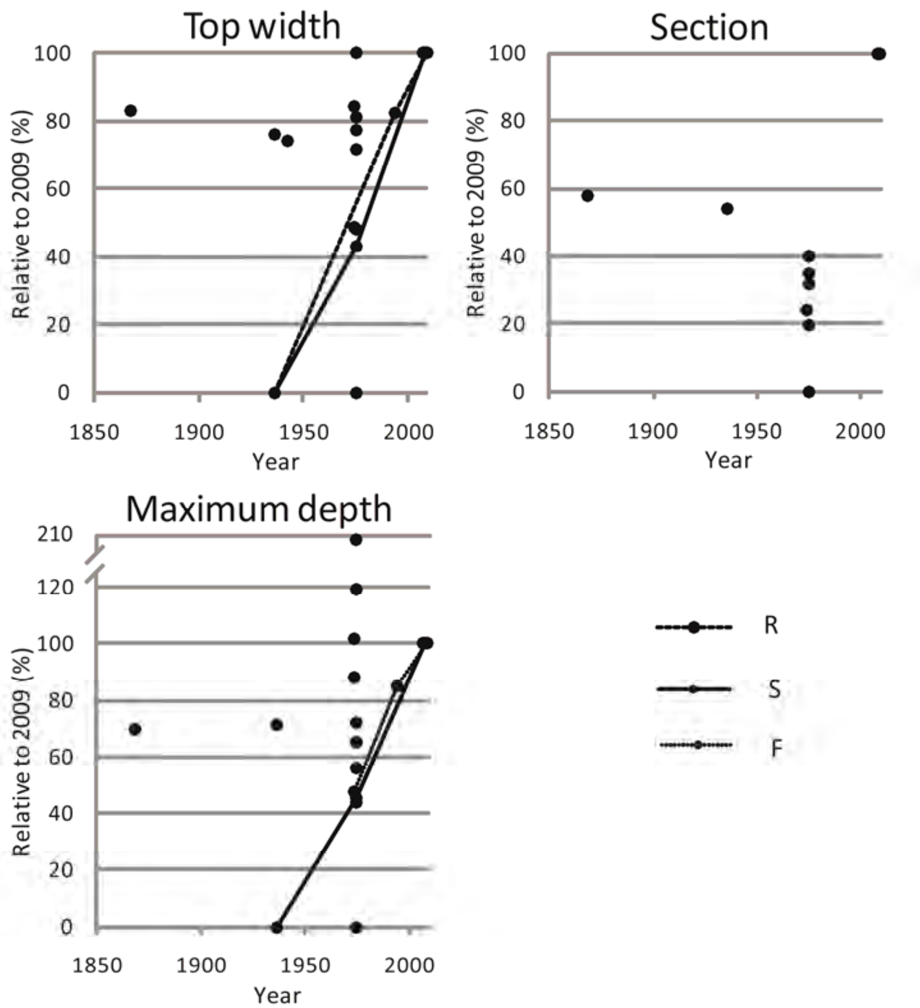

Figure 2.3 Historical cross-sectional top width, maximum depth and cross-sectional area shown relative to the 2009 situation (100%). Lines indicate the change of cross-sectional properties that could be quantified three times over the studied period (see **Table 2.2**).

Figure 2.4 While river width strongly increased, maximum depth equally decreased. A stabilization level in the left river bank (arrow) that is well displayed on the historical photograph was almost completely buried in 2009. Flooding of the adjacent land occurred during an extreme rainfall event at the end of August 2009, which caused sediment deposition on the arable land close to the river. Flood marks were recorded 0.80 m above the right river shoulder. The lady on the 1975 photograph carries a traditional Mogogo oven cover to the market. Cross-section properties: historical photograph: D = 6.13 m; repeat photograph: D = 2.93 m (Cross-section E, **Table 2.2**). Location: Agula, 13° 41’ 33’’ N, 39° 34’ 11’’ E. Note that exclosures were established on the distant steep slopes (historical photograph: Rita Ions, repeat photograph: Amaury Frankl).

The quantitative analysis indicates that gullies were already common features of the landscape in the late 19th century (e.g., **Figure 2.5**). However, significant increase in gully cross-sectional area especially occurred after 1975 (**Figure 2.3**). For six cross-sections, only a median area of 27.6% of the 2009 situation came into existence before 1974–1975. The top width of nine cross-sections reached a median of 71.4% of their 2009 size in 1974–1975 and for the maximum depth of 12 cross-sections, a median of 65.5% of the 2009 size was eroded by 1974–1975.

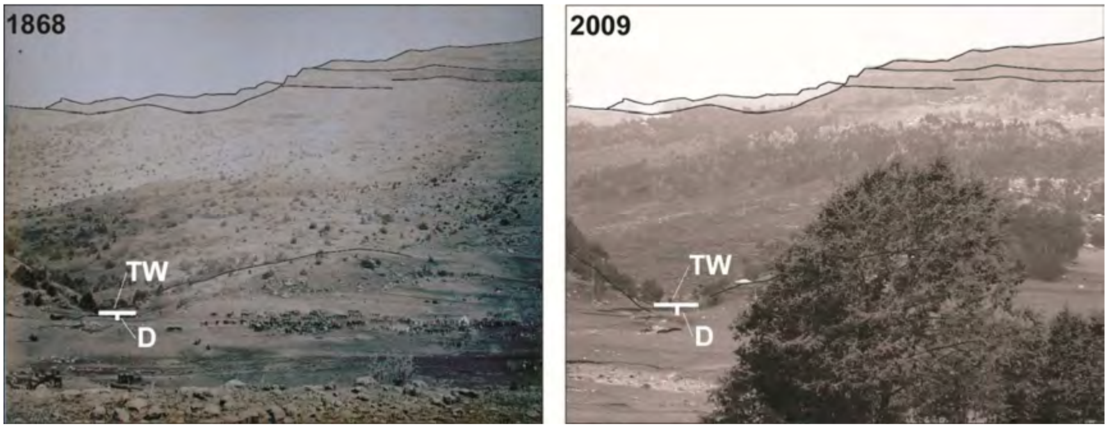

Figure 2.5 View over the valley of Seytan (Bolago village), original photograph taken by the Royal Engineers (obtained from the KingsOwn Museum, Lancaster, U.K.). Though we could not quantify it, a certain effect of tectonics should not be excluded. Markham (1868) noted about this area: “There are deep cracks round the base of Afaji, which are said to have been caused by the earthquakes in 1864, and the natives assert that these earthquakes also caused great changes in the water system of the Doba valley, some springs drying up and others appearing.”. Local etymology “Seytan” (Satan, devil) tends to confirm the occurrence of severe events. The surface morphology, and the current inhabitants, did not give any evidence of recent tectonic activity that could be related to gully development. Note the channel aggradation due to bank erosion upstream which is shown on photo-couple 45 (Thesis Appendix A). Cross-section properties: historical photograph: TW = 13.30 m, D = 1.60 m, CSA = 13.97 m²; repeat photograph: TW = 16.00 m, D = 2.30 m, CSA = 24.25 m² (Cross-section P, **Table 2.2**). (repeat photograph: Amaury Frankl)

2.3.2 Gully development around Atsela and Lake Ashenge

With regard to the catchment of Ashenge, the photographs of the period 1936–1939 (Thesis Appendix A, photo-couples 46–50) display a landscape affected by intensive agricultural exploitation and wood harvesting (**Figure 2.6**). Trees are particularly scarce and the cropland showed a similar extent to the present, covering all gentle slopes. However, there was still a dense shrub cover on the hills surrounding the valley floor, on which the steeper slopes are covered by shrubs and where soil lynchets have good vegetation growth on their risers. As in the Atsela catchment, terracing of the hills surrounding the valley floor is rare. The gully that drains the catchment is 14.42 m wide and 4.84 m deep in 1936 (Cross-sectional Q, **Table 2.2**). It appears well stabilized as seen from the abundant vegetation in its channel and the smooth walls, such that the gullies could be rehabilitated and converted into cropland (**Figure 2.6**). The lower gully end is situated at 2479 m a.s.l. and is prolonged by a small diversion channel to protect the cropland from flooding. On the historical photographs, small nucleated settlements appear on top of the hills.

The aerial photographs of 1965 show that gully activity remained limited and that their expansion was similar to the 1930s situation. Moreover, most of the present-day first order gullies were already present and their upstream extent was almost at maximum, with gully heads being close to the divides (**Figure 2.7**). The position of the lower gully end remained unchanged between the 1930s and 1965. The most important changes in network extension probably resulted from the road construction of 1936–1937 which led to the initiation of small gullies under the road outlets (where no gullies are normally expected) and the reactivation of gullies that were already present in slope depressions. In 1965, the total length of the gully network was 2515 m and the drainage density was 22.26 m ha^{-1}. Of this, only 740 m was composed of highly dynamic major or minor gullies.

Figure 2.6 Gully channel evolution in Lake Ashenge (photograph location is indicated on **Figure 2.7**). Although wood harvesting and agricultural exploitation in 1939 severely affected the environment, shrub cover on the land (white arrow) and on the surrounding hills (black arrow) of this small catchment draining to Lake Ashenge is still relatively high. The gully draining the valley is dormant and has been partially converted to cropland (zoom). By 2009, the gully had extended downstream by 294 m. It is freshly incised and remains active despite the recent soil and water conservation efforts. *Eucalyptus* trees were planted along the gully in an attempt to stop widening. As deepening of the gully continues, these efforts might be wasted as mass failures still occur in the gully bank. Original photograph (left): Maugini (Istituto Agronomico per l'Oltremare, Firenze, I). Repeat photograph: Amaury Frankl.

From the 1930s onwards, the vegetation clearance on the steep slopes progressed, extending bare land on the hillsides. Settlement density also progressively increased. In 1971–1975, the historical photographs show that the gully which drains the valley reactivated and expanded downstream by 239 m (**Figure 2.7**). In 1975, in contrast to the earlier situations, the gully was freshly incised and cut through the lower valley floor with a channel of 5.00 m wide and 1.73 m deep (Cross-section R, **Table 2.2**). At the lower gully end, there was a sediment splay.

By 1986, the network expanded further by 55 m downslope, and reached its lowest position at 2464 m a.s.l., where there was a debris cone. The total gully network expanded to a length of 2820 m and the drainage density was 24.96 m ha^{-1}. Despite expansion, changes also occurred in network configuration, when compared to the situation of 1965. The minor gully network especially changed, with gullies disappearing between 1965 and 1986 on the hillside. On the other hand, an important new network developed in the valley located mostly to the west, on the hillside (**Figure 2.7**). The total length of the minor and major gully networks being highly dynamic increased to 2163 m, and possibly longer, since 493 m of gullies that were in the shadow of the hill were not visible.

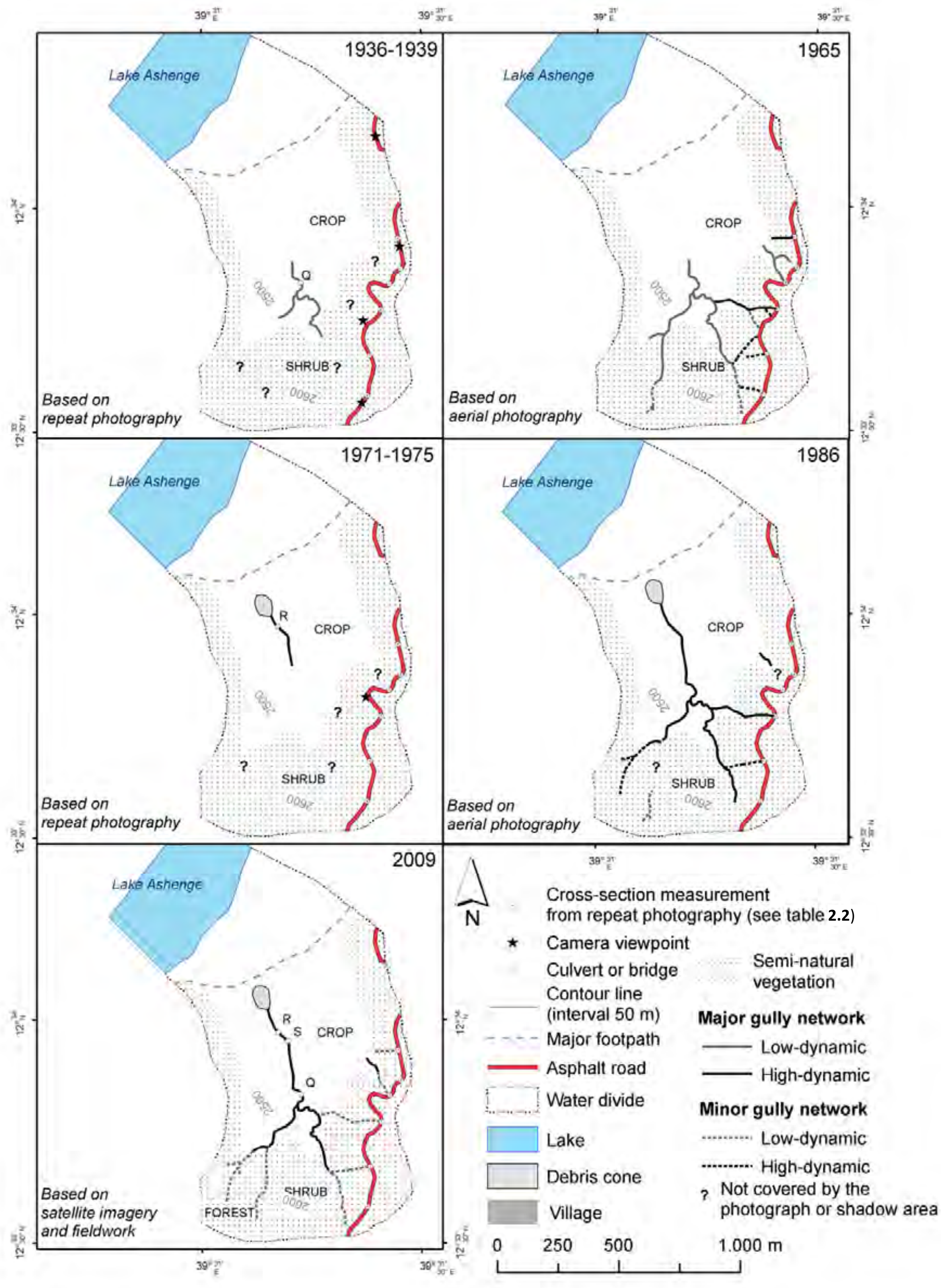

Figure 2.7 Gully network development in the Lake Ashenge catchment site.

From the photograph of 1994, it can be deduced that the gully cutting through the valley floor is still active and widening. The gully width increased from 10.27 m to 12.50 m between 1994 and 2009 at the level of cross-section S (**Table 2.2**). The vegetation cover remained similar to the situation in 1975, but shrub cover was less dense and *Eucalyptus* trees were recorded for the first time in the catchment. Housing density further increased and iron roofs were introduced, contributing to increased surface runoff.

Starting in 2000 until 2009, terracing of the steep slopes was increased on a large scale with systematic planting of *Eucalyptus* trees (**Figure 2.6**), in a campaign to control gully erosion with better land management. Check dams were built in the gully reaches located on steep slopes and especially in the area that was protected from grazing since the collapse of the Dergue regime in 1991 and where dense forests occurred in 2009. This effort resulted in the total stabilization of the gullies. Elsewhere on the hillsides, gullies were discontinuous and showed limited activity, and can be related to runoff concentration into roadside ditch outlets higher up on the slope. The total length of the gully network was 2779 m, with 1234 m of highly dynamic gullies and a drainage density of 24.59 m ha^{-1}.

In the thick valley bottom deposit, gullying was more severe than on the hillsides that are mantled by shallow soils. Gullies therefore quickly increase in cross-sectional area when they reach the valley floor. Here, gullying remains very active, although – according to local informants – soil and water conservation measures on the hills and in the cropland seem to have reduced flooding, ever since 2000–2005. At several places, one or two terrace levels could be observed in the gully walls, thus proving the existence of three distinct incision periods (**Figure 2.8**). The top of the highest terrace, which is present only in the higher valley bottom, corresponds to the bottom of the gully between 1936 and 1965. At cross-section Q the height of this terrace measured in the field is 3.53 m. Between 1965 and 1994–1999, the highest terrace was formed, when the gully floor depressed to the top of the lower terrace. Between 1965 and 1994–1999, the incision rate was 0.12 m y^{-1} and continued at almost the same rate (0.11 m y^{-1}) after 1994–1999, i.e. when local informants date the initiation of the lower terrace. This terrace was between 1.05 m and 1.73 m high and could be observed on cross-sections 2 to 4 and 6 (**Figure 2.8**). Between 1994–1999 and 2009, the volumetric erosion rate for the 1074.50 m long gully system in the valley floor was 1.17 10^3 m^3 y^{-1}.

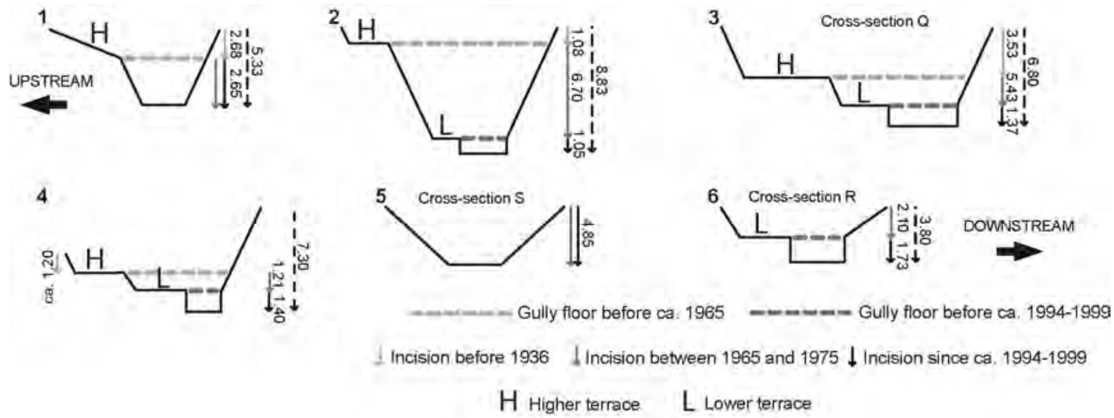

Figure 2.8 Gully cross-sections along the main gully in the valley floor deposits of Lake Ashenge catchment site marking three distinct incisive periods. See **Figure 2.6** for the location of the cross-sections Q, R and S; **Table 2.2** for the cross-sectional change. Values are in meters.

In the period 1936–1944 (Thesis Appendix A, photo-couples 37–40), it is evident that the Atsela catchment was poorly managed and bore the signs of intensive agricultural exploitation (**Figure 2.9**). The overall vegetation cover was reduced with trees being almost absent, and slopes covered only by sparse shrubs. Farmland extended beyond its 2009 area to the lower steep mountain slopes, where terracing was absent. The three gullies (A–C) that nowadays cut through the valley floor were already present in the early 20th century. However, their lower ends were located higher in the valley bottom at approximately 2490 m a.s.l. (**Figure 2.10**). As indicated by smooth gully walls and the presence of shrubs in the channel, their erosive activity was limited. This indicates that the initiation of the gullies was not related to the road construction a short time before the first photographs were taken of the catchment in 1936. Gully A on the historical photograph of **Figure 2.8** is 9.87 m wide in 1942 (Cross-section M, **Table 2.2**).

The aerial photographs from 1965 show the low dynamic character of the gullies, and it can be inferred that the location of the lower gully ends was unchanged compared to 1936–1944 (**Figure 2.10**). Small gullies cutting through the steep mountain slopes were already present close to the crestlines, but drainage density was much lower compared to more recent situations. The effect of the road in 1965 was thus limited, not affecting the main gully draining the catchment but only initiating small gullies starting under the road ditch outlets, in locations where no gullies are expected. In 1965, the total length of the network was 10 396 m, from which 2876 m were highly dynamic major or minor gullies. The drainage density was 25.32 m ha^{-1}.

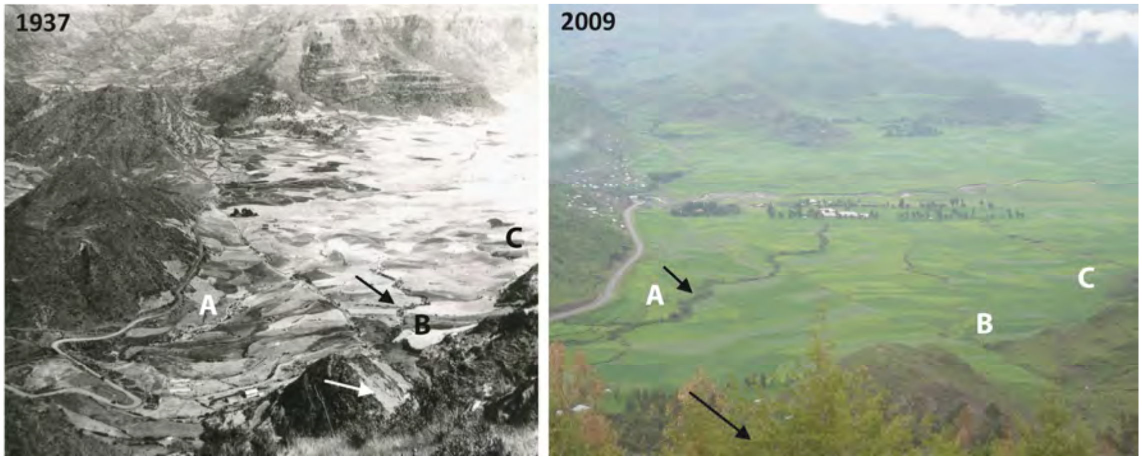

Figure 2.9 Gully channel evolution in Atsela (photograph location is indicated on **Figure 2.10**). In 1937 gullies (A–C) cutting through the upper valley bottom are stable, as indicated by their smooth transverse profiles and vegetation cover in the channel (black arrow) and some steep slopes started to be converted into cropland (white arrow). The black arrow on the 1937 photographs indicates the location of the 1975 cross-section measurement (In 2009 much more care is being given to the environment resulting in the reforestation of the steep slopes (arrow) and building of terraces. This affects the gullies that became established in the intermediate period and which are deactivating and stabilizing as a result of the building of check dams and the planting of shrubs and trees (arrow). Original photograph (left): Maugini (Istituto Agronomico per l'Oltremare, Firenze, I). Repeat photograph: Amaury Frankl.

Hereafter, the photographs of 1971–1975 show that the overuse of the landscape continued and that the erosive activity of the gullies strongly increased. The channels are re-incised and prolonged downstream by a total length of 1663 m, ending in large debris cones. Gully C connected to the main valley drainage. The gully cross-section N was 6.35 m wide in 1975 (**Table 2.2**). Terracing of the valley floor has started and *Eucalyptus* trees were introduced in the catchment. Population density also increased in the catchment, as indicated by the growth of the villages at the foot of the mountain slopes.

The aerial photographs of 1986 show that the downstream extension of the gully network continued after 1975, with both gullies A and C being connected to the main valley drainage (**Figure 2.10**). Compared to the situation in 1975, the network extended another 948 m downstream and cut through the 1975 sediment cones. More significant were the changes in the upper catchment, where gully densities strongly increased, with a network extension similar to the 2009 situation. Drainage density reached a maximum at 43.62 m ha^{-1} and the total gully length was 17 906 m.

In 1994, a similar situation as in 1986 could be observed, with gullies having a highly erosive activity. The gullies in the lower valley bottom all evolved to single channel streams, decreasing the total gully length to 17 232 m and the drainage density to 41.98 m ha^{-1}.

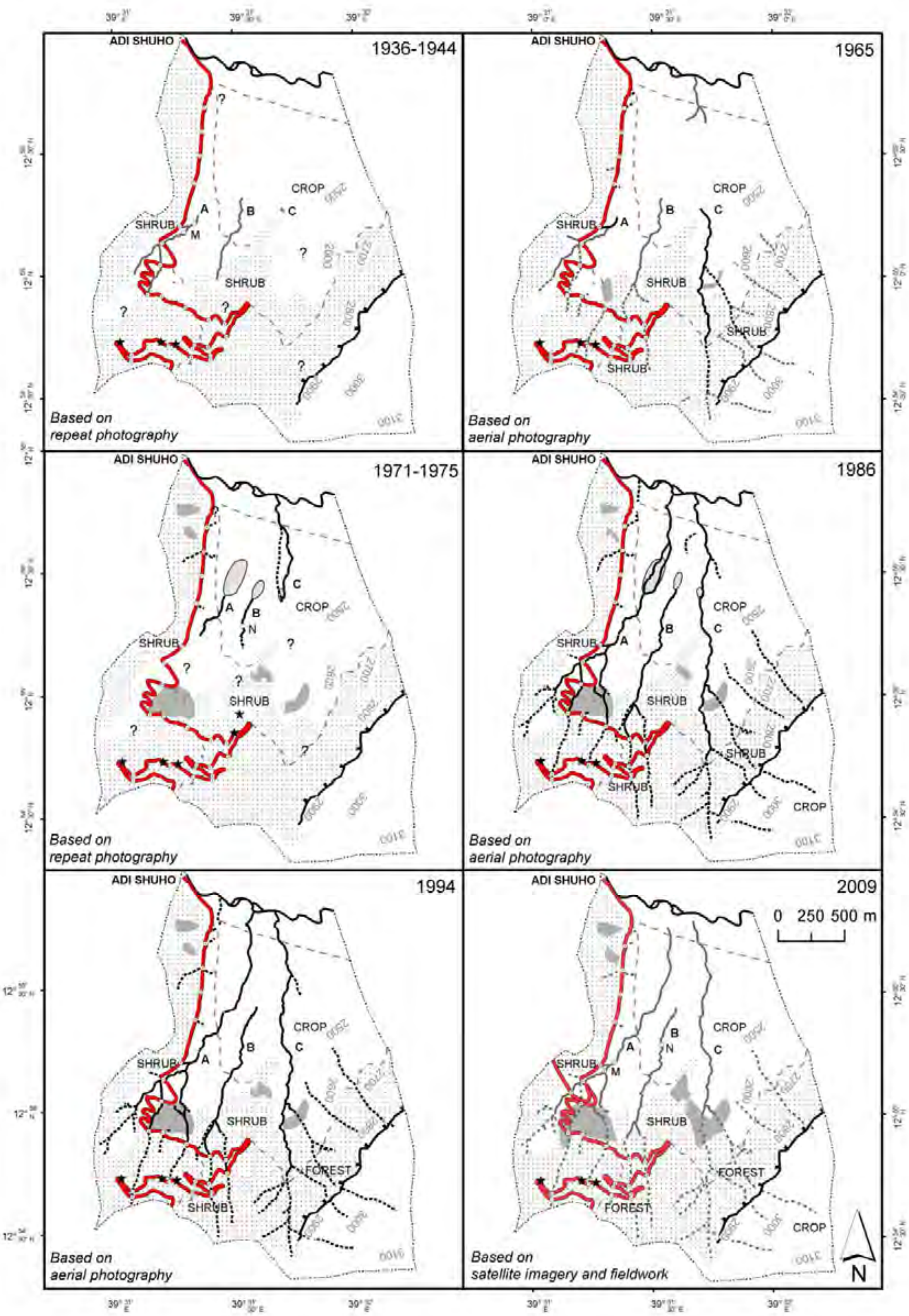

Figure 2.10 Gully network development in the Atsela catchment since the 1930s. For cross-sections M and N, see **Table 2.2**. For legend see **Figure 2.7**.

By 2008–2009, the landscape had undergone some major changes (**Figure 2.9**). Land management strongly improved, and soil and water conservation measures were widely implemented. The steep mountain slopes on which rehabilitation had been stimulated since the Dergue regime (1974–1991) developed into a dense forest, and terracing of all slopes in the catchment became frequent (and is still ongoing). *Eucalyptus* trees are now widely planted because of their diverse uses in the urban sprawls and rural settlements.

This environmental recovery has resulted in an almost complete deactivation of the gully network. On the steep mountain slopes, the gully network is reduced to discontinuous streams with smooth cross-sections, filled check dams and a high vegetation cover. The active channel width is narrower. In the valley floor, even important rainfall events do not initiate strong flash floods, as evidenced by the low-active gully system. Here, the construction of (gabion) check dams and accelerated vegetation recolonization (thanks to planting programs) strongly favor the recovery of the gullies. In some cases, the gully floor has been converted to cropland. Compared to 1994, the gully network has shrunk and is now 16 659 m long. This is caused by the upslope retreat of the lower gully ends, which are no longer connected to the main valley drainage (**Figure 2.10**). Drainage density is 40.58 m ha^{-1}.

2.4 Discussion: use of repeat photography

Repeat photography is proving to be a powerful tool, which is not yet fully exploited, for precisely assessing environmental change and channel response. It validates previous studies indicating a fast degrading environment in Northern Ethiopia (e.g., Brown, 1973; Virgo and Munro, 1978; Billi and Dramis, 2003; Nyssen et al., 2004a, 2006). In addition, this study shows that efforts in soil and water conservation are starting to pay off. As demonstrated, gullies are slowly stabilizing and, when managed well, can be converted back into agricultural land.

The major disadvantage of using repeat photography is that generally only small areas are covered by the historical photographs, so that generalizations of the observations can seldom be made. In addition, the interpretation of time series of terrestrial and aerial photographs, all picturing the landscape from different viewpoints and at different scales, can be difficult when assessing an elastic concept such as gully or river channel dynamics. Therefore, interpretations should be based primarily on repeat photographs aerial photographs exclusively. However, when large datasets of randomly distributed historical photographs are available, repeat photography can capture the full story of a region, documenting and quantifying change beyond living memory.

2.5 Conclusions

In the late 19th and early 20th centuries, gullies were common features of the Northern Ethiopian landscape. Gullies that nowadays drain small headwater catchments were already present. Low-active gullies and river channels existed, which can be derived from their smooth cross-sections and vegetation cover within the channels. A sudden change in slope stability and resulting activation of the gullies and river channels occurred soon after 1965. Historical photographs from the second half of the 20th century show gully and river sections with clear-cut walls, active head cuts, and large volumes of debris transported by the channels. A comparison of gullies and river channels on 57 historical photographs with their 2006–2009 photographs, led to the conclusion that 92.7% of the cross-sections increased in area. The quantitative analysis of 30 cross-sections revealed that important increase in cross-sectional area occurred after 1975. In 2009, gullies and river channels were becoming less active. The successful implementation of soil and water conservation measures has yielded positive results, with 23% of the gully and river sections stabilizing and displaying cross-sectional properties indicating stability.

2.6 References

Betts, H.D., Derose, R.C., 1999. Digital elevation models as a tool for monitoring and measuring gully erosion. Int. J. Applied Earth Obs. Geoinfo. G 1, 91-101.

Beyene, A., Gibbon, D., Mitiku Haile, 2006. Heterogeneity in land resources and diversity in farming practices in Tigray, Ethiopia. Agric. Syst. 88, 61-74.

Billi, P., Dramis, F., 2003. Geomorphological investigation on gully erosion in the Rift Valley and the northern highlands of Ethiopia. Catena 50, 353-368.

Brown, L.H., 1973. Conservation for Survival, Ethiopia’s Choice. Haile Sellassie I University Press, Addis Ababa.

Dervieux, A., Picon, B., 1997. Entre plaque de verre et pellicule photographique; les changements paysagers dans la vallée de l’Hérault depuis le début du siècle. Image et Sc. Soc. 5, 131-145.

Descheemaeker, K., Nyssen, J., Rossi, J., Poesen, J., Mitiku Haile, Moeyersons, J., Deckers, J., 2006. Sediment deposition and pedogenesis in exclosures in the Tigray Highlands, Ethiopia. Geoderma 132, 291-314.

Dramis, F., Umer, M., Calderoni, G. and Haile, M., 2003. Holocene climate phases from buried soils in Tigray (northern Ethiopia), comparison with lake level fluctuations in the Main Ethiopian Rift. Quat. Res. 60, 274-283.

FAO, 2009. The State of Food Insecurity in the World – Economic Crises, Impacts and Lessons Learned. FAO, Rome.

Fjellstad, W.J., Dramstad, W.E., 1999. Patterns of change in two contrasting Norwegian agricultural landscapes. Landscape Urban Plan. 45, 177-191.

Graf, W.L., 1982. Spatial variation of fluvial processes in semi-arid lands. In, Thornes, C.E. (Ed.), Space and Time in Geomorphology. Geogre Allen and Unwin, London, pp. 193-217.

Hall, F., 2001. Ground-based Photographic Monitoring. Gen. Tech. Rep. PNW-GTR-503. U.S. Department of Agriculture, Forest Service, Pacific Northwest Research Station, Portland, OR.

HTS, 1976. Tigrai Rural Development Study (TRDS). Hunting Technical Services Ltd. Government of Ethiopia and UK Ministry of Overseas Development,. Hunting Technical Services, Borehamwood.

Markham, C.R., 1868. Geographical results of the Abyssinian expedition. J. R. Soc. London 38, 12-49.

Martinez-Casasnovas, J.A., 2003. A spatial information technology approach for the mapping and quantification of gully erosion. Catena 50, 293-308.

Merla, G., Abbate, E., Azzaroli, A., Bruni, P., Canuti, P., Fazzuoli, M., Sagri, M., Tacconi, P., 1979. A geological map of Ethiopia and Somalia (1973) 1,2.000.000 and comment. University of Florence, Firenze.

Miller, S., 2004. Photogrammetric Products. In, McGlone, J.C., Mikhail E.M., Bethel, J. (Eds.), Manual of Photogammetry, Fifth Edition. ASPRS, Bethesda, MA, pp. 983-1013.

Moges, A., Holden, N.M., 2008. Estimating the rate and consequences of gully development, a case study of Umbulo catchment in southern Ethiopia. Land Degrad. Develop. 19, 574-586.

Molina, B.F., Karpilo, R.D., Pranger, H.S., 2004. Post-Little-Ice-Age landscape and glacier change in Glacier Bay National Park, documenting more than a century of variability with repeat photography. Eos Trans. AGU 85(47), Fall Meet. Suppl., Abstract C42A-03.

Muhindo Sahani, 2011. Le contexte urbain et climatique des risques hydrologiques de la ville de Butembo (Nord-Kivu/RDC). Thèse présentée en vue de l'obtention du grade de Docteur en Sciences, Université de Liège, Collège de doctorat en géographie, pp. 273.

Munro, R.N., Deckers, J., Grove, A.T., Mitiku Haile, Poesen, J., Nyssen, J., 2008. Soil and erosion features of the Central Plateau region of Tigrai - Learning from photo monitoring with 30 years interval. Catena 75, 55-64.

Munroe, J.S., 2003. Estimates of Little Ice Age climate inferred through historical rephotography, northern Uinta Mountains, USA. Art. Antart. Alpine Res. 35, 489-498.

Nachtergaele, J., Poesen, J., 1999. Assessment of soil losses by ephemeral gully erosion using high-altitude (stereo) aerial photographs. Earth Surf. Processes Landforms 24, 693-706.

NMA (National Meteorological Agency), 2010. NMA, Addis Abeba.

Nyssen, J., Poesen, J., Moeyersons, J., Deckers, J., Haile, M., Lang, A., 2004a. Human impact on the environment in the Ethiopian and Eritrean highlands - a state of the art. Earth Sci. Rev. 64, 273-320.

Nyssen, J., Veyret-Picot, M., Poesen, J., Moeyersons, J., Mitiku Haile, Deckers, J., Govers, G., 2004b. The effectiveness of loose rock check dams for gully control in Tigray, Northern Ethiopia. Soil Use Manage. 20, 55-64.

Nyssen, J., Vandenreyken, H., Poesen, J., Moeyersons, J., Deckers, J., Mitiku Haile, Salles, C., Govers, G., 2005. Rainfall erosivity and variability in the Northern Ethiopian Highlands. J. Hydrol. 311, 172-187.

Nyssen, J., Poesen, J., Veyret-Picot, M., Moeyersons, J., Mitiku Haile, Deckers, J., Dewit, J., Naudts, J., Kassa Teka and Govers, G., 2006. Assessment of gully erosion rates through interviews and measurements, a case study from Northern Ethiopia. Earth Surf. Processes Landforms 31, 167-185.

Nyssen, J., Poesen, J., Descheemaeker, K., Nigussie Haregeweyn, Mitiku Haile, Moeyersons, J., Frankl, A., Govers, G., Munro, R.N., Deckers, J., 2008a. Effects of region-wide soil and water conservation in semi-arid areas, the case of northern Ethiopia. Z. Geomorph., 52, 291 - 315.

Nyssen, J., Naudts, J., De Geyndt, K., Mitiku Haile, Poesen, J., Moeyersons, J., Deckers, J., 2008b. Soils and land use in the Tigray highlands (Northern Ethiopia). Land Degrad. Dev. 19, 257-274.

Nyssen, J., Haile, M., Naudts, J., Munro, N., Poesen, J., Moeyersons, J., Frankl, A., Deckers, J., Pankhurst, R., 2009. Desertification? Northern Ethiopia re-photographed after 140 years. Sci. Total Environ. 407, 2749-2755.

Preciso, E., Salemi, E., Billi, P., 2010. Land use changes, torrent control works and sediment mining, effects on channel morphology and sediment flux. Hydrol. Processes, in press.

Robinson, P.J., Henderson-Sellers, A., 1999. Contemporary Climatology. Pearson Education Ltd., Essex.

Roush, W., Munroe, J.S. and Fagre, D.B., 2007. Development of a spatial analysis method using ground-based repeat photography to detect changes in the alpine treeline ecotone, Glacier National Park, Montana, USA. Art. Antart. Alpine Res. 39, 297-308.

Showers K, 1996. Soil erosion in the Kingdom of Lesotho and development of Historical Environmental Impact Assessment. Ecol. Appl. 6,653–64.

Thornthwaite, C.W., 1948. An approach toward a rational classification of climate. Geogr. Rev. 38, 55-94.

Trimble, S.W., 1998. Dating fluvial processes from historical data and artifacts. Catena 31, 283-304.

Trimble, S.W., Lund, S.W., 1982. Soil conservation and the reduction of erosion and sedimentation in the Coon Creek Basin, Wisconsin, U.S. Geol. Surv. Prof. Pap., 12-34.

UNEP, 1992. World Atlas of Desertification. Edward Arnold, London.

Valentin, C., Poesen, J., Li, Y., 2005. Gully erosion, impacts, factors and control. Catena 63, 132-153.

Van de Wauw, J., Baert, G., Moeyersons, J., Nyssen, J., De Geyndt, K., Nurhussen Taha, Zenebe, A., Poesen, J., Deckers, J., 2008. Soil-landscape relationships in the basalt-dominated highlands of Tigay, Ethiopia. Catena 75, 117-127.

Vandaele, K., Poesen, J., deSilva, J.R.M., Govers, G., Desmet, P., 1997. Assessment of factors controlling ephemeral gully erosion in Southern Portugal and Central Belgium using aerial photographs. Z. Geomorph. 41, 273-287.

Virgo, K.J., Munro, R.N., 1978. Soil and erosion features of the Central Plateau region of Tigrai, Ethiopia. Geoderma 20, 131-157.

Webb, R.H., Leake, S.A., 2006. Ground-water surface-water interactions and long-term change in riverine riparian vegetation in the southwestern United States. J. of Hydr. 320, 302-323.

Webb, R.H., Boyer, D.E., 2004. Repeat photography and changes in geomorphology and vegetation in national parks of the southwestern United States. Geological Society of America, Denver Annual Meeting (November 7–10, 2004), Colorado Convention Center, Denver.

Wilkins, D.E., Ford, R.L., 2007. Nearest neighbor methods applied to dune field organization, The Coral Pink Sand Dunes, Kane County, Utah, USA. Geomorphology 83, 48-57.

Williams, G.P., 1978. The case of the shrinking channels - the North Platte and Platte Rivers in Nebraska. U.S. Geol. Surv. Prof. Pap., 1286.

Williams, M., Williams, F., 1980. Evolution of the Nile basin. In, Williams, M., Faure, H. (Eds.), The Sahara and the Nile. Quaternary Environments and Prehistoric Occupation in Northern Africa. Balkema, Rotterdam, pp. 207-224.

Wilson, R., 1977. The vegetation of central Tigre, Ethiopia, in relation to its land use. Webbia 32, 235-270

Chapter 3
Quantifying gully development patterns since 1963 from small-scale aerial photographs and high-resolution satellite images

This chapter is modified from:

Frankl, A., Poesen, J., Scholiers, N., Jacob, M., Mitiku Haile, Deckers, J., Nyssen, J., 2012. Assessment of decadal gully network and volume development in Northern Ethiopia using small-scale aerial photographs and high-resolution satellite images. Earth Surface Processes and Landforms, submitted.

Frankl, A., Zwertvaegher, A., Poesen, J., De Dapper, M., Nyssen, J., Transferring Google Earth observations to ArcGIS: an example for the study of gully erosion. International Journal of Digital Earth, submitted.

Abstract

Understanding historical and present-day gully erosion is essential when addressing the causes and consequences of land degradation. For Northern Ethiopia, several reports exist on the severity of gully erosion, yet few studies quantified gully erosion development. In this Chapter, gully network and volume development were quantified over the period 1963-2010 for an area of 123 km^2, representative for the regional variability in environmental characteristics. Gully networks were mapped from small-scale aerial photographs and high-resolution satellite images. For the latter, visualizing Google® Earth images in 3D proved to be very suitable to investigate gully erosion. As only gully length could be accurately defined from the aerial photographs and satellite images, quantifying gully volume development required to establish relations between gully network volume (V) and length (L) (or catchment area, A). Field observations indicated that the lithology and the presence/or absence of check dams or low-active channels were the most important controls of gully cross-sectional shape and size. The median cross-sectional area in shales was 36.7% larger than cross-sections in volcanics, while the median cross-sectional area of gully with check dams was 33.5% smaller than for gullies without check dams. Cross-sectional area could be fairly well predicted by their drainage area. From the network and volume development over the period 1963-2010, the occurrence of one cut-and-fill cycle is apparent. From a largely low-dynamic gully system in the 1960s, network expansion and increased erosion rates in the 1980s and 1990s caused the drainage density and volume to peak in 1994. The total gully density (D_{total}) was then 2.52 km km^{-2} and the area-specific gully volume (V_a) 59.59 10^3 m^3 km^{-2}. This coincides with soil losses of 17.6 ton ha^{-1} y^{-1} by gullying over the period 1963/1965-1994. By 2010, improved land management and the region-wide implementation of soil and water conservation measures caused 25% the gully network to stabilize, resulting in a net infilling of the gully channels over the period 1994 – 2008/2010. This study demonstrates the potential of small-scale aerial photographs and high-resolution satellite images to investigate decadal gully erosion development in a data-poor and mountainous country like Ethiopia. It illustrates that $V-L$ and $V-A$ relations can be very suitable for planners to assess gully volume, but that the establishment of such relations is necessarily region-specific. The study validates previous statements that land degradation by gullying was indeed severe in Northern Ethiopia in the second half of the 20th century, but also shows that when proper land management is applied, gullies can be transformed into a linear oasis, which increases the resistance of gullies to further erosion.

Key words Aerial photographs, Ethiopia, Google® Earth, Gully erosion, Gully morphology.

3.1 Introduction

Understanding historical and present-day gully erosion is essential when addressing the causes and consequences of land degradation (Poesen et al., 2003; Valentin et al., 2005). For instance, land managers need to foresee the impacts of land use changes, infrastructure construction or urbanization on gully erosion. Without such projections, future developments may be unsustainable and yield much higher costs than originally budgeted. In addition, soil losses may strongly increase at the expense of agricultural production (Poesen et al., 2003). Furthermore, the rapid expansion of gullies enhances shifts in the hydrological regime of landscapes (Knighton, 1998), by which runoff and soil water rapidly drains into gullies. This often results in flash floods of polluted water which threaten human health (e.g., Valentin et al., 2005). As a first step, gaining insights into the development of gully erosion requires the acquisition of data on historical and present-day gully networks and volume over sufficiently large areas.

During field surveys, time constraints and difficult terrain allow only partial or local measurements of gully morphology. Gullies may remain unobserved when visually obstructed by vegetation, and recording their dimensions can be quite challenging when gullies are large or when they expand over vast mountainous landscapes. Moreover, field observations only provide limited information on the historical importance of gully erosion. Therefore, several studies explored the potential of (time-series of) remote sensing products to facilitate research on gully erosion (e.g., Patton and Shumm, 1975; Vandaele et al., 1997; Betts and Derose, 1999; Nachtergaele and Poesen, 1999; Martinez-Casasnovas, 2003; Ionita, 2006; Parkner et al., 2006; James et al., 2007; Marzolff et al., 2011).

The ability to quantify gully networks and volumes from aerial photographs or satellite images largely depends on their spatial resolution. Considering aerial photographs, the spatial resolution is mainly determined by the scale of the photographs. Large-scale aerial photographs, with a scale exceeding 1 : 10 000, have a high spatial resolution, generally less than 0.5 m. They allow to accurately map gully networks, but, as they cover small surfaces, their acquisition and processing for large areas is very expensive. Therefore, their usefulness is limited when considering the mapping of gully networks. To compute gully volume, large-scale aerial photographs are more valuable as they allow to precisely resolve gully morphology. This is commonly done through the creation of a Digital Elevation Model (DEM; e.g., Marzolff et al., 2002; Ries and Marzolff, 2003; Martinez-

Casasnovas et al., 2009; Marzolff and Poesen, 2009). The accuracy of the quantification strongly depends on the ratio between the dimension of the gully and the resolution of the DEM (the DEM resolution ought to reflect the resolution of the photographs). Landforms should have dimensions of at least twice the DEM resolution to be defined in a grid-based DEM (Warren et al., 2004). In an empirical study, Giménez et al. (2009) concluded that, in order to keep the accuracy high, the maximum spatial resolution of aerial photographs should not exceed 15 cm. Medium- to small-scale aerial photographs (scale between 1 : 10 000 and ca. 1 : 50 000) have ground resolutions typically ranging between 0.5 and 2 m. They cover large surfaces and thus allow to map gully networks quite rapidly. The precise delineation of gullies can however be challenging, especially when the contrast with the surrounding bare surface is low or when the incision is limited. Computing gully volume from medium- to small-scale aerial photographs has also been done using DEMs (e.g., Betts and Derose, 1999; Martinez-Casasnovas, 2003; Wensheng et al., 2005; Parkner et al., 2006). Such assessments however suffer from large errors in the positional and vertical accuracy of the DEMs. Moreover, the proposed methodologies are often difficult to adapt as important (and often complex) DEM modifications are required using software that is complex and often difficult to access (e.g., Daba et al., 2003). Considering satellite images, the spatial resolution is given by the pixel size. Best resolutions are provided by sensors like IKONOS® (1 m) or GeoEye-1® (0.41 m). Accessing high-resolution images is costly, especially when stereo images for DEM extraction are required. Therefore, few studies use satellite images to quantify gully erosion (e.g., Satter et al., 2010). However, with the launch of virtual globes like Google® Earth or NASA World Wind®, the free access to high-resolution images strongly increased, allowing earth scientists to rapidly investigate the Earth's surface, and more specifically, gully networks.

Indeed, virtual globes allow 3D-visualizations or on-screen measurements that can facilitate fieldwork and its planning, and to some extent, even replace it (Smith and Pain 2009). As a result, the number of studies that use digital earth imagery to visualize, map or analyse landforms is increasing fast. For example, Google® Earth images were used to visualize and inspect dunes in Chad (Warren et al. 2007), karst phenomena in Slovenia (Podobnikar et al. 2009), and glacial landscapes in Tibet (Heyman et al. 2008). Complementing qualitative observations is frequently done by quantifying landforms on-screen, like measuring dune size in Peru (Hesse 2009), pre-landslide topography in Taiwan (Tsou et al. 2011), or treeline elevation in Ethiopia (Jacob et al. 2011). Very few studies, however, transferred their data (i.e. points, lines, polygons) into a conventional Geographic Information System (GIS) in order to allow advanced analysis of geographic features . Some even prefer to georeferrence images from Google® Earth in CAD software (Iglesias et al. 2009).

When the spatial resolution of aerial photographs or satellite images only allows to outline gully networks, calculating their volume requires understanding the determinants of gully cross-section shape. In the case of ephemeral gullies, Poesen (1992) reported that the cross-sectional width-depth ratio (determined in the field) is mainly controlled by the thickness and resistance properties of the soil horizons. Knowing the average cross-section of ephemeral gullies for a specific area, in combination with their length, allows to calculate their volume (e.g., Vandaele et al., 1997; Nachtergaele and Poesen, 1999). As ephemeral gullies do not grow subsequently but are erased by tillage (Poesen et al., 1996), the average cross-section can also be applied when using historical photographs or images to assess gully volume. In the case of permanent gullies, because of their continuous increase (or decrease) in size over time, an average cross-section does not allow to calculate historical gully volume. Therefore, several authors explored the relation between gully volume (V) and gully length (L). As a result, a number of power relations of the type $V = aL^b$ were proposed, that generally closely fit the datasets (e.g., Nachtergaele et al., 2001a; Capra et al., 2005; Zucca et al., 2006; Zhang et al., 2007; Kompani-Zare et al., 2010). Such relations reflect the fact that, when gullies increase in length, their volume increases by a power function, which is the consequence of gullies becoming deeper and wider as their catchment size increases downslope (Graf, 1988; Knighton, 1998). The coefficients a and b reflect environmental characteristics (soil, lithology, land use, climate) that determine gully cross-sectional shape. To our knowledge, most studies established $V – L$ relations for ephemeral gullies and did not consider permanent gullies. For the latter, larger values for the exponent b can however be expected as ephemeral gullies are often reported as having a more or less constant cross-sectional area (e.g., “winter gullies” in Nachtergaele et al., 2001a). In addition to $V – L$ relations, which allow to calculate gully volume from their length, our interest was also to investigate the relation between gully volume and catchment area (A), as the latter is the only parameter that can easily be derived from a topographical map.

For Ethiopia, many studies report severe historical and present-day gully erosion (e.g., Virgo and Munro, 1978; Nyssen et al., 2002; Billi and Dramis, 2003; Frankl et al., 2011), yet few studies quantified gully erosion networks or volumes over large areas. Nyssen et al. (2006) investigated the development of four gully systems in Northern Ethiopia by developing a field-method which is based on how local people remember the historical extent of gullies. Although this approach yields accurate results, it is rather difficult to apply over large areas. That is why, in Southern Ethiopia, Moges and Holden (2008) limited their analysis on the importance of historical gully erosion to eight gullies. A small gully network in Eastern Ethiopia was studied by Daba et al. (2003), using a time-series of DEMs derived from small-scale aerial photographs. Analyzing the development of gully headcuts and cross-sections at regional scale was done by Frankl et al. (2011, 2012). By using small-scale orthophotographs and repeat (terrestrial) photography, these authors could define important phases in gully erosion development.

This paper proposes a inexpensive yet comprehensive methodology to quantify gully network and volume development over large areas using field data, small-scale aerial photographs and (freely accessible) high-resolution satellite images. The specific objectives are:

(i) to demonstrate the potential of small-scale aerial photographs and high-resolution satellite images to study gully development,
(ii) to determine the controls of gully cross-sectional shape,
(iii) to establish $V – L$ *and* $V - A$ relations for gullies in the Northern Ethiopian Highlands that take the regional variability in environmental characteristics into account,
(iv) to investigate gully erosion network and volume development patterns at a regional scale since 1963 in Northern Ethiopia.

3.2 Materials and Methods

3.2.1 Study area

The study area consists of eight catchments that are located in the Northern Ethiopian Highlands and which are representative for the regional variability in environmental characteristics: Ablo (15.2 km²), May Mekdan (44.7 km²), May Ba'ati (4 km²), May Tsimble (8.1 km²), Atsela (4.9 km²), Ayba (37 km²), Seytan (8.2 km²) and Lake Ashenge (1.1 km²) (Figure 1.1). May Tsimble drains to the Rift Valley, Lake Ashenge is an endorheic or marginal graben of the Rift Valley and all other catchments drain to the Tekeze-Atbara river system. Elevations range between 2100 and 3900 m a.s.l. The deeply incised valleys developed over the past 25 million years, as a result of the rapid uplift of the Ethiopian Highlands at the western margin of the Rift Valley (Williams and Williams, 1980). Consequently, Mesozoic limestones, sandstones and Tertiary volcanics were exposed (Merla et al., 1979), and their differential resistance to erosion gave the valleys their typical stepped relief, dominated by flat-topped mountains, called *amba*. The Ablo catchment exposes sandstone; May Mekdan and May Tsimble shale with limestone cliffs and occasionally dolerite at the summits; Atsela, Ayba, Seytan and Lake Ashenge expose volcanics (flood basalt, rhyolites and consolidated volcanic ashes) and May Ba'ati exposes volcanics (= basalt) at higher elevations, while sandstone, limestone and shale occur at lower elevations.

The rainfall regime is driven by the position of the Inter Tropical Convergence Zone (Robinson and Henderson-Sellers, 1999). Its passage over the Highlands from March until

May announces the beginning of the monsoon-type rainy season, which is intense from June until September. Average annual rain increases from north to south, ranging between 500 and 900 mm y^{-1}, and usually falls as intense showers that seldom last longer than ten minutes (Nyssen et al., 2005). Rain is however highly unreliable and droughts frequently occur.

Due to active geomorphologic processes, most soils are young (HTS, 1976; Nyssen et al., 2008a). Leptosols are found in high landscape positions while Regosols or Cambisols occur on steep slopes. In footslope positions, more developed fine-textured soils occur, with Vertisols on basalt (colluvium) and Calcisols on limestone. Under remnant forests, Phaeozems occur (Descheemaeker et al., 2006).

Land degradation is severe in Northern Ethiopia (Virgo and Munro, 1978; Nyssen et al., 2004). Gullies affect nearly all slopes and frequently exceed 2 m in depth and 5 m in top width (**Figure 3.1**). Their occurrence is related to the vulnerable environment, which exposes steep slopes, where rainfall intensities are high and where deforestation and overgrazing depleted the landscape of most vegetation. As pointed by Frankl et al. (2011, 2012a), improved land management and gully rehabilitation programs are having a positive effect on the stabilization of gullies in Northern Ethiopia. Especially for headwater streams, where hillslope-channel links are strong, reforestation and soil and water conservation programs are beneficial. These measures include the terracing of slopes, the establishment of exclosures, and the construction of check dams in gullies (Nyssen et al., 2004). The implementation of the latter usually started after 1994. Vertisols remain very susceptible to gully erosion (Frankl et al., 2012).

Figure 3.1 Examples of high- and low-active gullies in different material. **A**: High-active gully incised in alluvium/colluvium (on volcanics, Ayba), **B**: Low-active gully in a Vertisol (on shale, May Mekdan), **C**: High-active gully in landslide material with large amounts of rock fragments on the gully floor (on shale, May Mekdan), **D**: Gabion check dam in a gully which led to an almost completely filled gully (on sandstone, Ablo). Photographs by Amaury Frankl and Nelles Scholiers.

3.2.2 Fieldwork and laboratory analysis

It takes about a full day's work to measure the volume of gullies in 1 km² in Northern Ethiopia. Considering that the areas of study cover 123 km² in total, we needed about 123 days to acquire data on the variability in gully cross-sections and the expansion of gully networks. This was done during subsequent campaigns in 2008, 2009 and 2010.

In total 811 cross-sections were quantified at an equal number of gully segments. This involved measuring the maximum depth (*D*, in m), top width (*TW*, in m) and bottom width (*BW*, in m), of the bankfull channels. Where the gully cross-section shape was trapezoidal or wedge-shaped $((TW + BW) / 2) * D$ gave the cross-sectional area (*CSA*, in m²). In other cases, additional measurements of the channel dimension were required. For practical reasons, measurements were conducted with a measuring tape. Errors in the calculation of *CSA* are less than 2% (which is equal to a measurement error on *TW* and *D* of 0.01 m for a gully of 1 m deep and wide, and an error of 0.1 m on a gully of 10 m deep and wide). When using the *CSA* to compute gully volume, it is however very important to carefully select the average cross-section of a gully segment, which can imply a much larger error.

Local environmental characteristics that ought to determine the dimensions of the cross-sections were recorded. These included the presence of check dams, gully activity, lithology, gully bank material, the presence of a rock fragment floor in the gully, land use/cover and local slope gradient (S_l, m m^{-1}). When check dams were present in gullies, the cross-section was measured in between two check dams, in order to record the mean gully-filling effect of the structures. Gully activity was assessed visually, by making a distinction between low- and high-active channels. This was based on the cross-sectional shape of the channel, the presence of vegetation in the channel, the occurrence of mobile bed material, bank gullying, and tension cracks or mass failure in the channel banks (Frankl et al., 2011). Considering the lithology, measurements were done in shale-, volcanic-, and sandstone-derived deposits. The effect of gully bank material on gully morphology and size was taken into account in May Mekdan, where shales occur. A distinction could be made between Vertisol, floodplain alluvium, colluvium and landslides. Originally, the effect of bank material was also targeted for gullies in volcanics of the Ayba catchment, but due to problems in the texture analysis, this could not be done. For each gully bank material type, a mixed soil sample taken from the gully wall was collected at representative sites in order to examine particle-size distribution. This was done by wet sieving using sieves with 0.063 mm, 0.5 mm and 2 mm openings and by analyzing the fraction smaller than 0.063 mm with a sedigraph (Sedigraph III®). The stoniness in the gully wall was also considered separately. As the stoniness had to be assessed visually, rough subdivisions were used: 0-20%, 20-50%, 50-80% and 80-100%. Many gullies had important deposits of coarse bedload on their floor. The effect of the presence of such a rock fragment floor was therefore analyzed. Assessing the effect of land use/cover on cross-section morphology and size was done by considering gullies that cut through rangeland and grazing land, cropland and exclosures. Cross-sections where land use/cover was different on both sides were not considered. The local slope gradient S_l of the soil surface next to the cross-section was defined between locations five meter upslope and five meter downslope the cross-section.

Gully cross-sections and headcut locations were recorded by Global Positioning System (GPS) measurements, using a Garmin GPSMap 60® with a standard deviation of 5 m. For the creation of DEMs and orthophotographs, GPS measurements of stable landscape elements, like churches, rock outcrops or road junctions were conducted using an accurate differential Trimble® GEO XH 2005 series GPS. This GPS allows a reference-rover correction and provides planimetric and altimetric accuracies at submeter level.

3.2.3 Creating time-series of aerial photographs and satellite images

A database of satellite images and digitized stereographic aerial photographs was created for all eight study areas. Aerial photographs of 1963, 1965, 1986 and 1994 having scales ranging between 1 : 35 000 and 1 : 60 000 were collected from the Ethiopian Mapping Authority. They were scanned at a resolution of 1200 dpi with a desktop scanner. IKONOS-2® satellite images (resolution of 1 m) of 2006 were available from the VLIR MU-IUC for the study areas of Ablo and May Ba’ati. For all other study areas, images were consulted on Google® Earth. This platform offers high resolution GeoEye® - 1 (resolution of 0.50 m) images of 2005, Digital Globe (resolution of 0.60 m) images of 2006, and Cnes SPOT® (resolution 2.5 m) images of 2011, and allow 3D visualization of the images.

Next, the aerial photographs and satellite images were geometrically rectified into the UTM-WGS1984 coordinate system. Considering the satellite images, a good rectification was already provided by reading the IKONOS-2® images into ArcGIS® 9.2 together with the period rational polynomial coefficient (RPC) data. In order to increase the accuracy for the areas of interest, Ground Control Points (GCPs) were used to perform a second order polynomial transformation on the images. Considering the aerial photographs, the geometric rectification was done from a photogammetric restitution or, when this yielded poor results, from a co-registration. Photogammetric restitutions were done with Supersoft® Inc VirtuoZo 2.2 and were based on a DEM devised for the same area. Producing the DEMs from the aerial photographs required inner and exterior orientation. The relative orientation was based on >300 tie points per stereo pair, and the exterior orientation on seven to fifteen GCPs. When the number of GCPs suitable for the DEM production was too low for a specific area and period; the photogammetric restitution proved to be unsuccessful. This was especially the case when considering the oldest aerial photographs that display a landscape that has undergone important changes. Within decades of fast population growth, rural settlements, infrastructure and land management structures may have changed considerably. Moreover, the low level of technological development implies that few human-build structures were stable. For instance, the position of footpaths may change over time, trees may be cut and traditional houses and fences rebuild. Therefore, the geometric rectification of some aerial photographs was done by co-registration. Second or third order polynomial transformations (with ArcGIS® 9.2) were performed, using points that were derived from the most recent orthophotographs or Google® Earth images. The advantage of such an image-to-image registration is that a large number of corresponding points can be identified on both layers, assuring a density of 2 to 9 points per km². As shown by Hughes et al. (2006) and James et al. (2012), such an approach can yield reasonable results when considering small areas and using enough control points that are located close to the features of interest.

Once all photographs and images were geometrically rectified, they were organized as layers in a Geographic Information System (GIS) environment. Switching the layers on or off allowed to easily and rapidly observe gully channel development in the study areas. As could be visually observed, some orthophotographs produced from DEMs showed relatively large lateral displacements when compared to each other. This was solved by performing a co-registration of these layers to the most recent situation. As a result, observed changes in the gully networks that were the result of mismatches between the different layers were kept minimal and are presented in the results section.

Assessing the horizontal positional accuracy of each layer was done by measuring the distance between an independent set of ten points measured by GPS in the field, and their location on the different layers. This approach allowed to quantify the true locational error that is not influenced by the type of data used, or the way in which they were geometrically rectified.

3.2.4 Quantifying gully network development patterns

Gully networks observed on the time-series of aerial photographs and satellite images were mapped on-screen using ArcGIS® 9.2 or Google® Earth, and were updated with more recent modifications as observed in the field. A distinction was made between high- and low-active channels. High-active channels have steep, well delineated walls, which make them very distinctive (**Figure 3.1**). Their detection is often accentuated by shadow cast in the gullies. Low-active channels have smooth cross-sectional profiles as a result of gully stabilization, and are often covered by vegetation (**Figure 3.1**). For the most recent situation, the stabilization of low-active channels was typically (re-)enforced by check dams. In order to accurately make the distinction between the high- and low-active channels, a stereographic analysis of the aerial photographs was often required.

Before analyzing changes in gully network development, networks mapped in Google® Earth needed to be integrated in ArcGIS® 9.2. In order to transfer the points, lines and polygon created in Google® Earth into ArcGIS®, the R-freeware was used to convert .kml-files into .shp-files. Therefore, firstly, the points, lines and polygons were saved as .kml-files from Google® Earth into a designated folder on the computer. Secondly, the R-freeware (version 2.14.0) was downloaded from http://www.r-project.org/ and installed. The *rgdal*-library was unpacked from the Packages menu. To convert the .kml-files to .shp-files, a script was applied which allows to convert all the files at once:

```
library(rgdal)
for (i in n:m)
{
a = paste("Folder location of the .kml-files",i,".kml",sep="")
```

```
b = paste(i,".kml",sep="")
import<-readOGR(a,b)
c = paste(i,sep="")
writeOGR(obj=import,dsn="Folder location for the .shp-files", driver = "ESRI Shapefile",layer=c)
}
```

By running this script for features *n* to *m*, .shp-files are written to the designated folder. The .shp-files could then be loaded into ArcGIS® 9.2 and further analysed in combination with existing datasets of gully networks derived from aerial photographs.

Subsequently, the gully network density could be calculated and analyzed for the different study areas and periods. The gully network maps for each study area and period can be found in Appendix B of the thesis, except for the maps of Lake Ashenge and Atsela which are given in Chapter 2.

A preliminary study on the controls of the drainage density was made by analyzing the effect of catchment area (A, in km²), lithology and average catchment slope gradient (S_c, in m m^{-1}) of 21 subcatchments smaller than 10 km². S_c was obtained from SRTM data (90 m resolution, available on http://srtm.csi.cgiar.org). The effects of A and S_c were analyzed with a linear regression ($\alpha = 0.05$) and the effects of lithology with Analysis of Variance (one-way ANOVA, $\alpha = 0.05$).

3.2.5 Factors controlling gully cross-sections

In order to understand the determinants of gully cross-sectional shape, a first step was to analyze the variability in gully *TW*, *BW*, *D* and *CSA*. This was done by producing boxplots and by computing minima, maxima, the interquartile range and median of the frequency distributions.

Secondly, we assessed the effect of gully and environmental characteristics that were recorded during the field survey (Section 3.2.2) on gully cross-sectional area and gully morphology. The latter was explained by using the ratio between gully top width and depth (*TW/D*) and the ratio between gully bottom width and top width (*BW/TW*). Gullies that display a large *TW-D* ratio are much wider then they are deep, and vice versa, while the *BW-TW* ratio, that ranges between 0 and 1, determines whether the gully is V or U shaped. An analysis of variance (ANOVA, $\alpha = 0.05$) was performed on the logarithm of the morphologic ratios in order to compare the distributions at different levels of the explanatory variables: check dam (and stabilized cross-sections), lithology, gully bank material, stoniness of the gully bank, rock fragment floor, land use/cover and local slope gradient. The levels of these variables are listed in Section 3.2.2 and **Table 3.2**. Performing a similar analysis for *CSA* did not necessarily mean that that levels of a variable had different distributions. Diverging means between subgroups could also be the result of sampling gullies of a different size. Therefore, obtaining meaningful results required to rescale *CSA* by dividing it with the *TW*, thus correcting for differences in sampled gully size. Normality of the distributions and variance homogeneity was tested with a Kolmogorov-Smirnov test ($\alpha = 0.05$) and a Levené test ($\alpha = 0.01$).

Finally, we investigated whether cross-sectional gully properties could be predicted on the basis of catchment characteristics. With the purpose to efficiently transfer water and sediment downslope, channel shape and size mainly adjusts to runoff properties (Knighton, 1998). As a result, channel *TW*, *D* and *CSA* will generally increase downstream. Departures from this trend are caused by variations in slope gradient, gully bank material and vegetation cover (Knighton, 1998).

In order to relate cross-sectional properties to runoff mean discharge, discharge data would be needed for a variety of small gully catchments. Such data is however not available for Northern Ethiopia. Gauging stations are only present at a limited number of large rivers with catchments that range between 121 km² and 4592 km² (Zenebe et al., 2012). For these catchments, mean seasonal discharge shows a strong positive power relation to catchment area (*A*), indicating that the biophysical setting was similar in the different catchments. Such an assumption can also be made for the basins studied here, and thus the importance of catchment area as a proxy for mean discharge was used to explain the gross variability in cross-sectional properties, without considering variations in rainfall.

3.2.6 Quantifying the evolution of gully volume

Assessing gully volume development over the period 1963-2010 required establishing relations between the present-day volume of the gully networks and their length. This was done by selecting 33 mutually exclusive catchments, with areas varying between 0.02 km² and 8.0 km². For these catchments, the length of the 2008-2010 gully network varied between 106 m and 18 366 m. Quantifying volumes was done by summing-up the mathematical products of the length of each gully section and its average cross-sectional area. $V – L$ relations were produced by taking factors that determine gully cross-sectional size into account (Section 3.2.5). The resulting $V – L$ relations were then applied on networks obtained for the period 1963-1994, and this allowed to compute the volume of historical gullies.

In addition, the relation between the volume of the gully networks and their catchment area ($V – A$) was also explored for the present-day data. As the average catchment slope gradient (S_c, in m m^{-1}) was important in explaining the variability in drainage density, the effect of S_c on the $V – A$ relation was also considered. *A* was mapped from contour lines derived from DEMs or from topographical maps, and S_c was calculated from SRTM data (available on http://srtm.csi.cgiar.org); using ArcGIS® 9.2.

3.3 Results

3.3.1 Horizontal positional accuracy of the small-scale aerial photographs and high-resolution satellite images

Assessing the horizontal positional accuracy of the rectified layers used to map gully networks was done from an independent set of GPS-recordings. Consequently, the average locational error (± standard deviation) of the different layers could be compared to each other. **Table 3.1** indicates that all the layers have a similar horizontal positional accuracy, and that this was not related to the type of rectification process. For all periods and catchments the average horizontal positional accuracy was 8.4±3.3 m. Best accuracies were given by the images displayed in Google® Earth. In some cases, observations from one layer were transposed to another. This was done for the 1963 situation of the Seytan catchment, for which only 47% of the catchment could be observed, and for the situations of Atsela 1965 and 1986, and Lake Ashenge 1986 and 1994, which were largely adapted from Frankl et al. (2011).

Table 3.1 Horizontal positional accuracy (in m) of the aerial photographs and satellite images. The average locational error ± standard deviation is based on ten independent test points that were measured in the field with a Trimble® GEO XH 2005 series GPS with submeter accuracy.

Catchment	Year					
	1963	1965	1974	1986	1994	2005-2011
Ablo					12.6±7.3 [c]	6.7±3.8 [b]
May Mekdan		8.1±3.2 [a]			5.5±3.4 [a]	
May Ba'ati	9.6±4.8 [a]		7.1±4.4 [c]		7.0±4.4 [a]	5.6±2.7 [b]
May Tsimble					16.4±10.0 [c]	12.6±8.2 [b]
Astela [d]		TRANS 1994		TRANS 1994	9.3±5.6 [a]	5.1±1.8 [b]
Ayba		7.2±3.2 [c,e]		10.4±6.1 [c]	12.9±6.6 [a,c]	5.1±1.8 [b]
Seytan	TRANS 1994 [f]			10.6±5.6 [c]		5.1±1.8 [b]
Lake Ashenge [d]		6.7±2.5 [a]		TRANS 2006	TRANS 2006	5.1±1.8 [b]

(a) Orthophotograph; (b) Satellite image; (c) Georectified aerial photograph; (d) Data largly adapted from Frankl et al. (2011); (e) 91% of the catchment could be observed; (f) 47% of the catchment could be observed.
TRANS 1994: transponed on the 1994 situation

3.3.2 Factors controlling gully cross-sectional shape

For the 811 gully cross-sections surveyed in Northern Ethiopia, the gully top width (*TW*) varied between 0.35 m and 31.90 m with a median of 6.34 m. The gully depth (*D*) varied between 0.20 m and 12.77 m with a median of 2.15 m and the bottom width (*BW*) ranged between 0.10 m and 19.50 m with a median of 3.00 m. The median cross-sectional area (*CSA*) was 10.1 m² and ranged between 0.15 m² and 236.5 m². As the boxplots suggest (**Figure 3.2A**), the distributions are right-skewed and the variability of the observations, as indicated by interquartile range, is higher for *TW* (5.20) and *BW* (2.70) than for *D* (1.79). The median *TW-D* ratio was 2.7, while the median *BW-TW* ratio was 0.5 (**Table 3.2**). Note that for *TW*/*D* and *BW*/*TW*, median and mean do not differ much as the distributions are nearly Normal. As shown in **Figure 3.2B**, plotting *D* over *TW* shows wide scatter around a linear relation purged through the origin (0, 0).

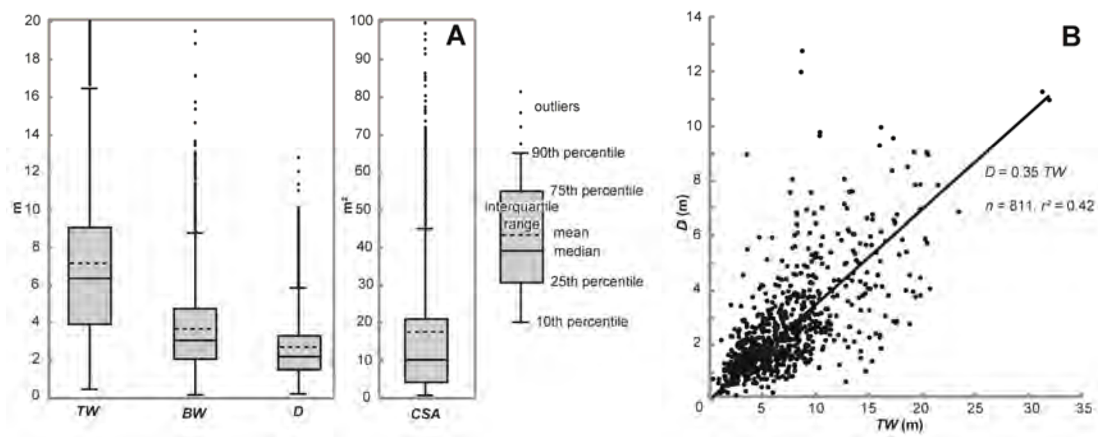

Figure 3.2 Cross-section characteristics of the studied gullies in Northern Ethiopia. **A**: Boxplots for gully top width (*TW*), bottom width (*BW*), depth (*D*) and cross-sectional area (*CSA*) for 811 sections. Outliers larger than 20 m and 100 m² are not displayed. **B**: Plotting gully depth (*D*) over gully top width (*TW*) shows a linear relation.

In the following analysis, the effect of gully and environmental characteristics that were recorded during the fieldwork (Section 3.2.2) on gully morphology (*TW-D* and *BW-TW* ratios) and on *CSA* are presented. In order to reduce the effect of extreme values in the dataset, cross-sections for which the shape was controlled by rock exposure were not considered. For instance, on cliffs edges, rock exposure causes gullies to become very wide and shallow. Omitting these observations did not affect the median of the distributions much, but did increase statistical significance.

The results that are summarized in **Table 3.2** show median values for the morphologic ratios and *CSA*. The latter were obtained by multiplying the standardized *CSA* of the different subgroups to the median *TW* (= 6.34 m) of the surveyed gullies in Northern Ethiopia, and thus corrects for differences in sampled gully magnitude between the different subgroups. The reported statistics (**Table 3.2**) apply on the logarithmic transformation of *TW*/*D*, *BW*/*TW* and standardized *CSA*.

Table 3.2 Median values for the gully top width - depth ratio (*TW*/*D*), bottom width - top width ratio (*BW*/*TW*) and cross-sectional area (*CSA*).

Explanatory variables	Levels	n	TW/D	BW/TW	CSA[1] (m²)
All data		811	2,7	0,5	10,1
Presence of (gabion) check dams or stabilized sections	Yes	336	3,7	0,6	8,4
	No	376	2,5	0,5	12,6
Lithology[2]	Shale	198	2,0	0,5	15,6
	Volcanics	94	3,2	0,6	9,9
	Sandstone	7	2,5	0,8	13,8
gully bank material[2] (case May Mekdan)	Vertisol	41	1,4	0,2	20,0
	Floodplain alluvium	42	2,1	0,4	15,0
	Colluvium	70	2,3	0,6	13,1
	Landslide	30	1,8	0,5	17,2
Stoniness of the gully bank[2]	0% - 20%	136	2,2	0,4	13,7
	20% - 50%	81	2,3	0,5	13,8
	50% - 80%	71	2,6	0,7	12,7
	80% - 100%	21	2,6	0,8	12,6
Presence of a rock fragment floor[2]	Yes	135	2,3	0,5	13,9
	No	157	2,3	0,5	13,4
Land use/cover[2]	Cropland	150	2,0	0,7	14,9
	grassland	93	2,4	0,3	13,1
	Exclosure	8	3,2	0,7	9,8
Local slope gradient (S_l)[2]	0% - 10%	112	1,8	0,4	16,6
	10% - 20%	83	2,3	0,6	13,3
	20%-30%	55	2,8	0,8	11,6

[1] Median values were obtained by multiplying the standardized *CSA* of the subgroups to the median *TW* (= 6.34 m) of the surveyed gullies in Northern Ethiopia, and thus corrects for differences in gully magnitude between the different subgroups.

[2] For cross-sections without check dams or which are stabilized

The black bars should be read vertically within blocks of explanatory variables and represent levels of a variable for which the distributions significantly differ from each other.

Measurements of cross-sections were made in 376 gullies without check dams and in 294 gullies with (gabion) check dams. In addition, 42 sections that were partly infilled and stabilized without check dams in their immediate proximity were also recorded. As observed in the field, the effect on *TW/D*, *BW/TW* and *CSA* for both gullies with check dams and stabilized gullies is very similar (one-way ANOVA test, P<0.05), so that both subgroups were considered together. From a one-way ANOVA (P<0.05), we could conclude that the median *TW-D* ratio for gullies with check dams (or stabilized sections) was 32.8% higher than for gullies without check dams and that the median *CSA* of gullies with check dams (or stabilized sections) was 33.5% smaller than for gullies without check dams. This means that the implementation of check dams resulted in the decrease in gully depth by circa one-third. No significant effect could be demonstrated for the effect of check dams and stabilized sections on the *BW-TW* ratio (one-way ANOVA, P=0.46). **Table 3.2** presents median values for *TW/D*, *BW/TW* and *CSA* for the different subgroups.

Assessing the effect of lithology and their derived deposits on *TW/D*, *BW/TW* and *CSA* was done for 322 gully sections where no check dams were present and which were not stabilized: 198 in shale, 94 in volcanics and 7 in sandstone. From a one-way ANOVA Scheffé test (P<0.05), we could conclude that the median *TW-D* ratio was 38.2% smaller in shale than in volcanics, and that the median *BW-TW* ratio was 21.8% larger for shale when compared to volcanics. The combined effect on *CSA* was that cross-sections in shale had a median that was 36.7% larger than in volcanics. This indicates that, for a given *TW*, *D* and *BW* are larger in shale when compared to volcanics. No significant effects could be observed for sandstone versus shale or volcanics.

The effect of the gully bank material on cross-sectional shape and area was analysed by investigating particle-size distribution and rock fragment content of the gully banks. In May Mekdan, where shale occur, a distinction could be made between gullies that developed in Vertisol (n = 41), floodplain alluvial deposits (n = 42), fine colluvium (n = 70) and landslides (n = 30). Sections that developed in weathered travertine or that cut through unweathered rock were not considered. Soil texture properties are given in **Table 3.3**. Finer particle-size distributions of the gully sidewalls tended to have a positive effect on *CSA* and a negative effect on *TW-D* and *BW-TW* ratios in May Mekdan (**Table 3.2**). In other words, the finer the particle-size distribution gets, the larger the cross-section tends to be, which is the result of the gully incising deeper while becoming more V-shaped. Although this general trend applies, not all subgroups showed distributions that were significantly different from each other (**Table 3.2**). When considering the cross-sectional morphology, sections incised in Vertisol had a median *TW-D* ratio that was 31.8% smaller than sections in floodplain alluvium and 39.2% smaller than sections in colluvium (one-way ANOVA Scheffé test, P<0.05). For the *BW-TW* ratio, gully segments that incised in Vertisol had a median *BW-TW* ratio that was 50% smaller than sections in floodplain alluvium, 66.5% smaller than sections in colluvium and 61.2% smaller than sections in landslides (one-way ANOVA Scheffé test, P<0.05). When considering the median *CSA*, sections that developed in Vertisol were 34.9% larger than sections which were in colluvial deposits (one-way ANOVA Scheffé test, P<0.05). An important anomaly to the trend described here-above is that sections that developed in landslides did not tend to give a smaller *CSA* or a larger *TW-D* ratio when compared sections that developed in finer material (**Table 3.2**).

Table 3.3 Gully bank material composition of the deposits studied in May Mekdan.

	Soil texture (mass %)			
	Clay	Silt	Sand	Average gully wall stoniness (volume %)
Vertisol	74	23	3	18
Floodplain alluvium	52	32	16	24
Colluvium	54	27	17	22
Landslide	60	28	12	37

When considering the stoniness of the gully banks separately for 309 cross-sections, no significant effect could be demonstrated for variations in *TW-D* ratio and *CSA* (one-way ANOVA, P = 0.22 and P = 0.68). However, when considering *BW-TW* ratio, a higher stoniness of the gully wall tends to give higher *BW-TW* ratios (**Table 3.2**). Stoniness levels 50-80% and 80-100% gave *BW-TW* ratios that where significantly higher than level 0-20%, by 40.5% and 50.72% respectively (one-way ANOVA, P<0.05).

The presence of many rock fragments armoring the gully floor did not have a significant effect on gully cross-sectional morphology or area. Results of the one-way ANOVA performed on 292 sections are P = 0.99 and P = 0.81 for *TW-D* and *BW-TW* ratios respectively, and P = 0.53 for *CSA*.

Analyzing the effect of land use/cover on 251 sections did only yield significant results for the *BW-TW* ratio. This ratio was 34.2% larger in grazing land than in cropland (one-way ANOVA, P<0.05).

The local slope gradient of the soil surface had a positive effect on both *TW-D* and *BW-TW* ratios and a negative effect on *CSA*. Gullies that developed on gentle slopes tend to have cross-sections that are deeper, more V –shaped and larger than gullies that developed on steep slopes. The median *TW-D* ratio of gullies that developed on slopes ranging between 0% and 10% was 21.1% smaller than gullies that developed on slopes ranging between 10% and 20% and 33.2% smaller than gullies that developed on slopes ranging between 20% and 30% (one-way ANOVA, P<0.05). The *BW-TW* ratio was 35.1% smaller for slopes of 0-10% when compared to slopes of 10-20%, and 31.3% smaller for slopes of 10-20% when compared to slopes of 20-30% (one-way ANOVA, P<0.05). The combined effect on the median *CSA* was that on slopes of 0-10%, the *CSA* was 24.7% larger than on slopes of 20-30% and 42.6% larger than on slopes of 20-30% (one-way ANOVA, P<0.05; **Table 3.2**).

Explaining the variability in *TW*, *D* and *CSA* on the basis of the catchment area (A, m²) was done for active gullies without check dams and without rock exposure. **Figure 3.3** shows the power relations between *TW*, *D*, *CSA* and *A* respectively. Both *TW*, *D* and *CSA* increase with increasing *A*. As the trend lines for “all data” show, this increase is more marked for *CSA* than for *TW* and *D*. The rather low r^2 values indicate that the variability on this trend is rather high, as can also be visually observed.

In addition, the effect of local slope gradient of the soil surface (S_l, m m^{-1}) and the lithology on these relationships was analyzed. In contrast to other variables, these can easily be derived from topographical and geological maps, that thus can serve as a basis to predict gully morphology and *CSA*. As can be derived from **Table 3.2**, these are also the most important factors that control gully shape and size, when no check dams are present. Before investigating the importance of S_l, the relation between *A* and S_l was analyzed. With an correlation coefficient *r* equal to 0.71 ($n = 60$; $P < 0.01$), *A* and S_l showed to be highly interrelated. This is the consequence of catchments becoming steeper and smaller when situated higher in the valley. However, in the stepped relief of the Ethiopian Highlands where a succession of structural flats and steep valley sides is displayed, gentle slopes may also occur in high topographical positions. Adding S_l to the regression analysis did not result in a significant increase in model r^2, and thus, S_l was excluded as a predictive variable.

When looking at the effect of lithology, the analysis yields similar results as those presented in the previous paragraphs (**Figure 3.3**). For a given *A*, *TW*, *D* and *CSA* were larger in deposits derived from shale than from volcanics. The effect of sandstone-derived deposits is somehow intermediate.

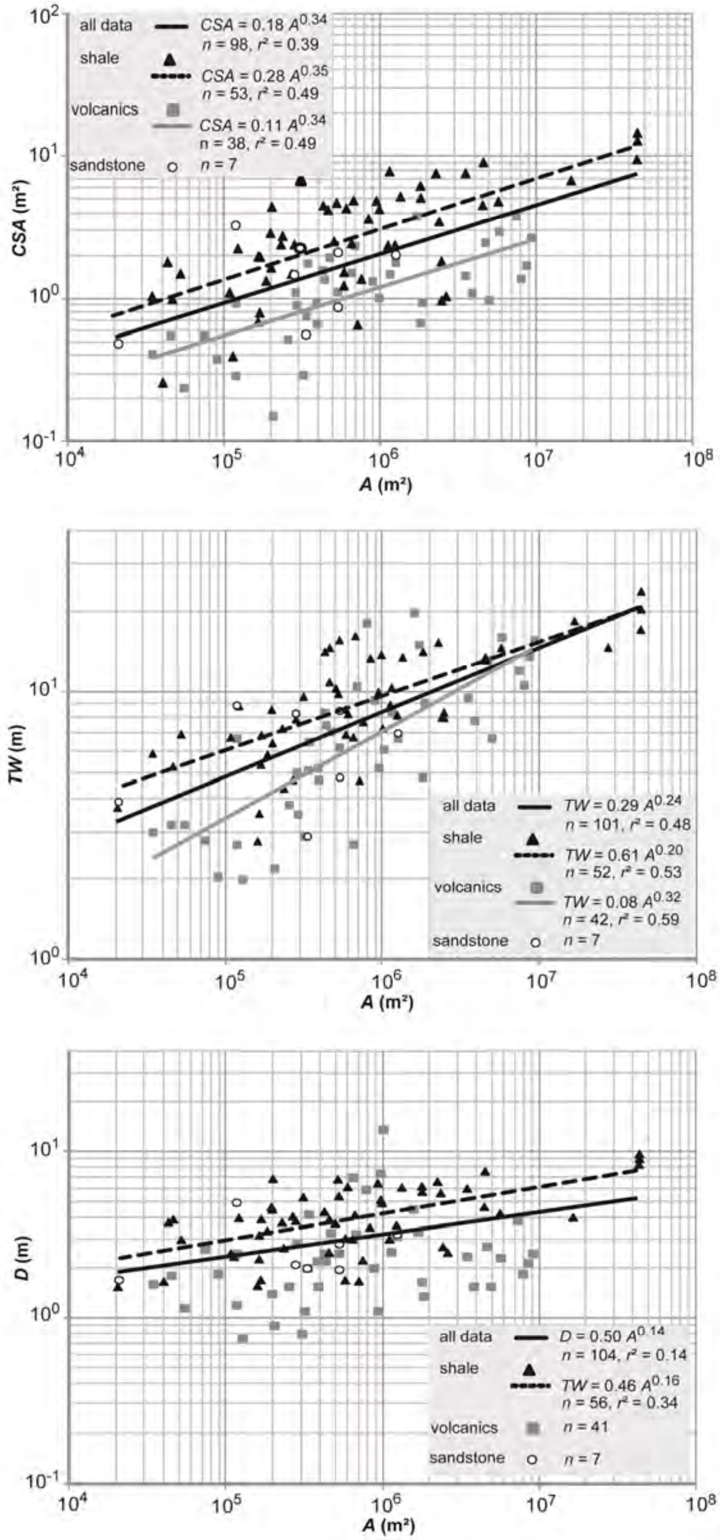

Figure 3.3 Power relation between gully top width (*TW*), depth (*D*), cross-sectional area (*CSA*, in m²) respectively, and catchment area (*A*). The effect of the lithology on these relations is also shown and trend lines are plotted when significant (*P*-value less than 0.05).

3.3.3 Gully network development since 1963

Table 3.4 presents the results of the gully network development analysis. For each catchment and period, data is given on the gully length (L, km), the length of the high-active gullies ($L_{\text{high-active}}$, km) and the length of the low-active gullies ($L_{\text{low-active}}$, km). Given the catchment area (A, km²), the drainage density of the total gully network (D_{total}, km km^{-2}) and the drainage density of the high-active gullies ($D_{\text{high-active}}$, km km^{-2}) could also be calculated. The development of D_{total} and $D_{\text{high-active}}$ through time is shown on **Figure 3.4A-C**. For the gully network maps we refer to Appendix B of the thesis, except for the maps of Lake Ashenge and Atsela which are given in Chapter 2.

In 1963-1965, D_{total} ranged between 1.20 km km^{-1} and 2.29 km km^{-2}, and was on average 1.86 km km^{-2}. From **Table 3.4** and **Figure 3.4B**, it can be observed that only a limited part of the 1963-1965 network was composed of high-active gullies, $D_{\text{high-active}}$ being on average 0.89 km km^{-2}. The bulk of the 1963-1965 network consisted of low-active gullies. For the catchment of May Ba'ati, which could be observed on 1974 aerial photographs, the situation after a decade showed that D_{total} increased from 1.20 km km^{-2} to 1.62 km km^{-2}. This increase of 35% was the result of the expansion of the gully network with high-active gullies.

In 1986, a strong increase in D_{total} could be observed for the catchments of Atsela, Ayba, Seytan and Lake Ashenge. Network expansion resulted in high D_{total} values that ranged between 2.28 km km^{-2} and 3.63 km km^{-2}, with an average of 2.48 km km^{-2}. These figures reflect closely $D_{\text{high-active}}$, as nearly all gullies could be classified as high-active. Especially for the catchment of Atsela, a strong increase in D_{total} and $D_{\text{high-active}}$ could be observed, with 72% and 523% respectively.

In 1994, the average D_{total} and $D_{\text{high-active}}$ were at their highest value, being 2.52 km km^{-2} and 2.35 km km^{-2} respectively. D_{total} and $D_{\text{high-active}}$ both ranged between 0.50 km km^{-2} and 3.35 km km^{-2}. The low minimum D_{total} and $D_{\text{high-active}}$ values were caused by observations in the Ablo catchment, which was only studied as from 1994. In **Figure 3.4B**, it can clearly be observed that for the period 1986-1994, the gully network was in a very active phase, with most of the gullies being high-active while important network extensions took place.

In 2008-2010, D_{total} decreased for most catchments, with the exception of the small catchments of May Tsimble and May Ba'ati. Values for D_{total} were however still relatively high, ranging between 0.50 km km^{-2} and 3.37 km km^{-2}, with an average of 2.20 km km^{-2} (**Table 3.4**, **Figure 3.4A**). Hence, a sharp decline could be noted for $D_{\text{high-active}}$ in most catchments. The average $D_{\text{high-active}}$ dropped to 1.65 km km^{-2}, and represented 75% of the total gully network.

From **Figure 3.4A-C**, a regional pattern in gully network development can clearly be observed. From 1963-1965 to 1986-1994, a strong increase by 32%in D_{total} occurred, which was the result of network expansions and an important increase in $D_{\text{high-active}}$ (by

164%). Hereafter, by 2008-2010, D_{total} decreased by 12%. An even more important decrease occurred for $D_{high\text{-}active}$, which dropped by 29%.

In smaller catchments, the site-specific situation led to patterns that diverged to some extent from the general picture. For example, the May Tsimble 1994 situation shows D_{total} and $D_{high\text{-}active}$ that were higher than for any other catchment. With these figures increasing by 2008-2010, the gully development pattern in May Tsimble strongly diverges from the other observations. Another remarkable trend can be observed in the Atsela catchment, which shows a very strong increase in $D_{high\text{-}active}$ from 1963-1965 to 1986, and an equally sharp decline in $D_{high\text{-}active}$ from 1994 to 2008-2010.

A preliminary analysis of the controls on D_{total} revealed that lithology and average slope gradient of the catchment (S_c, in m m^{-1}) explain a large fraction of the variability in D_{total}. As shown on **Figure 3.4C**, the overall development in D_{total} plots is higher for shale than for volcanics. The difference in D_{total} was on average 0.38 km km^{-2} for the period 1963-1965, 0.27 km km^{-2} in 1994 and 0.12 km km^{-2} for the period 2008-2010. In percentages, these departures represent respectively 18%, 9% and 5% of increased D_{total} when comparing shales to volcanics and express a slight higher vulnerability of shales compared to volcanics. Selecting 22 subcatchments smaller than ten square kilometer revealed that the distributions in D_{total} were significantly different from each other when comparing catchments that developed in shale, to catchments that developed in volcanics (One-way ANOVA, $P < 0.05$). In addition, the effect of S_c was added to the analysis. As shown in **Figure 3.4D**, equal values of D_{total} occur on slopes with much lower S_c-values when comparing shales to volcanics. Given the relative small number of observations, the linear regression lines explain relatively large fractions of the variability in D_{total} (**Figure 3.4D**). This amplifies the higher vulnerability to gully erosion of soils that developed on shales when compared to soils that developed on volcanics. The outlier “Atsela road” on **Figure 3.4D** was not considered in the linear regression as here, the road that zigzags in the upper catchments clearly had an aggravating effect on gully erosion. Catchment area did not show a significant effect on D_{total} (linear regression, $n = 22$, $P = 0.09$).

Table 3.4 Gully network and volume development for the studied catchments (in total 123 km²) over the period 1963 - 2010.

Catchment	1963 - 1965								1986							
	L	$L_{high-active}$	$L_{low-active}$	V	A	D_{total}	$D_{high-active}$	V_a	L	$L_{high-active}$	$L_{low-active}$	V	A	D_{total}	$D_{high-active}$	V_a
	(km)	(km)	(km)	(10^3 m^3)	(km^2)	(km km^{-2})	(km km^{-2})	(10^3 m^3 km^{-2})	(km)	(km)	(km)	(10^3 m^3)	(km^2)	(km km^{-2})	(km km^{-2})	(10^3 m^3 km^{-2})
Ablo																
May Mekdan	96.65	62.25	34.4	2321	44.73	2.16	1.39	51.89								
May Ba'ati	4.82	3.85	0.98	38	4,00	1.2	0.96	9.48								
May Tsimble				0												
Atsela	10.40	2.88	7.52	64	4.94	2.11	0.58	12.88	17.91	17.91	0,00	196	4.94	3.63	3.63	39.66
Ayba	49.42	8.82	40.61	452	33.8	1.46	0.26	13.36	84.52	76.63	7.89	1217	37.00	2.28	2.07	32.9
Seytan	8.43	(a)	(a)	90	3.91	2.16	(a)	22.95	22.12	22.12	0,00	306	8.27	2.68	2.68	37.03
Lake Ashenge	2.52	0.74	1.78	17	1.1	2.29	0.67	15.01	2.82	2.16 [b]	0.22 [b]	24	1.1	2.56	2.23	22.25
Total	172.23	78.53	85.27	2980	92.48	1.86	0.89	32.23	127.37	118.82	8.11	1719	51.3	2.48	2.32	33.52
Total shale	96.65	62.25	34.4	2321	44.73	2.16	1.39	51.89								
Total volcanics	70.76	12.43	49.9	622	39.84	1.78	0.31	15.6	127.37	118.82	8.11	1719	51.3	2.48	2.32	33.52
	1974															
May Ba'ati	6.49	5.46	1.04	60	4.00	1.62	1.36	15.06								

Catchment	1994								2008- 2010							
	L	$L_{high-active}$	$L_{low-active}$	V	A	D_{total}	$D_{high-active}$	V_a	L	$L_{high-active}$	$L_{low-active}$	V	A	D_{total}	$D_{high-active}$	V_a
	(km)	(km)	(km)	(10^3 m^3)	(km^2)	(km km^{-2})	(km km^{-2})	(10^3 m^3 km^{-2})	(km)	(km)	(km)	(10^3 m^3)	(km^2)	(km km^{-2})	(km km^{-2})	(10^3 m^3 km^{-2})
Ablo	7.79	7.79	0,00	89	15.52	0.5	0.5	5.76	7.84	0.74	7.1	69	15.52	0.5	0.05	4.43
May Mekdan	126.79	111.41	15.37	4209	44.73	2.83	2.49	94.09	100.63	87.81	12.82	3266	44.73	2.25	1.96	73.01
May Ba'ati	10.81	10.81	0,00	159	4,00	2.7	2.7	39.77	12.1	1.48	10.62	135	4,00	3.02	0.37	33.7
May Tsimble	29.4	29.4	0,00	971	8.14	3.35	3.35	119.26	30.41	29.32	1.09	1002	8.14	3.22	3.16	123.15
Atsela	17.23	17.23	0,00	186	4.94	3.49	3.49	37.59	16.66	0,00	16.66	120	4.94	3.37	0,00	24.4
Ayba	89.77	84.01	5.76	1270	37.00	2.43	2.27	34.33	75.25	57.95	17.3	1059	37.00	2.03	1.57	28.63
Seytan	27.7	27.7	0,00	422	8.27	3.35	3.35	51.11	26.16	26.04	0.12	385	8.27	3.16	3.15	46.59
Lake Ashenge									2.78	1.23	1.55	20	1.1	2.53	1.12	18.02
Total	309.47	288.34	21.14	7306	122.6	2.52	2.35	59.59	271.83	204.57	67.26	6056	123.7	2.2	1.65	48.96
Total shale	156.18	140.81	15.37	5179	52.87	2.95	2.66	97.96	131.05	117.13	13.91	4268	52.87	2.48	2.22	80.73
Total volcanics	134.7	128.94	5.76	1878	50.2	2.68	2.57	37.42	120.85	85.23	35.63	1585	51.3	2.36	1.66	30.89

L: Total gully length; $L_{high-active}$: Length of the high-active gullies; $L_{low-active}$: Length of the low-active gullies; V: Total gully volume; A: Catchment area; D_{total}: Drainage density of the total gully network; $D_{high-active}$: Drainage density of the high-active gullies, V_a: area-specific gully volume.

(a) Could not be calculated due to the poor quality of the aerial photographs. (b) 493 m of gullies were poorly visible due to shadow.

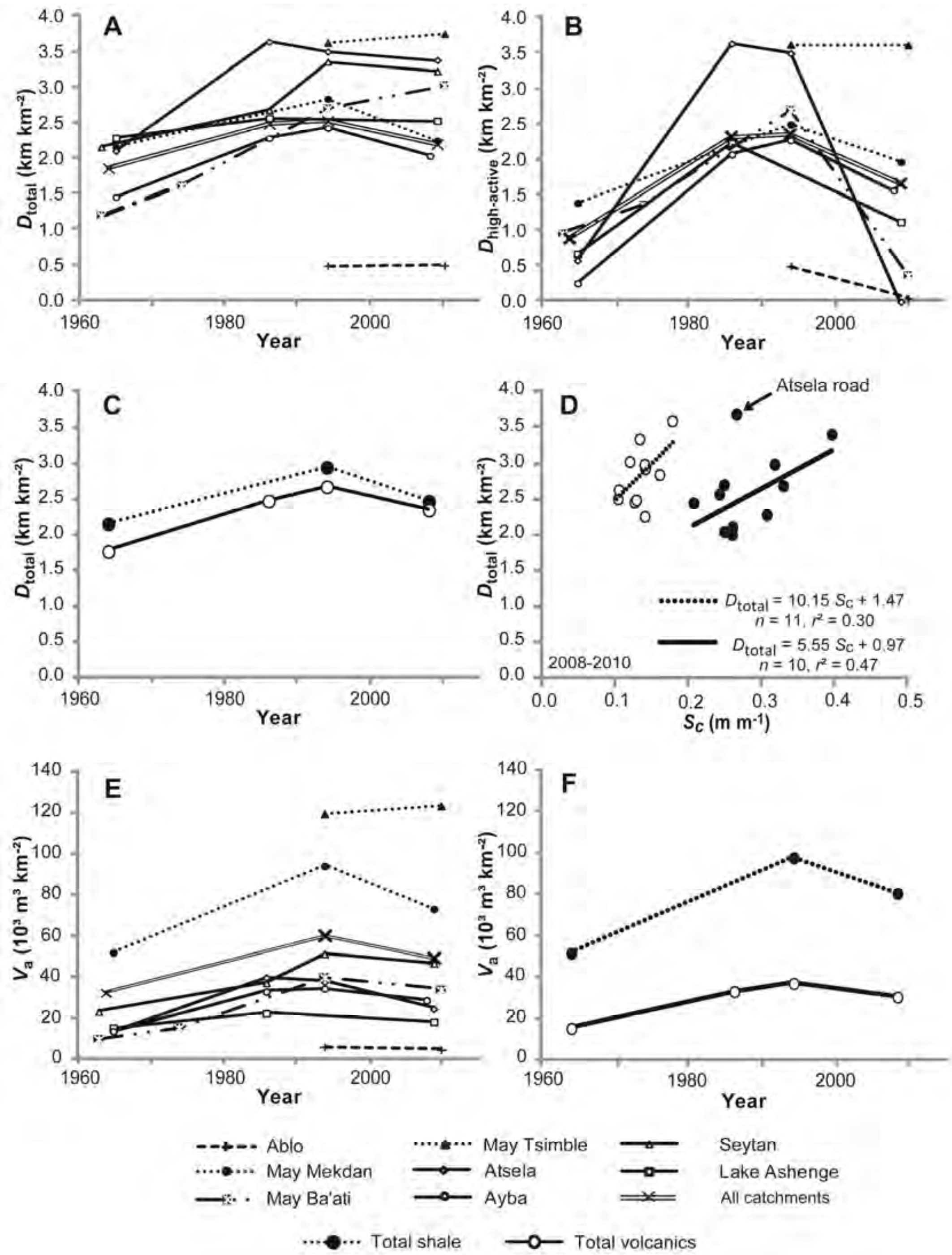

Figure 3.4 Trends in gully drainage density and area-specific gully volume for the studied catchments during the period 1963-2010. **A**: Total drainage density (D_{total}). **B**: Drainage density of the high-active gullies ($D_{high\text{-}active}$), **C**: D_{total} totals for networks that developed in deposits derived from shale and from volcanics. **D**: Relation between D_{total} and the average basin slope gradient (S_c) for 2008-2010. **E**: Area-specific volume development (V_a). **F**: V_a totals for networks that developed in deposits derived from shale and from volcanics.

3.3.4 $V-L$ and $V-A$ relations

Relating gully volumes to their length was done for the 2008-2010 situation. This relation was best described by a power equation of the form $V = aL^b$. From the different parameters that influence gully cross-sectional size, we only considered the lithology of gullied catchments and the presence of check dams in gullies (including the effect of low-dynamic sections). As shown in Section 3.3.2, these are the most important characteristics that explain the variability in *CSA*, both of which are rather easily observed in the field, or derived from topographic maps. Other parameters, like gully bank material or land use/cover, have similar distributions along gully networks, making different networks difficult to contrast in terms of $V-L$ relations. Moreover, including such parameters, which are labour intensive to map, would make $V-L$ relations difficult to apply in other areas or periods. The resulting $V-L$ equations for the different lithologies are (**Figure 3.5A)**:

$V_{\text{all data}} = 0.562\ L^{1.381}$ (n = 33, r^2 = 0.94, 34.9% of the network treated with check dams and/or low-active) (3.1)

$V_{\text{shale}} = 0.349\ L^{1.465}$ (n = 16, r^2 = 0.96, 22.2% of the network treated with check dams and/or low-active) (3.2)

$V_{\text{volcanics}} = 0.343\ L^{1.399}$ (n = 12, r^2 = 0.90, 28.9% of the network treated with check dams and/or low-active) (3.3)

$V_{\text{sandstone}} = 2.94\ L^{1.149}$ (n = 5, r^2 = 0.81, 90.1% of the network treated with check dams and/or low-active) (3.4)

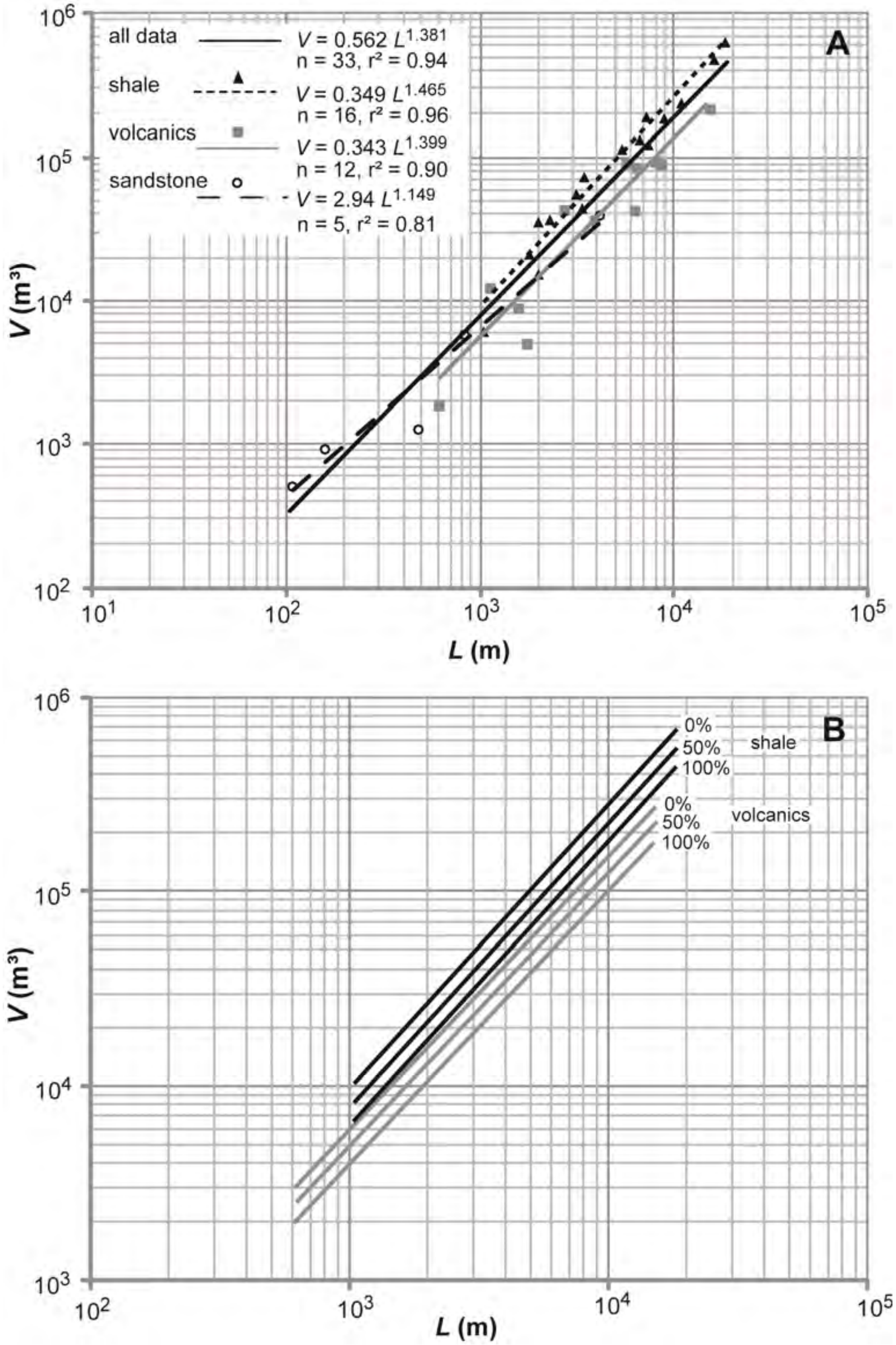

Figure 3.5 **A**: $V - L$ relations obtained for the 2008-2010 situation. **B**: Simulating the effect of 0%, 50% and 100% of the networks treated with check dams and/or low-active for networks that developed in deposits derived from shale and from volcanics.

The relations (3.1) – (3.4) are valid for the given fraction of the network which is treated with check dams and/or low-active. For example, the $V - L$ equation that applies for gully networks that developed in shale-derived deposits, is valid for 22.2% of the network treated with check dams and/or low-active. From Section 3.3.2, we know that the median *CSA* of gullies decreases on average by 33.5% when they are treated with check dams and/or are low-active. In our example, the $V - L$ equation established for shale-derived deposits thus takes an infilling of 22.2% x 33.5% = 7.4% into account. This filling is reflected in the a-coefficient of the equation. Thus, simulating the effect of 0% to 100% of the gully networks treated with check dams and/or being low-active, results in a decreasing a-coefficient (**Table 3.5**). For sandstone, simulating the effect of 0% to 100% of the networks treated with check dams and/or low-active on the a-coefficient was not done, as the dataset proposed here is limited (n = 5) and covers only a small area (= 1.62 km²) when compared to the other datasets. **Figure 3.5B** displays the resulting equations at 0%, 50% and 100%.

Table 3.5 a-coefficients related to a given percentage of the networks treated with check dams and/or low-active for catchments that developed in the lithologies shale and volcanics.

% of gully length treated with check dams or low-active	Shale $V = a L^{1.465}$ with a	Volcanics $V = a L^{1.399}$ with a
0	0.3746	0.3760
10	0.362	0.3634
20	0.3495	0.3508
30	0.3369	0.3382
40	0.3244	0.3256
50	0.3118	0.3130
60	0.2993	0.3004
70	0.2867	0.2878
80	0.2742	0.2752
90	0.2617	0.2626
100	0.2491	0.2500

As for the relation between gully network volumes and their catchment area for the 2008-2010 situation, good associations (with high r^2 values) could be established for shale and volcanics (**Figure 3.6A**). Due to the limited dataset, the $V - A$ relation for sandstone was weak and not significant. Adding S_c as an explanatory factor to these equations increased the r^2 values, especially for the networks that developed in volcanic deposits (**Figure 3.6B**). Note that the $V - A$ and $V - A$ x S_c relations for all data were not produced, as the catchments in sandstone are of a different order of magnitude and, therefore, should not be merged with those in shale and volcanics.

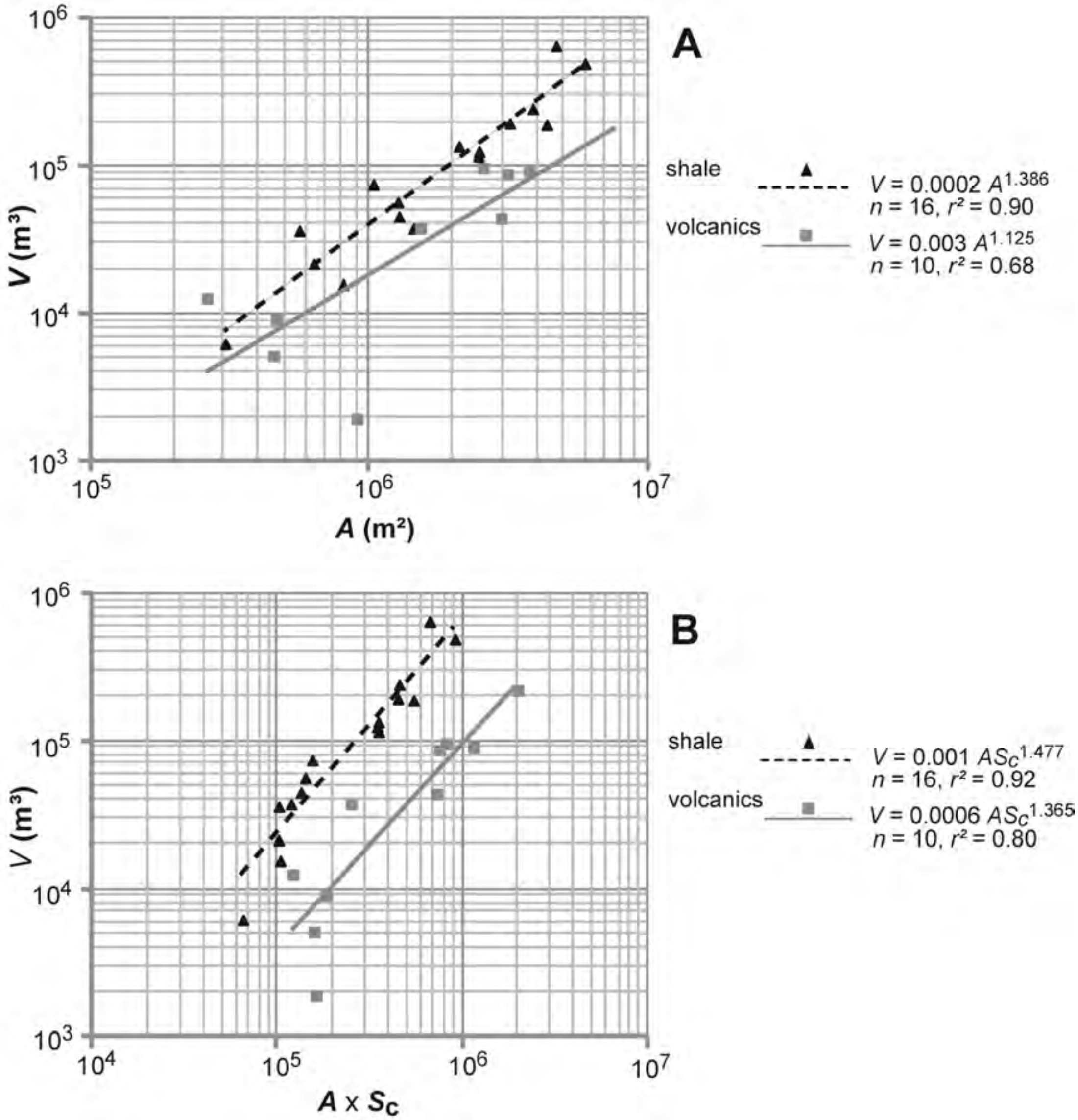

Figure 3.6 The relationship between gully volume (V), catchment area (A) and average catchment slope gradient (S_c) (A) **A**: $V – A$ and **B**: $V – A$ x S_c relations obtained for the 2008-2010 situation.

3.3.5 Evolution of gully volume

The development in gully volume is similar to the network development presented in Section 3.3.3. **Table 3.4** presents the results of the gully volume development analysis. For each catchment and period, data is given on the total gully volume (V, 10^3 m^3) and the area-specific gully volume (V_a, 10^3 m^3 km^{-2}). The development of V_a through time is given in **Figure 3.4E-F**.

In 1963-1965, V_a varied between 9.48 10^3 m^3 km^{-2} and 51.89 10^3 m^3 km^{-2}, with an average of 32.23 10^3 m^3 km^{-2}. Summed over all the study areas that could be observed in 1963-1965, the gully volume was 2980 10^3 m^3. As can be observed in **Table 3.4** and on **Figure 3.4E-F**, V_a was on average 3.3 times larger when comparing the May Mekdan catchment, that developed in shale, to the catchments that developed volcanics. For the catchment of May Ba'ati, which could be observed on 1974 aerial photographs, V_a strongly increased after a decade, from 9.48 10^3 m^3 km^{-2} to 15.06 10^3 m^3 km^{-2}.

By 1986-1994, a strong increase in V_a could be observed (**Table 3.4**, **Figure 3.4E-F**). In 1986, the average V_a doubled in the study areas that developed in volcanics, increasing from 15.60 10^3 m^3 km^{-2} to 33.52 10^3 m^3 km^{-2}, and ranging from 22.25 10^3 m^3 km^{-2} to 39.66 10^3 m^3 km^{-2}. In 1994, the average V_a for these areas further increased to 37.42 10^3 m^3 km^{-2}. Also considering the catchments of May Mekdan and May Tsimble, which developed in shale, gives an average V_a of 59.59 10^3 m^3 km^{-2}. This corresponds to a total volume of 7306 10^3 m^3, which is more than the double of the 1963-1965 volume. Values for V_a were on average 2.6 times higher in shale catchments than in volcanics catchments. The highest value for V_a was quantified in May Tsimble (= 119.26 10^3 m^3 km^{-2}). The lowest value for V_a (= 5.76 10^3 m^3 km^{-2}) was quantified in the Ablo catchment, which was only studied as from 1994. In the steep-sloped catchment of Seytan, a marked increase in V_a occurred between 1986 and 1994.

In 2008-2010, V_a decreased for all areas with the exception of May Tsimble (**Table 3.4**, **Figure 3.4E-F**). The average V_a was 48.96 10^3 m^3 km^{-2}, ranging from 4.43 to 123.15 10^3 m^3 km^{-2}. The effect of lithology still caused V_a values for catchments in shale to be on average 2.6 times larger than for catchments in volcanics. Summed for all the study areas, the gully volume was 6056 10^3 m^3, which is twice the volume of 1963-1965, and a decrease by 17% when compared to the 1994 situation.

3.4 Discussion

3.4.1 Using small-scale aerial photographs and Google® Earth

Using small-scale aerial photographs proved to be very useful for the analysis of gully network and volume development, even in a mountainous country like Ethiopia for which old aerial photographs are of poor quality and difficult to orthorectify. This study indeed confirms that, with a minimal geomorphologic background and stereographic view, gully networks can be delineated with relative ease. Assessing their volumes requires the establishment of *V – L* or *V – A* relations, based on *in situ* observations. Essential for truly understanding the dynamics of the gully system, is to make the distinction between low- and high-active gullies. It requires field experience and good practice with aerial photographs, and to a certain extent remains subjective. Historical terrestrial photographs that give partial views on the gully network in the same period as the aerial photographs can highly benefit the interpretations. For this study, such insights were provided by the repeat terrestrial photography study of Frankl et al. (2011).

High resolution satellite images complete the data series for the present. Especially the use of Google® Earth showed to be very helpful. This platform allows to map features in 3D on-the-screen with a planimetric accuracy comparable to that of a handheld GPS (e.g. Garmin GPSMap 60®, standard deviation of 5 m). With the ability to import mapped features into a GIS-environment, the potential of Google® Earth for geomorphologic studies is strongly increasing. Several studies exist that use Google® Earth, but mostly these are limited to 3D-visualizations or on-screen measurements (e.g., Warren et al. 2007; Heyman et al., 2008; Hesse, 2009; Podobnikar et al., 2009; Huaixiang and Zhaoyin, 2011; Tsou et al. 2011). Few studies explored its potential for analyzing landforms (e.g., Iglesias et al., 2009; Mc Innes et al., 2011).

3.4.2 Gully cross-sectional shape

As pointed out by Knighton (1998, p. 167), “the cross-sectional form of natural channels is characteristically irregular in outline and locally very variable”. Understanding the variability in gully morphology and size therefore mostly requires large datasets to get the general trend. This is well illustrated in **Figure 3.2B**, which displays a large scatter around the trend line when plotting gully depth (*D*) over top width (*TW*) for 811 cross-sections of permanent gullies.

Natural channels will adjust their shape and size to the hydrological regime, i.e. the quantity of water delivered to the channel and the characteristics of runoff discharge (Leopold and Maddock, 1953; Knighton, 1998; Schumm, 2005). Empirical approaches to understand the variability in *TW* and *D* along channels therefore mainly take runoff discharge (annual, peak, bankfull) into consideration. For example, in semi-arid areas, where the hydrological regime is dominated by the occurrence of flash floods, channels tend to develop wider than in humid regions (Knighton, 1998). Hence, *TW* and *D* are explained as a power function ($Y = \mathrm{a}X^{\mathrm{b}}$) of mean runoff discharge. Such relations were essentially developed for rivers, indicating that *TW* varies approximately as the square root of discharge (b-coefficient ~ 0.5; Knighton, 1998; Poesen et al., 2003). For ephemeral gullies, Nachtergaele et al. (2002) demonstrated that the equation $W = \mathrm{a}Q_{\mathrm{peak}}^{\mathrm{b}}$ has a b-coefficient of approximately 0.4.

Given the discharge properties, channel shape and size will adjust to the constraints imposed by local controls. As discussed by Knighton (1988) and Schumm (2005), these are especially the gully bank material of the channel, vegetation growing on the banks and the local slope gradient of the soil surface. Numerous studies reported by these authors indicate that the *TW-D* ratio of rivers will be larger for non-cohesive (sand) soils than for cohesive soils (silt-clay), smaller with increasing vegetation cover, and larger when the slope gradient increases. As for gullies, this study and the findings of Muñoz-Robles et al., (2010) confirm the increasing effect of local slope gradient on the *TW-D* ratio. Regarding the gully bank material, this study also confirms that particle fining causes the *TW-D* ratio to decrease. As gullies become deeper, they also tend to become more V-shaped. Despite our findings, some studies claim that the *TW-D* ratio for gullies in cohesive soils is larger than for non-cohesive soils (Radoane, 1995). The lithology has an important effect of the *TW-D* ratio, with higher ratios in shale when compared to volcanics. The effect of vegetation on the cross-sectional shape could not be demonstrated in this study. This was also not expected for the reason that the free-grazing system restricts the development of dense vegetation and because most gullies are older than the exclosures which they incise.

As mentioned before, the cross-sectional size is mainly controlled by discharge properties. Regarding the effect of lithology, channel cross-sections in shale are 37.7% larger than cross-sections in volcanics (**Table 3.2**). An important explanatory variable for this might be the occurrence of incised travertine dams in shale catchments (**Figure 3.7**). As they represent the local base-level of gully networks, their deep incision causes the gullies to degrade. The build-up of the May Mekdan travertine dam, which forms the outlet of the studied catchment, occurred at least between 7310 ± 90 y BP and 5160 ± 80 yr BP (Berakhi et al., 1998). The incision of such dams is often related to the deforestation which started some 3000 years ago (Moeyersons et al., 2008). Rainfall variability was not taken into account for the explanation of cross-section variability. However, considering that the average annual precipitation is larger in the volcanics catchments (Atsela, Seytan, Ayba and Lake Ashenge) than in the shale catchments (May Mekdan and May Tsimble) (Jacob et al., 2012), **Figure 3.3** suggests that the effect of lithology is far more important than the effect of average annual precipitation. On average, the volcanics catchment receive 200-300 mm more rain on a yearly basis. More important might be the variability in peak flow discharge, as in dryland environments, high-magnitude low-frequency flash floods accomplish most of the morphologic changes (Graf, 1988; Vanmaercke et al., 2010). This was however beyond the scope of this study.

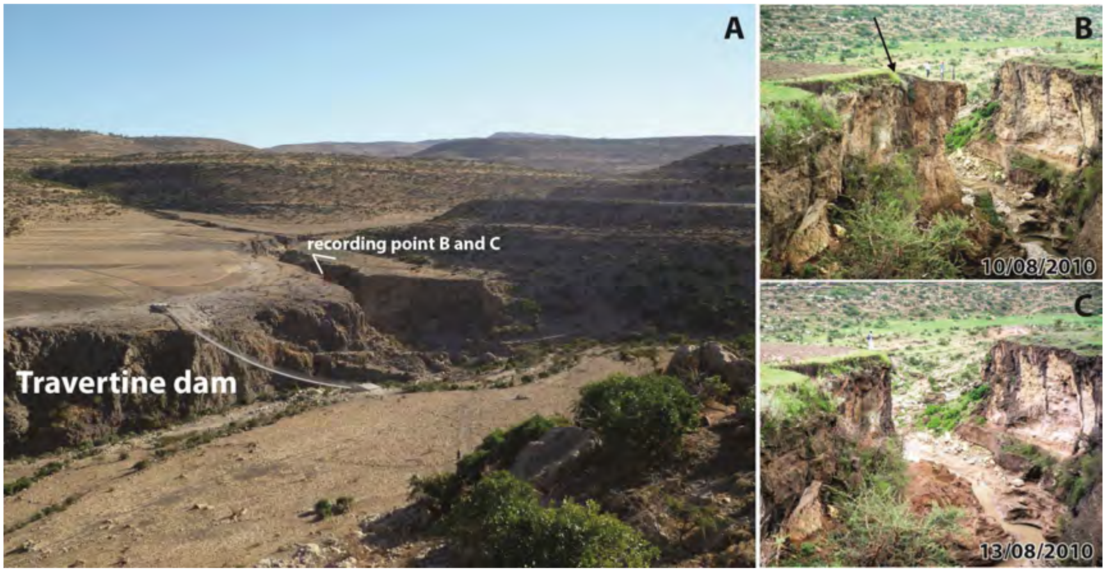

Figure 3.7 Extreme example of the effect of incised travetine dams on gully erosion. **A**: The deeply incised travertine dam near to the town of May Mekdan and gully network upslope. **B**: View from inside the gully before the occurrence of an important flash flood event on 12/08/2010 when flood marks were recorded at 3.5 m above the gully floor. The arrow indicates where cracks were visible in the land at the time when the photograph was taken. **C**: The flash flood event caused important geomorphic changes as shown here by the occurrence of a slab failure. The arrow indicates the same location as the arrow on B. Photographs by Amaury Frankl. Note that A was taken during the dry season on 28/02/2011.

In order to predict the variability in gully cross-sectional shape and size, the use of catchment area as a proxy of mean discharge was assessed in this study. This shows that indeed, channel *TW*, *D* and *CSA* are positively related to catchment area according to a power relation (**Figure 3.3**). However, the large scatter around the trend lines indicates that predicting channel shape and size at a specific location upon these equations can be in gross error.

3.4.3 *V* – *L* and *V* – *A* relations

Figure 3.8 presents the *V* – *L* relation for Northern Ethiopia (equation 3.1) as compared to other regions in the world. As can be deduced from **Table 3.6**, such relations were especially established in arid to dry sub-humid regions. For humid environments, power relations exist for winter and summer ephemeral gullies in Belgium. The r^2-values of the power equations are relatively high (**Table 3.6**). Only for the study considering the Fars Province in Southwestern Iran, the r^2 of the pooled dataset proved to be low. However, clustering gullies according to their morphology gave r^2-values up to 0.86 (Kompani-Zare et al., 2011). The high r^2-values indicate that gully length is a good predictor of gully volume. As pointed out by Nachtergaele et al. (2001b) and Capra et al. (2005), such empirical relations are more suitable to predict gully volume and simpler to apply than the Ephemeral Gully Erosion Model (Woodward, 1999). Adding the 24-h rainfall as a predictive variable to the $V - L$ equation slightly increased the model fit (r^2 from 0.64 to 0.74) in Sicily (Capra et al., 2005).

Empirical $V - L$ relations reflect the environmental setting (climate, topography, lithology, soil, vegetation) of the area they were developed for, and can thus not easily be applied to wider regions or similar areas worldwide (Graf, 1988). This is especially true when the datasets used to produce these relations are limited or when the area taken into consideration is small. In such cases, the risk exists that the sampled gullies do not reflect the regional variability in gully morphology. The study of the $V - L$ relation, which aims at being representative for the Northern Ethiopian Highlands, covers 5 380 ha and considers 151 767 m of gullies for the establishment of the $V - L$ relation. As can be read from **Table 3.6**, the size of the study areas for (a) – (i) is limited in most studies, ranging from 54 ha to 1 199 ha. Whether the gully length range is representative for the area is difficult to assess, but in general, the smaller the study area considered, the larger the risk that the empirical relation does not cover the magnitude of the gullies in the wider region. However, studies (a) – (i) mostly do consider a fairly large total gully length. Total gully length varies from 480 m up to 19 216 m.

The discussed $V - L$ relations can roughly be subdivided in two groups. The first group represents the ephemeral gullies, equations (e) to (i). As ephemeral gullies do not grow subsequently but are erased after tillage, these lines plot lower on the graph. The second group represents the permanent gullies, which increase in size after subsequent rainfall events. These are equations (a) – (c) and this study. Equation (d) includes both ephemeral and permanent gullies and is somewhat transitional.

As observed in **Table 3.6**, the b-coefficients for the different equations are very similar, ranging between 1.04 and 1.429. The larger the b-coefficient, the more important the increase in cross-sectional area becomes with increasing length, and thus, the more erodible the incised deposits are. Gullies with coefficients close to 1 will thus display relatively constant cross-sectional areas along their channel. In Zucca et al. (2006), b-coefficients close to 1 for a subgroup of gullies that developed in coarse granites was explained by the presence of bedrock at shallow depths limiting the deepening of gullies. The larger b-coefficient for summer gullies than winter gullies in Belgium was explained by the occurrence of higher rainfall intensities during summer months, thus producing stronger floods and creating larger channels (Nachtergaele et al., 2001a). As a result of the large similarity for the $V - L$ relations for summer gullies in Belgium and for gullies in Portugal and Spain, Nachtergaele (2001a) presented an equation including both datasets. Given the b-coefficient, the a-coefficient determines the height of the power relation on the Y-axis and therefore reflects the general environmental vulnerability of the area. As can be observed on **Figure 3.8**, gullies in Northern Ethiopia plot higher than those in Australia. This can be expected as the environmental setting in the Australian study area is less vulnerable than the Ethiopian context of this study. The study presented by Muñoz-Robles et al. (2010) considers an area with undulating terrain for which precipitation is uniformly distributed throughout the year with an annual mean of 441 mm y^{-1} and storms having low to moderate intensities. Considering the power relation that was developed for the Northeastern Iran, the small dataset of only six gullies with a total length of 480 m suggests that the sampling might is not be fully representative for the wider region.

Table 3.6 Overview of the characteristics of the volume – length relations ($V = aL^b$) established in different regions.

Reference on Figure 7	Area	Climate	Lithology	Gully type	Size of the study area (ha)	Total gully length (m)	*n* (gullies or gully networks)	a	b	r^2
this study	Northern Ethiopia	semi-arid / dry sub-humid	shale, volcanics, sandstone	permanent	5 380	151 767	33	0.562	1.381	0.94
a	New South Wales (Australia)	semi-arid	highly metamorphosed sandstone	permanent	1 199	19 216	16	0.43	1.36	0.81
b	Golestan Province (NE Iran)	arid / semi-arid	shale?	permanent	500	480	6	5.64	1.24	0.52
c	Fars Province (SW Iran)	arid	Quaternary sediments and marl	permanent	gullies randomly selected from 5 very large areas (ca. 5-10 10^4 ha)	2 556	146	0.9483	1.097	0.33 (-0.09 - 0.86)
d	Sardinia (Italy)	dry-sub humid	granites and metamorphic rocks	ephemeral / permanent	720	17 405	32	0.235	1.12	0.55
e	SE Spain, SE Portugal	semi-arid / humid	shist	ephemeral	54	4 461	86	0.05	1.27	0.91
f	"summer gullies" Belgium	humid	loess	ephemeral	38	3 221	26	0.1	1.16	0.74
g	NE China	semi-humid	lacustrine and fluvial sand beds and loess	ephemeral	85	9 090	21	0.015	1.429	0.67
h	"winter gullies" Belgium	humid	loess	ephemeral	197	7 885	32	0.1	1.04	0.82
i	Sicily (Italy)	Mediterranean	?	ephemeral	120	13 340	92	0.0082	1.416	0.64

References: (a) Munoz-Robles et al. (2010), (b) Soufi and Isaie (2012), (c) Kompani-Zare et al. (2011), (d) Zucca et al. (2006), (e) Nachtergaele et al. (2001b), (f) Nachtergaele et al. (2001a), (g) Zhang et al. (2007), (h) Nachtergaele et al. (2001b), (i) Capra et al. (2005).

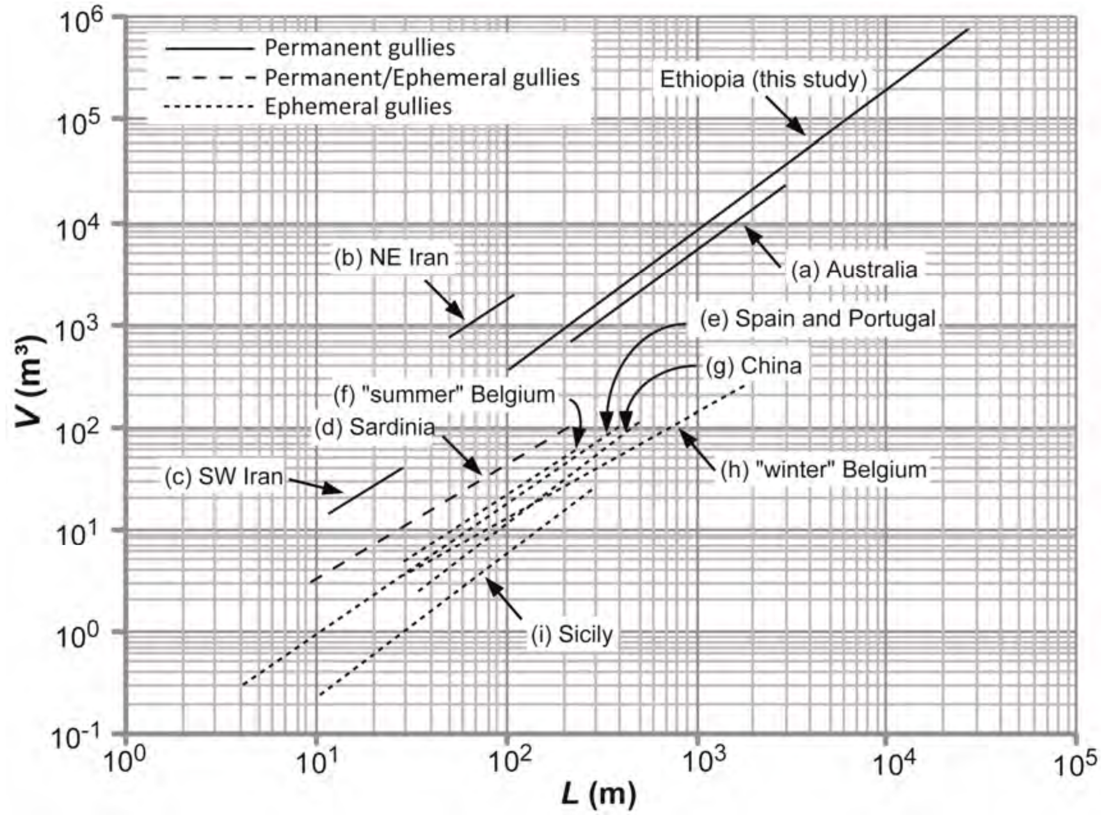

Figure 3.8 Gully Volume (V) – Length (L) relation in Northern Ethiopia as compared to elswhere in the world. For references see **Table 3.6**.

Applying $V – L$ relations to assess gully volume still requires to map gully networks in the field or to derive them from aerial photographs. For general planning purposes, collecting data on gully lengths might be too labour intensive. Therefore, the value of catchment characteristics that are easy to quantify was assessed in this study. We found that catchment area is a fairly good predictor of gully erosion volume. Including average slope gradient of the catchment yields even better results, as network density proved to increase with S_c. For gullies that developed in deposits derived from shale and volcanics, $V – A$ x S_c relations (**Figure 3.6B**) gave r^2-values of 0.92 and 0.80 respectively. The limited dataset of small gully networks in sandstone catchments did not allow to develop a satisfactory relation. A could be mapped from topographical maps and S_c could be determined from SRTM data. As is the case for the $V – L$ relations, the $V – A$ and $V – A$ x S_c relations defined here take environmental characteristics into account. Developing such relations was also done elsewhere in the world, for example, by Khosla (1953) in India ($V = 0.00323A^{0.72}$) and by Vandekerckhove et al. (2000) for bank gullies in Spain ($V = 1.75A^{0.59}$). Differences in the a- and b-coefficients of such equations are the result of higher gully densities or a higher erodibility of the deposits the gullies developed in (~ $V –$

L relation). The good association between *V* and *A* is not surprising, as many studies indicated that *A* is the major control of gully head retreat (Frankl et al., 2012; Poesen et al., 2003).

3.4.4 Gully network and volume development

The gully network and volume development patterns shown on **Figure 3.4A-C** and **E-F** indicate that the gully system is experiencing a cut-and-fill cycle over the period 1963-2010. In 1963-1965, the quite extensive gully network merely consisted of low-active gullies. By 1984-1994, with a marked increase in high-active gullies, the gully network became highly active, with the expansion of the network and the increase in gully volume as a result. At present, in 2008-2010, the proportion of high-active gullies decreased at the benefit of low-active gullies. Moreover, the gully network shrunk and the total gully volume decreased. This cut-and-fill cycle can best be observed when considering the largest catchments, i.e. those of May Mekdan (44.7 km^2) and Ayba (37 km^2) (**Figure 3.4A** and **E**).

These findings are in-line with those of Frankl et al. (2011). On the basis of repeat photography, gully development in Northern Ethiopia was explained in terms of hydrogeomorphic phases. From ca. 1868 to 1965, gullies were low-active, displaying smooth (vegetated) cross-sections. This corresponds to the large proportions of low-active gullies for the period 1963-1965 in this study. It indicates that environmental vulnerability did not yet reach a critical point for large-scale channel extension and degradation to occur. After 1965, a marked transition from low- to high-active gullies occurred, which is also apparent in this study. This is probably related to arid pulses that occurred in the 1970s and 1980s (Frankl et al., 2011). Such phases alter biomass production and increase the human pressure on land and vegetation. In order to secure food production, farmers will be forced to cultivate steeper land and grazing will deplete slopes from most vegetation. Analyses of region-wide land use and cover on the basis of Landsat imagery by de Mûelenaere et al. (2012) in the 1970s and 1980s confirmed that in 1984/1986, the surface covered by bare ground was extensive and that the surface covered by cropland peaked. From the analysis of land use and land cover on old terrestrial photographs, Meire et al. (2012) also indicate a minimum in vegetation cover in the period 1940s-1990s. Jacob et al. (2012) showed that the length of the growing period decreases with increasing drought in Northern Ethiopia, making croplands very vulnerable to high-intensive rainfall in the summer rainy season. Since ca. 2000, the large-scale implementation of soil and water conservation measures started to yield positive effects on the environmental rehabilitation and the on stabilization of gullies. Several studies indeed indicate that vegetation cover and land management strongly improved in recent decades (e.g., Gebremedhin et al., 2004; Munro et al., 2008; Alemayehu et al., 2009; Mekuria et al., 2009; Nyssen et al., 2009; de Mûelenaere et al., 2012; Meire et al., 2012). Frankl et al. (2011) indicated that in 2009, 23% of the studied gully sections were stabilizing. In this study, low-active gully segments count for 25% of the gully network, which is very close to the previous findings. The decrease in gully volume is essentially the result of the siltation behind check dams on low-active sections. Environmental rehabilitation proves to be very successful for gully stabilization in Atsela (**Figure 3.9**). In this steep-sloped catchment, the road – built by the Italians in the 1930s – that zigzags in the upper catchment causes a high runoff concentration, and strongly contributed to the peeked increase in $D_{\text{high-active}}$ from 1963-1965 to 1986 (**Figure 3.4**). The sharp decline in $D_{\text{high-active}}$ after 1994 is the result of a thorough land rehabilitation. The reforestation of steep slopes, dense soils and water conservation structures (stone bunds, trenches) and management of the gullies led to an almost total gully stabilization, where even important rainstorms, as was observed multiple times in the period 2008-2011, result in little or no runoff in the gully. The success of the gully rehabilitation in Atsela is most probably related to proximity to the small town of Adi Shuho and the threatening by gullying of the road which used to be the main thoroughfare from Addis Ababa to Mekelle (**Figure 3.9**). As a result, the deep gully was transformed into a linear oasis (black arrow and zoom, **Figure 3.9**) which can decrease landscape fragmentation and, therefore, is beneficial for ecological recovery (cf. Aerts et al., 2008). Moreover, the forestation of gullies will increase their resilience to the effects of drought or land use changes on the runoff response of the land and the occurrence of flash floods in gullies. The afforestation of gullies is rather rare in Northern Ethiopia and a similar example was studied for a gully near to the catchment of May Ba’ati (Reubens et al., 2009).

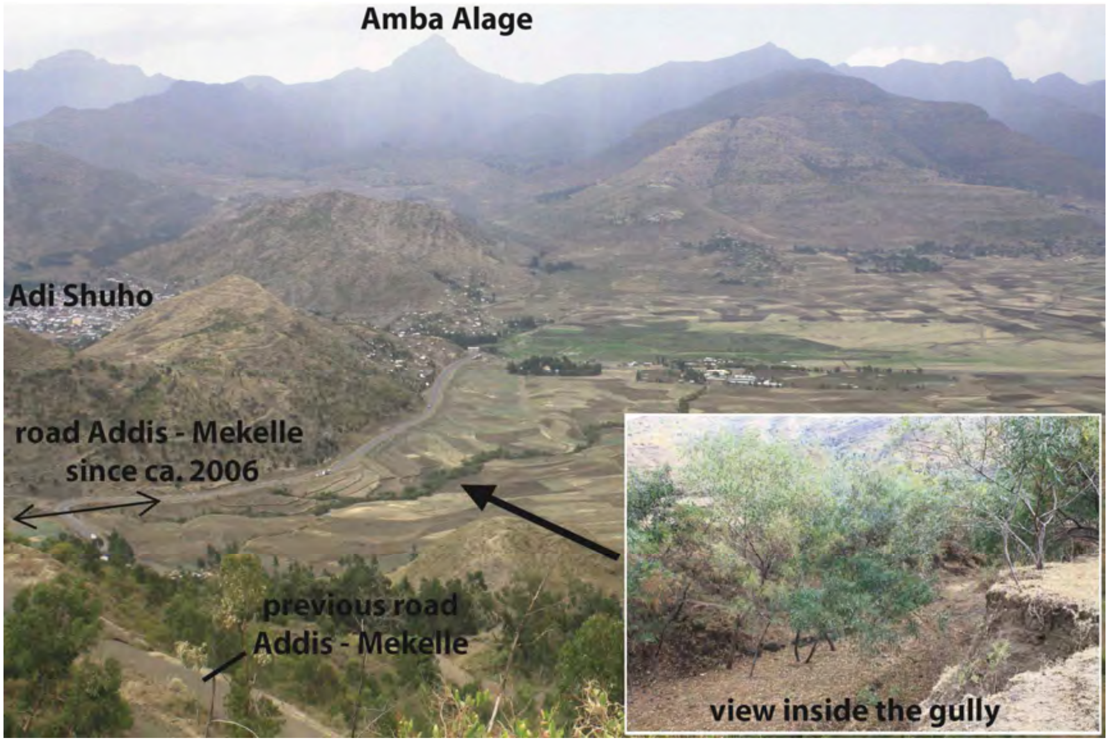

Figure 3.9 Gully rehabilitation in the catchment of Atsela. Thanks to the improved land management and the application of soil and water conservation measures, like the reforestation of the steep slope on the photograph foreground, the gully indicated by the black arrow was transformed into a green oasis in the landscape. (Photographs by Cleo De Wolf, March 2012)

Drainage densities by gully erosion are relatively high in Northern Ethiopia as compared to other regions in the world (Ionita, 2006). An important determinant of drainage density, besides the effect of catchment slope gradient, proved to be the lithology of the catchments. As can be observed on figure 4C, the total drainage density in shale catchments is higher than in catchments in volcanics. With cross-sections in shale-catchments being 36.7% larger than in catchments in volcanics, the V_a-values are on average 2.6 to 3.3 times larger when comparing catchments in shale to catchments in volcanics (**Figure 3.4F**). Such effects of lithology on the sediment export from catchments were also demonstrated for rivers (Schumm, 2005) and gullies in other regions (Zucca et al., 2006).

In order to compare our results to other reports of soil erosion by gullying in Northern Ethiopia and in other drylands, the soil loss was also expressed as soil loss by gullying (*SL*g, ton ha^{-1} y^{-1}). As no soil bulk density measurements were performed in this study, we used a standard soil bulk density of 1.5 g cm^{-3}. Average soil bulk density values for topsoils in Northern Ethiopia varied between 1.28 and 1.38 g cm^{-3} (Girmay et al., 2009).

Soil losses by gullying (*SL*g) are considerable in Northern Ethiopia. Over the period 1963/1965 – 2008/2010, the average *SLg* was 8.3 ton ha^{-1} y^{-1}. This is similar soil losses of 9.7 ton ha y by sheet and rill erosion (Nyssen et al., 2009). For shales and for volcanics, the average *SLg*-values were 12.28 ton ha^{-1} y^{-1} and 6.3 ton ha^{-1} y^{-1} respectively. Over the same period, Nyssen et al. (2006) obtained average *SLg*-values of 6.2 ton ha^{-1} y^{-1}, for several gullies near the catchment of May Ba'ati. Low *SLg*-values of 4.1 ton ha^{-1} y^{-1} were reported by Nyssen et al. (2008b) over the period 1998-2001 in a well managed catchment also near May Ba'ati. Calculating *SLg* over the period 1963/1965 - 1994, when the gully system was in a pronounced cut-phase, gave a much higher value of 17.6 ton ha^{-1} y^{-1}. Differentiating between shales and volcanics gave values of 27.0 ton ha^{-1} y^{-1} and 12.5 ton ha^{-1} y^{-1} respectively. Over the period 1994-2008/2010 a net infilling of 8.3 ton ha^{-1} y^{-1} was calculated. This of course does not imply that no active gullying occurs (headcut retreat, bank erosion, etc.), but merely indicates that soil is efficiently being trapped into gullies. Compared to *SL*g-values reported in Poesen et al. (2003), soil loss by gullying is severe in Northern Ethiopia. Gully sediment yields are locally very variable, but may be as high as 3.4 ton ha^{-1} y^{-1} in Kenya, 32 ton ha^{-1} y^{-1} in Niger, 16.1 ton ha^{-1} y^{-1} in Portugal, 64.9 ton ha^{-1} y^{-1} in Spain and 36.8 ton ha^{-1} y^{-1} in the USA (Poesen et al., 2003). Poesen et al. (2002) conclude that gully erosion contributes to 50% to 80% of the overall sediment production in dryland environments.

3.5 Conclusions

Small-scale aerial photographs of the period 1963-1994 proved to be very valuable to map and understand historical gully erosion, even for a mountainous country like Ethiopia for which old aerial photographs are of poor quality and difficult to orthorectify. With basic geomorphic background and stereographic view, gully networks could be mapped relatively easily and a distinction between low- and high-active gullies could be made. High-resolution satellite images offer similar resolutions like those of aerial photographs, and could thus be used to collect data on present-day gully erosion. At no cost and at good spatial accuracy, we mapped gully networks in Google® Earth using 3D visualization of the images. Networks defined from this platform could be imported into a conventional GIS-environment using R-freeware.

As a proxy of mean runoff discharge, catchment area of the cross-sections proved to be a fairly good predictor of channel properties. Local controls that cause gully cross-secional shape and size to vary were the presence of check dams, channel activity, lithology, local slope gradient, gully bank material, and to a lesser extent the presence of a rock fragment floor and land use/cover. Considering the effect of lithology, cross-sections in shales were 36.7% larger in than in volcanics. This is probably largely explained by the incision of travertine dams.

As the spatial resolution of the aerial photographs or satellite images only allowed to outline gullies, quantifying gully volumes required the development of volume – length (V – L) relations. These are based on *in situ* observations of gully volume and thus require fieldwork. Based on fieldwork in Northern Ethiopia, the lithology, the presence of check dams, and the channel activity proved to be the most important controls of gully cross-sectional area. Different V – L relations were thus established and allowed to quantify historical gully volume with more precision. Comparing the V – L relations established for ephemeral and for permanent gullies in different regions around the world indicated that for the latter, the increase in V with L is more pronounced. In a comparable study in Australia, the gully volume increase over length prove to be less important when compared to this study, most probably as a result of the higher environmental vulnerability of Northern Ethiopia. As an alternative to V – L relations, which still require to map gully networks, V – A and V – A x S_c relations were also established. Both catchment area (A) and catchment slope gradient (S_c) could be easily determined and proved to be good predictors of gully volume as well.

From the development of gully network and volume from 1963 to 2010, this study confirms previous findings by Frankl et al. (2011) (Chapter 2) that the gully network is experiencing a cut-and-fill phase, related to alternating environmental conditions. Although network density was relatively high (1.86 km km^{-2}) in the 1960s, 50% of the network was low-active, and the area specific gully volume (V_a) was 32.23 10^3 m^3 km^{-2}. These figures changed dramatically towards the 1980s and 1990s. The total (D_{total}) and high-active ($D_{high\text{-}active}$) network density then peaked reaching 2.52 km km^{-2} and 2.35 km km^{-2} in 1994. This coincided with a V_a of 59.59 10^3 m^3 km^{-2}. With improved land management and the region-wide implementation of soil and water conservation measures in the recent decades, the gully network density and volume decreased. D_{total} and $D_{high\text{-}active}$ declined to 2.2 km km^{-2} and 1.65 km km^{-2} respectively, and 25% of the gully network is low-active. V_a in 2008-2010 is 48.96 10^3 m^3 km^{-2}. Comparing catchments of similar size showed that the drainage density is largely controlled by catchment slope gradient and that for the same gradient, densities in shales are higher than in volcanics (= flood basalt, rhyolites and consolidated volcanic ashes).

Soil losses by gullying (*SL*g) are considerable in Northern Ethiopia. Over the period 1963/1965 – 2008/2010, *SL*g was on average 8.3 ton ha^{-1} y^{-1}. However, average *SL*g-values between shales and volcanics differ considerably. Considering the gully cut-phase from 1963/1965 - 1994 gave a much higher average *SL*g-values of 17.6 ton ha^{-1} y^{-1}. Over the period 1994-2008/2010 a net filling of 8.3 ton ha^{-1} y^{-1} was calculated.

This study shows that land degradation by gullying was indeed severe in Northern Ethiopia in the second half of the 20th century. However, the huge efforts in environmental rehabilitation undertaken in the recent decades are starting to result in gully stabilization. When proper land management is applied, gullies can even be transformed into a linear oasis (**Figure 3.9**) which will increase the resistance of gullies possible further erosion.

3.6 References

Aerts, R., Lerouge, F., November, E., Lens, L., Hermy, M. and Muys, B., 2008. Land rehabilitation and the conservation of birds in a degraded Afromontane landscape in northern Ethiopia. Biodiversity Conserv. 17, 53-69.

Alemayehu, F., Taha, N., Nyssen, J., Girma, A., Zenebe, A., Behailu, M., Deckers, S. and Poesen, J., 2009. The impacts of watershed management on land use and land cover dynamics in Eastern Tigray (Ethiopia). Resour. Conserv. Recy. 53, 192-198.

Betts, H.D., Derose, R.C., 1999. Digital elevation models as a tool for monitoring and measuring gully erosion. International Journal of Applied Earth Observation and Geoinformation 1, 91-101.

Berakhi, O., Brancaccio, L., Calderoni, G., Coltorti, M., Dramis, F., Umer, M.M., 1998. The Mai Maikden sedimentary sequence: a reference point for the environmental evolution of the Highlands of Northern Ethiopia. Geomorphology 23, 127-138.

Billi, P., Dramis, F., 2003. Geomorphological investigation on gully erosion in the Rift Valley and the northern highlands of Ethiopia. Catena 50, 353-368.

Capra, A., Mazzara, L.M., Scicolone, B., 2005. Application of the EGEM model to predict ephemeral gully erosion in Sicily, Italy. Catena 59, 133-146.

Daba, S., Rieger, W., Strauss, P., 2003. Assessment of gully erosion in eastern Ethiopia using photogammetric techniques. Catena 50, 273-291.

de Mûelenaere, S., Frankl, A., Mitiku Haile, Poesen, J., Deckers, J., Munro, N., Veraverbeke, S., Nyssen, J., 2012. Historical landscape photographs for calibration of LANDSAT land use/cover in the Northern Ethiopian Highlands. Land Degrad. Dev., Online Early View.

Descheemaeker, K., Nyssen, J., Rossi, J., Poesen, J., Mitiku Haile, Moeyersons, J., Deckers, J., 2006. Sediment deposition and pedogenesis in exclosures in the Tigray Highlands, Ethiopia. Geoderma 132, 291-314.

Frankl, A., Nyssen, J., De Dapper, M., Mitiku Haile, Billi, P., Munro, R.N., Deckers, J., Poesen, J., 2011. Linking long-term gully and river channel dynamics to environmental change using repeat photography (North Ethiopia). Geomorphology 129, 238-251.

Frankl, A., Poesen, J., Deckers, J., Mitiku Haile, Nyssen, J., 2012a. Gully head retreat rates in the semiarid Highlands of North Ethiopia. Geomorphology. in press.

Gebremedhin, B., Pender, J. and Tesfay, G., 2004. Collective action for grazing land management in crop-livestock mixed systems in the highlands of northern Ethiopia. Agr. Syst. 82, 273-290.

Gimenez, R., Marzolff, I., Campo, M.A., Seeger, M., Ries, J.B., Casali, J., Alvarez-Mozos, J., 2009. Accuracy of high-resolution photogrammetric measurements of gullies with contrasting morphology. Earth Surf. Processes Landforms 34, 1915-1926.

Girmay Gebresamuel, Singh, B.R., Nyssen, J., Borrosen, T., 2009. Runoff and sediment-associated nutrient losses under different land uses in Tigray, Northern Ethiopia. J. of Hydr. 376, 70-80.

Graf, W.L., 1988. Fluvial processes in dryland environments. The Blackburn Press.Caldwell, USA.

Hesse, R., 2009. Do swarms of migrating barchan dunes record paleoenvironmental changes? - A case study spanning the middle to late Holocene in the Pampa de Jaguay, southern Peru. Geomorphology 104, 185-190.
Heyman, J., Hattestrand, C., Stroeven, A.P., 2008. Glacial geomorphology of the Bayan Har sector of the NE Tibetan Plateau. Journal of Maps 4, 42-62.
HTS, 1976. Tigrai Rural Development Study (TRDS). Hunting Technical Services Ltd. Government of Ethiopia and UK Ministry of Overseas Development,. Hunting Technical Services, Borehamwood.
Huaixiang, L., Zhaoyin, W., 2011. The river geomorphology study by the application of Google Earth. Proceedings of the 2011 International Conference on Remote Sensing, Environment and Transportation Engineering, Nanjing, China, 24-26 June 2011, 5571-5574.
Hughes, M.L., McDowell, P.F., Marcus, W.A., 2006. Accuracy assessment of georectified aerial photographs: Implications for measuring lateral channel movement in a GIS. Geomorphology 74, 1-16.
Iglesias, G., Lopez, I., Castro, A., Carballo, R., 2009. Neural network modelling of planform geometry of headland-bay beaches. Geomorphology 103, 577-587.
Ionita, I., 2006. Gully development in the Moldavian Plateau of Romania. Catena 68, 133-140.
Jacob, M., Frankl, A., Beeckman, H., Mitiku Haile, Nyssen, J., 2011 Treeline dynamics in Afro-Alpine Ethiopia as affected by climate change and anthropo-zoogenic impacts.. Paper presented at the conference <Forests and climate change - Scientific insights and social leverages>. be-REDD-i project, Brussels, 9 November 2011. Book of Abstracts.
Jacob, M., Frankl, A., Haile, M., Nyssen, J., 2012. Cropping systems in afro-montane Northern Ethiopia as related to spatiotemporal rainfall variability. In preparation.
James, L.A., Watson, D.G., Hansen, W.F., 2007. Using LiDAR data to map gullies and headwater streams under forest canopy: South Carolina, USA. Catena 71, 132-144.
James, L.A., Hodgson, M.E., Ghoshal, S. and Latiolais, M.M., 2012. Geomorphic change detection using historic maps and DEM differencing: The temporal dimension of geospatial analysis. Geomorphology 137, 181-198.
Knighton, D., 1998. Fluvial Forms and Processes – A New Perspective. Hodder Education: London.
Kompani-Zare, M., Soufi, M., Hamzehzarghani, H., Dehghani, M., 2011. The effect of some watershed, soil characteristics and morphometric factors on the relationship between the gully volume and length in Fars Province, Iran. Catena 86, 150-159.
Khosla, A. N., 1953. Silting of reservoirs. CPIP Publ 51, New Delhi, India.
Martinez-Casasnovas, JA., 2003. A spatial information technology approach for the mapping and quantification of gully erosion. Catena 50, 293-308.
Martinez-Casasnovas, J.A., Concepcion Ramos, M., Garcia-Hernandez, D., 2009. Effects of land-use changes in vegetation cover and sidewall erosion in a gully head of the Penedes region (northeast Spain). Earth Surf. Processes Landforms 34, 1927-1937.
Marzolff, I., Ries, J.B., Albert, K-D., 2002. Kite aerial photography for gully monitoring in sahelian landscapes, Proceedings of the Second Workshop of the EARSeL Special Interest Group on Remote Sensing for Developing Contries, Bonn, Germany, 2-13.
Marzolff, I. and Poesen, J., 2009. The potential of 3D gully monitoring with GIS using high-resolution aerial photography and a digital photogrammetry system. Geomorphology 111, 48-60.
Marzolff, I., Ries, J.B., Poesen, J., 2011. Short-term versus medium-term monitoring for detecting gully-erosion variability in a Mediterranean environment. Earth Surf. Processes Landforms 36, 1604-1623.
McInnes, J., Vigiak, O., Roberts, A.M., 2011. Using Google Earth to map gully extent in the West Gippsland region (Victoria, Australia), 19th International Congress on Modelling and

Simulation, Perth, Australia, 12–16 December 2011, http://mssanz.org.au/modsim2011, 1-7.

Meire, E., Frankl, A., De Wulf, A., Mitiku Haile, Deckers, J., Nyssen, J., 2012. Mapping the 19th century landscape in Africa – warped terrestrial photographs of North Ethiopia. Reg. Environ. Change. Submitted.

Merla, G., Abbate, E., Azzaroli, A., Bruni, P., Canuti, P., Fazzuoli, M., Sagri, M., Tacconi, P., 1979. A geological map of Ethiopia and Somalia (1973) 1,2.000.000 and comment. University of Florence, Firenze.

Mekuria, W., Veldkamp, E., Haile, M., Gebrehiwot, K., Muys, B. and Nyssen, J., 2009. Effectiveness of exclosures to control soil erosion and local community perception on soil erosion in Tigray, Ethiopia. Afr. J. Agr. Res. 4, 365-377.

Moeyersons, J., Nyssen, J., Poesen, J., Deckers, J. and Mitiku Haile, 2006. Age and backfill/overfill stratigraphy of two tufa dams, Tigray Highlands, Ethiopia: Evidence for Late Pleistocene and Holocene wet conditions. Palaeogeogr. Palaeoclimatol. Palaeoecol. 230, 165-181.

Moges, A., Holden, N.M., 2008. Estimating the rate and consequences of gully development, a case study of Umbulo catchment in southern Ethiopia. Land Degrad. Dev. 19, 574-586.

Muñoz-Robles, C., Reid, N., Frazier, P., Tighe, M., Briggs, S.V. and Wilson, B., 2010. Factors related to gully erosion in woody encroachment in south-eastern Australia. Catena 83, 148-157.

Munro, R.N., Deckers, J., Grove, A.T., Mitiku Haile, Poesen, J. and Nyssen, J., 2008. Soil and erosion features of the Central Plateau region of Tigrai - Learning from photo monitoring with 30 years interval. Catena 75, 55-64.

Nachtergaele, J., Poesen, J., 1999. Assessment of soil losses by ephemeral gully erosion using high-altitude (stereo) aerial photographs. Earth Surf. Processes Landforms 24, 693-706.

Nachtergaele, J., Poesen, J., Steegen, A., Takken, I., Beuselinck, L., Vandekerckhove, L., Govers, G., 2001a. The value of a physically based model versus an empirical approach in the prediction of ephemeral gully erosion for loess-derived soils. Geomorphology 40, 237-252.

Nachtergaele, J., Poesen, J., Vandekerckhove, L., Wijdenes, D.O. and Roxo, M., 2001b. Testing the ephemeral gully erosion model (EGEM) for two Mediterranean environments. Earth Surf. Processes Landforms 26, 17-30.

Nachtergaele, J., Poesen, J., Sidorchuk, A. and Torri, D., 2002. Prediction of concentrated flow width in ephemeral gully channels. Hydrol. Processes 16, 1935-1953.

Nyssen, J., Poesen, J., J., M., Luyten, E., Veyret-Picot, M., Deckers, J., Mitiku Haile and Govers, G., 2002. Impact of road building on gully erosion risk: a case study from the Northern Ethiopian Highlands. Earth Surf. Processes Landforms 27, 1267-1283.

Nyssen, J., Poesen, J., Moeyersons, J., Deckers, J., Haile, M., Lang, A., 2004. Human impact on the environment in the Ethiopian and Eritrean highlands - a state of the art. Earth Sci. Rev. 64, 273-320.

Nyssen, J., Vandenreyken, H., Poesen, J., Moeyersons, J., Deckers, J., Mitiku Haile, Salles, C., Govers, G., 2005. Rainfall erosivity and variability in the Northern Ethiopian Highlands. J. Hydrol. 311, 172-187.

Nyssen, J., Poesen, J., Veyret-Picot, M., Moeyersons, J., Mitiku Haile, Deckers, J., Dewit, J., Naudts, J., Kassa Teka, Govers, G., 2006. Assessment of gully erosion rates through interviews and measurements: a case study from Northern Ethiopia. Earth Surf. Processes Landforms 31, 167-185.

Nyssen, J., Naudts, J., De Geyndt, K., Mitiku Haile, Poesen, J., Moeyersons, J., Deckers, J., 2008a. Soils and land use in the Tigray highlands (Northern Ethiopia). Land Degrad. Dev. 19, 257-274.

Nyssen, J., Poesen, J., Moeyersons, J., Mitiku Haile and Deckers, J., 2008b. Dynamics of soil erosion rates and controlling factors in the Northern Ethiopian Highlands - towards a sediment budget. Earth Surf. Processes Landforms 33, 695-711.

Nyssen, J., Mitiku Haile, Nauds, J., Munro, N., Poesen, J., Moeyersons, J., Frankl, A., Deckers, J. and Pankhurst, R., 2009. Desertification? Northern Ethiopia re-photographed after 140 years. Sc. Total Environ. 407, 2749-2755

Parkner, T., Page, M.J., Marutani, T., Trustrum, N.A., 2006. Development and controlling factors of gullies and gully complexes, East Coast, New Zealand. Earth Surf. Processes Landforms 31, 187-199.

Patton, P.C., Schumm, S.A., 1975. Gully erosion, Northwestern Colorado: a threshold phenomenon. Geology 3, 83-90.

Podobnikar, T., Schroener, M., Jansa, J., Pfeifer, N., 2009. Spatial analysis of anthropogenic impact on karst geomorphology (Slovenia). Environ. Geology 58, 257-268.

Poesen, J., 1992. Gully erosion in the loess belt of Northwestern Europe: typology and control measures. In Geographical Information System for Soil Erosion Management, Luk SH (ed.). Proceedings International Conference, Taiyuan, Shanxi Province, China, 163-174.

Poesen, J., Vandaele, K., van Wesemael, B., 1996. Contribution of gully erosion to sediment production in cultivated lands and rangelands. International Association of Hydrological Sciences Publication 236, 251-266.

Poesen, J., Vandekerckhove, L., Nachtergaele, J., Oostwoud Wijdenes, D., Verstraeten, G., van Wesemael, B., 2002. Gully erosion in dryland environments. In: Bull, L.J., Kirkby, M.J. (Eds.), Dryland Rivers: Hydrology and Geomorphology of Semi-Arid Channels. Wiley, Chichester, UK, pp. 229–262.

Poesen, J., Nachtergaele, J., Verstraeten, G., Valentin, C., 2003. Gully erosion and environmental change: importance and research needs. Catena 50, 91-133.

Radoane, M., 1995. Gully distribution and development in Moldova, Romania. Catena, 24(2): 127-146.

Ries, J.B., Marzolff, I., 2003. Monitoring of gully erosion in the Central Ebro Basin by large-scale aerial photography taken from a remotely controlled blimp. Catena 50, 309-328.

Robinson, P.J., Henderson-Sellers, A., 1999. Contemporary Climatology. Pearson Education Ltd., Essex.

Reubens, B., Poesen, J., Nyssen, J., Leduc, Y., Amanuel Zenebe, Sarah Tewoldeberhan, Bauer, H., Kindeya Gebrehiwot, Deckers, J. and Muys, B., 2009. Establishment and management of woody seedlings in gullies in a semi-arid environment (Tigray, Ethiopia). Plant Soil 324, 131-156.

Satter, F., Wasson, R., Pearson, D., Boggs, G., Ahmad, W., Nawaz, M., 2010. The development of geoinformatics based framework to quantify gully erosion. Proceedings of the International Multidisciplinary Scientific Geo-Conference & Expo-2010, 1-9.

Schumm, S.A., 2005. River Variability and Complexity. Cambridge University Press, Cambridge.

Smith, M.J., Pain, C.F., 2009. Applications of remote sensing in geomorphology. Prog. Phys. Geog. 33, 568-582.

Soufi, M., Isaie, H., 2012. The relationship between gully characteristics and sediment production in the Northeast of Iran, Golestan province. Accessed from http://www.tucson.ars.ag.gov/isco/isco15/pdf/Soufi%20M_The%20relationship%20between.pdf, on 10/03/2012, pp. 3.

Tsou, C-Y., Feng, Z-Y., Chigira, M., 2011. Catastrophic landslide induced by Typhoon Morakot, Shiaolin, Taiwan. Geomorphology 127, 166-178.

Valentin, C., Poesen, J., Li, Y., 2005. Gully erosion: Impacts, factors and control. Catena 63, 132-153.

Vandaele, K., Poesen, J., deSilva, J.R.M., Govers, G., Desmet, P., 1997. Assessment of factors controlling ephemeral gully erosion in Southern Portugal and Central Belgium using aerial photographs. Zeitschrift für Geomorphologie N. F. 41, 273-287.

Vandekerckhove, L., Poesen, J., Wijdenes, D.O., Gyssels, G., Beuselinck, L. and de Luna, E., 2000. Characteristics and controlling factors of bank gullies in two semi-arid mediterranean environments. Geomorphology 33, 37-58.

Vanmaercke, M., Zenebe, A., Poesen, J., Nyssen, J., Verstraeten, G. and Deckers, J., 2010. Sediment dynamics and the role of flash floods in sediment export from medium-sized catchments: a case study from the semi-arid tropical highlands in northern Ethiopia. J. Soils Sediments 10, 611-627.

Virgo, K.J., Munro R.N., 1978. Soil and erosion features of the Central Plateau region of Tigrai, Ethiopia. Geoderma 20, 131-157.

Warren, S.D., Hohmann, M.G., Auerswald, K., Mitasova, H., 2004. An evaluation of methods to determine slope using digital elevation data. Catena 58, 215–233.

Warren, A., Chappell, A., Todd, M.C., Bristow, C., Drake, N., Engelstaedter, S., Martins, V., M'Bainayel, S., Washington, R., 2007. Dust-raising in the dustiest place on earth. Geomorphology 92, 25-37

Wensheng, H., Jiyuan, L., Qiangguo, C., Zhiqiang, G., 2005. Assessment of gully erosion in a semi-arid catchment of the Loess Plateau, China using photogrammetric techniques. Proceedings of the SPIE - The International Society for Optical Engineering 5884, 1-9.

Williams, M., Williams, F., 1980. Evolution of the Nile basin. In, Williams, M., Faure, H. (Eds.), The Sahara and the Nile. Quaternary Environments and Prehistoric Occupation in Northern Africa. Balkema, Rotterdam, pp. 207-224.

Woodward, D.E., 1999. Method to predict cropland ephermeral gully erosion. Catena 37 393–399.

Zenebe, A., Vanmaercke, M., Poesen, J., Verstraeten, G., Haregeweyn, N., Haile, M., Amare, K., Deckers, J. and Nyssen, J., 2012. Spatial and temporal variability of river flows in the degraded semi-arid tropical mountains of northern Ethiopia. Z. Geomorph. N. F., in press.

Zucca, C., Canu, A., Della Peruta, R., 2006. Effects of land use and landscape on spatial distribution and morphological features of gullies in an agropastoral area in Sardinia (Italy). Catena 68, 87-95.

Zhang, Y., Wu, Y., Lin, B., Zheng, Q. and Yin, J., 2007. Characteristics and factors controlling the development of ephemeral gullies in cultivated catchments of black soil region, Northeast China. Soil & Tillage Research 96, 28-41.

Chapter 4
Gully head retreat rates

This chapter is modified from:

Frankl, A., Poesen, J., De Dapper, M., Deckers, J., Mitiku Haile, Nyssen, J., 2012. Gully head retreat rates in the semiarid Highlands of North Ethiopia. Geomorphology, online early view: DOI: 10.1016/j.geomorph.2012.06.011.

Abstract

Due to overgrazing and agricultural intensification, gully erosion severely affects sub-Saharan countries; however, insufficient quantitative studies exist for this part of the world. This paper presents data on gully head retreat rates in Northern Ethiopia and relates these rates to gully and environmental characteristics. The monitoring of headcuts over one rainy season (2010) revealed that present-day retreat rates are low, with average annual linear (R_l), areal (R_a) and volumetric (V_e) retreat rates of 0.34 m y^{-1}, 1.70 m^2 y^{-1} and 5.2 m^3 y^{-1}, respectively. These results express the positive effects of recent soil and water conservation practices on gully stabilization. Significantly higher values of R_l (up to 1.93 m y^{-1}) occurred in the Vertisol areas affected by soil piping. When considering the medium- to long-term time scale (1–47 years) using archival terrestrial (and aerial) photographs, headcut retreat rates proved to be significantly higher than those in the short-term. The averages for R_l, R_a and V_e are 3.8 m y^{-1}, 31.5 m^2 y^{-1} and 47.7 m^3 y^{-1}, respectively. Retreat rates are up to 10 times higher after road construction. On the medium- to long-term time scale, headcut retreat rates were positively related to the catchment area (A). A power relationship that best describes the relation between V_e and A is $V_e = 0.53\ A^{0.31}$ ($r^2 = 0.27$, $n = 18$). Compared to other areas worldwide, regressive erosion has been rapid in Ethiopia as a result of the degraded and steep landscape combined with erosive rains and the occurrence of Vertisols. In Vertisols, headcut retreat is controlled by soil piping. Because no adequate techniques exist to control gully initiation and development in Vertisols, alternative techniques should be developed that deactivate soil pipes.

Key words: Africa, Gully erosion; Headcut retreat, Northern Ethiopia, Repeat photography, Vertisol.

4.1 Introduction

In sub-Saharan Africa, gully erosion (Poesen et al., 2003) causes severe land degradation, which, in turn, disrupts the often-poor local communities. Gullies impede agricultural activities, while the reduction of water tables (Muhindo Sahani, 2011), caused by the incision of gullies, reduce agricultural production. Once deepened, gullies decrease the accessibility of the land and can cause severe damage to infrastructure. Human life and health is potentially endangered by bank failures, the flooding of valley bottoms and water pollution caused by sediment and urban wastewater. In developing countries, urban wastewater is generally diverted straight into gully systems.

Reported cases of gully erosion indicate that both urban and rural areas are affected in many African countries, e.g., Burkina Faso (Marzolff and Ries, 2007), the Democratic Republic of Congo (DRC; Ndona and Truong 2011), Ethiopia (Frankl et al., 2011), Kenya (Oostwoud Wijdenes and Bryan, 2001; Katsurada, 2007), Lesotho (Showers, 1996); Namibia (Eitel et al., 2002), Niger (Leblanc et al., 2008), Nigeria (Gobin et al., 1999), Rwanda (Moeyersons, 1991), Senegal (Poesen et al., 2003), South Africa (Boardman et al., 2003), Swaziland (Felix-Henningsen et al., 1997) and Zimbabwe (Stocking, 1980). In these regions, gully erosion is mainly related to the degradation of the vegetation cover, as a consequence of overgrazing, and the intensification of agriculture. This increases the runoff response of the land, often resulting in flash floods in semi-arid areas. Another major cause of gully erosion is runoff concentration resulting from modifications in the natural drainage pattern near settlements or roads. In urban areas, such as Kinshasa (DRC), the careless deforestation and urbanization of slopes has led to deep gullies in the midst of residential areas. Extreme examples of gully erosion are recorded for Southeast Nigeria (Poesen et al., 2003). Since the second half of the twentieth century, gullies reaching the unusual depth of 50 m have developed as a result of the degradation of the vegetation cover and the establishment of artificial drainage networks (near roads). In the Great Karoo in South Africa, gullies reaching up to eight meters deep originated as a result of overgrazing in the period between 1937 and the 1960s (Boardman et al., 2003). In the Southwestern Sahel in Niger, the drainage density almost tripled between 1950 and 1992 (from 6 to 15 m ha^{-1}; Leblanc et al., 2008). In Northern Ethiopia, gully systems were re-activated and expanded from the 1960s onwards as a result of intensified land use and a series of droughts in the 1970s and 1980s (Frankl et al., 2011). Gully systems that developed have a drainage density of approximately 25 m ha^{-1}, which is one of the densest networks in the world, with gullies that are ten to fifteen meters deep.

Despite the development of important gully networks in sub-Saharan Africa, quantitative research on gully headcut erosion rates is very limited. In Kenya, Oostwoud Wijdenes and Bryan (2001) studied eleven gully heads over a period of three years and found linear headcut retreat rates that varied between 0.8 and 15 m y^{-1}. During the same period, linear gully head erosion rates in Burkina Faso varied between 3.16 and 9.85 m y^{-1} for two gully heads (Marzolff and Ries, 2007). Although several studies reported significant gully erosion in Ethiopia (Virgo and Munro, 1978, Nyssen et al., 2000, 2002, 2004, 2006; Billi and Dramis, 2003; Daba et al., 2003; Moges and Holden, 2008; Munro et al., 2008; Reubens et al., 2009), there is insufficient data on gully head retreat rates, the size of the area affected by retreating gullies and the sediment volumes produced by gully head erosion in Ethiopia. This finding is especially true for the large areas covered by Vertisols, which are susceptible to soil piping.

Vertisols are churning, heavy clay soils that are rich in swelling clays and cover 2.4% of the global land surface area (311 million ha), mainly in Sudan, Ethiopia, India and Australia (FAO, 2007). They are usually found in lower landscape positions on (weathered) deposits that are rich in smectitic clays (e.g., Sudan) or on extensive basalt plateaus (e.g., Ethiopia), and they typically cover large surfaces suitable for agriculture (an estimated 150 million hectares worldwide; FAO, 2007). Vertisols especially develop in the semi-arid tropics, where the precipitation ranges from 500 to 1000 mm y^{-1} and the climate is marked by dry and wet seasons, which are favorable for the periodic shrinking and swelling of the soil (FAO, 2007).

Soil piping is recognized as an important reason for the development of gullies (Valentin et al., 2005). For Vertisols, this development is related to the periodic shrinking and swelling. In a dry Vertisol, shrinking results in the development of wide cracks, which can reach up to two meters deep. Runoff water subsequently infiltrates into the subsoil (bypass flow) and drains underground. Intense subsurface erosion of the dry, dispersive clays results in the development of soil pipes, which, once collapsed, initiates gullies (**Figure 4.1**). When a Vertisol gets wet, swelling causes cracks to close, and the Vertisol becomes almost impermeable. Consequently, the runoff production is very high, and large runoff volumes drain through pipes to the gully heads.

Few studies exist on the importance of soil piping in the development of gullies; for example, these studies have been performed only in Lesotho (Faber and Imeson, 1982), Spain (Ries and Marzolff, 2003; Faulkner et al., 2004) and Southwest USA (Parker, 1963; Swanson et al., 1989). For Southern Ethiopia, Moges and Holden (2008) stress the importance of soil piping in valley bottom deposits for the initiation and development of gullies. In Northern Ethiopia, Nyssen et al. (2000) indicate that piping is important for the development of gullies in Vertisols.

When considering techniques to study headcut retreat, most studies rely on monitoring by fieldwork (e.g., Oostwoud Wijdenes and Bryan, 2001; Wu and Cheng, 2005) or small-scale aerial photographs and their Digital Elevation Model derivatives (e.g., Martinez-Casasnovas et al., 2004; Parkner et al., 2006; Marzolff et al., 2011). In several cases, topographical maps (e.g., Radoane et al., 1995), dendrochronology (e.g., Vandekerckhove et al., 2001) or interviewing local residents serve as a basis (e.g., Nyssen et al., 2006; Moges and Holden, 2008). For a more complete overview, refer to Poesen et al. (2003). In a recent study, Frankl et al. (2011) showed that repeat terrestrial photography can also be of great value for studying gully erosion development, although this technique was rarely used previously (see Chapter 2). When recording gullies, historical photographs provide clear insights into the expansion, size and activity of gully networks. Furthermore, historical terrestrial photographs are often available for periods far before aerial photography data were available, and they can be used to increase the observation density in-between aerial photography surveys.

Figure 4.1 Gully erosion initiated by soil piping in a Vertisol near May Mekdan (see **Figure 4.2**, August 2010). The soil pipe inlet is located directly in front of the person standing and connects to the 4 m deep gully in the background.

The objective of this Chapter is to quantify short-term and medium-to-long-term (1-47 years) gully head erosion rates using, among other methods, terrestrial repeat photography. The linear headcut retreat, the size of the surfaces affected by the gully head retreat, as well as the volumes of sediment produced are quantified, and the erosion rates are related to gully and environmental factors. Particular attention is devoted to the effects of soil piping, which in Ethiopia, occurs in Vertisols, and to the impact of new road infrastructure on gully head erosion.

4.2 Materials and methods

4.2.1 Study area

The area of study (13°23'N, 14°05'N – 39°08'E, 39°36'E) covers an area of 50 km x 75 km near the city of Mekelle in Northern Ethiopia (**Figure 4.2**). This region is part of the source area of the Atbara River and features a young accidental relief between 1400 m and 2800 m a.s.l. The lithology consists mainly of (sub)horizontal strata of sandstone, limestone and basalt that have been uplifted with the formation of the East African Rift (Williams and Williams, 1980). The semi-arid climate is characterized by a major dry season lasting from October until March. The rainy season peaks from July until the beginning of September. The annual precipitation is approximately 700 mm y^{-1} and usually takes the form of heavy showers that seldom last longer than ten minutes (Nyssen et al., 2005). Compared to other regions in the world, rain erosivity is mainly due to the large raindrop sizes rather than high rainfall intensities because 88% of the rain falls with an intensity less than 30 mm h^{-1} (Nyssen et al., 2005). The volume-specific kinetic energy (Ek_{vol}) (in J m^{-2} mm^{-1}) is defined by $Ek_{vol} = 36.65(1 – (0.6/I))$, with I representing the rain intensity in mm h^{-1} (Nyssen et al., 2005). Young soils prevail in the study area (HTS, 1976). Leptosols are found in high landscape positions, while Regosols or Cambisols occur on steep slopes. In footslope positions, fine-textured soils are found with undifferentiated Vertisols and typically exceed one meter in thickness on basalt or basalt colluvium, and Calcisols are found on limestone. In remnant forests, Phaeozems occur (Descheemaeker et al., 2006). Far-reaching deforestation and overgrazing explain why the vegetation cover in Northern Ethiopia is low. The original Afro-Montane forest only appears as patches around churches. During the last twenty years, however, critical zones were selected, where vegetation is now protected against logging or grazing (Descheemaeker et al., 2006). Today (in the year 2011), such exclosures cover 10% to 15% of the land surface. Land degradation is severe in Northern Ethiopia, where significant soil losses occur because of sheet, rill and gully erosion (Nyssen et al., 2009a). Gullies affect nearly all slopes and all surfaces. During the last twenty years, measures have been taken to reduce the runoff response and soil erosion of the land, such as the terracing of slopes, demarcating exclosures and the construction of check dams in gullies (Nyssen et al., 2004). As a result of these measures, 23% of the gully and river network is currently stabilized (Frankl et al., 2011).

A detailed study of gullies was conducted in May Ba'ati (**Figure 4.2**), which contains the small headwater basin (4 km²) characteristic of the Northern Ethiopian Highlands. The topography, comprising a steep sloped, flat-topped *amba* relief, lies between 2100 and 2550 m a.s.l. Slope gradients vary between 0.03 and 0.56 m m^{-1}. Cliff-forming layers of limestone and sandstone have developed structural flats. On top of these flats are Vertisols that developed in basalt (colluvium) and cover 10% to 15% of the area, which is completely under arable land. Land use consists mainly of cropland. Twelve percent of the area is covered by forests or exclosures, which are typically located on the steepest slopes. Rangeland covers 8% of the area. The population density is approximately 200 persons km^{-2} (Stock, 2011).

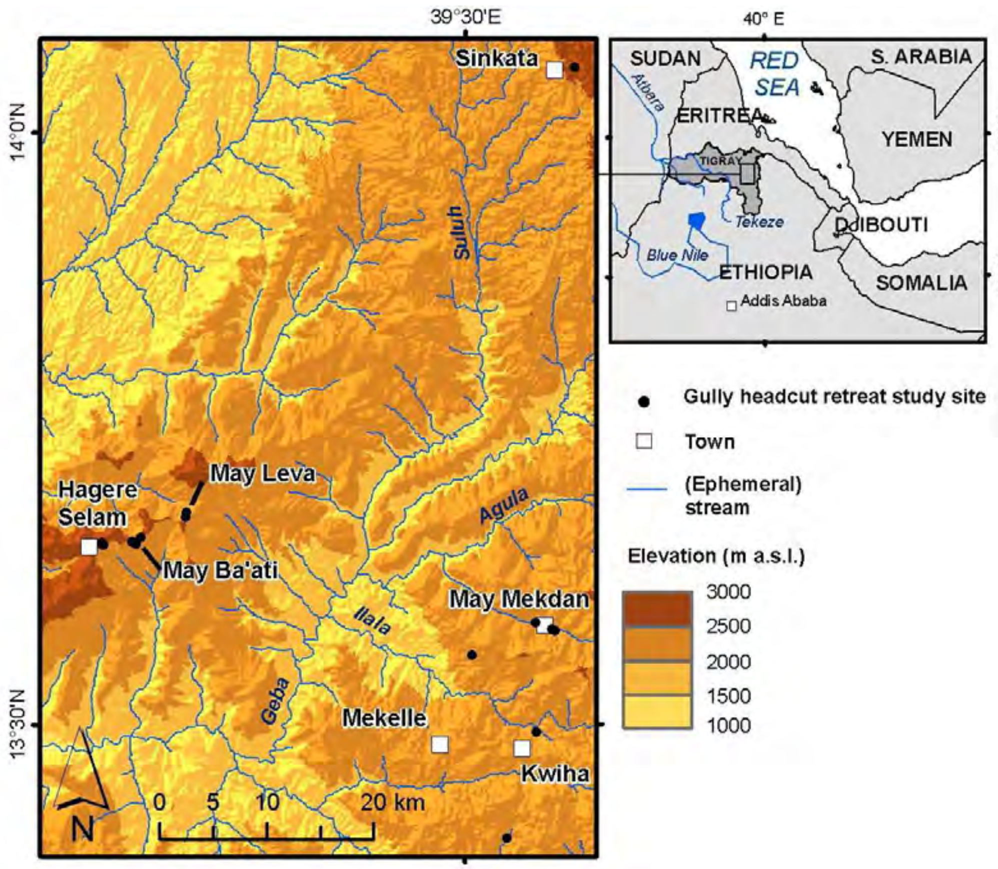

Figure 4.2 Gully headcut retreat study sites. Oro-hydrography based on SRTM data (http://srtm.csi.cgiar.org).

4.2.2 Monitoring short-term gully headcut retreat

Between July 9, 2010 and September 5, 2010, the linear, areal and volumetric headcut retreat rates were measured for 24 gully heads in May Ba'ati (**Figure 4.2**). These measurements can be equated to the annual headcut retreat rate for three reasons: (1) 71±7% of the annual precipitation occurs within the rainy season, between July 1 and September 15, calculated over the period of 1998-2006 for the nearby station of Hagere Selam (MU-IUC, 2007). In 2010, September 5th marked the abrupt end of the rainy season because no rainfall occurred between September 5th and September 15th when the field was last visited. (2) During the dry season and the early rainy season (September – June), rainfall events generate limited runoff (rarely entering gullies) because infiltration rates in the dry (cracked) soils are significantly high. (3) Observations in late July 2011 showed that practically no change occurred at the gully heads since the last measurement was obtained on September 5, 2010. Consequently, this allowed for the assessment of present-day (short-term) gully head activity.

Daily linear headcut retreat rates L_d (m d^{-1}) were established by taking daily measurements of the distance between the most upslope branch of the gullies and a fixed upslope point, such as the trunk of a shrub or a marked rock. Summing the values of L_d over the monitoring period provided us with the annual linear headcut retreat rates (R_l, m y^{-1}). The volumetric headcut retreat rates (V_e, in m^3 y^{-1}) were obtained by subtracting the volume of the gully heads at the beginning of the rainy season from the volume of the headcuts at the end of the rainy season. The volume, in turn, was determined by multiplying the gully head length and the average cross-sectional area of the headcut. Two to four channel cross-sections were positioned in the field by paint-marked rock fragments or wooden stakes. From the changes in the gully length and the average top width, the areal headcut retreat rate (R_a, in m^2 y^{-1}) could be calculated. The measurements in the field were conducted with a measuring tape. Minima, maxima, averages and standard deviations were calculated for L_d, R_l, R_a and V_e. To determine which gully and environmental characteristics control the variability of L_d, R_l, R_a and V_e, data were collected on the headcut type, the headcut height, the local slope gradient of the soil surface, the lithology, the occurrence of soil piping, land use in 2010 at the gully head, the catchment area and the precipitation. Concerning the headcut type, single, branched and rill-abrupt gully heads were distinguished, as is the case in previous classifications (Oostwoud Wijdenes et al., 1999; Nyssen et al., 2002). The slope gradient of the soil surface at the gully head was determined by measuring the inclination of the soil surface with a clinometer, between locations with a five-meter upslope and a five-meter downslope on the gully head. In the field, observations were made on the presence of soil piping to determine if pipes were active at the gully head. The catchment area (A, m^2) of the headcuts was delimited by Global Positioning System recordings (Garmin GPSMap 60®, 5 m standard deviation). This delimitation was performed shortly after rainfall events when the runoff paths could be easily observed. The daily precipitation was recorded by installing three simple rain gauges that were composed of a large tin installed in an open space 1–1.5 m above the ground on a farmer’s compound. The rain gauges were positioned in such a way that every gully head could be linked to a particular site.

The relation between L_d and the daily precipitation was analyzed using the Pearson correlation coefficient r, also taking into account other gully and environmental characteristics (see above) that control headcut retreat. Before analyzing the data on R_l, R_a and V_e in relation to the gully and environmental characteristics, a logarithmic transformation of the data was performed. This approach was necessary to obtain datasets with normal frequency distributions and homogeneous variances that are suitable for statistical analyses. This approach was verified using a Kolmogorov-Smirnov test (α = 0.05) and a Levene test (α = 0.01). Subsequently, significant associations (α = 0.05) between LogR_l, LogR_a, LogV_e and continuous explanatory variables were detected using a correlation matrix. For the categorical variables of headcut type, soil piping, lithology, and land use in 2010, *t*-tests (α = 0.05) were performed.

4.2.3 Medium- to long-term (1-47 years) gully headcut retreat rates

Eighteen gully heads, which could be clearly observed from terrestrial or aerial photographs, were selected in the Northern Ethiopian Highlands for the analysis of headcut retreat rates over a period of 1 to 47 years. Eight gully heads could be studied by means of historical terrestrial photographs, and ten gully heads could be studied by means of historical aerial photographs. In addition, intermediate observations could be performed for four gully heads using terrestrial or aerial photographs, focused interviews (see Nyssen et al., 2006) or field observations.

Eleven archival terrestrial photographs used in this chapter were taken during field visits in 1998 or 2008. Two terrestrial photographs from 1975 were originally taken by Neil Munro. The aerial photographs (scale ranging between 1:35,000 and 1:45,000) were collected from the Ethiopian Mapping Authority with dates of 1963, 1965, 1974 and 1994.

The assessment of the annual headcut retreat rates, R_l, R_a and V_e by means of terrestrial or aerial photographs could be completed using field measurements on the basis of the relocated historical gully heads. The latter was possible whenever the historical gully heads were situated close to landscape elements, such as stone bunds (**Figure 4.3**) or footpaths. Several gullies that developed as bank gullies did not yet exist at the time when the aerial photographs of 1963, 1965 or 1974 were taken. In those cases, it was sufficient to locate the downslope gully end for the calculations of R_l, R_a and V_e. Because the gully was not yet present in 1963, 1965 or 1975, the values for R_l, R_a and V_e were interpreted as minimum values. When interviews or field observations from 2009 served as the basis for the positioning of historical gully heads, people’s indications were used and cross-checked for consistency. Analogous to the previous section, the measurements of the gully dimensions in the field were performed using a measuring tape.

The maximum error of the relocation of the historical gully heads in the field was estimated to be 2 m, which introduced an error in the values of R_l, R_a and V_e that ranged between 0.2% and 31%, which was 8±1% on average.

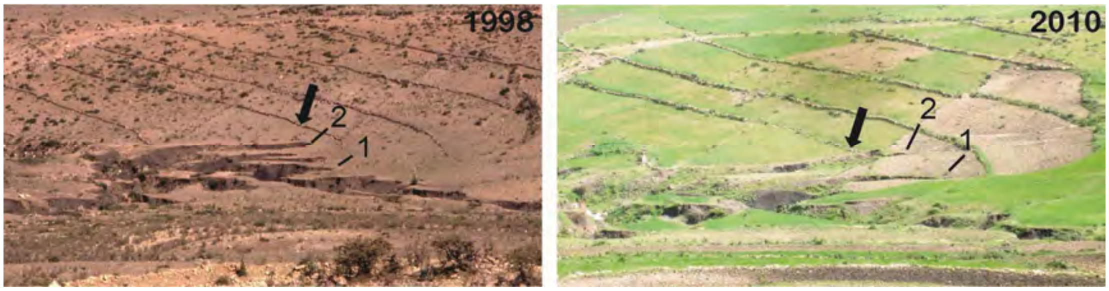

Figure 4.3 Quantifying gully head retreat from repeat photography. Due to the presence of stone bunds (black arrows), the 1998 location of two gully heads in May Leva could be detected in the field between 1998 and 2010. The May Leva 1 and May Leva 2 headcuts retreated by 13.1 m and 20.7 m, respectively. Both gullies did not yet exist in 1963. Photograph in 1998 was taken by J. Poesen, and a repeat photo was taken in 2010 by A. Frankl.

To analyze gully head erosion in relation to the controlling factors, descriptive statistics for R_l, R_a and V_e were computed: minima, maxima, averages and standard deviations. Subsequently, the effect of the following gully and environmental characteristics on LogR_l, LogR_a and LogV_e was determined: gully head type, headcut height, local slope gradient at the gully head, lithology, occurrence of soil piping, land use at the gully head in 2010, catchment area and precipitation. For the latter, data were collected from the Global Climatic Data database (accessed from www.worldclim.org; Hijmans et al., 2005) for the period of 1960-2000 and included averages for the annual precipitation, the precipitation during the wettest month and the Fournier Index. This index, which combines the annual precipitation (p) and the precipitation of the wettest month (P) in the equation $c = P^2/p$, expresses the relative importance of both variables and the rainfall erosivity (Fournier, 1960). The data were generated through the interpolation of average monthly climatic data from weather stations on a 30 arc-second resolution grid (Hijmans et al., 2005).

First, the analysis determined the strength of the relationship between LogR_l, LogR_a and LogV_e and the continuous and categorical explanatory variables. For the continuous variables of the gully (headcut height, local slope gradient, catchment area and precipitation), the significance of the association (α = 0.05) was determined using the correlation coefficient r. For the categorical variables, including gully head type, lithology, soil piping and land use in 2010, t-tests were performed to determine whether the averages of the populations were significantly (α = 0.05) different from each other.

Second, a multiple regression analysis (in SPSS) was performed to detect the relevant parameters (gully head type, headcut height, local slope gradient, lithology, occurrence of soil piping, land use at the gully head in 2010, catchment area and precipitation; α = 0.05), and a linear model was computed for the relationships between LogR_l, LogR_a or LogV_e and the relevant gully and environmental characteristics.

In the case of the four gully heads with multiple observations, the variabilities of R_l, R_a and V_e were analyzed.

4.2.4 Gully head erosion after road construction

To study the effects of the recent modifications to the road infrastructure (with relocations of road outlets) on gully head erosion, data from Nyssen et al. (2002) were adapted. These data comprise the catchment area, the gully width and depth, the total length of the headcut retreat and the eroded volume of 15 gullies after the construction of a new road during 1993-1994 east of Hagere Selam (**Figure 4.2**). For R_l, R_a and V_e, descriptive statistics were calculated (minima, maxima, averages and standard deviations). T-tests were performed to determine if the population averages of LogR_l, LogR_a or LogV_e after the recent road construction were significantly different from the data presented in Section 2.3 for which the recent road modifications had no influence on the drainage patterns.

4.3 Results

4.3.1 Short-term gully headcut retreat rates

The average seasonal precipitation for the three measuring sites was 359±42 mm with 30 days with rain (34%) and 58 days without rain during the period of study. In the former case, the daily precipitation was 12 mm on average with a maximum of 45 mm. These figures correspond to an average or above-average rainy season and were perceived by the farmers as a good year.

The 24 gully heads monitored in May Ba'ati during the rainy season of 2010 retreated by linear erosion during 2 to 16 rain events. The daily linear headcut retreat rate (L_d) varied between 0 and 0.55 m d^{-1} (**Figure 4.4**). Due to the 2 mm rainfall, the gullies were able to become active. The number of active gullies showed a strong positive correlation with the daily precipitation (r = 0.79, P <0.001). A linear regression indicates that 50% of the gullies retreat by linear erosion when the rainfall depth equals 20 mm. High rainfall events that should cause all of the gullies in the area of study to retreat at the same time did not occur during the monitoring period. This finding is mainly explained by the fact that rainstorms are generally small in size, and the correlation between L_d and daily precipitation was considerably low (average of r = 0.25, **Table 4.1**), with only thirteen gully heads showing a significant relationship. The strength of the correlation between L_d and the daily precipitation was not influenced by gully and environmental parameters. However, seven out of thirteen significant correlations occurred on degraded soils. The high variability in L_d and the weak correlation with the daily precipitation are the result of the discontinuous retreat of the gully heads, which does not always occur when the precipitation is at a maximum. Along the gully head, tension cracks develop that cause soil falls, which are likely to occur in-between rainfall events because of gravity. Therefore, the values for L_d were summed to equal the annual linear headcut retreat rates R_l (**Table 4.1**).

The linear retreat rates R_l varied from 0.02 m y^{-1} to 1.93 m y^{-1} with an average of 0.34±0.49 m y^{-1} (**Table 4.1**, **Figure 4.5**). The areal retreat rates R_a varied from 0.11 m^2 y^{-1} to 4.57 m^2 y^{-1}, with an average of 1.70 ±1.59 m^2 y^{-1} (**Table 4.1**). The volumetric headcut retreat rates V_e varied from 0.1 m^3 y^{-1} to 20.7 m^3 y^{-1}, with an average of 5.2±5.1 m^3 y^{-1} (**Table 4.1**). The values of R_l, R_a and V_e were not normally distributed, they were skewed towards lower values and high outliers occurred. A logarithmic transformation of R_l, R_a and V_e resulted in normal distributions of LogR_l, LogR_a or LogV_e with homogeneous variances (insignificant Kolmogorov-Smirnov and Levene tests).

Eighteen of the gully head-type headcuts could be classified as single, three headcuts were rill-abrupt, and the remaining three were branched. The headcut height varied between 0.40 m and 2.93 m and was, on average, 0.96±0.62 m (**Table 4.1**). The slope gradient of the soil surface at the gully head ranged between 1% and 49%, with an average of 14±11%. Soil piping occurred at six headcuts, which were all located in Vertisol areas. Ten gully heads were located in densely vegetated areas, such as exclosures, or in grassed seasonal waterways; five headcuts were in cropland; seven headcuts developed on surfaces with degraded vegetation and two headcuts showed mixed land use (**Table 4.1**). Six headcuts developed in limestone colluvium, twelve in sandstone colluvium and six in Vertisols. The catchment areas of the headcuts ranged from 590 m^2 to 243 380 m^2, with an average of 57 580±78 520 m^2.

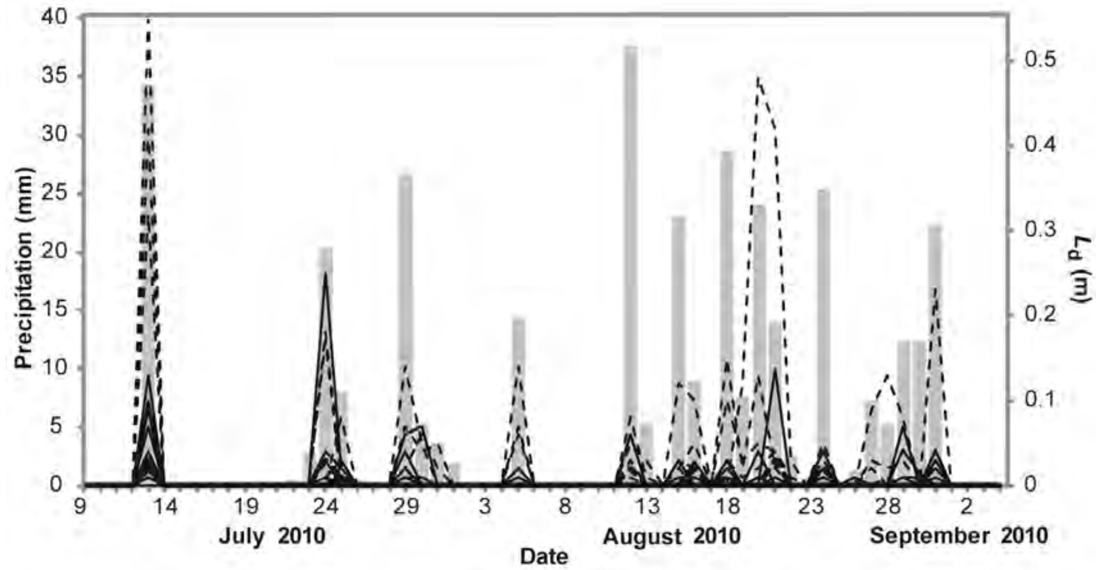

Figure 4.4 The daily gully headcut retreat rate L_d (shown with the black line) and its relationship with the daily precipitation (grey bars) for all of the studied headcuts in 2010. The gully heads where soil piping occurs (in Vertisols) are indicated by the dashed line. The daily precipitation shown is the average rain recorded at the three measuring sites.

Table 4.1 Headcut retreat of 24 gullies in May Ba'ati during the rainy season of 2010.

Gully head	R_l (m y^{-1})	R_a (m^2 y^{-1})	V_e (m^3 y^{-1})	Headcut height	r between L_d and daily precipitation	A (m^2)	Soil piping	Land use at gully head (2010)
1	.14	.90	1.1	.93	.32	591		Exclosure (Acacia trees, poor undergrowth)
2	.03	.94	2.1	.89	.13	142 348		Exclosure (Acacia trees, shrubs)
3	1.52	5.79	7.1	.45	.71*	243 376	x	Grazed footpath
4	.45	.73	1.5	.40	.47*	230 622	x	Grazed footpath
5	.76	3.51	7.9	1.4	.28	672	x	Cultivated
6	1.93	3.61	10.2	1.3	.38	220 187	x	Cultivated
7	1.02	4.57	5.5	.46	.52*	2 769	x	Cultivated
8	.08	1.71	.9	.66	.07	27 092		Seasonal waterway (grasses)
9	.13	.19	.5	.53	.18	3 427		Seasonal waterway (grasses)
10	.28	.32	1.9	.92	.42*	5 580		Exclosure (shrubs and small trees)
11	.09	1.17	3.3	.78	.36*	67 291		Exclosure (trees, shrubs, grasses)
12	.09	1.28	5.8	1.41	.29	35 548		Cultivated
13	.09	3.65		2.93	.32	147 632		Degraded rangeland
14	.17	.3	9.5	.47	.44*	44 721	x	Degraded rangeland
15	.03	1.41	20.7	2.26	.46*	83 909		Cultivated/Degraded rangeland
16	.02	2.07	3.8	.75	.29	31 850		Seasonal waterway (grasses)
17	.18	1.62	9.1	.75	.39*	16 085		Cultivated/Grazed waterway
18	.43			1.52	.35*	9 628		Degraded rangeland
19	.12	.11	11.5	.22	.59*	1 833		Exclosure (Acacia trees, grasses)
20	.10	.97	8.0	1.1	.33	28 427		Cultivated
21	.11	3.52	.1	.42	.41*	2 986		Exclosure (large trees, dense
22	.06	.11	.4	.89	.14	21 239		Eucalyptus plantation (dense undergrowth)
23	.19	.23	.2	.74	.44*	11 756		Degraded rangeland
24	.05	.26	2.6	.93	.45*	2 356		Degraded rangeland

* Correlation is significant at the 0.05 level.

R_l, R_a, V_e: annual linear/area/volumetric headcut retreat rate; L_d: daily linear headcut retreat; A: catchment area

The correlation between LogR_l and the continuous gully and the environmental characteristics (i.e., the catchment area, the local slope gradient and the headcut height) was low and insignificant. For the categorical variables (gully head type, lithology, land use in 2010 and the presence of soil pipes), only soil piping had a significant positive effect on LogR_l (t = -3.47, P = 0.003). Therefore, the soils that were located where piping occurred (Vertisols) had larger values of LogR_l (**Figure 4.5**). The effects of the gully and the environmental characteristics on LogR_a and LogV_e could not be demonstrated due to the expectation of a weak correlation between LogR_a and the local slope gradient (r = 0.43, P = 0.048).

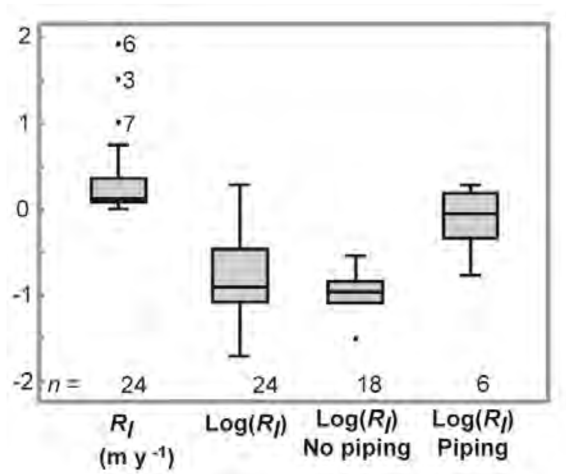

Figure 4.5 The linear headcut retreat rate before and after logarithmic transformation. The logarithmic transformation of R_l creates a normally distributed parameter LogR_l. is higher in soils where piping occurs.

4.3.2 Medium- to long-term (1-47 years) gully headcut retreat rates

Table 4.2 shows the values of R_l, R_a and V_e for the 18 gully heads, the methods used to calculate the retreat rates (terrestrial photographs, aerial photographs, interviews and field observations), the period over which observations were made, the headcut height, the catchment area (A) of the gully head and the occurrence of soil piping.

Table 4.2 Studied gully heads (n = 18) for the medium- to long-term retreat rates and their characteristics; and four intermadiate observations.

Gully head	Method*	Period	R_l (m y^{-1})	R_a (m² y^{-1})	V_e (m³ y^{-1})	Headcut height	A (m²)	Soil piping
Sinkata	AP	1994-2010	.64	3.5	3.3	.85	6 648	
May Leva 1	AP	1963-2010	1.10	8.2	13.0	1.72	10 086	x
May Leva 2	AP	1963-2010	.86	7.9	11.5	1.30 - 1.55	10 323	x
May Ba'ati 1	AP	1974-2010	.53	5.5	9.8	1.30	1 876	
May Ba'ati 2	AP	1974-2011	1.03	9.4	10.6	.47	44 721	x
May Mekdan 1	AP	1965-2010	9.79	63.1	40.1	.1 - 1.90	787 507	x
Hagere Selam 1a	TP	1998-2010	1.90	4.2	9.9	1.10	86 000	
May Ba'ati 3	AP	1994-2011	1.75	25.7	47.6	1.52	9 628	
May Ba'ati 4	AP	1974-2011	1.39	9.3	20.5	2.26	83 909	
May Ba'ati 5	TP	2008-2011	2.15	4.0	4.3	0.93	124 208	
Hagere Selam 2b	TP	1993/4-1999	7.27	58.2	58.1	0.82	141 000	x
Hagere Selam 2c	TP	2008-2011	8.93	33.7	45.1	1.76	141 000	x
May Mekdan 2	TP	1975-2010	.62	4.0	14.8	4.00	715 000	x
May Mekdan 3	AP	1965-2010	1.36	10.9	23.0	.50 - 1.30	24 531	x
May Mekdan 4	AP	1965-2010	18.4	201.6	425.4	.1 - 4.20	2 829 872	x
Mekelle Mesebo	TP	1998-2010	1.49	0.3	1.3	.85	138 826	
Kwiha 1	TP	1975-2010	1.85	69.2	66.9	.80 - 1.22	3 808 440	x
Kwiha 2	TP	1998-2010	7.33	48.3	52.5	1.10 - 1.15	1 558 857	x
Intermediate Observations								
May Leva 1	TP	1998-2010	1.73	8.1	10.9	1.72	10 086	x
May Leva 2	IV	1998-2010	1.09	6.3	8.2	1.30 - 1.55	10 323	x
May Leva 2	AP	2008-2011	3.15	7.1	7.0	1.30 - 1.55	10 323	x
May Ba'ati 1	TP	1998-2010	.65	5.1	6.9	1.30	1 876	
May Mekdan 2	FO	2009-2010	7.00	30.1	43.6	1.32	715 000	x

* TP: Terrestrial photography, AP: Aerial Photography, IV: Interview, FO: Field observation
R_l, R_a, V_e: annual linear/area/volumetric headcut retreat rate; A : catchment area

The average and standard deviation was 3.8±4.7 m y^{-1} for R_l, 31.5±48.3 m² y^{-1} for R_a, and 47.7±96.5 m³ y^{-1} for V_e (**Table 4.3**). The minima and maxima differ considerably as a result of extreme values and skewed distributions towards the lower values of R_l, R_a and V_e. The logarithmic transformation of R_l, R_a and V_e results in normal frequency distributions with homogeneous variances.

Table 4.3 Descriptive statisticsof the observed gully headcut retreat rates (R_l, R_a and V_e).

	R_l				R_a				V_e			
	All	Soils with piping	Other Soils	Recent road construction*	All	Soils with piping	Other Soils	Recent road construction*	All	Soils with piping	Other Soils	Recent road construction*
n	18	11	7	15	18	11	7	15	18	11	7	15
Minimum	.5	.6	.5	1.8	.3	4.0	.3	2.9	1.3	10.6	1.3	9.0
Maximum	8.9	18.4	2.2	91.6	201.6	201.6	25.7	280.0	425.4	425.4	47.6	2310.0
Mean	**3.8**	**5.3**	**1.4**	**21.3**	**31.5**	**46.8**	**7.5**	**21.5**	**47.7**	**69.2**	**13.8**	**554.7**
Std. Deviation	4.7	5.6	.6	24.4	48.3	57.1	8.5	83.1	96.5	119.9	16.2	849.5

* (calculated from Nyssen et al. 2002)

R_l, R_a, V_e: annual linear/area/volumetric headcut retreat rates

The head type of twelve gully headcuts was single, two headcuts were rill-abrupt, and four were branched. The headcut height varied between 0.47 m and 4.20 m and was, on average, 1.39±0.80 m (**Table 4.2**). The slope gradient of the soil surface at the gully head ranged from 2% to 22% with an average of 9±6%. Soil piping occurred at eleven headcuts in which the majority was located in Vertisols. Three gully heads were located in densely vegetated areas, such as in exclosures or in grazed seasonal waterways, thirteen headcuts were located in cropland and two headcuts were located on surfaces with degraded vegetation. Three headcuts developed in limestone colluvium, five developed in sandstone colluvium and one developed in basalt colluvium. Nine headcuts developed in Vertisols. The catchment area of the headcuts ranged between 1 880 m^2 and 3 808 440 m^2, with an average of 584 580±1 085 040 m^2. The average annual precipitation over the period from 1960-2000 for all of the measuring sites was 637±37 mm, with a minimum of 537 mm and a maximum of 678 mm. The average precipitation of the wettest month (August) during the same period ranged from 199 mm to 214 mm, with an average of 205±7 mm. The Fournier Index was 66±2 on average and ranged from 63 to 70.

Considering the relationship between the gully headcut retreat rate and the gully and environmental characteristics recorded, only the catchment area (Log$A$) had a strong positive association with LogR_l, LogR_a and LogV_e, with correlation coefficients of 0.65, 0.48 and 0.52, respectively, which were significant at the $\alpha = 0.05$ level. The correlations between the annual headcut retreat rates and the other characteristics, including the local slope gradient of the surface, the headcut height, the precipitation of the wettest month and the Fournier Index, were low and not significant ($\alpha = 0.05$). The positive effect of soil piping on the gully headcut retreat rates, as indicated by the numerical description (**Table 4.3**) and the graphical description (**Figure 4.6**), leads us to conclude that for this study, soils in which piping occurs are more vulnerable to gully erosion. A t-test, which was used to compare the means of the observations on the gully headcut retreat rates for soils with piping and soils without piping, reveals that the null hypothesis, which assumes equal means, could be rejected for LogR_a and LogV_e. The t-statistics are as follows: LogR_l, $t = -1.21$ ($P = 0.10$), LogR_a, $t = -2.88$ ($P = 0.01$) and LogV_e, $t = -2.73$ ($P = 0.015$). There proved to be no significant effect of the present land-use type on the gully headcut retreat rates, the lithology or the headcut type.

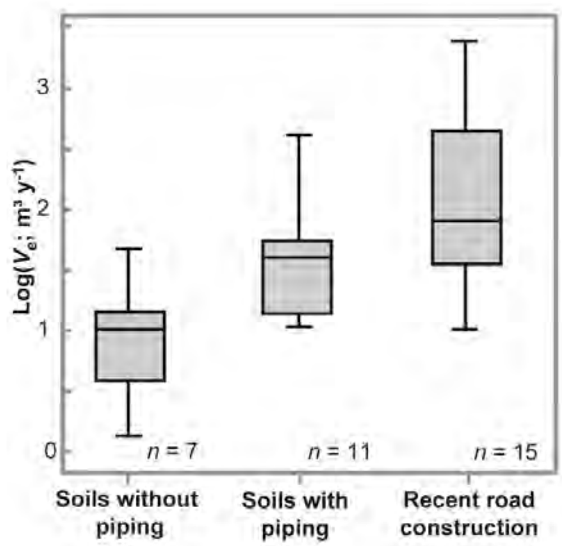

Figure 4.6 Boxplots showing the distribution of the gully headcut retreat rates (in $m^3\ y^{-1}$) after a logarithmic transformation for soils without piping, soils with piping (including Vertisols) and after road construction.

For the next step in the analysis, a multiple regression analysis was performed using LogR_l, LogR_a and LogV_e as response variables and gully and environmental variables as explanatory variables. The catchment area (A, m^2) showed to be the most important variable that is significantly related to the annual retreat rates (the power relations are shown by eqns. 4.1 to 4.3). Regarding the effect of soil piping, a trend could only be observed when considering the linear headcut retreat rate (P = 0.55). When considering the areal and volumetric headcut retreat rates, the effect of soil piping was such that significant associations could only be defined when considering gullies in which soil piping occurred. For these subgroups, given A, the retreat rates showed to be higher on the plot (Eq. 4.4 and 4.5; **Figure 4.7**).

$R_l = 0.06\ A^{0.31}$ (n = 18, r^2 = 0.42) (4.1)

$R_a = 0.27\ A^{0.33}$ (n = 18, r^2 = 0.23) (4.2)

$V_e = 0.53\ A^{0.31}$ (n = 18, r^2 = 0.27) (4.3)

$R_{a\ \text{“piping”}} = 0.23\ A^{0.38}$ (n = 11, r^2 = 0.47) (4.4)

$V_{e\ \text{“piping”}} = 0.45\ A^{0.36}$ (n = 11, r^2 = 0.52) (4.5)

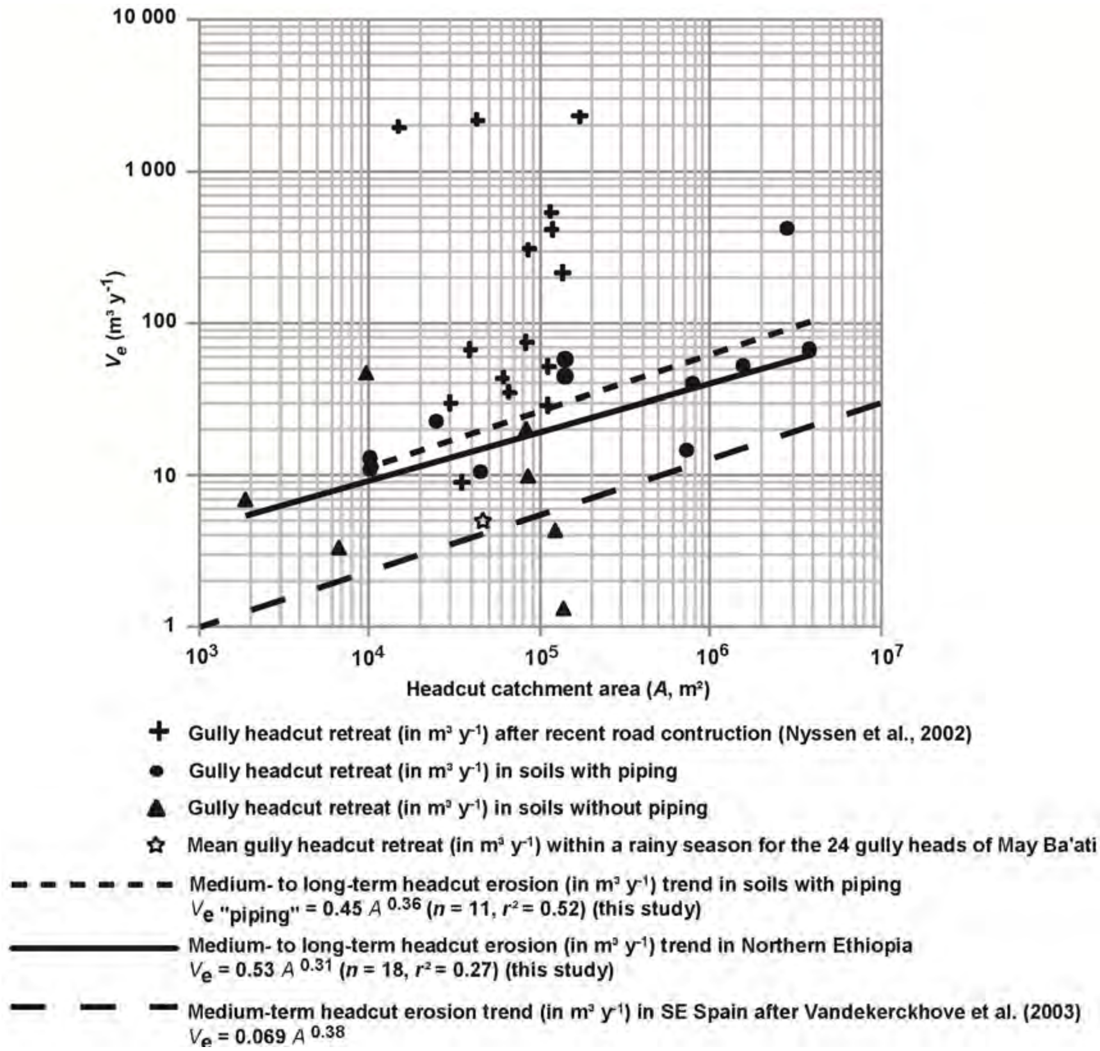

Figure 4.7 Relationship between the annual volumetric retreat rate (V_e) and the drainage area (A) in the area of study area.

In the case of the sites of May Leva 1 and 2, May Ba'ati 1 and May Mekdan 2, the development of the gully volume (**Figure 4.8**), the length and the surface over time could be determined. A negative exponential increase in the gully volume, the length and the surface could be observed over the period of study for three out of four gullies. For these gullies, the headcut retreat rates were larger during the early phases of gully development.

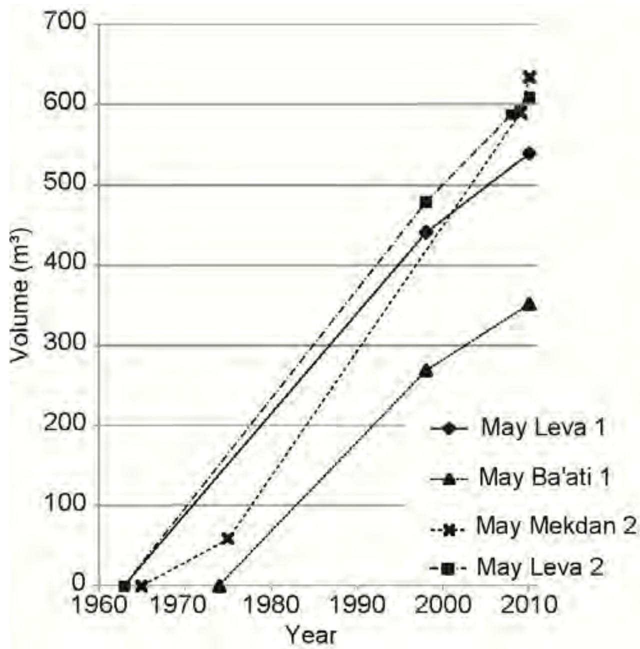

Figure 4.8 Growth of gully head volume over time for the sites of May Leva 1 and 2, May Mekdan 2 and May Ba'ati 1.

4.3.3 Gully headcut retreat after a recent road construction

Table 4.3 shows descriptive statistics for R_l, R_a and V_e that were obtained for the 15 gully heads studied after a recent road construction by Nyssen et al. (2002). The average values and the standard deviations for R_l, R_a and V_e were 21.3 m y^{-1}, 21.5 m² y^{-1} and 554.7 m³ y^{-1}, respectively. Both the descriptive statistics (average, maximum, minimum) and the boxplot (**Figure 4.6**) indicate that headcut retreat was more severe (up to 10 times greater) when a new road caused a significant increase in the catchment area of the gullies, compared to the gullies described in section 3.2, where no recent roads were built in their catchments. We tested this observation with a *t*-test after a logarithmic transformation of the observations: LogR_l, t = -4.62, P < 0.001; LogR_a, t = -1.05, P = 0.30; and LogV_e, t = -3.81, P < 0.001. These results illustrate that in the case of LogR_l and LogV_e, recent road construction had a significant positive effect on the headcut retreat rates. In the case of LogR_a, however, the averages for both populations (with/without recent road construction in the catchment) did not differ significantly. The 95% confidence interval for the increase in the gully head retreat rates due to the construction of a new road varied from 7.3 – 29.5 m y^{-1} for R_l and from 158.2 – 861.2 m³ y^{-1} for V_e. A regression between the response variables of LogR_l, LogR_a, LogV_e and Log$A$ could not be performed because these variables did not correlate with each other ($r \approx 0$). **Figure 4.7** shows, however, that for a given catchment area (A), the volumetric headcut retreat rates V_e were generally higher when considering the gullies in which a new road was constructed in a catchment.

4.4 Discussion

4.4.1 The use of repeat terrestrial photography for assessing gully head retreat rates

Repeat terrestrial photography offers a valuable tool for analyzing long-term changes in environmental features (Frankl et al., 2011). Gullies are often spectacular landscape features, attracting the attention of many photographers. Hence, they appear in many terrestrial photographs. In Northern Ethiopia, Nyssen et al. (2010) created a large dataset of historical landscape photographs, which allowed for repeat photography studies (e.g., Nyssen et al., 2009b; Munro et al., 2010) to analyze environmental changes over more than 140 years. However, photographing (mountainous) landscapes from the on-the-ground perspective results in large deformations of the scenery displayed on the photographs. For this reason, to date, few quantitative studies actually used repeat photography (e.g., Corripio, 2004). Such studies are primarily based on the projection of the photographs on a Digital Elevation Model (DEM) to create maps. Because this technique is difficult to apply and requires the availability of a high resolution DEM, Meire et al. (2011) developed a methodology that warps terrestrial photographs onto the horizontal plane of a map using GPS measurements of homogeneous topographies. To our knowledge, apart from the study of Frankl et al. (2011) (see Chapter 1) that quantifies historical gully cross-sections and the brief study of Vincente et al. (2009) that observed gully expansion, no other study has successfully used repeat photography in a quantitative way when considering gully erosion. This Chapter shows that repeat terrestrial photography can also be used to quantify gully head retreat rates, which enables the establishment of long-term headcut retreat rates when historical maps or large-scale aerial photographs are lacking for the period of interest. However, to avoid large errors, much care is required when determining the historical location of the headcuts. Only photographs that allow for the precise positioning of the historical headcut relative to the proximity of stable landscape elements should be selected.

4.4.2 Gully headcut retreat rates in Ethiopia compared to other semi-arid regions of the world

Headcut retreat rates are significantly smaller on the short-term compared to the medium-to-long-term time scale, which corresponds to results obtained in Spain (Vandekerckhove et al. 2001, 2003; Martinez-Casasnovas et al., 2003, 2004; Marzolff et al., 2011) and Romania (Ionita, 2006). This finding is partially explained by the occurrence of extreme rainfall events inducing strong headcut retreat, which are more likely to occur during longer observation periods. Furthermore, the soil and water conservation structures (e.g., exclosures, stone bunds, infiltration trenches and ponds) that have been implemented over the past 20 years in Tigray had a significant influence on the catchment hydrology through the decrease of both the runoff coefficients and the sediment production (Descheemaeker et al., 2006; Nyssen et al., 2009a). As a consequence, gully activity is decreasing (Frankl et al., 2011), and the correlation between gully head erosion rates and gully and environmental parameters is weak. This phenomenon is most evident in small headwater basins, such as in May Ba'ati, where nine out of 24 gully heads have a linear retreat rate of less than 0.1 m y^{-1}. Similar findings on the decreasing effect of soil and water conservation measures on gully erosion rates were also obtained for a study in Romania (Ionita, 2006).

As in other sub-Saharan countries (e.g., Marzolff and Ries, 2007, Oostwoud Wijdenes and Bryan, 2001) and semi-arid areas worldwide (e.g., Vandekerckhove et al., 2001, 2003; Wu and Cheng, 2005; Marzolff et al., 2011), the variability in gully head retreat rates is high in Ethiopia. For catchments of similar sizes and during the same observation period, the headcut retreat rates obtained in this study vary by a factor of ten. In Southeast Spain, Vandekerckhove et al. (2003) computed a regression equation linking drainage area and medium-term gully head retreat rates: $V_e = 0.069\ A^{0.38}$ (**Figure 4.7**). Marzolff et al. (2011) included observations from Northeast Spain and obtained an A - V_e equation similar to that reported by Vandekerckhove et al. (2003). Comparing these equations with the A - V_e equation obtained in this study, we conclude that for similar catchment areas, the gully headcut retreat rates (in $m^3\ y^{-1}$) that resulted from this study in Northern Ethiopia are approximately seven times larger than those obtained by the studies in Spain (**Figure 4.7**).

This finding is most likely due to an environment that is more vulnerable to soil erosion with steeper slopes, a more degraded vegetation cover, the occurrence of intense rainstorms during the short rainy season and the presence of Vertisols. The exponents of the equations for Ethiopia and Spain (Vandekerckhove et al., 2003; Marzolff et al., 2011) do not differ notably (Spain: 0.37, Ethiopia: 0.38), reflecting the similar importance of the catchment area and the gully headcut retreat rate in both environments.

As indicated by the medium-to-long-term data and previous studies (e.g., Seginer, 1966; US Soil Conservation Service, 1966; Stocking, 1980; Burkard and Kostaschuk, 1997; Vandekerckhove et al., 2003; Marzolff et al., 2011), the catchment area at the gully head is the most important factor controlling gully head retreat rates, which translates into the importance of the runoff volume entering the gully. Other gully and environmental parameters are generally weakly correlated to the gully head retreat rates and depend on site-specific characteristics.

Precipitation characteristics are important in controlling gully initiation and development (e.g., Thompson, 1964; USSCS, 1966; Radoane et al., 1995; Martinez-

Casasnovas et al., 2002). However, in this study, the annual headcut retreat rates weakly correlate with the precipitation characteristics. The reason for this is that the averages calculated over a 50-year time period do not reflect the large inter-annual variability in rainfall characteristics. Limited meteorological station data obtained over the period 2004-2006 for the towns of Hagere Selam, Mekelle and Wukro resulted in values for the annual precipitation, the precipitation of the wettest month and the Fournier Index that ranged between 390 mm and 850 mm, 171 mm and 314 mm and 74 and 164, respectively.

Graf (1977) suggested that gully head retreat rates display negative exponential growth on a long-term time scale. According to Oostwoud Wijdenes and Bryan (2001) and Nachtergaele et al. (2002), this finding is the result of the reduction in the contributing runoff area, while the headcut progresses upslope. Other site-specific explanations include the consequence of a decrease in the local slope gradient during headcut retreat, the increase of soil and water conservation practices through time and land abandonment. Laboratory (Kosov et al., 1978) and field studies (Oostwoud Wijdenes and Bryan, 2001; Nachtergaele et al., 2002; Nyssen et al., 2006) have confirmed this negative exponential growth. As is apparent in **Figure 4.8**, a similar trend can be observed in this study.

Regarding the effect of artificial modifications to the drainage patterns, this chapter supports the findings of Nyssen et al. (2002), which claim that road construction considerably increases the risk of gully head activity, which, in turn, can affect both rural (e.g., Moeyersons, 1991) and urban areas (e.g., Archibold et al., 2003). We can derive from the data in this chapter that a strong increase in the catchment area activates (or initiates) gullies that will develop rapidly upslope (linear erosion) and will deepen. Only in a later phase will the gully gradually widen due to an oversteepening of the gully walls. Special care is therefore required when altering runoff pathways to not destroy valuable land located downslope the newly built roads (Valentin et al., 2005). A possible solution consists of increasing the local drainage by decreasing the distance between drifts or culverts (Croke and Hairsine, 2001; Nyssen et al., 2002) based on threshold values that indicate the maximum size a drainage area may have after road construction.

4.4.3 The effect of soil piping (especially in Vertisols) on gully head retreat rates

Under normal conditions, footslope positions have a low susceptibility to gully initiation because their slope gradients are low (Knighton, 1998). The presence of smectite clays (such as those in Vertisols) strongly increases the susceptibility of these slopes to water erosion as a consequence of their susceptibility to soil piping. Once the gullies are initiated, they will be extended along the line of still-buried pipes (Knighton, 1998). Because of the frequent draining of large areas in footslope positions, high annual retreat rates can be observed. In California, the presence of smectite clays in valley floors strongly affects the gully erosion rates through soil piping (Swanson et al., 1989). Soil piping also plays an important role in the development of badlands in dispersive clays and silt-clays in the valley floors of the Ebro basin in Spain (Gutierrez et al., 1997). This chapter indicates that the occurrence of soil piping is related to the soil crack density and that in valley floors, large soil pipes (> 1 m in diameter) develop because of the increased infiltration on gentle slopes. In addition, in Spain, Faulkner et al. (2004) indicate that soil pipes develop into rills, which often precede gullies, after the collapse of the soil pipe roof. This finding explains part of the contrast in the headcut retreat rates between gullies with soil piping and gullies without soil piping on the medium-to-long-term time scale (**Figure 4.6** and **Figure 4.7**). However, more data are required to better contrast gully erosion rates in Vertisols. In the catchment of May Ba'ati, where the implementation of soil and water conservation measures has reduced gully headcut erosion rates, only the gullies incised in Vertisols remain notably active with retreat rates of up to 1.93 m y^{-1} (**Table 4.1**). This finding indicates that current measures to prevent gullies in Vertisol areas from expanding upslope have a limited effect. In these areas, gully headcut retreat is strongly controlled by the development of soil pipes and their collapse (**Figure 4.9**).

Figure 4.9 Gully development as a result of soil piping. The collapse of a soil pipe in the rainy season of 2008 resulted in the initiation of a gully at the site of Hagere Selam 2c (**Table 4.2**). Rapid regressive erosion occurred, resulting in a gully length of 26.8 m in 2011. The gully remains active with the occurrence of a 1.4-m-high and 0.6-m-wide soil pipe (see arrow). Photographs by Amaury Frankl.

Alternative measures are therefore needed to control sub-surface drainage in Vertisol areas, especially upslope of existing gully heads. A new method that is being tested in the catchment of May Ba'ati consists of introducing a subsurface geomembrane (vertical dam) at the gully head, which was enforced with a gabion check dam (**Figure 4.10A-E**). The subsurface dam extents 25 m at each side of the check dam and is inserted from 0.3 to 2.8 m deep. The aimed outcome of this technique is that the groundwater level upslope from the subsurface geomembrane dam would rise, and subsequently, that soil cracking and hence soil piping would decrease. Preliminary results from piezometric measurements indeed indicate that groundwater is retained longer in the Vertisol upslope of the dam after rainfall events. This is also apparent from field observations in April 2012, which show greenish grass upslope of the subsurface as a result of improved moisture conditions (**Figure 4.10F**).

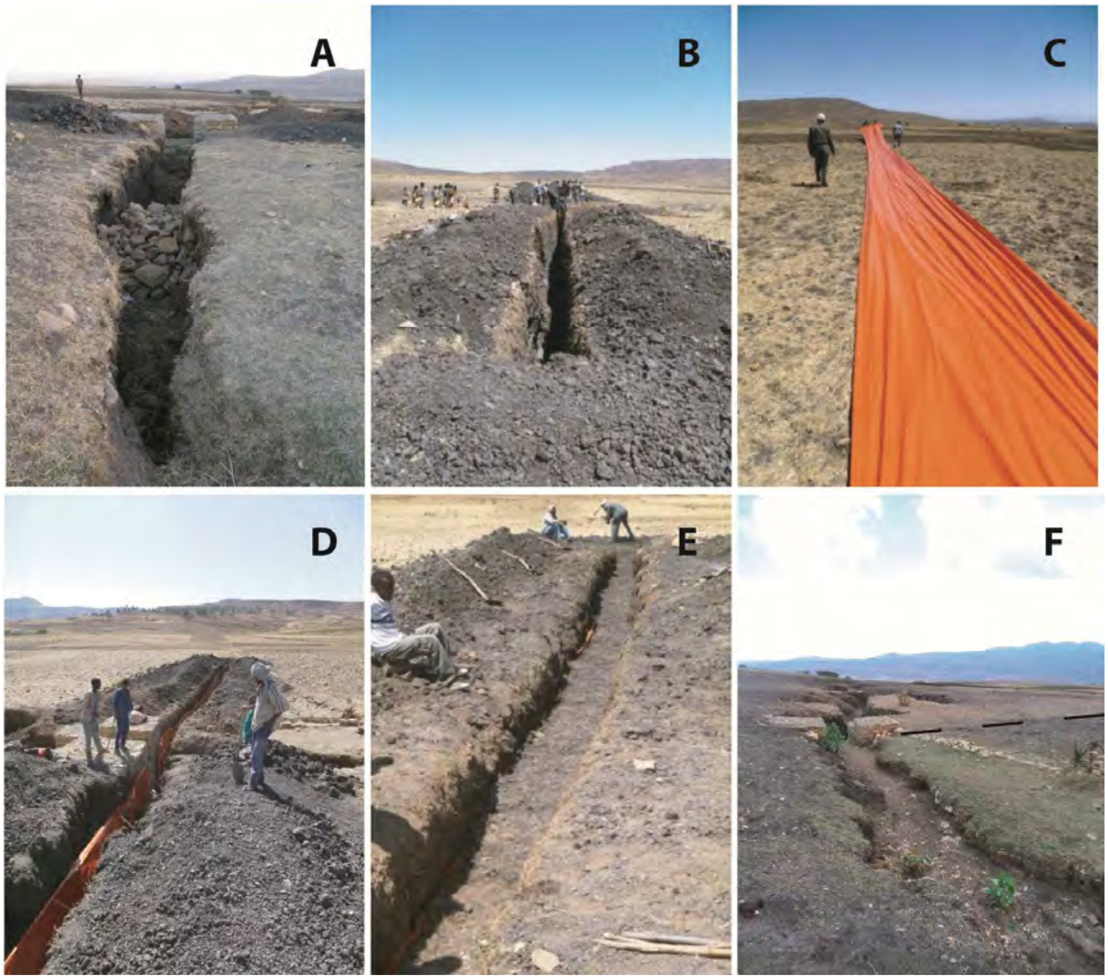

Figure 4.10 Introducing a subsurface geomembrane dam to stabilize gully heads in Vertisol areas. **A**: Reinforcement of the headcut with a gabion check dam, **B**: Digging of a 25 m long and approximately 2.8 m deep trench on both sides of the gabion check dam, perpendicularly to the gully, **C**: The geomembrane that was bought from a nearby shop, **D**: Introducing the geomembrane into the trench. The upper 0.3 m was not dammed to allow tillage and cropping, **E**: Filled trench. **F**: View on the gully head one year after installing the subsurface dam. Upslope from the dashed line, which indicates the position of the subsurface dam, the grass is greener and soil moisture is better as compared to the lower side of the dam.

4.5 Conclusions

As the first comprehensive quantitative analysis of gully head retreat rates in sub-Saharan Africa, this Chapter presents results from monitoring 24 gullies during the rainy season of 2010 and results from the study of 18 gullies on the medium-to-long-term time scale (1-47 years) in Northern Ethiopia. The study demonstrates the following conclusions:

(1) Repeat terrestrial photography is a valuable tool for assessing medium-to-long-term gully headcut retreat rates.

(2) Present (short-term) gully head retreat rates are an order of magnitude smaller than those on the medium-to-long-term time scale. The small values of R_l, R_a and V_e on the short-term time scale are explained by the increasing positive effect of gully stabilization through soil and water conservation structures that have been implemented at the catchment scale over the past 20 years and by the higher probability of extreme rainfall events during longer observation periods.

(3) Compared to similar areas worldwide, present-day gully headcut retreat rates in Northern Ethiopia occur at the same order of magnitude. On the medium-to-long-term time scale, gully head retreat appears to be more severe in Northern Ethiopia. The power relationship, $V_e = 0.53\ A^{0.31}$ ($r^2 = 0.27$), indicates that the vulnerability to gully headcut erosion rates is seven times higher in Ethiopia when compared to Southeast Spain as a result of a steeper topography, more degraded soils, more erosive rains and the presence of Vertisols.

(4) The catchment area at the gully head is the most important parameter explaining linear, areal and volumetric gully headcut retreat on the medium-to-long-term time scale. Additional gully and environmental characteristics (gully head type, headcut height, slope gradient, lithology, soil piping and land use at the gully head in 2010, average annual precipitation, average precipitation of the wettest month, Fournier Index) that were studied have no significant effect on headcut retreat. Regarding the effect of soil piping, however, a trend can be observed, which requires more observations to be fully confirmed. For the short-term observations, except for the increasing effect of soil piping on $\mathrm{Log}R_l$ and of the slope gradient on $\mathrm{Log}R_a$, there is insufficient evidence to state that the studied gully and environmental parameters, including the gully head type, the headcut height, the slope gradient at the gully head, the lithology, the soil texture at the gully head, the occurrence of soil piping and the land use at the gully head in 2010, have a significant effect on the headcut retreat rates.

(5) On the short-term and medium-to-long-term time scales, larger headcut retreat rates are observed in Vertisols where piping occurs. Particularly on the short-term, the occurrence of soil piping has clearly had an increasing effect on linear headcut retreat rates. This indicates that current soil and water conservation practices (e.g.,

slope terracing and exclosures) have only limited effects on regressive gully erosion in Vertisols where gully erosion is strongly influenced by soil piping. Therefore, alternative techniques should be developed to reduce the effect of soil piping on gully head erosion. One solution could be physically obstructing the soil pipes in Vertisol areas.

(6) The effect of recent modifications to road infrastructures was studied for 15 additional gullies. Based on these data, we conclude that headcut retreat rates for gullies in which a new road has been recently constructed in their catchment are significantly higher when compared to gullies studied on the medium-to-long-term time scale. The 95% confidence interval for an increase in gully head retreat rates to occur due to the construction of a new road is 7.3 – 29.5 m y^{-1} for R_l and 158.2 – 861.2 m^3 y^{-1} for V_e.

4.6 References

Archibold, O.W., Levesque, L.M.J., de Boer, D.H., Aitken, A.E., Delanoy, L., 2003. Gully retreat in a semi-urban catchment in Saskatoon, Saskatchewan. Appl Geogr 23, 261-279.

Billi, P., Dramis, F., 2003. Geomorphological investigation on gully erosion in the Rift Valley and the Northern highlands of Ethiopia. Catena 50, 353-368.

Boardman, J., Parsons, A.J., Holland, R., Holmes, P.J., Washington, R., 2003. Development of badlands and gullies in the Sneeuberg, Great Karoo, South Africa. Catena 50, 165-184.

Burkard, M.B. , Kostaschuk, R.A., 1997. Patterns and controls of gully growth along the shoreline of Lake Huron. Earth Surface Processes and Landforms 22, 901–11.

Croke JC, Hairsine PB. 2001. Management of road runoff: a design approach. In *Soil* Erosion Research for the 21st Century, Ascough J, Flanagan D (eds). Proceedings of International Symposium ASAE, 3–5 January 2001, Honolulu: 249–252.

Corripio, J. G., 2004. Snow surface albedo estimation using terrestrial photography. J Remote Sensing 25, 5705–5729.

Daba, S., Rieger, W., Strauss, P., 2003. Assessment of gully erosion in eastern Ethiopia using photogammetric techniques. Catena 50, 273-291.

Descheemaeker, K., Nyssen, J., Rossi, J., Poesen, J., Mitiku Haile, Moeyersons, J., Deckers, J., 2006. Sediment deposition and pedogenesis in exclosures in the Tigray Highlands, Ethiopia. Geoderma 132, 291-314.

Eitel, B., Eberle, J., Kuhn, R., 2002. Holocene environmental change in the Otjiwarongo thornbush savanna (Northern Namibia): evidence from soils and sediments. Catena 47, 43-62.

Faber, T., Imeson, A.C., 1982. Gully hydrology and related soil properties in Lesotho. Proceedings of the First Scientific General Assembly of the IAHS, July 19-30, Exeter, England, 135-144.

FAO IUSS Working Group WRB, 2007. World Reference Base for Soil Resources 2006, first update 2007. World Soil Resources Reports No. 103. FAO, Rome.

Faulkner, H., Alexander, R., Teeuw, R., Zukowsky, P., 2004. Variations in soil dispersivity across a gully head displaying shallow sub-surface pipes, and the role of shallow pipes in rill initiation. Earth Surf Process Land 29, 1143-1160.

Felix-Henningsen, P., Morgan, R.P.C., Mushala, H.M., Rickson, R.J., Scholten, T., 1997. Soil erosion in Swaziland: A synthesis. Soil Technol 11, 319-329.

Fournier, F., 1960. Influence des facteurs climatiques sur l'erosion du sol. Presses Universitaires de France, Paris.

Frankl, A., Nyssen, J., De Dapper, M., Mitiku Haile, Billi, P., Munro, R.N., Deckers, J., Poesen, J., 2011. Linking long-term gully and river channel dynamics to environmental change using repeat photography (Northern Ethiopia). Geomorphology 129, 238-251.

Gobin, A.M., Campling, P., Deckers, J.A., Poesen, J., Feyen, J., 1999. Soil erosion assessment at the Udi-Nsukka Cuesta (southeastern Nigeria). Land Degrad Dev 10, 141-160.

Graf, W.L., 1977. The rate law in fluvial geomorphology. Am J Sc 277, 178–191.

Gutierrez, M., Sancho, C., Benito, G., Sirvent, J., Desir, G., 1997. Quantitative study of piping processes in badland areas of the Ebro Basin, NE Spain. Geomorphology 20, 237-253.

Hijmans, R.J., Cameron, S.E., Parra, J.L., Jones, P.G., Jarvis, A., 2005. Very high resolution interpolated climate surfaces for global land areas. Int J Climatology 25, 1965-1978.

HTS, 1976. Tigrai Rural Development Study (TRDS). Hunting Technical Services Ltd. Governement of Ethiopia and UK Ministry of Overseas Development,. Hunting Technical Services, Borehamwood.

Ionita, I., 2006. Gully development in the Moldavian Plateau of Romania. Catena 68, 133-140.

Katsurada, Y., 2007. Regional scaled mapping of gully erosion sensitivity in Western Kenya. African J Environ Sc Technol 1, 049-052.

Knighton, D., 1998. Fluvial Forms and Processes — A New Perspective. Hodder Education, London.

Kosov et al., 1978. in Sidurchuk, A., 1999. Dynamic and static models of gully erosion. Catena 39, 11-31.

Leblanc, M.J., Favreau, G., Massuel, S., Tweed, S.O., Loireau, M., Cappelaere, B., 2008. Land clearance and hydrological change in the Sahel: SW Niger. Global Planetary Change 61, 135-150.

Martinez-Casasnovas, J.A., Ramos, M.C. and Ribes-Dasi, M., 2002. Soil erosion caused by extreme rainfall events: mapping and quantification in agricultural plots from very detailed digital elevation models. Geoderma, 125-140.

Martinez-Casasnovas, J.A., Anton-Fernandez, C. and Ramos, M.C., 2003. Sediment production in large gullies of the Mediterranean area (NE Spain) from high-resolution digital elevation models and geographical information systems analysis. Earth Surf Process Land 28, 443-456.

Martinez-Casasnovas, J.A., Ramos, M.C. and Poesen, J., 2004. Assessment of sidewall erosion in large gullies using multi-temporal DEMs and logistic regression analysis. Geomorphology 58, 305-321.

Marzolff, I., Ries, J.B., 2007. Gully erosion monitoring in semi-arid landscapes. Z Geomorph 51, 405-425.

Marzolff, I., Ries, J.B., Poesen, J., 2011. Short-term versus medium-term monitoring for detecting gully-erosion variability in a Mediterranean environment. Earth Surf Process Land 36, 1604-1623.

Meire E, Frankl A, De Wulf A, Mitiku Haile, Deckers J, Nyssen J, 2011. Land use and cover dynamics in Africa since the 19th century – warped terrestrial photographs of North Ethiopia. Regional Environ Change, submitted.

Moeyersons, J., 1991. Ravine formation on steep slopes: Forward versus regressive erosion. Some case studies from Rwanda. Catena 18, 309-324.

Moges, A., Holden, N.M., 2008. Estimating the rate and consequences of gully development, a case study of Umbulo catchment in southern Ethiopia. Land Degrad Develop 19, 574-586.

Muhindo Sahani, 2011. Le contexte urbain et climatique des risques hydrologiques de la ville de Butembo (Nord-Kivu/RDC). Thèse présentée en vue de l'obtention du grade de Docteur en Sciences, Université de Liège, Collège de doctorat en géographie, pp. 273.

Munro, R.N., Deckers, J., Grove, A.T., Mitiku Haile, Poesen, J., Nyssen, J., 2008. Soil and erosion features of the Central Plateau region of Tigrai - Learning from photo monitoring with 30 years interval. Catena 75, 55-64.

Nachtergaele, J., Poesen, J., Oostwoud Wijdenes, D., Vandekerckhove, L., 2002. Medium-term evolution of a gully developed in a loess-derived soil. Geomorphology 46, 223–239.

MU - IUC, 2007. Digital database of climatological and stream flow data of Geba catchment, obtained from National Meteorological Services Agency and Ministry of Water Resources. VLIR (Belgium) - Mekelle University Institutional University Cooperation Programme, Mekelle (Ethiopia) and Leuven (Belgium).

Nyssen, J., Moeyersons, J., Deckers, J., Mitiku Haile, Poesen, J., 2000. Vertic movements and the development of stone covers and gullies, Tigray Highlands, Ethiopia. Z Geomorph 44, 145-164.

Nyssen, J., Poesen, J., Luyten, E., Veyret-Picot, M., Deckers, J., Mitiku Haile, Govers, G., 2002. Impact of road building on gully erosion risk: a case study from the Northern Ethiopian Highlands. Earth Surf Process Land 27, 1267-1283.

Nyssen, J., Veyret-Picot, M., Poesen, J., Moeyersons, J., Mitiku Haile, Deckers, J., Govers, G., 2004. The effectiveness of loose rock check dams for gully control in Tigray, Northern Ethiopia. Soil Use Manage 20, 55-64.

Nyssen, J., Vandenreyken, H., Poesen, J., Moeyersons, J., Deckers, J., Mitiku Haile, Salles, C., Govers, G., 2005. Rainfall erosivity and variability in the Northern Ethiopian Highlands. J. Hydrol. 311, 172-187.

Nyssen, J., Poesen, J., Veyret-Picot, M., Moeyersons, J., Mitiku Haile, Deckers, J., Dewit, J., Naudts, J., Kassa Teka and Govers, G., 2006. Assessment of gully erosion rates through interviews and measurements, a case study from Northern Ethiopia. Earth Surf Process Land 31, 167-185.

Nyssen, J., Clymans, W., Poesen, J., Vandecasteele, I., De Baets, S., Nigussie Haregeweyn, Naudts, J., Amanuel Hadera, Moeyersons, J., Mitiku Haile, Deckers, J., 2009a. How soil conservation affects the catchment sediment budget - a comprehensive study in the Northern Ethiopian highlands. Earth Surf Process Land 34, 1216-1233.

Nyssen, J., Haile, M., Nauds, J., Munro, N., Poesen, J., Moeyersons, J., Frankl, A., Deckers, J., Pankhurst, R., 2009b. Desertification? Northern Ethiopia re-photographed after 140 years. Science of the Total Environment 407, 2749-2755.

Nyssen, J., Frankl, A., Munro, R.N., Billi, P. Mitiku Haile, 2010. Digital photographic archives for environmental and historical studies: the case of Ethiopia. Scottisch Geogr J 126, 185-207.

Ndona, A., Truong, P., 2011. Community mobilization for the control of ravine erosion with vetiver technology in the Congo. http://www.vetiver.org/ICV4pdfs/DC04.pdf, last accessed on 28 August 2011.

Oostwoud Wijdenes, D., Poesen, J., Vandekerckhove, L., Nachtergaele, J., De Baerdemaeker, J., 1999. Gully-head morphology and implications for gully development on abandoned fields in a semi-arid environment, Sierra de Gata, Southeast Spain. Earth Surf Process Land 24, 585-603.

Oostwoud Wijdenes, D.J., Bryan, R., 2001. Gully-head erosion processes on a semi-arid valley floor in Kenya: A case study into temporal variation and sediment budgeting. Earth Surf Process Land 26, 911-933.

Parker, G., G., 1963. Piping, a geomorphic agent in landform development of the drylands. International Association of Hydrological Sciences 1963, 103-113.

Parkner, T., Page, M. J., Marutani, T., Trustrum, N.A., 2006. Development and controlling factors of gullies and gully complexes, East Coast, New Zealand. Earth Surf Proces Land 31, 187-199.

Poesen, J., Nachtergaele, J., Verstraeten, G., Valentin, C., 2003. Gully erosion and environmental change, importance and research needs. Catena 50, 91-133.

Radoane, M., Ichim, I. and Radoane, N., 1995. Gully distribution and development in Moldova, Romania. Catena 24, 127-146.

Reubens, B., Poesen, J., Nyssen, J., Leduc, Y., Amanuel Zenebe, Sarah Tewoldeberhan, Bauer, H., Kindeya Gebrehiwot, Deckers, J., Muys, B., 2009. Establishment and management of woody seedlings in gullies in a semi-arid environment (Tigray, Ethiopia). Plant Soil 324, 131-156.

Ries, J., B., Marzolff, I., 2003. Monitoring of gully erosion in the Central Ebro Basin by large-scale aerial photography taken from a remotely controlled blimp. Catena 50, 309-328.

Scholiers, N., 2010. Development of gully networks and volumes since 1965 in the May Mekdan catchment (North Ethiopian highlands). MSc. thesis, Department of Geography, Ghent University, Ghent.

Seginer, I., 1966. Gully development and sediment yield. Journal of Hydrology 4, 236–53.

Stock, S., 2011. Land use/land cover and population dynamics in Northern-Ethiopia as derived from aerial photographs. MSc. thesis, Department of Geography, Ghent University, Ghent.

Showers, K., 1996. Soil Erosion in the Kingdom of Lesotho and Development of Historical Environmental Impact Assessment. Ecological applications 6, 653-664.

Stocking, M.A., 1980. Examination of factors controlling gully growth. In De Boodt M, Gabriels D (eds)Assessment of Erosion. John Wiley & Sons, Chichester, 505–20.

Swanson, M., Kondolf, G., M., Boison, P., J., 1989. An example of rapid gully initiation and extension by subsurface erosion: Coastal San Mateo County, California. Geomorphology 2, 393-403.

Thompson, J.R., 1964. Quantitative effect of watershed variables on rate of gully-head advancement. Transactions of the American Society of Agricultural Engineers 7, 54–5.

US Soil Conservation Service, 1966. Procedures for determining rates of land damage, land depreciation and volume of sediment produced by gully erosion. Technical Release 32, USDA, Washington, DC, 18 pp.

Valentin, C., Poesen, J., Li, Y., 2005. Gully erosion, impacts, factors and control. Catena 63, 132-153.

Vandekerckhove, L., Poesen, J., Oostwoud Wijdenes, D., Gyssels, G., 2001. Short-term bank gully retreat rates in Mediterranean environments. Catena 44, pp. 133-161.

Vandekerckhove, L., Poesen, J., Govers, G., 2003. Medium-term gully headcut retreat rates in Southeast Spain determined from aerial photographs and ground measurements. Catena 50, 329-352.

Vicente, F., Sanz, M. A., Lucía, A., Martín-Duque, J. F., 2009. Evolución geomorfológica en tiempos históricos recientes de cárcavas del borde del piedemonte norte del Guadarrama (Segovia, España). Estudio a partir de fuentes documentales. Bol. R. Soc. Esp. Hist. Nat. Sec. Geol. 103, 1-4.

Virgo, K.J., Munro, R.N., 1978. Soil and erosion features of the Central Plateau region of Tigrai, Ethiopia. Geoderma 20, 131-157.

Williams, M., Williams, F., 1980. Evolution of the Nile basin. In, Williams, M., Faure, H. (Eds.), The Sahara and the Nile. Quaternary Environments and Prehistoric Occupation in Northern Africa. Balkema, Rotterdam, pp. 207-224.

Wu, Y., Cheng, H., 2005. Monitoring of gully erosion on the Loess Plateau of China using a global positioning system. Catena 63, 154-166.

Part 2

Chapter 5
Land use and cover changes since the 19th century as evidenced by terrestrial photographs

This chapter is modified from:

Meire, E., Frankl, A., De Wulf, A., Mitiku Haile, Deckers, J., Nyssen, J., 2012. Mapping the 19th century landscape in Africa – warped terrestrial photographs of North Ethiopia. Regional Environmental Change. accepted for publication.

Abstract

Quantitative research on land use and land cover (LUC) in Africa usually addresses the second half of the 20th century, by using remote sensing data. Terrestrial photographs, which in Ethiopia are available since 1868, are seldom used in a quantitative way. This chapter presents a methodology that allows to produce land use and land cover (LUC) maps on the basis of old terrestrial photographs. Therefore, land use and land cover was investigated on historical and present-day photographs, and these interpretations were warped to the horizontal plane of the map. The resulting maps allow to gain better insights into LUC changes over a period of 140 years. The results show that woody vegetation increased strongly, together with an increase in built-up area. This occurred especially at the expense of bushland. The study validates pervious findings and shows that improved land management strategies in one of the world's most degraded areas can lead to environmental rehabilitation.

Keywords: Land use and land cover, Northern Ethiopia, Terrestrial photographs, Warping, Woody vegetation.

5.1 Introduction

It is commonly suggested that Ethiopia was far more forested 2-3 generations ago than it is at present, claiming that 40% of the country was covered by forests only 100 years ago (e.g., Taddesse, 1995). However, based on historical documents and observations from archival terrestrial photographs, such claims have been questioned and even contradicted (e.g., Pankhurst, 1995; Wøien, 1995; Mc Cann, 1997; Crummey, 1998; Nyssen et al., 2004; Nyssen et al., 2009). Quantitative assessments of land use and cover (LUC) so far relied on aerial photographs and satellite images, allowing the preparation of LUC maps from the 1950s onwards (e.g., Chapter 6; Wøien, 1995). Historical terrestrial photographs, which are available since 1868 in Ethiopia, were never used in a quantitative way for LUC studies.

Preparing LUC maps from terrestrial photographs can rather easily be done by the use of metric or calibrated cameras (e.g., Welch et al., 2002). From conventional ground-based photography, which use non-metric or uncalibrated cameras, LUC maps can not readily be prepared. Photographing landscapes from the on-the-ground perspective results in large distortions of the scenery as displayed on photographs. Most studies which are based on conventional terrestrial photographs therefore limit themselves to qualitiative assessments of LUC, and do not add real geographical positions to their interpretations (e.g., Butler, 1994; Kull, 2005; Byers, 2007). A semi-quantitative approach was proposed by Dervieux (2004), by visually transferring LUC entities to topographic maps. Strict quantitative assessments of LUC from terrestrial photographs were also proposed, but are usually difficult to apply. For example, Corripio (2004) presented a technique that georeferences oblique photographs to a high-resolution Digital Elevation Model (DEM), by defining a mapping function between photograph pixels and DEM cells. Web-based 3D-reconstructions of LUC from photographs have also been elaborated (e.g., Vergauwen and Van Gool, 2006; Frahma et al., 2010).

The presented study introduces a methodology to produce LUC maps from interpretations on terrestrial photographs, by warping topographic units observed on the photographs to the horizontal plane of the map. The methodology is illustrated for Northern Ethiopia. Results will allow to assess (and to a certain extent, to explain) the major land use and cover changes that occurred in the Northern Ethiopian Highlands since the late 19th century. To a further extent, this study will contribute to the understanding of LUC changes in African Highlands starting from the late 19th century.

5.2 Materials and Methods

5.2.1 Study area

5.2.1.1 General setting

The study was conducted in the Northern Ethiopian Highlands (Tigray Regional State), in an area located between 12°30' - 14°10' N and 39°15' - 39°45' E (**Figure 5.1**). Five study sites were selected along a 200 km north-south transect, based on the variability in environmental characteristics in terms of elevation, relief, geology, soils and land use (history). From north to south the study areas are: Sinkata (2200 m a.s.l.; 0.1 km^2), Adi Shuho (2600 m a.s.l.; 4.9 km^2), Ayba (2750 m a.s.l.; 2.6 km^2), Bolago (3500 m a.s.l.; 4.0 km^2) and Ashenge (2450 m a.s.l.; 0.3 km^2).

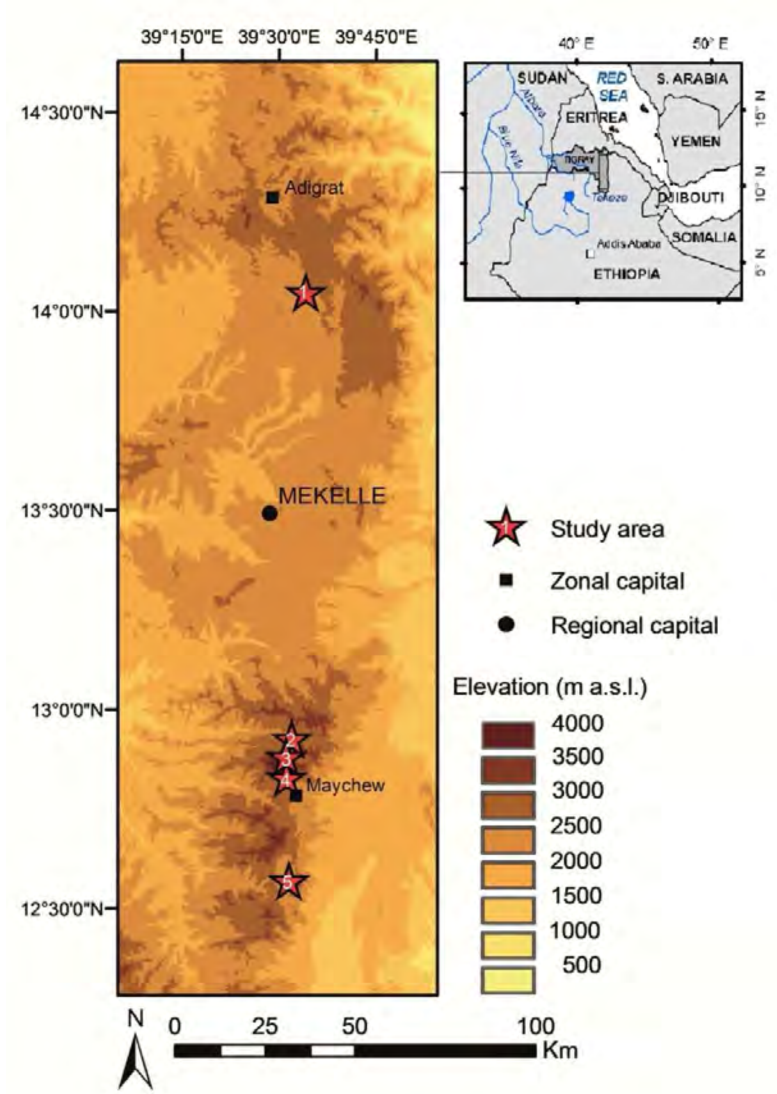

Figure 5.1 Map of the study areas in Tigray, Northern Ethiopia (1 Sinkata, 2 Adi Shuho, 3 Ayba, 4 Bolago, 5 Ashenge) (source: (a) DTM from NGA-NASA 2000, own processing, (b) after UNDP-EUE, 1998).

The Highlands border the Rift Valley on the west and are mainly composed of Mesozoic limestone and sandstone covered by Tertiary volcanics (Hofmann et al., 1997; Arndt and Menzies, 2005). The uplift of these lithological units over the past 25 million years (Cohen et al., 1993) and their differential resistance to erosion gave the Highlands their typical relief of stepped, flat topped mountains (*ambas*), dissected by canyon-like valleys. Elevations range between 1500 and 4000 m a.s.l.

Located in the sub-Saharan semi-arid belt, the Northern Ethiopian Highlands are one of the world's most drought-prone zones. The ustic rainfall regime is driven by the position of the Inter Tropical Convergence Zone (Robinson and Henderson-Sellers, 1999). Its passage over the Highlands from March until May announces the beginning of the monsoon type rainy season (called the *belg* season), intensifying from June until September (called the *kiremt* season). Precipitation occurs as intense rainstorms with large rain-drop sizes (Nyssen et al., 2005). Annual precipitation increases from north to south, ranging between 500 and 900 mm y^{-1}. The inter-annual variability, however, differs considerably. Mean annual temperatures range from 13° C (Bolago) to 21° C (Ashenge) (as derived from the FAO® New_LocClim V1.11 database).

5.2.1.2 Land use

The land use types that prevail in Northern Ethiopia comprise of: (i) cropland, (ii) villages, (iii) exclosures and (iv) pastures and rangelands (**Figure 5.2**). Small-scale rain-fed agriculture dominates the farming system (Virgo and Munro, 1978). Individual land holdings seldom cover an area larger than 1 ha (Atakilte et al., 2006). Croplands are preferably situated on flat areas, but also appear on (steep) hillslopes. There, soil and water conservation (SWC) measures like stone bunds or trenches are usually applied to constrain soil erosion. Villages mainly include clustered farms, community or commercial buildings, footpaths and Eucalypt trees. Exclosures are demarcated areas for woody vegetation recovery in which grazing and wood harvesting are restricted or prohibited (Badege, 2001). They are implemented on community land, most frequently on very steep and degraded slopes which suffer from severe erosion (Descheemaeker et al., 2006). Exclosures can eventually give rise to secondary forests, but contrast from the remnants of natural forests, which are usually church forests (Aerts, 2007). Pastures and rangelands constitute the areas primarily used for livestock grazing. Rangelands include all kinds of terrestrial ecosystems in which grazing is allowed (Szaro and Johnston, 1996), but in this study concern all grazing lands apart from grasslands (e.g., shrubland). Grasslands are areas with moist soil conditions that are used for livestock feeding.

Land use is typically related to the geomorphic setting. Croplands and grasslands are mostly situated in valley bottoms or on intermediate flats. Forests and rangelands usually cover mountain slopes, while villages generally occur on mountain slopes or breaks of slopes where shallow soils prevail (**Figure 5.2**).

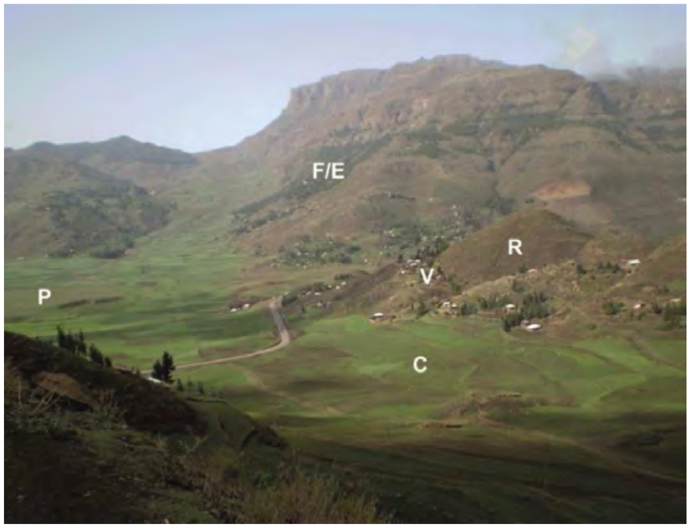

Figure 5.2 Dominant land use types of Northern Ethiopia: cropland (C), forest (F), exclosure (E), rangeland (R), pasture (P) and village (V) (photograph covers Ayba; photograph taken in July 2008).

5.2.1.3 Land cover

Main crops grown in the Northern Ethiopian Highlands are tef (*Eragrostis tef*), barley (*Hordeum vulgare* L.), wheat (*Triticum* sp.), sorghum (*Sorghum bicolor*), and maize (*Zea mays*), complemented by leguminous crops such as field peas (*Pisum sativum*), chickpeas (*Cicer arietinum*) and horse bean (*Vicia faba*). Around homesteads, *Gesho* (*Rhamnus prinoides*) is cultivated as an ingredient of a local beer called *sowa.* Major herb species are *Argemone mexicana*, *Aloe* spp., *Phytolacca dodecandra* and *Kniphofia foliosa*. Grass species have not been inventoried. *Opuntia ficus-indica*, *Carduus nyassanus* and *Rumex nervosus* constitute the largest part of the natural shrub cover, *Sansevieria trifasciata* is especially found in villages. Tree cover is dominated by *Eucalyptus globulus, Eucalyptus camaldulensis*, *Juniperus procera*, species of *Acacia*, *Olea europaea* ssp. *africana*, and *Euphorbia candelabrum*. *Eucalyptus* is by far the most encountered tree genus in the study areas and probably all over Northern Ethiopia. It occurs under the form of (i) large patches: plantations/exclosures and church forests, (ii) linear shapes: planted along gullies with the aim of limiting their lateral expansion; on land use boundaries near villages and (iii) small clusters: on farmlands and in villages. Species were determined following November et al. (2002) and Addis et al. (2005).

5.2.2 Repeat photography

Among the numerous existing historical terrestrial photographs of Northern Ethiopia (Munro et al., 2008; Nyssen et al., 2009; Frankl et al., 2011), a subset was selected that covers early periods for which remote sensing techniques are no option.
In total, ten photographs were selected from 1868, 1936, 1942, 1944 or 1961 (**Table 5.1**). Five 1868 photographs were taken during the British military expedition of 1867-1868 to former Abyssinia. The objective was to release a number of Europeans who had been imprisoned by Emperor Theodore (Sharf et al., 2003). During that campaign, sepia photographs were taken by the 10th Company of Royal Engineers, and represent the oldest landscape photographs of Ethiopia. They were made with a Dallmeyer's triplet achromatic camera (Gordenker and Cohen, 2006). The black-and white 1936 photograph was taken during the Italian occupation by an anonymous photographer. It was obtained from Ritler and Scheidegger (1999). Two black-and white photographs from 1942 and 1944 were taken by David Buxton while travelling in Ethiopia (Buxton, 1949). The 1961 color photographs considered in this study were taken by Alfred T. Grove while investigating Quaternary landforms in Eastern Africa (Adams et al., 1999).

The landscapes photographed have been revisited in the rainy season of 2008. Since the old photographs were not taken with the aim of being repeated, the camera locations were not permanently marked in the landscape. The repositioning was based on relocations carried out in 2007, by lining up landscape features in the fore- and background in a triangulation system (Nyssen et al., 2009; Frankl et al., 2011). Particular problems concerned atmospheric conditions and the lack of a clear, unobstructed view over the subject. For example, trees were an obstacle in Adi Shuho and Bolago. Repeat photographs were then taken by standing on top of large boulders or by ascending upon a near mountain slope at the back of the original viewpoint. The recent photographs were made using a digital Olympus© FE-210/X-775 camera. Several repeat photographs of the same historical photograph were taken successively; the one that closely matched the old one was selected for further research. As the repeat photographs had a larger angle of view, they were cropped to be precise repeat photographs. This created a uniform sampling area, which is a requisite for quantitative photo-analysis (Manier and Laven, 2002).

Table 5.1 Metadata of the historical and repeat photographs.

Study area		Photocouple*	Author	Year
Ashenge	1	KO-1936-AN-I19	Unknown	1936
		KO-1936-AN-I19-R1-2009-NY	J. Nyssen	2009
	2	KO-1961-GR-531	A. T. Grove	1961
		KO-1961-GR-531-R3-2008-ME	E. Meire	2008
	3	KO-1961-GR-528	A. T. Grove	1961
		KO-1961-GR-528-R3-2008-ME	E. Meire	2008
Bolago	4	MA-1868-RE-25	British Royal Engineers	1868
		MA-1868-RE-25-R2-2008-ME	E. Meire	2008
	5	MA-1868-RE-26/27	British Royal Engineers	1868
		MA-1868-RE-26/27-R2-2008-ME	E. Meire	2008
Ayba	6	MA-1942-DB-2	D. Buxton	1942
		MA-1942-DB-2-R1-2008-ME	E. Meire	2008
Adi Shuho	7	MA-1944-DB-26/27	D. Buxton	1944
		MA-1944-DB-26/27-R1-2008-ME	E. Meire	2008
	8	MA-1961-GR-526	A. T. Grove	1961
		MA-1961-GR-526-R2-2008-ME	E. Meire	2008
Sinkata	9	SE-1868-RE-19	British Royal Engineers	1868
		SE-1868-RE-19-R3-2008-ME	E. Meire	2008
	10	SE-1868-RE-20	British Royal Engineers	1868
		SE-1868-RE-20-R3-2008-ME	E. Meire	2008

* Photographs earlier than 1961 are black-and-white or sepia photographs

5.2.3 LUC classification

By investigation the LUC on the historical and repeat photographs and by making observations in the field, the following LUC classes could be distinguished: cropland, forest, Eucalypt plantation, bushland, grassland, village, bare ground and bedrock (**Table 5.2**). These classes and their definition are in accordance with Chapter 6, which investigates LUC changes from Landsat imagery in Northern Ethiopia.

Table 5.2 Description of the LUC classes.

LUC class or detailed LUC class	Description
I Cropland	Cultivated land with rainfed or irrigated, annual or rarely perennial crops
I.A Cropland	Without soil or stone bunds, always located on flat areas (e.g. plains)
I.B With soil/stone bunds	With soil and/or stone bunds, preferably located on areas with gentle slopes (e.g. foot slopes, plateaus, valley floors), herbs and grasses appear on the bunds
I.B.1 and scattered trees	With scattered Juniperus procera, seldom more than 2 trees per land unit
I.B.2 and clustered Eucalyptus	With groups of Eucalyptus (e.g. afforestation in gullies) that cover only a small area of the land units (< 5%)
I.B.3 and mixed shrubland	Including patches of shrubs that cover <50 % of total land unit area
I.B.4 and mixed shrubland and grassland	Including patches of grassland and shrubs, height < 30 cm, that cover <50 % of total land unit area
II Forest	Tree-plant patch, total canopy cover >20 %, shrubs, herbs and grasses can cover the lowest forest layer, generally found on steep slopes that are often provided with stone bunds
II.D Dense mixed forest	Total canopy cover >50 %, Juniperus procera and Eucalyptus mostly are the dominant tree species, or dominant tree species has not been identified
II.E Open mixed forest	Total canopy cover 20-50 %, Juniperus procera and Eucalyptus mostly are the dominant tree species, or dominant tree species has not been identified
II.F Dense Juniperus forest	Total canopy cover >50 %, Juniperus procera is dominant tree species
II.F.1 with mixed housing	Including patches of traditional/modern/mixed housing that cover <20 % of total land unit area
II.G Open Juniperus forest	Total canopy cover 20-50 %, Juniperus procera is dominant tree species
II.G.1 with high stoniness	Stoniness >40 %
III Eucalyptus plantation	Eucalyptus plant is main land cover, total canopy cover >20 %, shrubs, herbs and grasses can cover the lowest forest layer, found on steep slopes that are often provided with stone bunds
III.H Dense Eucalyptus plantation	Total canopy cover >50 %, Eucalyptus is dominant tree species, usually found around churches ('church forest') and steep slopes
III.H.1 with high stoniness	Stoniness >40 %
III.I Open Eucalyptus plantation	Total canopy cover 20-50 %, Eucalyptus is dominant tree species, usually found on the highest and steepest slopes

Table 5.2 continued

IV Bushland	Shrubs constitute the prevailing land cover, often related to rangeland, found on steep slopes, rangeland or exclosure
IV.I Shrubland	10-50 % of total land unit area is covered with shrubs, <50 % herbs and grasses, no woody vegetation
IV.I.1 with scattered trees	Including scattered trees (e.g. Acacia spp., Juniperus procera)
IV.I.2 with clustered Eucalyptus	Including patches of Eucalyptus plantation, total canopy cover <20 %
IV.I.3 with scattered trees and clustered Eucalyptus	Including scattered trees (e.g. Acacia spp., Juniperus procera) and patches of Eucalyptus plantation, total canopy cover <20 %
IV.I.4 with mixed cropland	Including patches of cropland that cover <50 % of total land unit area
IV.I.5 with traditional housing	Including traditional houses
IV.I.6 with mixed housing and scattered trees	Including mixed housing and scattered trees (e.g. Acacia spp., Juniperus procera), canopy cover <20 %
IV.I.7 with high stoniness	Stoniness >40 %
IV.I.8 with high stoniness and scattered trees	Including scattered trees (e.g. Acacia spp., Juniperus procera), canopy cover <20 %, stoniness >40 %
IV.J Degraded shrubland	10-30 % of total land unit area is covered with shrubs, <50 % herbs and grasses, exposing bedrock up to 60 % of total land unit area, no woody vegetation
IV.J.1 with clustered trees	Including clustered Olea europaea ssp. Africana or Eucalyptus, canopy cover <20 %
IV.K Dense bushland	>50 % of total land unit area is covered with shrubs, <50 % herbs and grasses, no woody vegetation
IV.K.1 with scattered trees	Including scattered trees (e.g. Acacia spp., Juniperus procera), canopy cover <20 %
V Grassland	Grasses and herbs constitute the prevailing land cover, usually related with grazing land, mainly found on flat areas
V.L Grassland	>90 % of total land unit area is covered with grasses and herbs, no woody vegetation
V.L.1 with scattered trees	Including scattered trees (e.g. Juniperus procera),intermediate between grassland and open forest
V.M Degraded grassland with scattered shrubs	<50 % of total land unit area is covered with grasses and herbs, exposing bedrock up to 30 % of total land unit area
VI Village	Rural settlement, including community buildings and houses, preferably located on gentle till sleep slopes
VI.N Modern village	Frequency of houses with a metal roof >50 %
VI.N.1 with mixed cropland and shrubland	Including patches of cropland and shrubland, total canopy cover < 50 %
VI.N.2 with mixed cropland and clustered Eucalyptus	Including patches of cropland and Eucalyptus clustered in patches or as living fences, total canopy cover <50 %

Table 5.2 continued

VI.N.3 with mixed cropland, scattered trees and clustered Eucalyptus	Including patches of cropland, scattered trees (e.g. Acacia spp., Juniperus procera) and Eucalyptus clustered in patches and/or as living fences, canopy cover <50 %
VI.N.4 with mixed cropland, shrubland and clustered Eucalyptus	Including patches of cropland, shrubland and Eucalyptus clustered in patches and/or as living fences, canopy cover <50 %
VI.N.5 with mixed cropland, shrubland, scattered trees and clustered Eucalyptus	Including patches of cropland, shrubland, scattered trees (e.g. Acacia spp., Juniperus procera) and Eucalyptus clustered in patches and/or as living fences, canopy cover <50 %
VI.N.6 with mixed shrubland, scattered trees and clustered Eucalyptus	Including patches of shrubland, scattered trees (e.g. Acacia spp,. Juniperus procera) and Eucalyptus clustered in patches and/or as living fences, canopy cover <50 %
VI.N.7 with mixed grassland and clustered Eucalyptus	Including patches of grassland and Eucalyptus clustered in patches and/or as living fences, canopy cover <50 %
VI.N.8 with mixed grassland, scattered trees and clustered Eucalyptus	Including patches of grassland, scattered trees (e.g. Acacia spp., Juniperus procera) and Eucalyptus clustered in patches and/or as living fences, canopy cover <50 %
VI.O Traditional village	Frequency of houses with straw roof >50 %
VIO.1 with clustered trees	Including clustered Olea europaea ssp. Africana or Eucalyptus, canopy cover <50 %
VI.O.2 with mixed shrubland and scattered trees	Including patches of shrubland and scattered trees (e.g. Juniperus procera, Acacia spp).
VI.O.3 with mixed shrubland and clustered Eucalyptus	Including patches of shrubland and Eucalyptus clustered in patches or as living fences, canopy cover <50 %
VI.P Mixed village	Frequency distribution of houses with a metal and a straw roof is 50 %-50 %
VI.P.1 with scattered trees and clustered Eucalyptus	Including scattered trees (e.g. Juniperus procera, Acacia spp). and Eucalyptus clustered in patches or as living fences, canopy cover <50 %
VI.P.2 with mixed cropland, shrubland and clustered Eucalyptus	Including patches of cropland, shrubland and clustered Eucalyptus, canopy cover <50 %
VI.P.3 with mixed cropland, shrubland, scattered trees and clustered Eucalyptus	Including patches of cropland, shrubland, scattered trees (e.g. Juniperus procera, Acacia spp.) and clustered Eucalyptus, canopy cover <50 %
V.I.P.4 with mixed shrubland, scattered trees and clustered Eucalyptus	Including patches of shrubland, scattered trees (e.g. Juniperus procera, Acacia spp.) and clustered Eucalyptus, canopy cover <50 %
VII Bare ground	No woody vegetation, <5 % shrubs, herbs and/or grasses, exposing soils up to 99 % of total land unit area, found on gentle to very steep slopes
VIII Bedrock	Exposing bedrock upt to 80 % of total land unit area

5.2.4 GPS measurements

Global Positioning System (GPS) measurements were done with a differential Trimble® GPS (Geo XH 2005 series) providing 0.30 m to 1 m planimetric accuracy and 1 to 3 m altimetric accuracy after postprocessing. GPS measurements were required for two purposes: (i) for the creation of orthophotographs and, (ii) to warp LUC units that were demarcated on the photographs to the horizontal plane of the map.

5.2.5 Preparation of othophotographs

Orthophotographs served as a base for the production of LUC maps. These were produced by digital image processing of the scanned aerial photographs (scale ~ 1:50 000, scanning at 1200 dpi with a desktop scanner) with Supersoft® Inc VirtuoZo 2.2. The geometric rectification was based on a digital elevation model (DEM) devised for the same area. The DEMs were produced through digital photogrammetric restitution and included inner and exterior orientations. The relative orientation was based on > 300 tie points per stereo pair, and the exterior orientation was based on ground control points (GCPs).

Typical GCPs were mountain tops, large trees, road crossings, remarkable points on cliffs, edges of rocks, large boulders and small churches. Recording the elevation of some features required reading the z-coordinate on a nearby rising slope or was calculated on the basis of trigonometry (Tovey, 1982). The GCPs were located at different elevations and as much as possible homogenously distributed over the area covered by the aerial photographs. This was not always the case since some areas were inaccessible. For example, in Ayba a few extreme mountain peaks were too steep to climb. In Sinkata, a minefield was avoided.

Several orthophotographs were created for each area, by using an increasing number of GCPs. The orthophotograph with the greatest positional accuracy was selected, based on (i) the lowest Root Mean Square Error (RMSE) in x and y and, (ii) the positional accuracy as compared to 1:50 000 topographic maps from the Ethiopian Mapping Authority.

5.2.6 Warping land use and cover interpretations to the horizontal plane of the map

The interpretation of LUC on the historical and repeat photographs was done primarily from the camera location, by looking over the photographed landscape. LUC was defined for the previous and current situation per land unit. A land unit corresponds to an area delimited on the photographs, which is homogeneous in LUC (according to **Table 5.2**) for a certain period. Every land unit was numbered and the historical and the current LUC types were specified. LUC units that were demarcated on the photographs were characterized in detail in accordance to Section 5.2.3. This involved observing and documenting the present-day LUC in the field.

The interpretation of LUC for the historical period was not always straightforward. For example, on sepia or black-and white photographs, a dark zone on a far-away mountainslope could equally be shadow from a cloud or a forest patch (Kull, 2005). Hence, such distant backgrounds were excluded from the analysis. Care was also required when assessing LUC on historical photographs that were not from the same season as the field visit. Especially differences in vegetation status between dry and rainy season needed to be accounted for.

Warping LUC interpretations to the horizontal plane of the map required to eliminate deformations in the photograph that are apparent when mountainous landscapes are photographed from the on-the-ground perspective. This was done by considering topographic units visible on the photographs separately. Each of these units, having a distinct slope gradient and orientation, has a specific angle of incidence (Aguiló and Iglesias, 1995). The incident angle introduces an optical effect that brings on a perspective distortion which influences the mapping resolution. Areas on the foreground and steep slopes oriented towards the observer's spot have larger incident angles than (nearly) flat areas in the background (**Figure 5.3**).

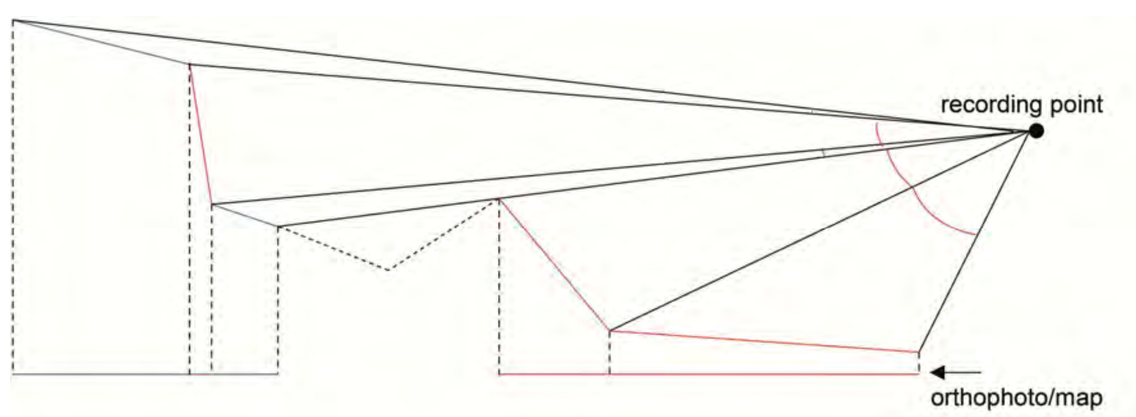

Figure 5.3 Incident angles of topographic units in relation to the orthogonal projection of the units on the map: (nearly) flat areas in the photograph background result in small incident angles (blue), flat areas on the foreground or steep slopes oriented towards the recording point produce large incident angles (red) and hidden zones of the scene (dotted lines) lead to blanks on the map.

Topographic entities were warped separately to the horizontal plane of the map. Therefore, numerous GPS measurements delimiting the topographic units were made in the field. As these recordings relate to the terrestrial photograph, they were called

Photograph Control Points (PCPs). Additionally, recordings derived from the orthophotographs were used. With this methodology, topographic units that were not visible from the observer's point were excluded (**Figure 5.3**).

5.2.7 Delineation of the mapping boundaries

The delineation of the mapping boundaries was done by transferring the area covered by the terrestrial photographs visually to the orthophotographs. In addition, two techniques were applied to minimize errors. Firstly, an ESRI® View Shed analysis with the photograph recording point as center was performed. This excludes all areas that cannot be viewed from the photograph location. Secondly, a method was developed to delineate left and right photograph boundaries when visually indefinable. Therefore, the horizontal field of view (β) was calculated for the uncropped repeat photographs (equation (1); Covington, 2007). β is the field of view of a photograph measured along the horizontal axis (Greene, 2001). Together with the vertical field of view, β determines the angle of view (Simmons, 1987). From β, the horizontal angle (α) between the midpoint of the uncropped image and the left or right boundary of the cropped or precise repeat photograph could be determined. Therefore, we assumed that (i) the image sensor of the camera was held nearly horizontally and, (ii) the midpoint of the historical landscape photograph, or another point on the photograph with perpendicular bisector could be located on the orthophotograph.

$$\beta = 2 \arctan (l/2f) \qquad (5.1)$$

where:

f = focal length, and

l = length of the digital image format

A three dimensional representation of β shows how to quantify α using goniometry (**Figure 5.4**). The elaborated technique could also provide additional points to delineate the lower or upper boundary of a photograph. For example, the intersection of the footpath on the foreground of photograph KO-1961-GR-531 and its lower boundary can be located by calculating δ (**Figure 5.4**)

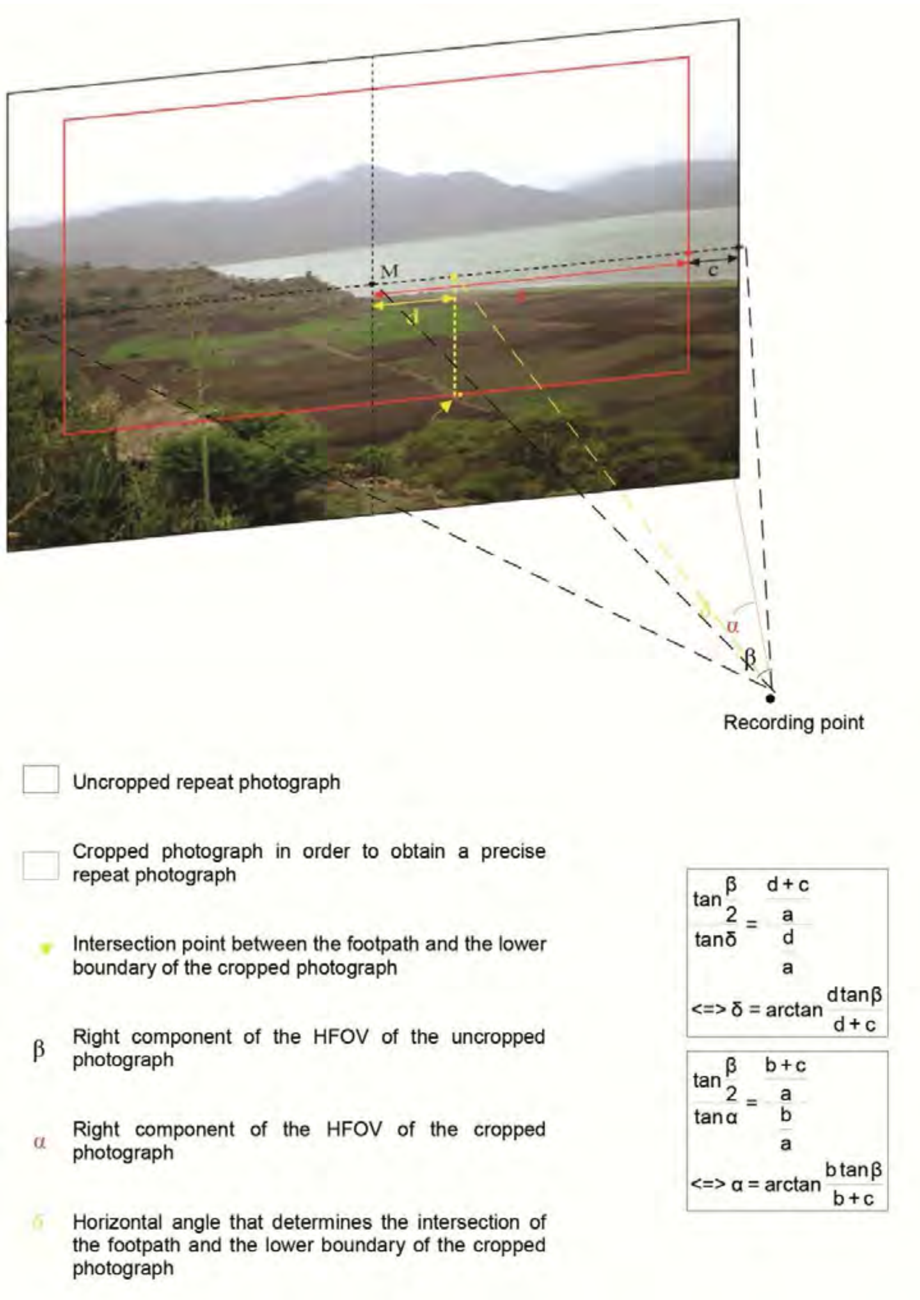

Figure 5.4 Calculation of α and δ using goniometry as part of a technique to delineate photograph boundaries on the two-dimensional plane of the map.

5.2.8 From interpreted terrestrial photograph to LUC map

Figure 5.5 shows the step-by-step method of creating LUC maps from terrestrial photographs, illustrated by the case of Bolago. The Geographic Information System package used for this was ArcGIS® 9.2.

STEP 1: Defining topographic units and characterizing land units.

Topographic units (TU) were defined on the photographs and LUC was interpreted per land unit. Targeted photo control points were indicated on the photographs.

STEP 2: Recording Photo Control Points in the field (PCPs) and selecting additional tie-points from orthophotographs

For each topographic unit, PCPs were measured in the field. In addition to PCPs, stable landscape features that could be recognized on the orthophotographs were also pointed on the terrestrial photographs.

STEP 3. Warping the topographic units to the horizontal plane of the map and delineation of the mapping boundaries

Warping the rasterized topographic units was done by a spline transformation method, which gave the best results. At least ten tie-points were required per topographic unit to optimize the warping. Next to PCPs, tie-points consisted of features visible on both the terrestrial photograph and the orthophotograph. The delineation of the mapping boundaries was done by a viewshed analysis and by calculating the horizontal field of view of the historical photographs.

STEP 4:Quality check

The quality check of the warping result involved:

- plotting view lines from the recording point toward the mapped area (locations that are in vertical alignment on the ground photographs should be located on a single view line on the plane of the map),
- the creation of a virtual photograph of every warping product in ESRI® ArcScene 9.2 - the warping procedure is optimal when this virtual image provides the same view as the ground photographs,
- analyzing LUC as related to contour lines derived from the DEM. This allows investigate on the accuracy at which the topographic unit boundaries have been warped.

STEP 5: Preparation of LUC maps

Finally, a LUC map was prepared according to mapping standards.

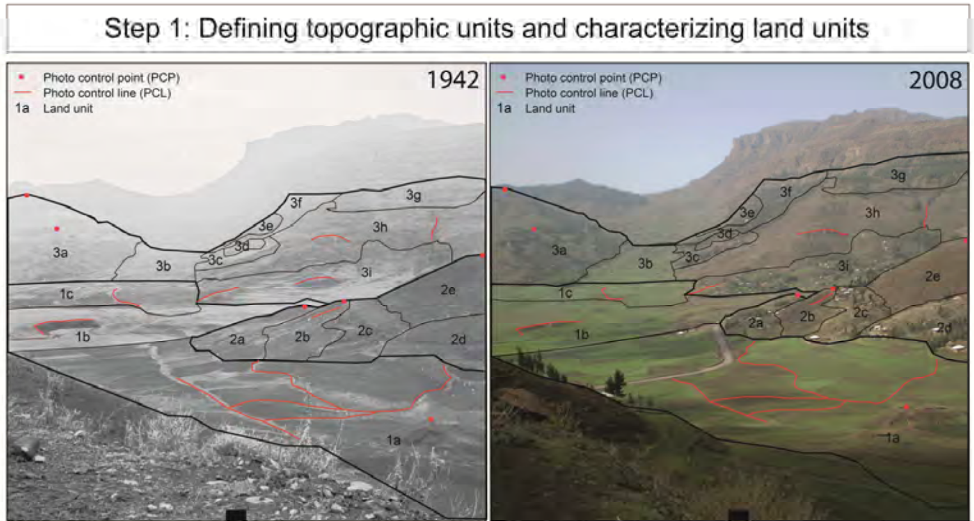

TU	LU	LUC 1942	LUC 2008
1	a	Cropland with soil/stone bunds	Cropland with soil/stone bunds
	b	Grassland	Grassland
	c	Cropland with soil/stone bunds	Cropland with soil/stone bunds
2	a	Dense bushland	Modern village with mixed cropland and shrubland
	b	Shrubland	Shrubland
	c	Shrubland	Modern village with mixed cropland, shrubland and clustered
	d	Dense bushland	Modern village with mixed cropland, shrubland and clustered
	e	Dense bushland	Shrubland
3	a	Dense bushland	Mixed village with mixed cropland, shrubland, scattered trees
	b	Cropland with soil/stone bunds	Cropland with soil/stone bunds
	c	Cropland with soil/stone bunds and mixed	Modern village with mixed cropland, shrubland and clustered
	d	Shrubland	Shrubland
	e	Open mixed forest	Dense mixed forest
	f	Shrubland	Dense mixed forest
	g	Shrubland	Open *Eucalyptus* plantation
	h	Dense bushland	Shrubland
	i	Cropland with soil/stone bunds	Modern village with mixed cropland and shrubland

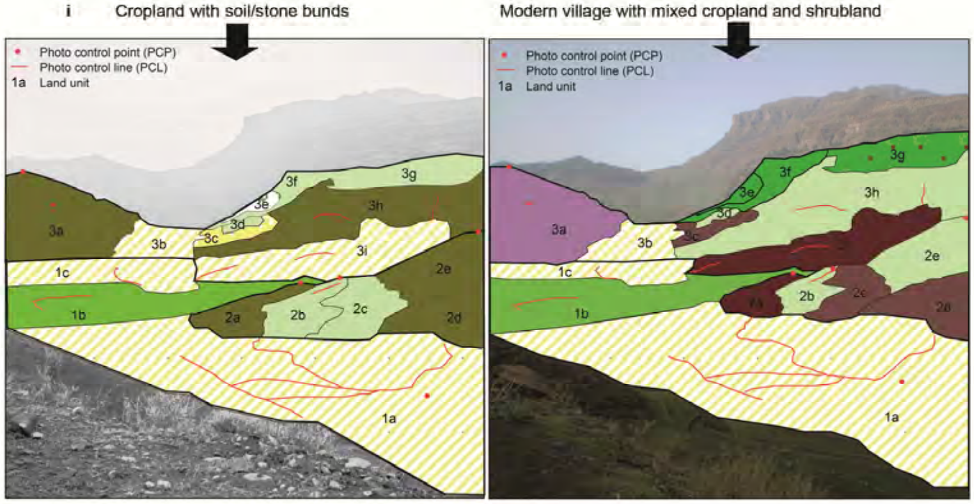

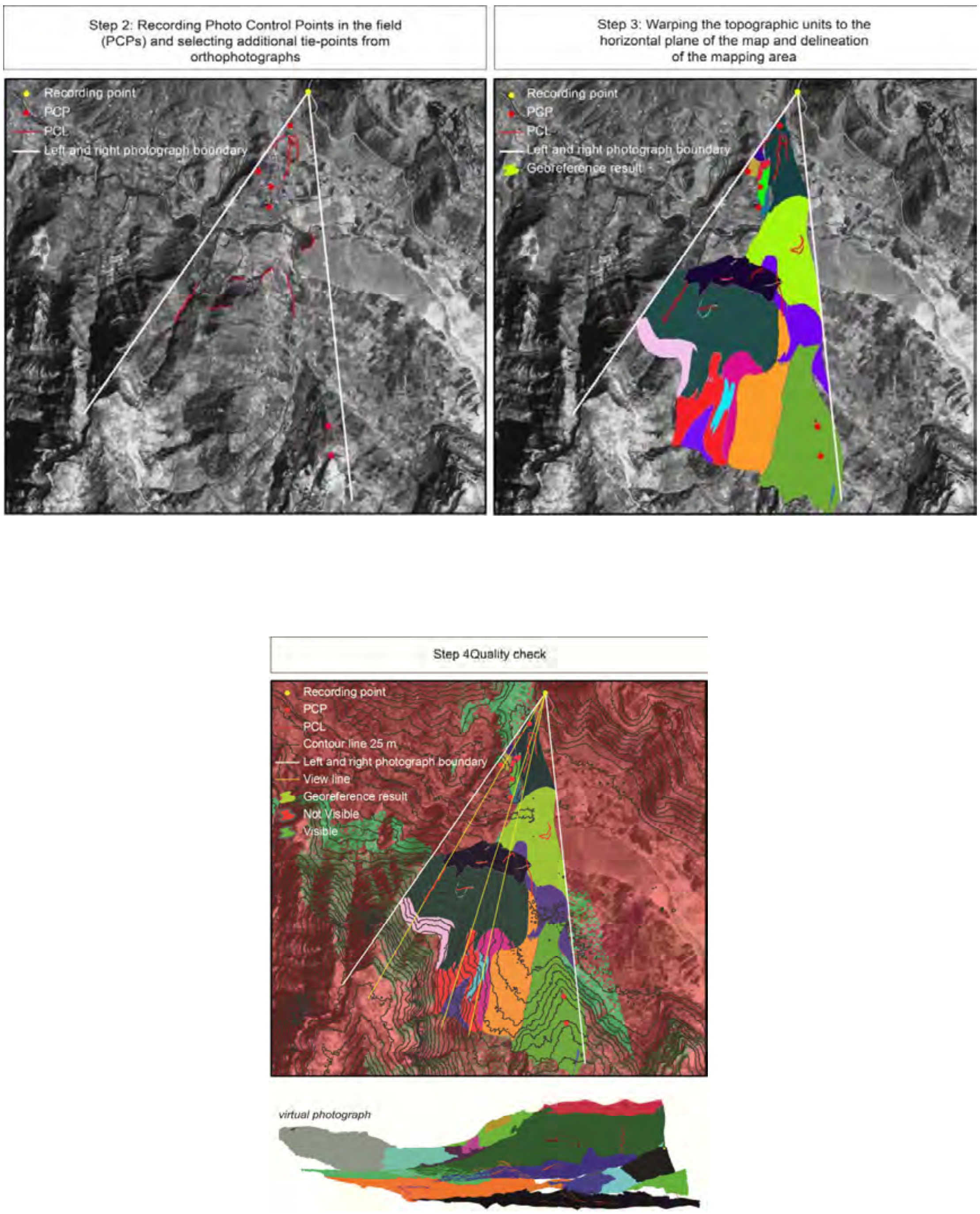
Step 2: Recording Photo Control Points in the field (PCPs) and selecting additional tie-points from orthophotographs
Recording point
PCP
PCL
Left and right photograph boundary
Step 3: Warping the topographic units to the horizontal plane of the map and delineation of the mapping area
Recording point
PCP
PCL
Left and right photograph boundary
Georeference result
Step 4Quality check
Recording point
PCP
PCL
Contour line 25 m
Left and right photograph boundary
View line
Georeference result
Not Visible
Visible
virtual photograph

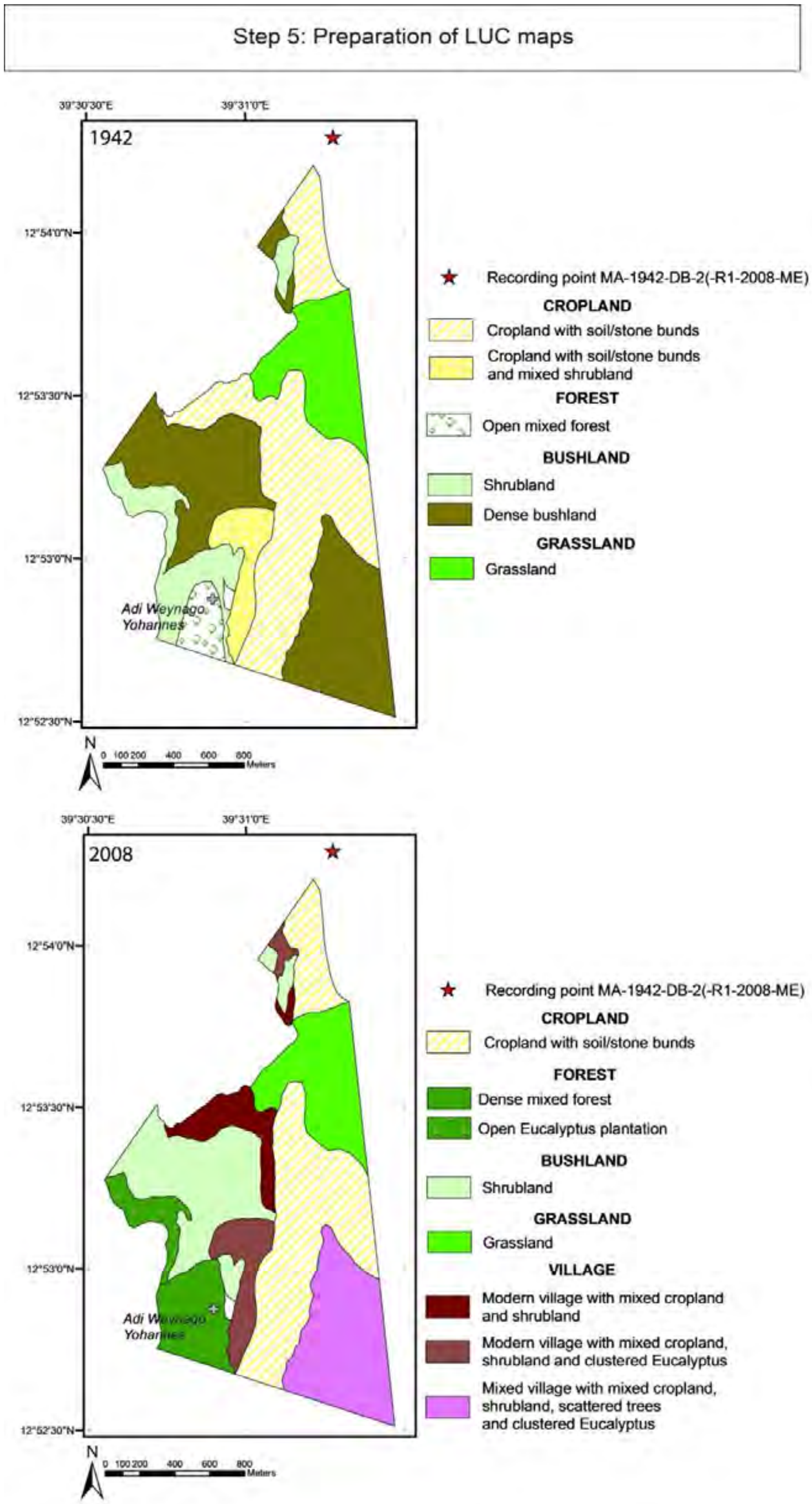

Figure 5.5 The step-by-step methodology to produce LUC maps from terrestrial photographs as illustrated for Ayba.

5.3 Results

LUC changes within the three study areas of Bolago, Ayba and Sinkata are presented here. The complete set of maps is provided by Meire (2009). LUC change patterns are represented using LUC transition matrices. LUC changes have been classified into two major classes: 'increase of woody vegetation cover' and 'decrease of woody vegetation cover' (**Table 5.3**).

Table 5.3 Defining LUC change patterns.

LUC $_{year\ 1}$	LUC $_{year\ 2}$	LUCC class	LUC $_{year\ 1}$	LUC $_{year\ 2}$	LUCC class
Cropland	Forest	Increase of woody vegetation cover	Bushland	Cropland Grassland	Decrease of woody vegetation cover
Cropland	Village				
Bushland	*Eucalyptus* plantation				
Bushland	Forest				

5.3.1 Land use and cover changes in Bolago (1868-2008)

The 1868 map of Bolago combines results from three terrestrial photographs, which were taken in panorama. The grassed plain in the lower center of the map corresponds to the overlapping part. Presumably, a fourth photograph taken towards the west completed the panorama.

Over the period 1868-2008, LUC has changed considerably in Bolago (**Table 5.4**, **Figure 5.6**). The 1868 situation shows a rather homogeneous landscape of extensive shrubland that includes some scattered *Juniperus procera* trees (3.4 km²). In the southern part, some large patches of juniper forest occur. A smaller patch is found as church forest, around the Tsibet Yohannes church. Central in the area there is some grassland.

Table 5.4 Land use and cover change matrix for Bolago valley (1868-2008) in km² (single border = decrease of woody vegetation cover, double border = increase in woody vegetation cover).

1868 \ 2008	Cropland	Forest	Eucalyptus plantation	Bushland	Grassland	Village	*Total*
Cropland	0.0	0.08	0.00	0.00	0.08	0.03	*0.20*
Forest	0.0	0.19	0.03	0.00	0.00	0.00	*0.25*
Eucalyptus plantation	0.0	0.00	0.00	0.00	0.00	0.00	*0.00*
Bushland	0.57	0.79	0.51	0.16	0.76	0.61	*3.40*
Grassland	0.0	0.00	0.00	0.00	0.21	0.00	*0.21*
Village	0.0	0.00	0.00	0.00	0.00	0.00	*0.00*
Total	*0.57*	*1.07*	*0.54*	*0.16*	*1.05*	*0.65*	*4.04*
Change (%) of the total area	*9*	*20*	*13*	*-80*	*21*	*16*	

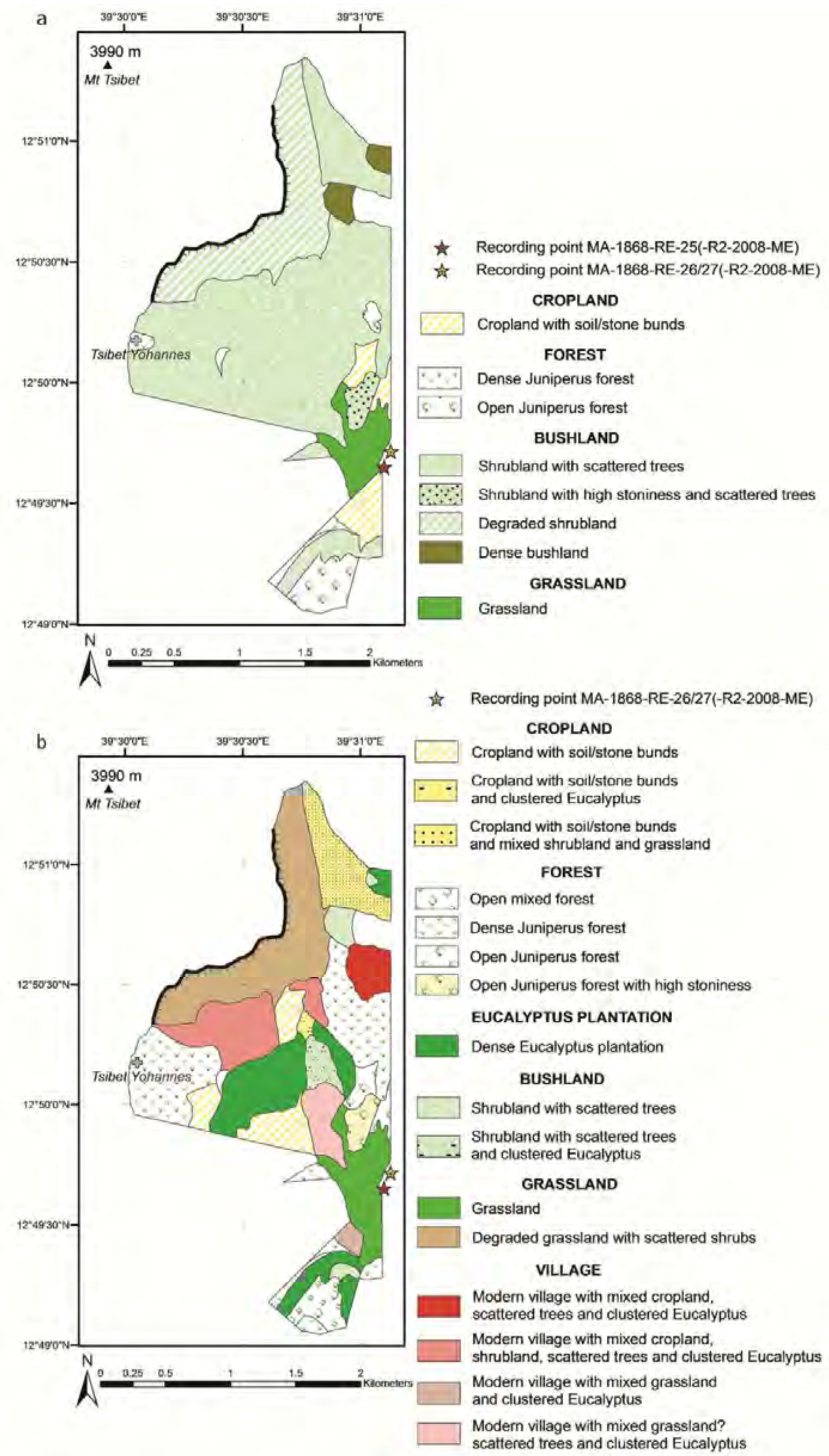

Figure 5.6 Detailed land use and cover maps of Bolago in **a**: 1868 and **b**: 2008.

The 2008 map of Bolago is more heterogeneous when compared to the previous situation. The number of LUC classes has doubled and the number of LUC patches strongly increased. Bushland was reduced from 3.4 km² to 0.2 km², or by 80%. Instead, the area covered by cropland (0.6 km²), forest (0.8 km²), Eucalyptus plantation (0.5 km²) and village (0.6 km²) increased. The small church forest of 1868 has expanded to 0.4 km², which is a sixteenfold increase.

The analysis of land use and cover change in the Bolago valley showed that important conversions took place over the past 140 years. Forests have expanded and became denser, which is often the result of the creation of exclosures since the mid-1980s, especially at the expense of bushland. In forests, Eucalypt trees were often introduced (**Figure 5.7**). The cropland in the valley bottom of 1868 has been displaced to steeper slopes by 2008. This all occurred together with the establishment or expansion of villages in the mapped area, which cover 16% of the area at present.

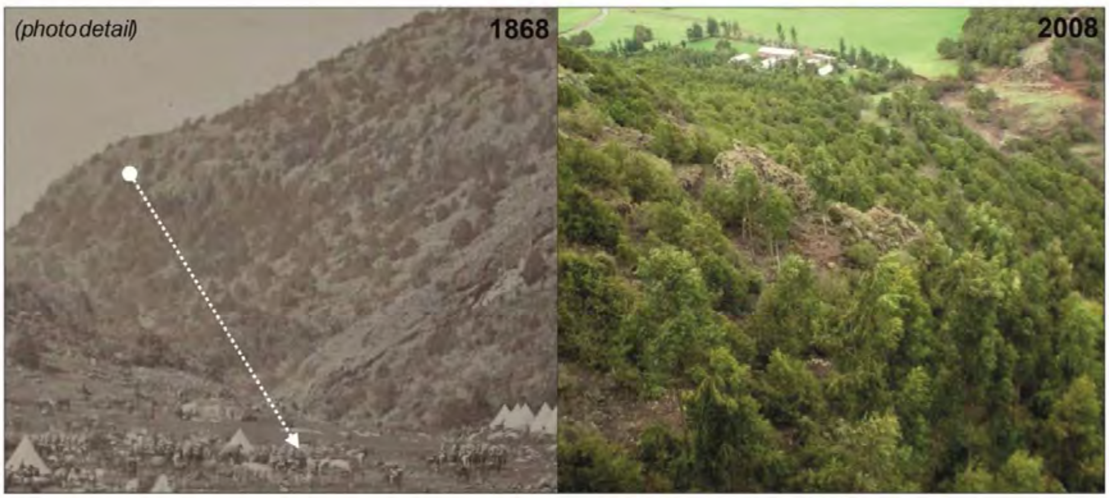

Figure 5.7 The introduction of eucalypt in the surroundings of natural forest (left) has resulted in a mixed forest at Debri Ridge in the Bolago valley (right) (photographs are taken from different viewpoints; the arrow indicates the direction of view of the 2008 photograph).

5.3.2 Land use and cover changes in Ayba (1942-2008)

Land use and cover changes between 1942 and 2008 in Ayba are summarized in **Table 5.5** and shown on **Figure 5.5**. The most apparent are the villages on the 2008 maps. In total, 28% of the study area has been subjected to village development. These villages developed mainly at the expense of cropland (0.3 km²). Villages are however not composed of built-up area only. They include patches of cropland, shrubland or *Eucalyptus* and *Acacia* trees (**Figure 5.8**). The apparent loss in cultivated land (-11%) is thus rather attributable to the classification system (the merging of detailed LUC classes into composite LUC classes) than to actual loss of cropland.

Table 5.5 Land use and cover change matrix for Ayba (1942-2008) in km² (double border = increase in woody vegetation cover).

1942 \ 2008	Cropland	Forest	Eucalyptus plantation	Bushland	Grassland	Village	*Total*
Cropland	0.75	0.00	0.00	0.00	0.00	0.28	*1.03*
Forest	0.00	0.09	0.00	0.00	0.00	0.00	*0.09*
Eucalyptus plantation	0.00	0.00	0.00	0.00	0.00	0.00	*0.00*
Bushland	0.00	0.12	0.09	0.47	0.00	0.46	*1.13*
Grassland	0.00	0.00	0.00	0.00	0.32	0.00	*0.32*
Village	0.00	0.00	0.00	0.00	0.00	0.00	*0.00*
Total	*0.75*	*0.20*	*0.09*	*0.47*	*0.32*	*0.73*	*2.56*
Change (%) of the total area	*-11*	*5*	*3*	*-26*	*0*	*28*	

About 12% of the former bushland (0.2 km²) has been replaced by *Juniperus* forest and *Eucalyptus* plantations. In the southwestern part of the study area, the 1942 situation shows a forest with apparently no settlements nearby. This suggests that it is a remnant of primary forest. Whether the Adi Weynago Yohannes church was already present in 1942 remains unclear, as it could have had a thatched roof at that time and thus remains unobserved (**Figure 5.9**). More to the east, an open *Eucalyptus* plantation was established on the highest and steepest part of the study area, at the expense of bushland.

Figure 5.8 The establishment of villages in the study areas has typically been accompanied by the planting of clustered Eucalyptus (south-eastern slope of the study site in Ayba) (photos are taken from different viewpoints; the arrow indicates the direction of view of the 2008 photo).

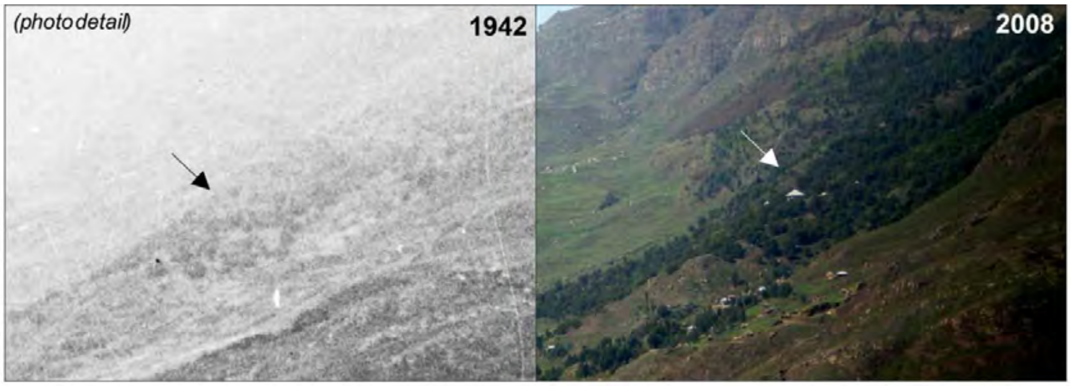

Figure 5.9 Remnant primary forest is generally protected because of religious reasons; its expansion eventually gives rise to secondary forest (Adi Weynago Yohannes church forest, south Ayba).

5.3.3 Land use and cover changes in Sinkata (1868-2008)

Land use and cover changes between 1868 and 2008 in Sinkata are summarized in **Table 5.6** and shown on **Figure 5.10**. The studied area of Sinkata is the smallest one, as it merely covers an area of 0.046 km². It is composed of two small maps, based on two 1868 photographs that were taken about 3 km apart.

The northern study site (Figure **Figure 5.10 a** and **b**) was relatively forested in 1868, with centrally a forest of primarily *Acacia* and *Olea*. By 2008, this has been replaced by dense *Eucalyptus* plantations covering 0.024 km². Under the cliff, the large bedrock patch of 1868 improved to degraded shrubland in 2008. The area of cropland, which is represented on the foreground of the photographs, has remained unchanged. It takes up a minor part of the study site (0.001 km² or 12 %).

The southern study area included a traditional village in 1868. This village has been abandoned and a dense bushland is now at place, including *Opuntia ficus-indica*. Probably, the 1868 village used to be a military camp, as it occurred around a fortification (**Figure 5.11**) of which the foundations are still visible today. The degraded shrubland that takes up the largest part of the southern area (0.003 km²) has been enriched with some *Eucalyptus* and *Olea*.

Table 5.6 Land use and cover change matrix for Sinkata area (1868-2008) in km² (double border = increase in woody vegetation cover).

1868 \ 2008	Cropland	Forest	Eucalyptus plantation	Bushland	Village	Bedrock	*Total*
Cropland	0.0018	0.0000	0.0000	0.0000	0.0000	0	*0.0018*
Forest	0.0000	0.0007	0.0148	0.0000	0.0000	0	*0.0155*
Eucalyptus plantation	0.0000	0.0000	0.0000	0.0000	0.0000	0	*0.000*
Bushland	0.0000	0.0000	0.0090	0.0056	0.0000	0	*0.0148*
Village	0.0000	0.0000	0.0000	0.0001	0.0027	0	*0.0028*
Bedrock	0.0000	0.0000	0.0000	0.0111	0.0000	0	*0.0109*
Total	*0.0018*	*0.0007*	*0.0238*	*0.0168*	*0.0027*	*0.000*	*0.0459*
Change (%) of the total area	*0*	*-32*	*52*	*5*	*-<1*	*-24*	

Vegetation cover has increased considerably near Sinkata during the studied period (1868-2008). The dominating LUC in the considered areas has changed from a relatively open forest (34%) to dense *Eucalyptus* plantation (52%).

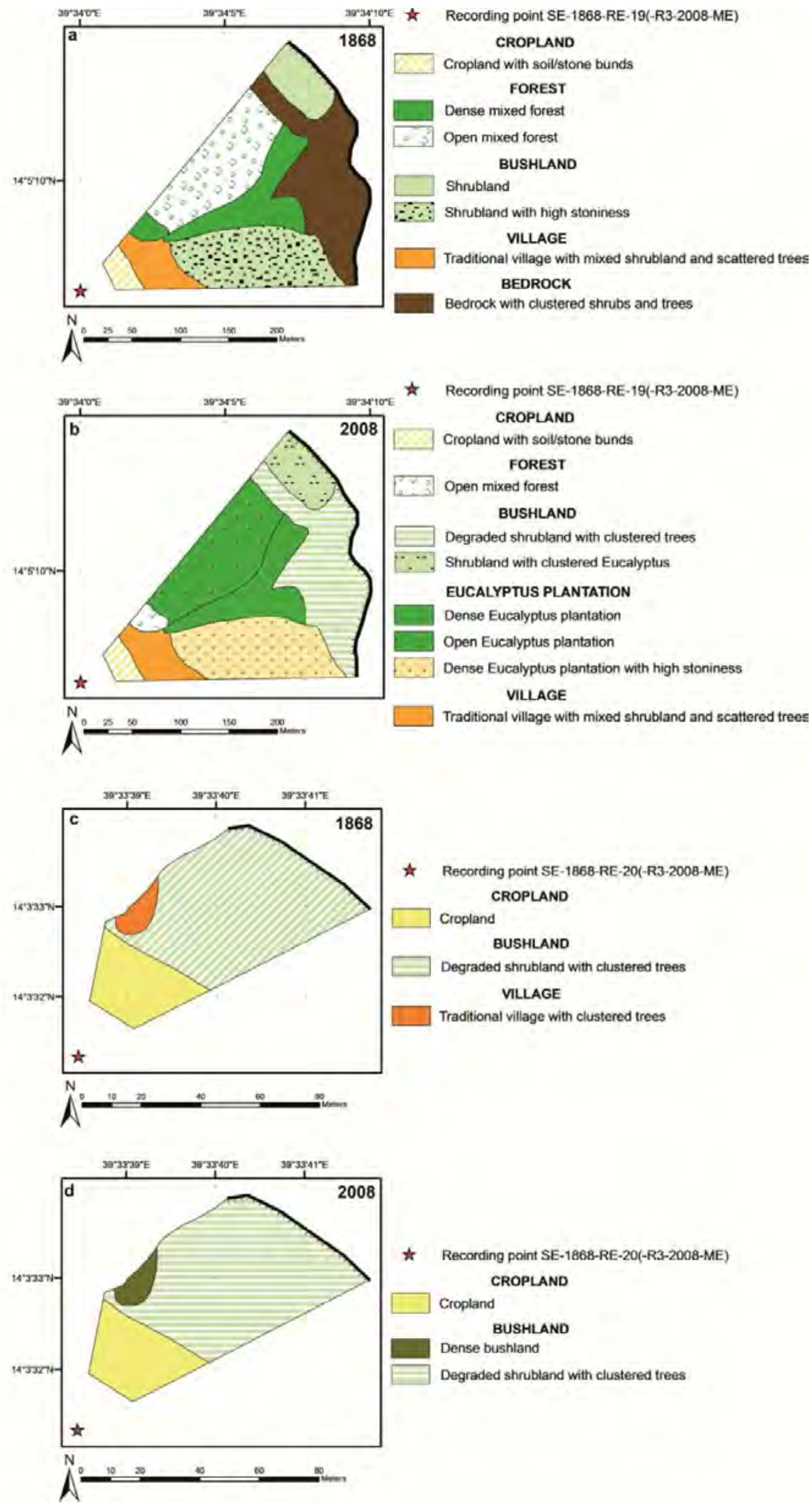

Figure 5.10 Detailed land use and cover maps of two areas near Sinkata in (a) 1868 and (b) 2008 are based on photographs SE-1868-RE-19(-R3-2008-ME); (c) 1868 and (d) 2008 are based on photographs SE-1868-RE-20(-R3-2008-ME).

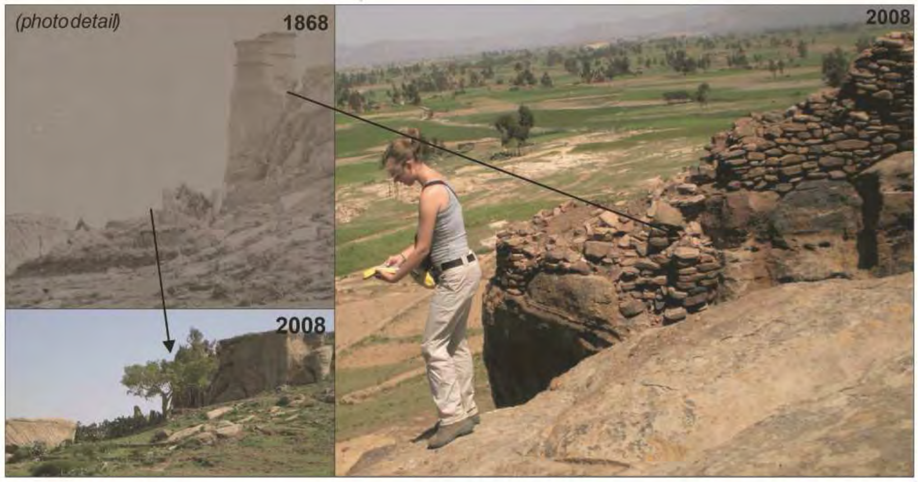

Figure 5.11 The rise of a *Ficus* sp. in front of the abandoned fortification is eye-catching (arrows indicate identical locations on the 1868 and 2008 photo).

5.3.4 Land use and cover changes in North Ethiopia (1868-2008)

In addition to the three already discussed areas, **Table 5.7** summarizes findings on LUC for the combined historical time span 1868-1942 and the 2008 situation, encorporating the sites Ashenge and Adi Shuho (for details see Meire, 2009). Information is also given on the total area of LUC patches with presence of *Eucalyptus*, trees in general and houses, both in historical and in recent times. In order to contrast between the late 19th-early 20th century and the present, the 1961 photographs are not discussed in this section.

Table 5.7 Overview of land use and cover changes in the combined study sites (for each epoch, the percentage occupied per LUC class/detailed LUC class is represented).

Period	1868-1940s		2008	
Total area	6.65 km²	%	6.65 km²	%
I Cropland	1.41	21	1.01	15
II Forest	0.36	5	1.28	19
III Eucalyptus plantation	0	0	0.98	15
IV Bushland	4.65	70	0	0
V Grassland	0.21	3	1.37	21
VI Village	< 0.01	< 1	2.02	30
VII Bare ground	0	0	< 0.01	< 1
VIII Bedrock	0.01	< 1	0	0
Total area w ith presence of eucalypt	0	0	4.11	62
Total area w ith presence of trees[1]	2.91	44	6.24	94
Ttoal area w ith presence of houses	< 0.01	< 1	2.14	32

[1]All tree species, including Eucalyptus

Bushland covered the majority of the area in 1868-1942 (4.65 km² or 70%), followed by croplands (1.41 km² or 21 %), forests (0.36 km² or 5 %), grassland (0.21 km² or 3 %), bedrock and villages (both <0.01 km² or <1 %). *Eucalyptus* trees did not occur in the 1868-1942 landscape. Other trees did however cover 2.91 km² (25%) of the total area and only a small fraction of the total area did include housing (<0.01 km²).

In 2008, the situation changed considerably. Villages are now the first LUC class of the area (2.02 km² or 30%), followed by grassland (1.37 km² or 21%), forests (1.28 km² or 19%), cropland (1.01 km² or 15%) and *Eucalyptus* plantations (0.98 km² or 15%). Clearly, woody vegetation cover has increased considerably over the period 1868-2008. Forests became larger and Eucalypt plantations were introduced. In total, 94% of the total area included trees, of which 62% were Eucalypt. Clearly, villages increased in size and number. These changes merely occurred at the expense of bushland.

5.4 Discussion

5.4.1 Land use and cover trends in Northern Ethiopia (1868-2008)

The important increase in built-up area over the period 1868-2008 from less than 1% to 32% can be explained by a strong increase in population density. An extrapolation by Nyssen et al. (2009), based on data presented by Maddison (2006) and McEvedy and Jones (1978), indicated that the population of Ethiopia in its current boundaries has increased 8- to 10-fold between 1868 and 2008.

Surprisingly, the woody vegetation cover increased over the same period from, especially after 1961. The surface covered by forest increased from 5% in 1868-1942 to 19% in 2008. The situation of 1868-1942 shows an environment where trees are scarce. With the increase in population density and in built-up area, the demand of construction wood and fuelwood strongly increased. According to Woldeamlak (2002), this motivated the local communities to protect vegetated areas and to start reforestation programs. Indeed, since the 1980s, environmental recovery programs were established in order to reverse the decline in woody vegetation (Nyssen et al., 2004), resulting in, for example, the creation of exclosures. This also prove to decrease gully erosion rates (Frankl et al., 2011, 2012). For building purposes, *Eucalyptus* trees were introduced as an alternative to endemic species especially since the 1970s (Jagger and Pender, 2003; Nyssen et al., 2009). At present, they occur everywhere in the landscape, planted as individual trees or small clusters by individual farmers or introduced as plantations on a community basis. Eucalypt trees were also introduced to forests (**Table 5.7**).

The observed relative small increase in cultivated areas might be explained by the fact that the remaining areas were rather unsuitable for cultivation or that, especially since the 1980s, they were under the protection of local and regional administrations (Descheemaeker et al., 2006). Other studies (*e.g.* Nyssen *et al.*, 2008; de Mûelenaere *et al*., 2009) reported an increase of the cropped area in Northern Ethiopia till 1980 and a decrease afterwards.

Significant improvement of the biomass production in the Tigray Highlands between 1975 and the years 2000 has also been indicated by previous research (e.g., Munro et al., 2008; Nyssen et al., 2009; de Mûelenaere et al., 2011). Similar findings are noticed in studies that were carried out in Amhara Region, which is situated south of Tigray. Over the time span 1957-1986, Wøien (1995) reported a remarkable increase in forests and in Eucalypt woodlots at the Mafud escarpment. Crummey (1998) compared terrestrial photographs of the 1930s to the situation in the 1990s, and concluded that tree cover strongly increase in Welo. Such tendencies of woody vegetation recovery were also noted by Woldeamlak (2002) in the Chemoga watershed (period 1957-1998), and by Girmay (2003) in the Tehuledere district (period 1936-1994).

As regarding to the people’s perception of the state of the 19th century environment, the information collected by interview has to be considered with much care. For instance, in Bolago the inhabitants told us that “at the time of our grandparents everything was forest here”. When we showed the 1868 photographs depicting a much poorer woody vegetation cover than the actual landscape, they simply did not believe it. Local people are mostly not used to be confronted with photographs displaying their village.

5.4.2 Quantifying land use and land cover from repeat photography

Using historical terrestrial photographs for LUC change assessments is not new (for examples see the Introduction Section). However, using 1868 photographs in a quantitative way is rather innovative. Furthermore, few work on LUC changes cover the period before 1950s, especially when considering Africa.

Much care is required when extrapolating results of repeat photography studies at a regional scale. Terrestrial photographs usually cover only small areas and are therefore not necessarily representative for the broader region. More reliable results can be obtained when a large dataset of photographs is at hand. Furthermore, the lack of uniform time scales of historical photographs make time-generalizations difficult. However, when using a random set of photographs in representative environments and when tendencies are straightforward, even a limited set of photographs can give valuable insights on historical LUC.

The accuracy of the warping results was strongly related to the incident angle at which topographic units were displayed. Warping flat areas located in the photograph background usually resulted in large positional errors, which needed to be resolved during the quality check. The warping of moderate to steep slopes oriented towards the recording proved less problematic. Warping results also showed to be more accurate when the number of tie-points was large for a topographic unit. Units for which the number of tie-points were too limited had to be analysed visually, based on contour lines and land boundaries observed on the orthophotograph. The method was rather time-consuming.

5.5 Conclusions

The proposed methodology allowed to produced land use and cover (LUC) maps on the basis of old terrestrial photographs. LUC tendencies could therefore be studied over a period of 140 years, which is rather unique for Africa. Results indicate that woody vegetation cover, and in particular tree cover, has increased in Northern Ethiopia over the period 1868-2008. This essentially occurred after 1961. Forests (especially composed of *Juniperus procera*) enlarged and *Eucalyptus* trees widely introduced. These developments particularly occurred at the expense of bushland. The increase in woody vegetation has been accompanied by an increasing population density, as evidenced by the increase in both size and number of villages. Our study is in line with other studies, and confirms that land management strategies improved in the Northern Ethiopian Highlands, which resulted in improved livelihoods.

5.6 References

Adams W, Goudie A, Orme A (1999) The physical geography of Africa. Regional Environments, Oxford

Addis G, Urga K, Dikasso D (2005) Ethnobotanical study of edible wild plants in some selected districts of Ethiopia. Human Ecology 33: 83-118

Aerts R. (2007) Church forests in Ethiopia. Frontiers in Ecology and the Environment 5 (2): 66

Aguiló M, Iglesias E (1995) Landscape inventory. In: Martínez-Falero E, González-Alonso S (eds) Quantitative Techniques in Landscape Planning. CRC Lewis Publishers, Boca Raton, FL, pp 47-83

Arndt N, Menzies M A (2005) The Ethiopian Large Igneous Province. http://www.largeigneousprovinces.org/print/05jan. Accessed 11 July 2009

Atakilte Beyene, Gibbon D, Mitiku Haile (2006) Heterogeneity in land resources and diversity in farming practices in Tigray, Ethiopia. Agricultural Systems 88: 61-74

Butler D R (1994) Repeat photography as a tool for emphasizing movement in physical geography. Journal of Geography 93 (3): 141-151

Buxton D (1949) Travels in Ethiopia. Lindsay Drummond Ltd, London

Byers A (2007) An assessment of contemporary glacier fluctuations in Nepal's Khumbu Himal using repeat photography. Himalayan Journal of Sciences 4 (6): 21-26

Cohen A S, Soreghan M J, Scholz C A (1993) Estimating the age of formation of lakes: An example from Lake Tanganyika, East African Rift system. Geology 21: 511-514

Corripio J G (2004) Snow surface albedo estimation using terrestrial photography. International Journal of Remote Sensing 25 (24): 5705–5729

Covington M A (2007) Digital SLR astrophotography. Cambridge University, Cambridge

Crummey D (1998) Deforestation in Wällo: process of illusion? Journal of Ethiopian Studies 21 (11): 1-41

de Mûelenaere S, Frankl A, Mitiku Haile, Veraverbeke S, Poesen J, Deckers J, Nyssen J. (2011) Historical landscape photographs for calibration of Landsat land use/cover (1972) in the Ethiopian highlands. Land Degradation & Development. Accepted

Dervieux A (2004) Que peuvent nous dire les anciennes photographies sur les changements paysagers. Arles: Dynamique Écologique et Sociale en Milieu Deltaïque (DESMID). http://www.enfa.fr/ACI/doc_pdf/01-Dervieux.pdf. Accessed 10 April 2008

Descheemaeker K, Nyssen J, Rossi J, Poesen J, Mitiku Haile, Raes D, Muys B, Moeyersons J, Deckers S (2006) Sediment deposition and pedogenesis in exclosures in the Tigray highlands, Ethiopia. Geoderma 132: 291-314

Frahma J-M, Pollefeys M, Lazebnika S, Gallupa D, Clippa B, Ragurama R, Wua C, Zach C, Johnson T (2010) Fast robust large-scale mapping from video and internet photo collections. ISPRS Journal of Photogrammetry and Remote Sensing 65 (6): 538-549.

Frankl A, Nyssen J, De Dapper M, Mitiku Haile, Billi P, Munro RN, Deckers J, Poesen J, (2011) Linking long-term gully and river channel dynamics to environmental change using repeat photography (North Ethiopia). Geomorphology 129: 238-251.

Girmay K W (2003) GIS Based Analysis of Land Use/Land Cover, Land Degradation and Population Changes. A Study of Boru-Metero Area of South Wällo, Amhara Region. Unpublished Msc Thesis, Addis Ababa University, College of Social Science,Department of Geography

Gordenker E, Cohen A (2006) Inventory of the Winterton Collection of East African Photographs: 1860–1960. Northwestern University Library, Evanston, IL

Greene A (2001) Primitive photography: A guide to making cameras, lenses, and calotypes. Focal Press, Oxford

Hofmann C, Courtillot V, Feraud G, Rochette P, Gezahegn Yirgu, Ketefo E, Pik R (1997) Timing of the Ethiopian flood basalt event and implications for plume birth and global change. Nature 389: 838-841

Jagger P, Pender J (2003) The role of trees for sustainable management of less-favored lands: the case of eucalyptus in Ethiopia. Forest Policy and Economics 5 (1): 83-95

Kull C (2005) Historical landscape repeat photography as a tool for land use change research. Norwegian Journal of Geography 59: 253–268

Maddison A (2006) The World Economy. Paris: OECD, Development Centre Studies

Manier D, Laven, R (2002) Changes in landscape patterns associated with the persistence of aspen (Populus tremuloides Michx.) on the western slope of the Rocky Mountains, Colorado. Forest Ecology and Management 167: 263-284

Mc Cann J (1997) The Plow and the Forest: Narratives of Deforestation in Ethiopia, 1840-1992. Environmental History 2 (2): 138-159

McEvedy C, Jones R (1978) Atlas of World Population History. Middlesex, Penguin

Meire, E. (2009) Mapping of land use and cover in the North Ethiopian highlands since 1868 using warped terrestrial photographs. Unpublished MSc. thesis, Ghent Univeristy, Department of Geography

Munro R N, Deckers J, Mitiku Haile, Grove A T, Poesen J, Nyssen J (2008) Soil landscapes, land cover change and erosion features of the Central Plateau Region of Tigray, Ethiopia: photo-monitoring with an interval of 30 years. Catena 75: 55–64

NGA-NASA (2000) Shuttle Radar Topography Mission – DTM 44_10

November E, Aerts R, Behailu M, Muys B (2002) Species list Tigrinya-Scientific technical note 2002/4. Mekelle University, Ethiopia and Forest Rehabilitation Project, K.U. Leuven, BE. https://lirias.kuleuven.be/bitstream/123456789/223190/1/Species+list+TGY-SCI+_TN-2002-4.pdf. Accessed 23 May 2009

Nyssen J, Poesen J, Moeyersons J, Deckers J, Mitiku Haile, Lang A (2004) Human impact on the environment in the Ethiopian and Eritrean Highlands – a state of the art. Earth Science Reviews 64 (3-4): 273-320

Nyssen J, Vandenreyken H, Poesen J, Moeyersons J, Deckers J, Mitiku Haile, Salles C, Govers G (2005) Rainfall erosivity and variability in the Northern Ethiopian Highlands. Journal of Hydrology 311: 172 –187

Nyssen J, Getachew Simegn, Nurhussen Taha (2008) An upland farming system under transformation: Proximate causes of land use change in Bela-Welleh catchment (Wag,Northern Ethiopian Highlands). Soil and Tillage Research 103: 231-238

Nyssen J, Mitiku Haile, Naudts J, Munro N, Poesen J, Moeyersons J, Frankl A, Deckers J, Pankhurst R (2009) Desertification? Northern Ethiopia rephotographed after 140 years. Science of the Total Environment 407: 2749-2755

Pankhurst R (1995) The history of deforestation and afforestation in Ethiopia prior to World War I. Northeast African Studies 2 (1): 119-33

Ritler A, Scheidegger D (1999) Landschaftswandel in Äthiopien anhand historischer Photographien. Afrikanische Studien 13: 260-278

Robinson P J, Henderson-Sellers A (1999). Contemporary Climatology. Pearson Education Ltd., Essex

Sharf F A, Northrup D, Pankhurst R (2003) Abyssinia, 1867-1868: artists on campaign : watercolors and drawings from the British expedition under Sir Robert Napier. Tsehai Publishers, Addis Ababa

Simmons S (1987) Using the View Camera: A creative guide to large format photography. Amphoto, New York

Szaro R, Johnston D W (1996) Biodiversity in managed landscapes: Theory and practice. Oxford University Press, Oxford

Taddesse Berisso (1995) Deforestation and environmental degradation in Ethiopia: the case of Jam Province. Northeast African Studies 2 (2): 139-56.

Tovey N K (1982) Surveying. In: Haynes R (ed) Environmental science methods. Chapman and Hall, New York, pp 317-347

UNDP-EUE (1998) Administrative Map of Tigray Region (http://peacei.com/peacei/map_tigray.html, 20/04/2008).

Vergauwen M, Van Gool L (2006) Web-based 3D reconstruction service. Machine Vision and Applications 17: 411-426

Virgo K, Munro R (1978) Soil and erosion features of the central plateau region of Tigray, Ethiopia. Geoderma 20: 131-157

Webb R H, Leake S A, Turner R M (2007) The ribbon of green: change in riparian vegetation in the Southwestern United States. The University of Arizona Press, The Arizona Board of Regents, AZ

Welch R, Madden M, Jordan T (2002) Photogrammetric and GIS techniques for the development of vegetation databases of mountainous areas: Great Smoky Mountains National Park. Journal of Photogrammetry and Remote Sensing 57 (1-2): 53-68

Wøien H (1995) Deforestation, information and citations : a comment on environmental degradation in Highland Ethiopia. Geojournal 37 (4): 501-12

Woldeamlak Bewket (2002). Land cover dynamics since the 1950s in Chemoga Watershed,Blue Nile Basin, Ethiopia. Mountain Research and Development 22: 263-269

Chapter 6
Land use and land cover changes since 1973 as quantified from Landsat imagery

This chapter is published as:

de Mûelenaere, S., Frankl, A., Mitiku Haile, Poesen, J., Deckers, J., Munro, N., Veraverbeke, S., Nyssen, J., 2012. Historical landscape photographs for calibration of LANDSAT land use/cover in the Northern Ethiopian Highlands. Land Degradation & Development, online early view: DOI: 10.1002/ldr.2142.

Abstract

The combined effects of erosive rains, steep slopes and human land use have caused severe land degradation in the Ethiopian Highlands for several thousand years, but since the 1970s, however, land rehabilitation programmes have been established to try to reverse deterioration. In order to characterize and quantify the transformations in the Northern Ethiopian Highlands, a study was carried out over 8884 km^2 of the Tigray Highlands of Northern Ethiopia. Using Landsat Multispectral Scanner and later Thematic Mapper imagery (1972, 1984/1986 and 2000), historical terrestrial photographs (1974–1975) and fieldwork (2008), land use and cover maps were prepared. For assessing the use of the historical terrestrial photographs, Landsat images from 1972 were classified using two different methods, namely conventional change detection (image differencing) and ground truthing (using the historical photographs of 1974–1975). Results show that the use of terrestrial photographs is promising, as the classification accuracy based on this method (Kappa coefficient 0.54) is better than the classification accuracy of the method based on image differencing (Kappa coefficient 0.46). Major land use and cover changes indicate the following: (1) a gradual but significant decline in bare ground (32% in 1972 to 8% in 2000); (2) a significant increase of bushland (25 to 43%) and total forest area (including eucalypt plantations, 2.6 to 6.3%); and (3) creation of numerous lakes and ponds. The dominant change trajectory (27% of the study area) indicates a gradual or recent vegetation increase. These changes can be linked to the population growth and the introduction of land rehabilitation initiatives, complemented by growing awareness of land holders.

Keywords: Ethiopia, Land use and land cover change, Remote sensing, Satellite imagery, Terrestrial photographs, Tigray.

6.1 Introduction

Since the origin of settled agriculture perhaps ten thousand years ago, human land use has interfered with the natural process of land cover change (Houghton, 1994; Ojima et al., 1994). During the last three centuries, the global human population has increased dramatically, and people's activities have become an important factor in global change processes (Petit and Lambin, 2002). Tropical mountain regions are often very densely populated and are thus more vulnerable to changes of the environment (Nyssen et al., 2009b). During the last few decades in the region under study, however, efforts have been made towards land rehabilitation, and these initiatives have proven that land recovery is possible and is economically viable (Boyd and Turton, 2000).

Land use can be defined as 'the human employment of the land' and land cover as 'the physical and biotic character of the land surface' (Meyer and Turner, 1992). Because land use is often linked to the land cover type, these concepts are frequently used interchangeably in land use and cover (LUC) studies (Green et al., 1994). LUC change processes are caused by interactions between physical, biological and social forces and can lead not only to enhanced productivity and long-term sustainability but also to conversion of potentially productive land into degraded land, loss of species and emission of (greenhouse) gases into the atmosphere (Houghton, 1994; Ojima et al., 1994; Turner et al., 1994). Sustainable management of natural resources therefore requires knowledge and quantification of LUC change processes.

Temporal series of remotely sensed data and analysis of change trajectories are useful in measuring LUC change and have been widely applied (e.g. Mertens and Lambin, 2000; Petit et al., 2001; Serneels et al., 2001; Petit and Lambin, 2002; Muñoz-Villers and Lopez-Blanco, 2008). Most LUC change studies use aerial photographs, satellite imagery or a combination of both. Especially if satellite imagery is used, ancillary data are needed for establishing training areas and performing accuracy assessments. For recent periods, ancillary data can be easily collected through field observations. However, for satellite imagery up to four decades old, these data are often not readily available. As an alternative, aerial photographs (e.g. Mertens and Lambin, 2000; Petit et al., 2001), vegetation maps (Muñoz-Villers and Lopez-Blanco, 2008) or interview methods (e.g. Atwell et al., 2009) have been used. However, old aerial photographs often require ground truthing themselves (Rembold et al., 2000) and are therefore not an optimal data source. The limited scope and often questionable reliability are major drawbacks of interview methods (Tra and Egashira, 2004; Aynekulu et al., 2006). Historical terrestrial photographs could be a promising alternative ancillary data source. Although there are studies using historical terrestrial photographs to study LUC change (Chapter 4; Hoffman and Rohde, 2007; Munro et al., 2008), sometimes also comparing interpreted historical terrestrial photographs to observations on Landsat imagery (McClaran et al., 2010), there is no record of any studies using such photographs as training sites to classify LUC types observed in old satellite images.

Land use and cover change studies in the Northern Ethiopian Highlands have thus far only been performed at a local scale (e.g. Crummey, 1998; Tekle and Hedlund, 2000; Zeleke and Hurni, 2001; Munro et al., 2008). The aim of this study is to assess LUC change (1972–2000) in Northern Ethiopia at a regional scale, using a unique dataset consisting of historical terrestrial photographs, field observations, satellite-based remote sensing and geographic information systems (GIS).

6.2 Study area

6.2.1 Geographical Context

The study area (Figure 1) is located in the Tigray Highlands, the northernmost Ethiopian regional state, between 12°30’to 14°10’ N and 39°00’ to 39°45’ E and comprises an area of 8884 km^2 at an altitude ranging from 1500 to 3939 m above sea level (a.s.l.).

The geological structure of Tigray results from the evolution of the East African Rift System. Precambrian metasediments and metavolcanics are unconformably overlain by subhorizontal Palaeozoic and Mesozoic sedimentary rocks. In turn, these are unconformably overlain by Tertiary lavas and basalts (Bussert, 2010). After the Miocene and Plio-Pleistocene tectonic uplift, erosion processes formed the benched landscape that is characteristic throughout the study area (Nyssen et al., 2007a). Quaternary alluvium, colluvium and tufa have been mainly deposited in river valleys, depressions and topographic concavities (Nyssen et al., 2004a).

Soil development in the Northern Ethiopian Highlands depends strongly on topography and parent material (Virgo and Munro, 1978). On basaltic parent materials, a typical red-black soil catena has developed (Van de Wauw et al., 2008) with deep, black Vertisols in colluvial lowlands and on the basalt plateaux and Luvisols and Cambisols on steeper sections. On limestone parent material, Phaeozems, dark organic soils, can be found in remnant forests (Descheemaeker et al., 2006). Intensive land use in other limestone areas led to soil erosion, high sediment deposition rates and the development of Leptosols and Regosols on slopes, whereas Cambisols occur in less steep areas (Van de Wauw et al., 2008).

The study area (**Figure 6.1**) corresponds to a wider region in which a high density of historical terrestrial photographs is available from the mid-1970s. The eastern boundary is the Rift Valley escarpment, at 1500 m a.s.l. The northwestern and western boundaries of the study area relate to the commencement of the outcrop of Precambrian and lower Palaeozoic lithologies. The geological map of Ethiopia (Merla et al., 1979) and the hydrogeological map of Mekelle (EIGS, 1978) were used to delineate these formations.

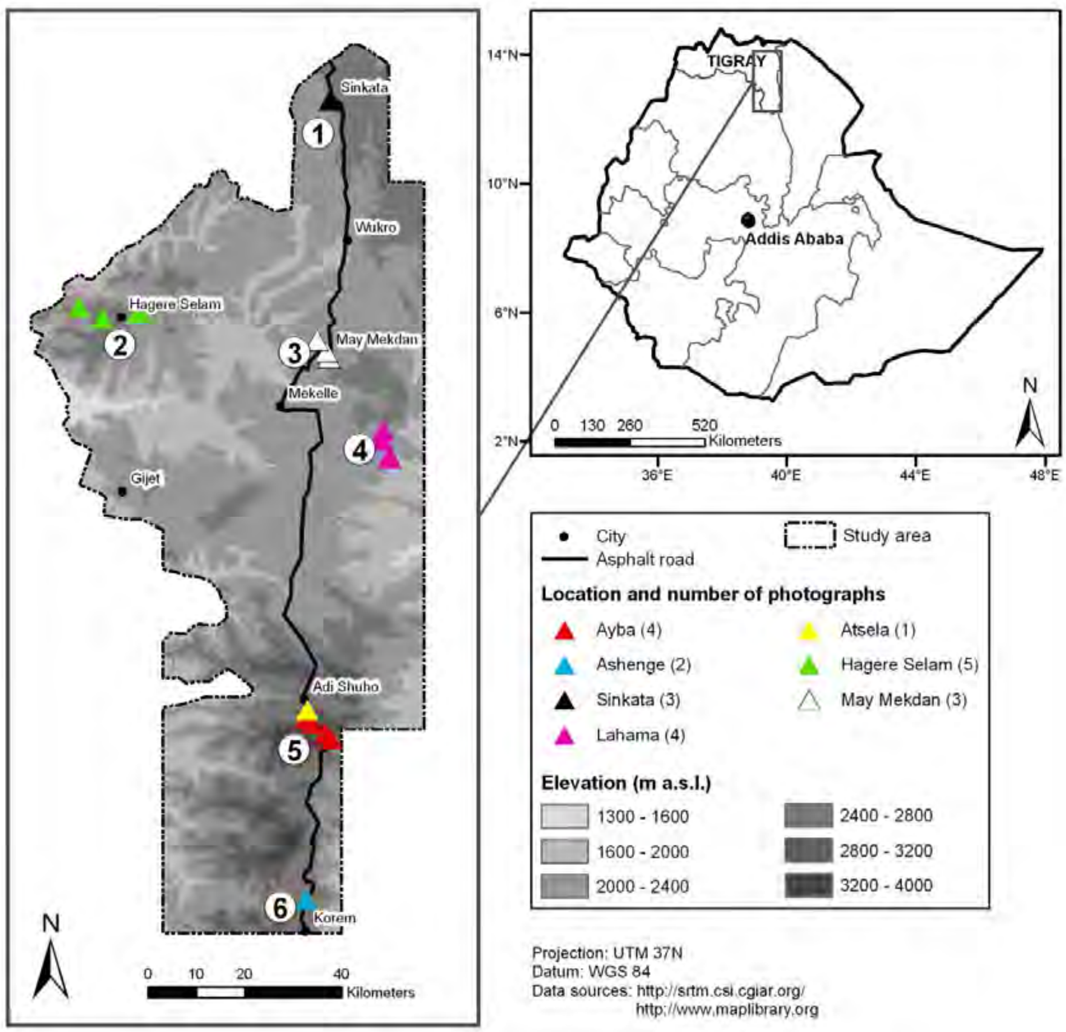

Figure 6.1 Location of the study area and areas of ground truthing (1: Sinkata, 2: Hagere Selam, 3: May Mekdan, 4: Lahama, 5: Ayba and Atsela, 6: Lake Ashenge, Bahri Hatsera).

6.2.2 Climate

Rainfall in the Northern Ethiopian Highlands is linked to the position of the Intertropical Convergence Zone (Nyssen et al., 2005). The current climate is tropical semi-arid (Virgo and Munro, 1978) with 400–900mm of annual precipitation, which varies with slope aspect and altitude. Although temperature varies with altitude, the average air temperature for the region is 18°C. There are three seasons: a dry season in the winter (October–

April), a rainy season in the summer with maximum precipitation in July and August and an unreliable small rainy season from March to May, which is most marked in the southern part of the study area. Analyses of time series of annual rainfall in Northern Ethiopia, as reported by Nyssen et al. (2004a), have shown that there is no significant long-term change in the annual precipitation regime.

6.2.3 Vegetation

The original climax vegetation in the Northern Ethiopian Highlands consisted of three types of vegetation (Wilson, 1977; Bard et al., 2000; Aerts et al., 2006). Dry evergreen montane forest dominated by *Juniperus procera* and *Olea europaea ssp. africana* was present above 2200 m a.s.l. In moister areas between 1400 and 2200 m a.s.l. was a mixed *Podocarpus gracilior* and *J. procera* forest. Deciduous wooded grassland was present at altitudes below 2200 m a.s.l. with tree species consisting mainly of *Acacia*, *Ficus*, *Euphorbia*, *Olea* and *Terminalia*.

It has been claimed that deforestation in Ethiopia is a recent process with 40% of the country still covered with forests in 1900 (Allen-Rowlandson, 1988; Taddesse, 1995; Bewket, 2002; and many others). However, no evidence is available to support this hypothesis. The current viewpoint about deforestation is that it commenced between 3000 and 2000 BP because of growing human land cultivation (Bard et al., 2000; Nyssen et al., 2004a). Today, most of the vegetation is semi-natural and consists of cropland and semi-arid degraded savanna, as well as non-indigenous species such as *Eucalyptus spp*. and *Opuntia ficus-indica*. Small remnants of the forest climax vegetation are found near churches and in isolated areas (Wilson, 1977; Descheemaeker et al., 2006). Land cover can generally be categorized into bare ground, grassland, cropland, bushland, (church) forest, Eucalyptus plantation and village. The crops that are grown in the study area mainly include annual food crops, e.g. *Eragrostis teff L*. (tef), *Hordeum vulgare L*. (barley), *Triticum sativum L*. (wheat), *Eleusine coracana L*. (millet), *Sorghum bicolor L*. (sorghum), *Zea mays L*. (maize) and *Vicia faba L*. (beans).

6.2.4 Socio-economic Environment

Ethiopia has a long human settlement history, with land cultivation starting around 7000–5000 BP (Hurni, 1990). Historically, the earliest and most powerful kingdom within the contemporary boundaries of Ethiopia was situated in the Highlands North and West of Addis Ababa (Crummey, 2000). Christianity was introduced in the early fourth century. By the 15th century, the state increasingly dominated the church, mainly by granting land (gult rights) to monasteries and churches. The gult system implied that farmers owed one-fifth of their harvest to the clerical gult holders and one-tenth to the king. By the early–1970s, centuries-long feudalism had led to a great inequality in land holding. In 1974, a communist military government, the Derg, took over and eliminated all private land titles; they also controlled the agricultural market. Droughts, famine and growing opposition led to the downfall of the Derg in 1991. After the new constitution (1995), all land remained as state property and is now managed by the rural communities, who allocate land to their members as equitably as possible and manage the remainder as common grounds (Crummey, 2000).

Ethiopia is ranked the 12th least developed country in the world according to the Human Development Index (UNDP, 2010). The average life expectancy is 54.7 years (UNDP, 2010). The economy is based on subsistence agriculture, and more than 85% of the population live in rural areas and rely on land resources for their livelihood (Diao and Pratt, 2007). The agricultural system in the Highlands is described as the ‘grain-plough complex’, with barley, wheat and tef as the main crops (Westphal, 1975). The upland farming system entailing livestock keeping (Ruthenberg, 1980) prevails in the Tigray Highlands. Agriculture practices are traditional, tillage being performed with an ox-drawn ard plough, locally called maresha. Crop production almost exclusively is based on the summer rainy season. Poverty and food shortages are severe in Tigray, and although absolute food production has increased, food production per capita has stagnated because of the fast population growth. Many households rely on food aid (Nyssen et al., 2004a).

6.2.5 Land Degradation

The mountainous terrain combined with the climatic conditions make the Ethiopian Highlands vulnerable to land degradation. Land use conflicts have caused further land degradation, such as deforestation, conversion of bushland to cultivated areas, overgrazing, shorter crop rotation cycles, soil erosion and desertification (e.g. Hurni, 1990; Epema et al., 2000; Feoli et al., 2002; Mekuria et al., 2007).

As a response, soil and water conservation (SWC) measures were intensively promoted in Tigray from 1975 onwards (Munro et al., 2008). This resulted in the establishment of stone or soil bunds along slopes, check dams in gullies, reforestation, exclosures (areas closed for grazing and agriculture) and reservoirs (Gebremichael et al., 2005; Descheemaeker et al., 2006; Haregeweyn et al., 2006). Many of the sloping cropland areas in the study area contain contour stone or soil bunds, which reduce soil erosion rates. Reforestation mainly included plantation of *Eucalyptus*, which grows rapidly and supplies timber wood, and exotic Australian *Acacia* species, mainly planted on shallow soils and steep slopes.

6.3 Materials and Methods

6.3.1 Data Collection

Land use and cover was derived for 1972, 1984–1986 and 2000 from the following:

- Historical terrestrial photographs (1974–1975);
- Fieldwork (2008);
- Landsat Multispectral Scanner (MSS) (1972), Thematic Mapper (TM) (1984–1986) and Enhanced TM Plus (ETM+) (2000) imagery.

Historical terrestrial photographs

In 1974 and 1975, R.N. Munro, G. Edgeley and K. Virgo (and numerous others) photographed Northern Ethiopia as part of the Tigray Rural Development Study (Munro et al., 2008), a technical assistance and development planning project that was aimed to counteract the consequences of drought and famine. Part of this project studied the natural resources of central Tigray and recorded the Tigrayan landscape through several thousand terrestrial photographs. Twenty-two of these historical terrestrial photographs (**Figure 6.2**) were selected and related to different sites throughout the study area (**Figure 6.1**).

(a) Atsela in October 1975 (left, N. Munro) and August 2008 (right, S. de Mûelenaere)

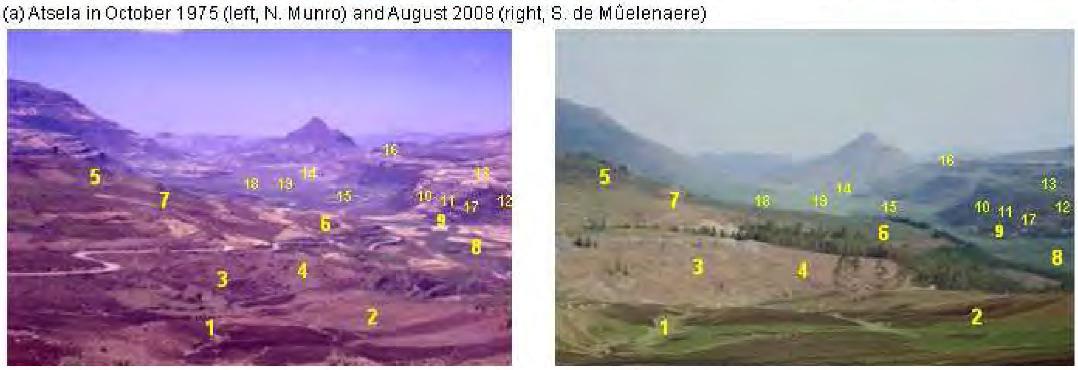

(b) Ayba valley in October 1975 (left, N. Munro) and July 2008 (right, S. de Mûelenaere)

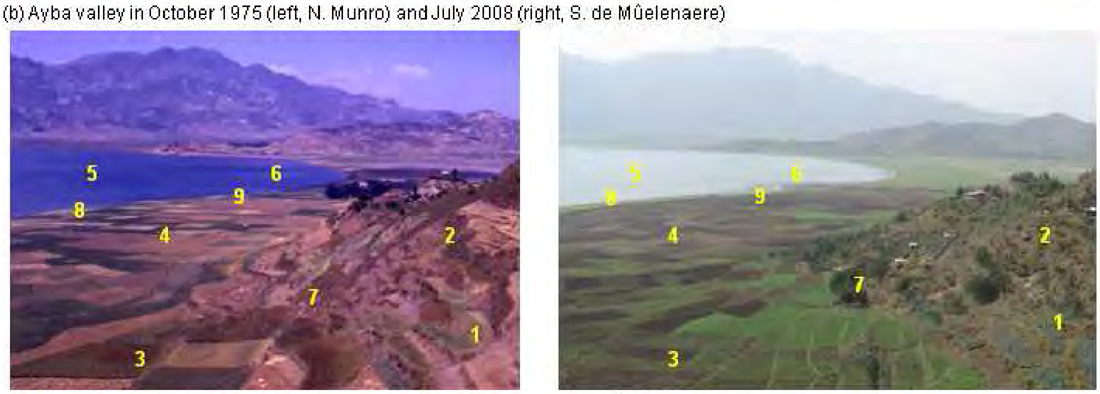

(c) Ashenge in October 1975 (left, N. Munro) and July 2008 (right, S. de Mûelenaere)

Figure 6.2 Example of interpreted terrestrial photographs in (a) Atsela, (b) Ayba and (c) Ashenge. The numbers indicate the land units that were used as training sites for land cover and land use classification.

Collection of ground truth data

Ground truth data were collected during the rainy season of 2008 from 9 July until 3 September, followed by a shorter campaign in November 2008, in six study sites spread throughout the study area (**Figure 6.1**). At each site, the historical terrestrial photographs were re-photographed and compared with the current landscape to determine training sites for land cover and land use classification (**Figure 6.2**). Given the accuracy of the positioning of the Global Positioning System (Garmin eTrex VistaW, Olathe, KS, USA, 7 m on average) and the pixel size of the Landsat images, training sites had to be areas of minimum 100m x 100m with homogenous land use/cover both in 2008 and in 1974–1975. Every land unit was visited in order to register its location (using Global Positioning System) and register its LUC properties. Parameters that influence spectral response (e.g. tree species, tree density, canopy cover, lithology, soil texture, stoniness) were also recorded for every land unit for the current (based on fieldwork) and the 1975 (based on the historical terrestrial photographs) situation. Because the most recent Landsat images date from 2000 and fieldwork was performed in 2008, the LUC situation of 2000 was obtained through interviews with the local population and field observations. A total of 196 training sites were observed during fieldwork.

Satellite imagery and pre-processing

Landsat MSS (2 November 1972), TM (22 November 1984/ 5 January 86) and ETM+ (27 January and 5 February 2000) imagery (metadata details are given in Appendix C), collected in the dry season, were corrected geometrically, radiometrically, atmospherically and topographically in order to meet the requirements for change detection. The ETM+ images were georeferenced using image-to-map rectification. The location of 321 ground control points, mostly at river junctions, was derived from the Ethiopian 1:50 000 scale topographic map series.

The effects of atmospheric absorption and scattering (Du et al., 2002) were removed using the cosine theta method (Chavez, 1996). Because of the mountainous nature of the study area, the imagery contained shadowing effects; hence, topographical correction was performed using the method of Riaño et al. (2003), using ground reflectance. Topographical slope and aspect data were derived from a missing-value corrected Shuttle Radar Topography Mission digital elevation model, with information about the azimuth and zenith angles taken from image metadata. Finally, all preprocessed Landsat images were mosaicked into single images for the periods 1972, 1984–1986 and 2000.

6.3.2 Image classification

The Landsat ETM+ (2000) image was spectrally classified using the supervised classification method. Training areas were selected on the basis of the ground truth information of the 196 land units that had been collected during fieldwork. The spectral separability of the LUC classes was assessed using the transformed divergence (TD) statistical measure (Swain, 1973; Bourne and Graves, 2001), and the maximum likelihood classifier, which generates very accurate classification results (Dewidar, 2004), was applied to classify the six non-thermal bands of the Landsat ETM + image. From the TD values and visual inspection of the classification result, LUC classes were joined or added until a satisfactory result was achieved.

No ground truth or other reference data were available for the period in which the Landsat 5 TM images were recorded (1984–1986 was in a period of civil war in the study area, and its access was extremely difficult). Therefore, the TM images were classified using the image differencing method, which is based on the subtraction of two spatially registered images from different periods to define change and no-change areas (Rogerson, 2002).

In order to test the performance of the Landsat MSS classification based on the historical terrestrial photographs, these images were also classified using image differencing. Because Landsat 1 MSS and Landsat 7 ETM+ have different spectral resolutions, it is not justified to difference their image bands. Therefore, the image differencing was performed using the Normalized Difference Vegetation Index (NDVI), an objective index of vegetation that is calculated using the red and near-infrared image bands (Lillesand et al., 2008). From the image difference result, change and no-change areas were identified. In both cases, classifications were performed by selecting training pixels in the no-change areas.

Last but not least, as an alternative to conventional change detection (e.g. image differencing) methods, the Landsat 1 MSS images were classified using information from ground-truthed historical terrestrial photographs, a method that has not been applied before. During fieldwork, the location and LUC properties of land units were registered for the current situation (2008) and for 1974–1975 (based on the historical photographs). This ‘ground truth’ was thus used to define training pixels for the classification of the MSS imagery. Originally, the LUC classes were the same as the ones used for the classification of the ETM+ images. On the basis of the TD values, some LUC classes were merged or left out. This iterative process was executed until a satisfactory classification result was produced.

6.3.3 Accuracy Assessment

The accuracy of the Landsat 7 ETM+ and Landsat 1 MSS classifications was assessed using repeated historical ground-based photographs (1974–1975 and 2007–2008) from the Tigray Repeat Photography Database (Nyssen et al., 2009a) that had not been used during the classification process. The classification result was tested against reality by comparing selected spots in the photographs with the classified images. Unfortunately, no reference data were available to assess the accuracy of the Landsat 5 TM classification (1984–1986).

The 1972 LUC maps were validated from 24 historical terrestrial photographs (1974–1975), and the 2000 LUC map was validated using the equivalent repeat photographs (2007–2008). Accuracy assessment was performed in ArcGIS® 9.2 (Image Analyst Extension) and resulted in a confusion or error matrix (Foody, 2002). From this matrix, the omission error (error of exclusion, linked to producer accuracy), commission error (error of inclusion, linked to user accuracy) and overall accuracy were calculated. Fleiss' Kappa (K) values (Stehman, 1997) were also calculated. This statistic is a measure of classification accuracy that ranges from -1 (complete discordance between datasets) to 1 (no misclassified pixels).

6.3.4 Analysis of Land Use and Cover Change (1972/1984–1986/2000)

LUC change was quantified using post-classification comparison, despite the disadvantage that the accuracy of the change map strongly depends on the accuracies of the compared maps (Singh, 1989). This analysis was performed in ArcGIS® 9.2. First, each period was analysed separately by calculating the proportion of each LUC class and comparing the LUC proportions of all observation years afterwards. Second, to quantify the extent and nature of LUC change, a change matrix and change maps (from–to change) were prepared for both pairs of observation years (i.e. 1972/1984–86 and 1984–86/2000). The change matrix gives the proportions of the study area by type of LUC in the first period that changed to a different class in the second. Third, all periods were combined into LUC change maps, with the following: (1) a map that visualizes the LUC change trajectories that have occurred over the observed period and (2) a map that visualizes the stability (number of changes) of each image pixel.

6.4 Results

6.4.1 Image Classification

2000 land use and cover map

During fieldwork, different types of settlement were observed, namely traditional villages, mixed villages and modern villages (depending on the proportion of houses with a traditional thatched or soil roof and metal sheet roof). In order to determine the spectral separability of these classes, a preliminary classification of settlements was performed. TD values pointed out that traditional and mixed villages were the most difficult to distinguish, so these classes were merged.

Initially, all training pixels were assigned to one of the 11 LUC classes (**Table 6.1**). However, the first classification result was unsatisfactory because field knowledge and comparison with topographical maps indicated that the LUC classes ‘modern village’ and ‘traditional village’ were over-represented. As closer examination pointed out that these wrongly classified areas were mainly roads and wetland areas, LUC classes ‘road’ and ‘wetlands’ were added to the previously defined LUC classes. In view of the difficulty to spectrally distinguish ‘shrubland’ from ‘dense bushland’, ‘open forest’ and ‘traditional village’ (TD lower than 1000), these classes were merged into one class, i.e. ‘bushland’. The excessive area of modern villages was reduced, but fragments remained present. According to the geological map (EIGS, 1978), these correspond mostly to areas with Precambrian-age or Palaeozoic-age lithologies that contain many high-reflecting minerals such as mica and quartz. Also, classification problems in the east of the study area were attributed to the different rainfall pattern (rain in the winter in the Rift Valley and its western escarpment). Lack of ground truth on such areas clearly caused classification problems. Therefore, a new LUC class ‘other’ was defined, with training pixels in areas on distinct different lithology or with a different rainfall pattern. Eventually, 11 LUC classeswere defined (**Table 6.1**). The average TD value was 1889, four pairs of LUC classes were spectrally difficult to separate, i.e. cropland and bare ground (TD 870), cropland and bushland (TD 1124), *Eucalyptus* plantation and bushland (TD 1231) and bare ground and bushland (TD 1310). The 2000 LUC map (**Figure 6.3**) was achieved with equal prior probabilities for each LUC class and after applying a 3 x 3 kernel majority filter.

Table 6.1 Definition of land use and cover classes.

No.	Class	Land cover (LC) and land use (LU)
1	Cropland	LU: cultivated land, not irrigated[a]; LC: (at the moment of image recording) bare with some weeds
2	Grassland	LC: 0 per cent trees, 0 per cent shrubs, > 90 per cent herbs and grasses; LU: grazing area, sometimes set aside for a few months to allow regeneration
3	Bare ground	LC: 0 per cent trees, < 10 per cent shrubs (< 3 m), < 10 per cent herbs and grasses; LU: no visible use or used as rangeland
4	Bushland	
	4 1 Shrubland	LC: 0 per cent trees, 10–50 per cent shrubs (< 3 m), 10–80 per cent herbs and grasses; LU: rangeland and fuelwood source or exclosure
	4 2 Dense bushland	LC: 0 per cent trees, > 50 per cent shrubs (< 3 m), 10–80 per cent herbs and grasses; LU: rangeland and fuelwood source or exclosure
	4 3 Open forest	LC tree canopy cover 10–50 per cent; LU: rangeland and fuel wood source or exclosure
	4 4 Traditional village	LC: mix of houses, roads, paths, stone walls, gardens and trees (mainly Eucalyptus), where more than 50 per cent of the houses has a thatched or traditional soil roof
5	Forest	LC: tree canopy cover > 50 per cent; LU: mainly church forest, exclosure
6	Eucalyptus plantation	LC: plantation of Eucalyptus trees, canopy cover > 50 per cent; LU: wood source, exclosure
7	Modern village	LC: mix of houses, roads, paths, stone walls, gardens and trees (mainly Eucalyptus), where more than 50 per cent of the houses has a metal sheet roof
8	Water	LC: Lakes and ponds
9	Wetland	LC: Rivers, shallow ponds, riparian vegetation
10	Road	LC: Asphalt and gravel roads
11	Other	Areas not covered during eldwork (with different lithology or rainfall pattern)

[a]Irrigated croplands were not included in this classi cation because no ground truth was recorded in such areas, given their limited area and their complexity (the phenological stage of vegetation in such areas can vary greatly)

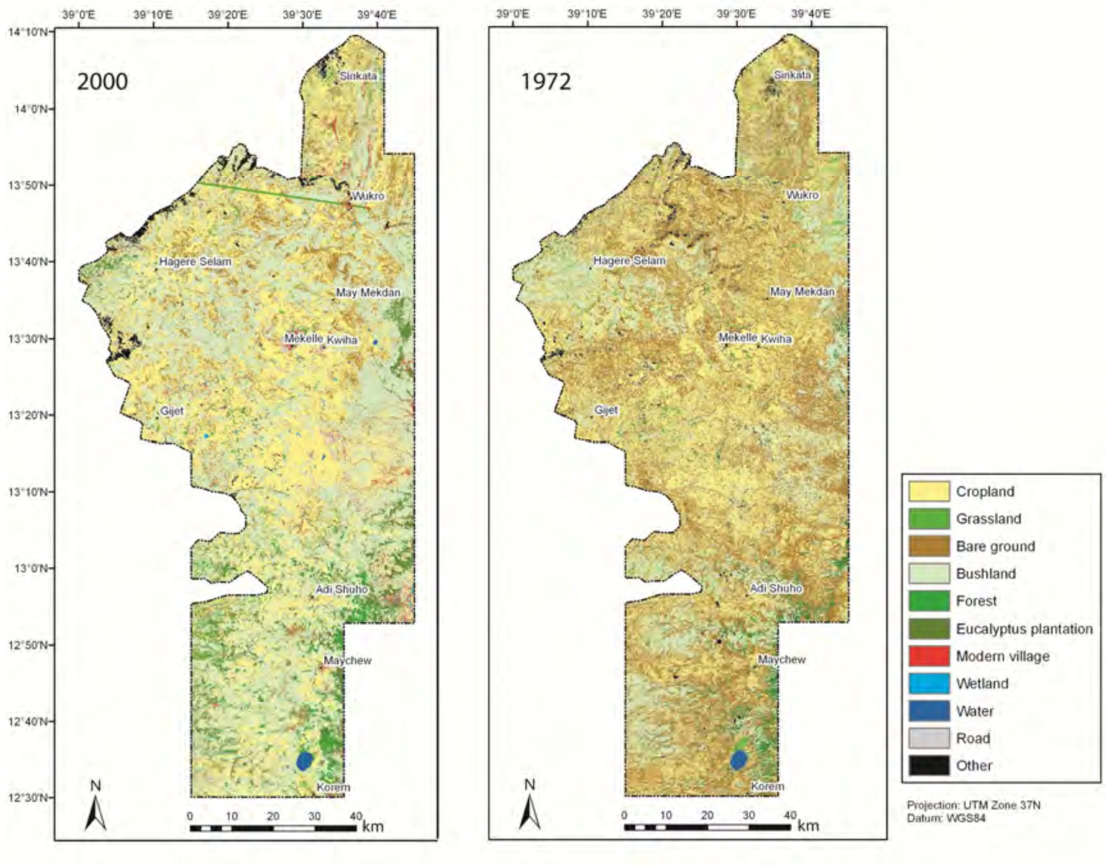

Figure 6.3 Land use/cover classification of Landsat Enhanced ThematicMapper Plus imagery (2000) using ground truthing in the field (left) and LandsatMultispectral Scanner imagery (1972) using information from ground-truthed historical terrestrial photographs (right).

1972 land use and cover map (based on historical terrestrial photographs)

On the basis of contemporary ground truthing (derived from the historical terrestrial photographs during fieldwork), training areas were selected on the Landsat MSS image. Because there was no ground-truthed information for eucalypt plantations, which only existed in a few localities in 1975, this class was left out. Roads could not be identified on the MSS images, most likely because of the combined effect of low MSS resolution (60m x 60m) and the fact that the road network mainly consisted of narrow earth roads in 1972. The class other was defined using exactly the same training areas as for the ETM+ images but was expanded with training areas of cloudy pixels present in the Southern part of the study area. TD values indicated low separability (TD<1500) for many LUC class pairs. Given the limited number of training areas, very little could be done to address this problem. Because separability problems were most severe for the LUC class ‘traditional village’, this class was combined with the class it spectrally resembled the most, i.e. ‘cropland’. TD values were still low for six pairs of LUC classes, mainly bare ground–cropland, bushland– cropland and bushland–bare ground (**Figure 6.3**, right).

1984–1986 and 1972 land use and cover map (based on image differencing)

Six normalized difference images were created by subtracting each TM image band (1–5 and 7) from the according ETM+ image band. From these difference images, a mean difference image was constructed. The change and no-change areas were determined from the mean and standard deviation of this image. Several threshold values (ranging from 1 to 3 standard deviations with an increment of 0.5) were tested and evaluated visually. A threshold value of 1.5 standard deviation around the mean was considered optimal. On the basis of the Landsat 7 ETM+ classification result, training pixels were selected in the no-change areas, and the observed LUC class was applied. After repetitive evaluation of the TD values and adjustment of the training pixels, an average TD of 1820 was obtained. Image classification was performed using the maximum likelihood classifier, and a mode (3 x 3 kernel) filter was applied (**Figure 6.4**).

Image differencing was also performed and was based on the NDVI of the Landsat ETM+ and MSS images. A threshold value of 1.5 standard deviations around the mean was used to distinguish change from no-change areas. Training pixels were selected in the no-change areas from the Landsat 7 ETM+ classification result, and after optimizing TD values to an average TD of 1790, a maximum likelihood classification was performed (**Figure 6.4**). Band 1 contains considerable noise (striping) that influences the classification results by causing stripes of alternating LUC classes in some areas. This was taken into account with the interpretation of the 1972 LUC map.

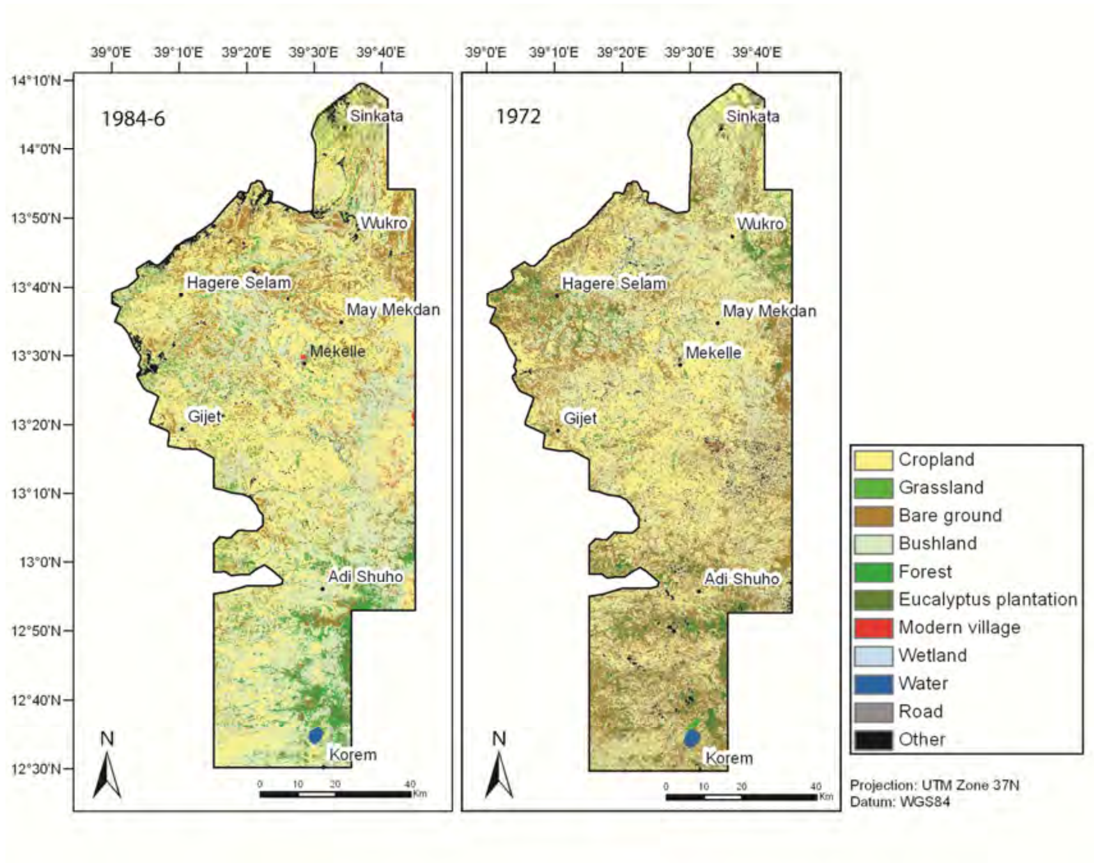

Figure 6.4 Land use/cover classification of Landsat Thematic Mapper imagery (1984‑1986) (left) and of Landsat Multispectral Scanner imagery (1972) (right), both based on image differencing.

6.4.2 Accuracy Assessment

A confusion matrix was produced for the 1972 LUC maps and the 2000 LUC map. First, all LUC classes were included in the confusion matrix. Later, classes with less than four sample locations were left out (wetland and water). Sample points that were classified as 'other' were not taken into account. A total of 107, 101 and 97 land units were eventually used to assess the accuracy of the ETM+, MSS (ground truth) and MSS (image differencing) classification results, respectively. The required minimum of 50 samples per LUC category (Congalton and Green, 1999) was not achieved, with even less than ten ground data points for grassland, forest and road.

The Kappa coefficient (0.75) indicates that there is a substantial level of agreement between the classification result and reality for the 2000 classification (**Table 6.2**). The user accuracy percentage is lowest for forest (25%), which was often misclassified as bushland. The bare ground class (user accuracy of 58%) was also difficult to differentiate and is mixed up with cropland, modern village, bushland and road.

There is a better agreement between the classification result and reality for the Landsat 1 MSS classification based on ground-based photographs (overall accuracy of 64%, **Table 6.3**) compared with the classification based on image differencing (overall accuracy of 59%, **Table 6.4**). Major differences in user accuracy are bare ground (86 vs 53%) and forest (14 vs 0%). The classification based on image differencing only has a higher user accuracy for bushland (79 vs 68%). The producer accuracy varies most for grassland (75 vs 56%) and bare ground (47 vs 63%). Details on user, producer and overall accuracy are given in Appendix C.

6.4.3 Analysis of Land Use and Cover Change from 1972 until 2000

The LUC maps for three periods (1972, 1984–1986 and 2000) were used to quantify the LUC change in the study area. For the 1972 period, the classification based on the historical ground-based photographs was used because it had the highest Kappa coefficient and overall accuracy.

Land use and cover proportions in 1972, 1984–1986 and 2000

In 1972, the study area was dominated by cropland (36%), bare ground (32%) and bushland (25%) (**Figure 6.5**). In 1984–1986, cropland (42%) and bushland (32%) were the major LUC classes. By 2000, bushland further increased to 43% whereas bare ground only occupied 8% of the total area and cropland diminished again (35%). The overall trend of LUC change in the study area between 1972 and 2000 is a significant decrease in bare ground (especially from 1972 to 1984–1986) and an increase in bushland, *Eucalyptus spp*. plantations and modern villages.

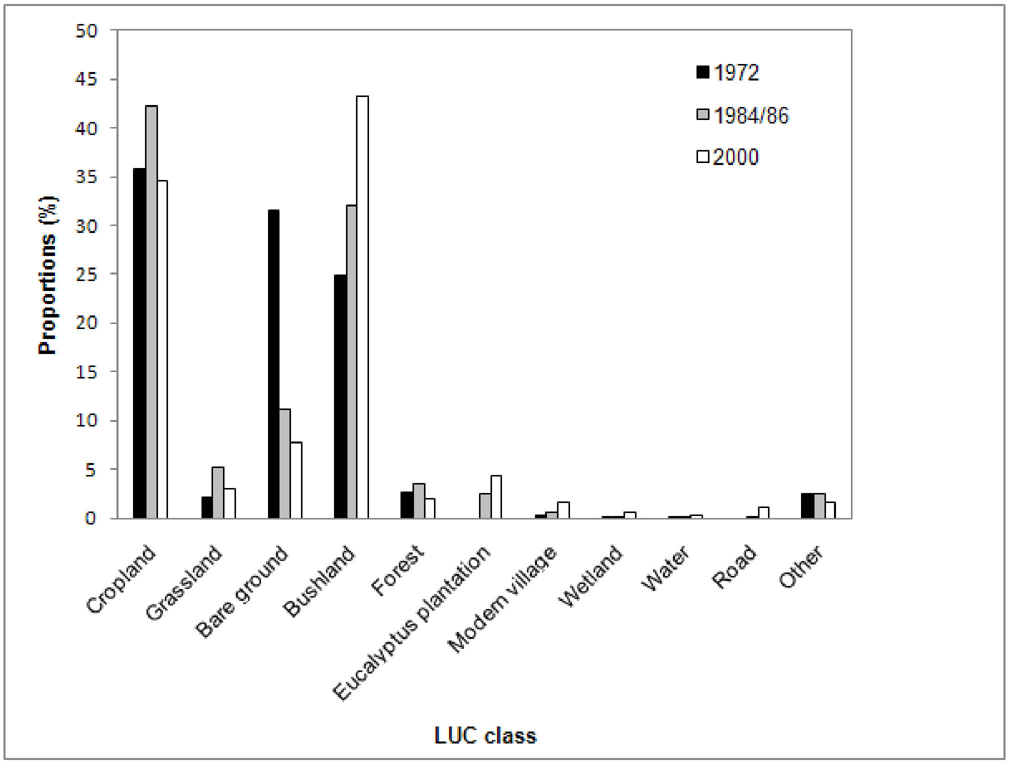

Figure 6.5 Land use and cover class proportions in 1972, 1984-1986 and 2000.

Change maps and matrices

The spatial pattern and nature of LUC change in the study area was analysed by producing a change matrix and map for two periods (1972/1984–1986 and 1984–1986/2000). Before analysis, the number of classes was reduced by merging ‘water’ with ‘wetland’ for all classifications and ‘road’ with ‘modern village’ for the 2000 and 1984–1986 classifications. The 1972 classification result was resampled to match the spatial resolution of the other classifications (30 x 30 m) using nearest-neighbour resampling. All areas classified as ‘other’ in one or more LUC maps were left out from the analysis (4.93%).

Land use and cover change between 1972 and 1984–1986.

In order to achieve an interpretable change map, the initial 49 from–to change categories (change matrix, **Table 6.2**) were reduced to six major LUC change classes, which were then visualized in a change map (**Figure 6.6**, left). Between 1972 and 1984–1986, 62% of the study area has undergone LUC change (**Table 6.2**, bottom). The most significant change is the decrease of bare ground as more than two-thirds of the 1972 bare ground area was converted to cropland or bushland by 1984–1986. During these 12 years, *Eucalyptus* plantations increased, mainly comprising former bushland and bare ground, and the grassland area more than doubled. Forestation and other increase in vegetation mainly took place in the southeastern part of the study area (**Figure 6.6**, left). The major degradation area is situated in the northeastern part of the study area. The increase of cultivated land is spread throughout the study area, but concentrations are present in the central (Mekelle) and western (Hagere Selam) parts of the study area.

Table 6.2 Land use and cover change matrix between 1972 and 1984‑1986 (total surface area in per cent).

1984-86 / 1972	Crop land	Grass land	Bare ground	Bush land	Forest	Eucalyptus plantation	Modern village	Water	1972 total
Cropland	19.2	1.4	4.4	8.5	0.2	0.2	0.2	0.02	34.1
Grassland	0.8	0.6	0.2	0.4	0.0	0.0	0.0	0.00	2.1
Bare ground	12.1	1.4	3.1	12.5	1.2	0.7	0.2	0.03	31.2
Bushland	8.7	1.1	2.9	9.3	1.2	1.1	0.2	0.04	24.4
Forest	0.3	0.0	0.2	0.8	0.9	0.4	0.0	0.00	2.6
Modern village	0.0	0.1	0.1	0.1	0.0	0.0	0.0	0.00	0.3
Water	0.1	0.0	0.0	0.0	0.0	0.0	0.0	0.14	0.3
1984-86 total	41.2	4.6	10.8	31.7	3.5	2.4	0.7	0.24	

Legend of major LUC change categories for the period between 1972 and 1984-86.

	Description	Proportion of study area (%)
	Deforestation	1.3
	Forestation	5.5
	Degradation	7.5
	Vegetation increase	21.4
	Conversion to water	0.1
	Bare ground/bushland to crop/grassland	23.3
	Other change	3.7
Bold	No change	33.3
	Areas classified as other	4.9

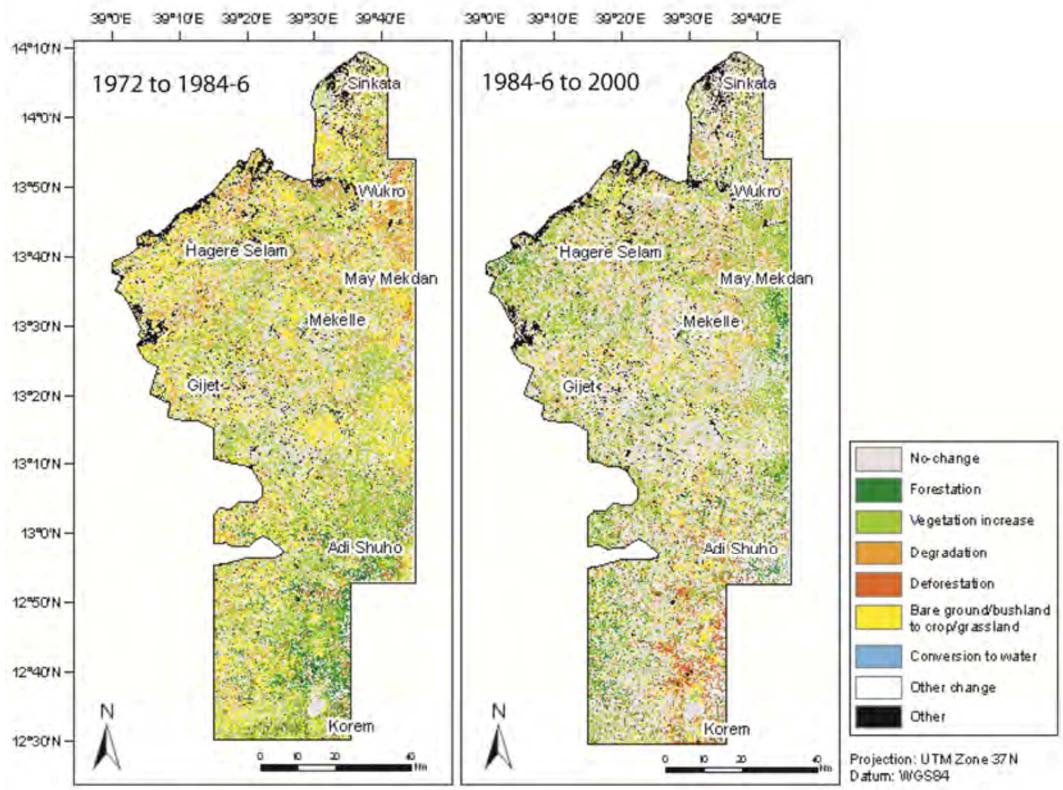

Figure 6.6 Land use and cover (LUC) change between 1972 and 1984‑1986 (left) and between 1984‑1986 and 2000 (right). LUC changes, limited to eight major LUC change classes, are indicated by different colours.Areas classified as ‘other’ LUC in the classification results were left out of the change analysis and are represented in black.

Land use and cover change between 1984–1986 and 2000.

From 1984–1986 to 2000, LUC has changed in almost half of the study area (49.7% or 4412 km^2). The change matrix (**Table 6.3**) indicates that the change area mainly consists of conversion from cropland to bushland (13% of the total area), bushland to cropland (around 6%) and bare ground to bushland (around 5%). The forest area decreased by 1.5% of the study area and was mainly changed into bushland and *Eucalyptus* plantation (mainly in the eastern and southwestern parts of the study area). This LUC change is mainly found in the southeastern part of the study area (**Figure 6.6**, right). Change to cultivated land is limited and mainly occurs in the southeastern part of the study area (Adi Shuho, Maychew and near Ashenge). Vegetation increase dominates the Northern part of the study area, whereas deforestation occurred mainly in the southeastern part of the study area.

Table 6.3 Land use and cover change matrix between 1984‑1986 and 2000 (total surface area in per cent).

1984-86 \ 2000	Crop land	Grass land	Bare ground	Bush land	Forest	Eucalyptus plantation	Modern village	Water	1984/86 total
Cropland	22.1	1.0	2.9	13.3	0.1	0.7	0.9	0.24	41.2
Grassland	1.1	0.8	0.5	1.8	0.0	0.1	0.3	0.04	4.6
Bare ground	3.0	0.3	1.9	5.3	0.1	0.2	0.1	0.01	10.8
Bushland	6.3	0.6	1.8	19.5	0.6	2.0	0.8	0.13	31.7
Forest	0.1	0.0	0.1	1.8	1.0	0.6	0.0	0.00	3.5
Eucalyptus plantation	0.2	0.1	0.1	0.8	0.2	0.1	0.1	0.85	2.4
Modern village	0.2	0.0	0.1	0.2	0.0	0.2	0.1	0.01	0.7
Water	0.0	0.0	0.0	0.0	0.0	0.1	0.2	0.00	0.2
2000 total	33.0	2.8	7.2	42.7	1.9	3.9	2.4	1.3	

Land use and cover change trajectory map

In order to analyse LUC change over the three periods, an LUC trajectory map was generated. Because representing all 418 occurring LUC change trajectories would not generate an interpretable map, specific LUC trajectories were defined by taking into account major LUC changes that occurred in each time interval. These trajectories (**Table 6.4**) encompass the difference between early (between 1972 and 1984–1986) and recent (between 1984–1986 and 2000) vegetation increase or decrease. Cropland areas are vegetated for only three months a year and are comparable to bare ground in the dry season (and therefore difficult to distinguish). It is concluded that a change from bushland to cropland (for example) is considered to be (woody) vegetation decrease. A change trajectory region map (**Figure 6.7**) was generated by generalizing the trajectorymap applying the Idrisimode filter (7 x 7 kernel) 15 times. In 19% of the study area, LUC did not change in the periods 1972/1984–1986/2000. The dominating change trend (27% of the study area) is a gradual or recent increase in vegetation. Main regions of recent vegetation increase are situated in the May Mekdan area and in eastern parts of the study area (Rift Valley escarpment). The area south of Adi Shuho has undergone a gradual increase in vegetation. Vegetation decrease occurred only in 7% of the study area and is mainly situated near Hagere Selam and in the central part of the study area.

Table 6.4 Classification of land use and cover change trajectories over the period 1972 - 1984-1986 - 2000.

Change trajectory name	Trajectory definition*					Percentage of total study area
	1972	→	1984/86	→	2000	
No-change	X	→	X	→	X	19%
Early vegetation decrease	Bu/F	→	Ba/C	→	Ba/C	5%
Recent vegetation decrease	Bu/F	→	Bu/F/E	→	Ba/C	2%
Gradual vegetation increase	Ba/C	→	Bu	→	Bu/F/E	14%
Recent vegetation increase	Ba/C	→	Ba/C	→	Bu/F/E	13%
Other change trajectories						42%

* X (any LUC class), Ba (Bare ground), Bu (Bushland), C (Cropland), F (Forest), E (Eucalyptus plantation)

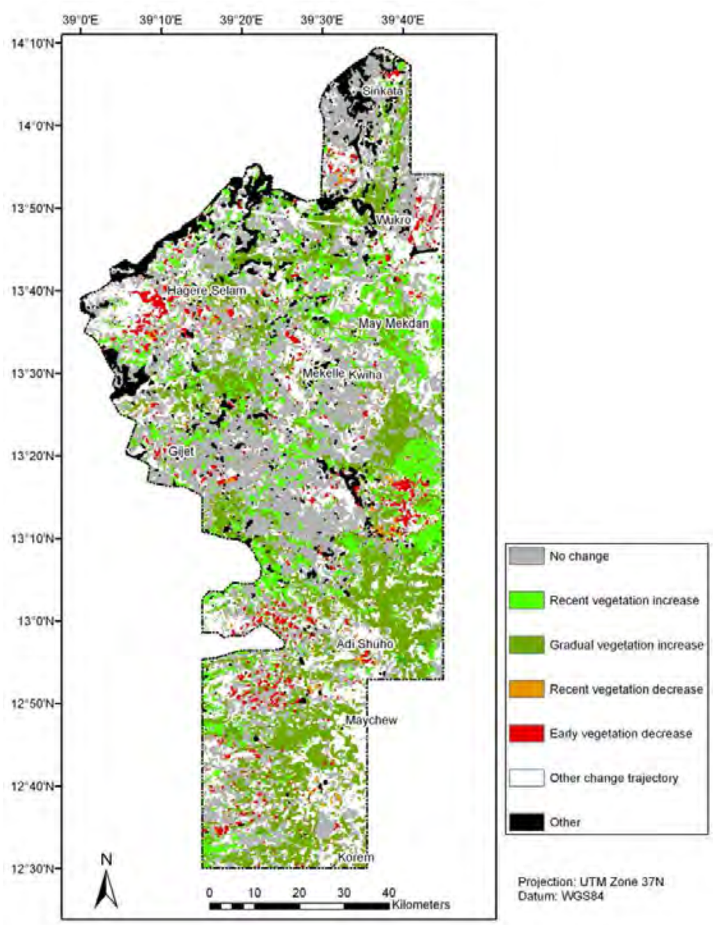

Figure 6.7 Overview of land use and cover (LUC) change in the study periods 1972/1984-1986/2000. The six major LUC change trajectories are indicated by different colours. Areas classified as 'other' LUC in the classification results were left out of the change analysis.

6.5 Discussion

6.5.1 Methodology

In contrast to former LUC research in Northern Ethiopia that focused on local-level changes, this study assessed LUC change on a regional level (over 8884 km^2) in a study area that is considered to be representative of the Northern Ethiopian Highlands. Furthermore, our research put particular emphasis on developing a methodology using historical photographs as ground truth for 1973 Landsat imagery.

The classification based on historical ground-based photographs yielded a Kappa coefficient of 0.54 and an overall accuracy of 64%, which still differs greatly from the required accuracy of 85% (Thomlinson et al., 1999). Although all satellite imagery had been captured during the dry season, the specific recording date varies from November to January–February. Because the rainy season lasts until September, there is significantly more vegetation in November (which is part of the harvest season) than in February. Although this does not have consequences for individual image classification, it does influence the process of image differencing because the phenological stage of the vegetation differs.

Ground truth data were collected in the summer of 2008 to perform a classification of the Landsat 7 ETM+ (2000) images. Because landscapes are dynamic and significant changes may occur in a time span of 8 years, efforts were made to retrieve the 2000 LUC properties, but this was not always possible. Furthermore, the accuracy of the 2000 classification result was assessed using field photographs that date from 2006 to 2008. Such time difference could lead to misinterpretation in rapidly changing environments. Further classification improvements can be made by collecting ground truth data in all geological sub-areas and agroclimatic zones (especially the eastern part) of the study area, as these have proven to cause misclassification.

Class separability is problematic for cropland and bare ground in all classifications. Although these classes have different land use, their land cover (especially in the dry season) and thus spectral response are very similar. In the MSS classification based on information from ground truthing the historical photographs, there is also low separability for cropland–bushland and bushland–bare ground. Both the season in which the images are recorded (early dry season) and the possible misinterpretation of historical ground-based photographs (especially for distant areas on the photographs) probably contributed to this confusion.

Although the image differencing technique can perform well when images from the same sensor are used (e.g. Landsat 7 ETM+ and Landsat 5 TM), images from sensors with different spectral resolutions such as Landsat 7 ETM+ and Landsat 1MSS are more difficult to compare. This problem was solved by differencing the NDVI of both images instead of the original image bands, which is not an ideal solution. The second problem with image differencing is the difficulty in determining the change/no-change threshold value, which is a subjective process. The shortcomings of this method are expressed by the accuracy of this classification, the Kappa coefficient is 0.46. Comparatively, the classification based on historical ground-based photographs yielded a Kappa coefficient of 0.54, which is an improvement.

All in all, the use of ground-based historical photographs is considered to be very promising and generates significantly better results compared with the more classic method of image differencing. This classification result could be further enhanced by improving ground truth recording by doing the following: (1) increasing the number of historical photographs used and (2) doing the fieldwork in the same season as the historical photographs were taken.

6.5.2 Land Use and Cover Change and Explaining

Factors Land use and cover change trend

From 1972 to 2000, LUC has undergone major changes in the Northern Ethiopian Highlands. Bare soil area has declined from 32 to 8% of the study area. It has been replaced mainly by bushland (25 to 43%) and the total forest area (including *Eucalyptus spp*. plantations), which more than doubled (2.6 to 6.3%). These findings are in line with observations made in specific (smaller) areas of the Northern Ethiopian Highlands (Wøien, 1995; Crummey, 1998; Bewket, 2002; Nyssen et al., 2009c). It contrasts however with decreasing forest cover and woody vegetation areas observed by Epema et al. (2000) who studied an area nearby ours over a period of 11 years only (1987–1998) and also with those by Tekle and Hedlund (2000), Zeleke and Hurni (2001) and Tegene (2002) who studied areas more to the SW; those studies also cover the decades between 1957 and 1986–2000, a period that includes a most probable decline in vegetation cover in its first half and a partial recovery in the second half, in contrast to our study that concerns only the decades after 1972, a period with regenerating vegetation.

Causes of land use and cover change

Although a thorough explanation of LUC change is not the objective of this study, some explanatory factors can be elucidated. Ethiopia has recently known two major shifts in land tenure system (Crummey, 2000). Prior to 1974 and for more than 900 years, feudalism (the gult system) had led to increasing inequalities in land holdings. In 1974, the Marxist government declared all land state property, thus reducing land holder inequality and controlled the grain market. In 1991, the post-Derg government legislated on ownership rights and freed the agricultural market. However, all land remained state property with tenured user rights on cropland. Increasingly, common land management focuses on land rehabilitation and sustainability. The population of Tigray has increased from 3.1 million in 1994 to 4.3 million in 2007 (CSA, 2008), which has led to increasing cultivation of land, more livestock and greater exploitation of wood for fuel and timber. The upland farming system faces increasing competition between livestock and crops. This has led farmers to allow grazing on croplands between harvest and sowing (Grepperud, 1996). Eventually, increased land cultivation, compaction and removal of crop residues and deforestation cleared the land and made it more vulnerable to land degradation. Ethiopia has been subject to recurring droughts and famine in 1972, 1980 and 1984. From 1975 onwards, but mainly since the 1990s, SWC measures have been undertaken (Nyssen et al., 2004b; Descheemaeker et al., 2006; Vancampenhout et al., 2006), aimed at environmental rehabilitation and income generation. At the onset, some farmers feared negative consequences (e.g. rodent shelter, loss of cultivated land) and therefore destroyed the physical structures. The establishment of exclosures also caused more pressure on the remaining grazing land. SWC efforts however continued, and their positive results (as reported by Nyssen et al., 2007b) have increased farmers' interest and awareness.

The progressive changes in Tigray in land tenure policy, population growth and SWC have been major factors in LUC change. In 1972, the main LUC class was bare soil (32%), but afterwards, vegetation cover has rapidly increased in most of the study area. The increase of bushland and forest is considered mainly due to SWC initiatives, which stimulated also agroforestry initiatives and established exclosures. Of course, the awareness of farmers is also crucial to preserving and expanding such areas. SWC, too, caused the recent creation of numerous earth dams and ponds, and these have offered increased water availability and irrigation possibilities. These results demonstrate that growing population pressure does not necessarily lead to irreversible land degradation. Similar conclusions were drawn by Tiffen et al. (1994) and Boyd and Slaymaker (2000). Tiffen et al. (1994) introduced the 'more people, less erosion' hypothesis based on a case study in the Machakos district (Kenya), where an increase in human population also resulted in more sustainable land use practices. Boyd and Slaymaker (2000) further discussed the 'more people, less erosion' hypothesis based on six cases in Africa and concluded that there are other examples of degradation reversal. Further study is needed to fully understand the dynamics of LUC change in the Northern Ethiopian Highlands and to determine its causes and driving factors.

6.6 Conclusions

The objective of this chapter was to detect LUC change in the Northern Ethiopian Highlands at a distinctive regional scale, using a unique dataset consisting of historical terrestrial photographs, field observations, satellite-based remote sensing and GIS.

Overall, the use of ground-based photographs, fieldwork, satellite-based remote sensing and GIS has proven to be very useful in the study of LUC change in the Northern Ethiopian Highlands. Although the satellite imagery has shortcomings (e.g. noise, acquisition date) and the combination of Landsat 1 MSS, Landsat 5 TM and Landsat 7 ETM+ images presents specific difficulties (mainly due to their different spectral resolution), satisfying classification results were achieved.

Two classification methods were compared to classify Landsat 1 MSS imagery. The first is based on historical ground-based photographs and the second on image differencing with recent Landsat imagery. Historical groundbased photographs are a useful ground truth resource for the classification of old satellite images. This method allows one to generate an independent classification of Landsat 1 MSS imagery. It does however require a sufficient number of ground-based photographs, preferably spread throughout the study area, and field observations to determine the location of training areas. Although the aspect of retrieving the exact location and angle of the historical photographs was not part of this study, it requires both time and field knowledge and thus has to be taken into account.

The study area showed significant LUC change over the last three decades. Major changes have been a decrease in bare soil and a considerable increase in bushland and forest. In 1972, the study area consisted mainly of bare ground and cropland. There was only a limited area covered by forest. By 2000, bushland dominates and bare soil has been reduced to a fourth of its former area. Numerous lakes and ponds were created in the central part of the study area. Although the forest area decreased slightly, the total area of *Eucalyptus spp*. plantations almost doubled over in the last 15 years. These results demonstrate that growing population pressure does not necessarily lead to irreversible land degradation. This change can be attributed to the SWC initiatives and the growing awareness of local communities.

6.7 References

Aerts, R., Van Overtveld, K., Haile, M., Hermy, M., Deckers, J., Muys, B., 2006. Species composition and diversity of small Afromontane forest fragments in northern Ethiopia. Plant Ecology 187, 127–142.

Allen-Rowlandson, T., 1988. A new approach to wildlife conservation in Ethiopia and its relevance to the control of desertification. Paper presented at the Nature Management and Sustainable Development, University of Groningen, Netherlands, 6–9 December.

Atwell, R.C., Schulte, L.A., Westphal, L.M., 2009. Landscape, community, countryside: linking biophysical and social scales in US Corn Belt agricultural landscapes. Landscape Ecology 24, 791–806.

Aynekulu, E., Wubneh, W., Birhane, E., Begashawl, N., 2006. Monitoring and evaluating land use/land cover change using Participatory Geographic Information system (PGIS) tools: a case study of Begasheka Watershed, Tigray, Ethiopia. Electronic Journal of Information Systems in Developing Countries 25, 1–10.

Bard, K.A., Coltorti, M., DiBlasi, M.C., Dramis, F., Fattovich, R., 2000. The environmental history of Tigray (northern Ethiopia) in the middle and late Holocene: a preliminary outline. African Archaeological Review 17, 65–86.

Bewket, W., 2002. Land cover dynamics since the 1950s in Chemoga Watershed, Blue Nile Basin, Ethiopia. Mountain Research and Development 22, 263–269.

Bourne, S.G., Graves, M.R., 2001. Classification of land-cover types for the Fort Benning ecoregion using Enhanced Thematic Mapper data. U.S. Army Engineer Research and Development Center, SERDP Technical Notes Collection, ERDC/EL TN-ECMI-01-01.

Boyd, C., Slaymaker, T., 2000. Re-examining the more people less erosion hypothesis: special case or wider trend? ODI Natural Resource Perspectives 63, 1–6.

Boyd, C., Turton, C., (eds). 2000. The Contribution of Soil and Water Conservation to Sustainable Livelihoods in Semi-arid Areas of Sub-Saharan Africa (vol. 102). The Agricultural Research and Extension Network: London.

Bussert, R., 2010. Exhumed erosional landforms of the Late Palaeozoic glaciation in northern Ethiopia: indicators of ice-flow direction, palaeolandscape and regional ice dynamics. Gondwana Research 18, 356–369.

Chavez, P.S., 1996. Image-based atmospheric corrections revisited and improved. Photogrammetric Engineering and Remote Sensing 62, 1025–1036.

Congalton, R.G., Green, K., 1999. Assessing the Accuracy of Remotely Sensed Data. Principles and Practices. Lewis Publishers, Boca Raton, FL.

Crummey, D., 1998. Deforestation in Wällo: process or illusion? Journal of Ethiopian Studies 31, 1–41.

Crummey, D., 2000. Land and society in the Christian Kingdom of Ethiopia. From the thirteenth to the twentieth century. University of Illinois Press, Addis Ababa.

CSA, 2008. Summary and statistical report of the 2007 population and housing census. Population size by age and sex. Central Statistical Agency of Ethiopia, Addis Abbaba.

Descheemaeker, K., Nyssen, J., Rossi, J., Poesen, J., Haile, M., Raes, D., Muys, B., Moeyersons, J., Deckers, J., 2006. Sediment deposition and pedogenesis in exclosures in the Tigray Highlands, Ethiopia. Geoderma 132, 291–314.

Dewidar, K.M., 2004. Detection of land use land cover changes for the northern part of the Nile delta (Burullus region), Egypt. International Journal of Remote Sensing 25, 4079–4089.

Diao, X.S., Pratt, A.N., 2007. Growth options and poverty reduction in Ethiopia—an economy-wide model analysis. Food Policy 32, 205–228.

Du, Y., Teillet, P;M., Cihlar, J., 2002. Radiometric normalization of multitemporal high-resolution satellite images with quality control for land cover change detection. Remote Sensing of Environment 82, 123–134.

EIGS, 1978. Hydrogeology of Mekele. Sheet Number ND 37-11. Ethiopian Institute of Geological Surveys: Addis Ababa.

Epema, G.F., Botoro, M.F., Deurloo, H., de Jong, S.M., 2000. Monitoring land use in Tigray (Ethiopia). Paper presented at the 1st Workshop of the EARSEL Special Interest Group on Remote Sensing for Developing Countries.

Feoli, E., Vuerich, L.G., Zerihun,W., 2002. Evaluation of environmental degradation in northern Ethiopia using GIS to integrate vegetation, geomorphological, erosion and socio-economic factors. Agriculture, Ecosystems & Environment 91, 313–325.

Foody, G.M., 2002. Status of land cover classification accuracy assessment. Remote Sensing of Environment 80, 185–201.

Gebremichael, D., Nyssen, J., Poesen, J., Deckers, J., Haile, M., Govers, G., Moeyersons, J., 2005. Effectiveness of stone bunds in controlling soil erosion on cropland in the Tigray Highlands, northern Ethiopia. Soil Use and Management 21, 287–297.

Green, K., Kempka, D., Lackey, L., 1994. Using remote-sensing to detect and monitor land-cover and land-use change. Photogrammetric Engineering and Remote Sensing 60, 331–337.

Grepperud, S., 1996. Population pressure and land degradation: the case of Ethiopia. Journal of Environmental Economics and Management 30, 18–33.

Haregeweyn, N., Poesen, J., Nyssen, J., De Wit, J., Haile, M., Govers, G., Deckers, S., 2006. Reservoirs in Tigray (Northern Ethiopia): characteristics and sediment deposition problems. Land Degradation & Development 17, 211–230.

Hoffman, M.T., Rohde, R.F., 2007. From pastoralism to tourism: the historical impact of changing land use practices in Namaqualand. Journal of Arid Environments 70, 641–658.

Houghton, R.A., 1994. The worldwide extent of land-use change. Bioscience 44, 305–313.

Hurni, H., 1990. Degradation and conservation of soil resources in the Ethiopian Highlands. Mountain Research and Development 8, 123–130.

Lillesand, T.M., Kiefer, R.W., Chipman, J.W., 2008. Remote Sensing and Image Interpretation (6th edn). John Wiley & Sons, Inc., New York, NY.

McClaran, M., Browning, D., Huang, C., 2010. Temporal dynamics and spatial variability in desert grassland vegetation. In repeat Photography: methods and applications in the natural sciences,Webb, R.H., Boyer, D.E., Turner, R.M. (eds). Island Press, Washington, DC, 145–166.

Mekuria, W., Veldkamp, E., Halle, M., Nyssen, J., Muys, B., Gebrehiwota, K., 2007. Effectiveness of exclosures to restore degraded soils as a result of overgrazing in Tigray, Ethiopia. Journal of Arid Environments 69, 270–284.

Merla, G., Abbate, E., Azzaroli, A., Bruni, P., Canuti, P., Fazzuoli, M., Sagri, M., Tacconi, P. 1979. A geological map of Ethiopia and Somalia (1973) 1:2.000.000 and comment.

Mertens, B., Lambin, E.F., 2000. Land-cover-change trajectories in southern Cameroon. Annals of the Association of American Geographers 90, 467–494.

Meyer, W.B., Turner, B.L., 1992. Human population growth and global land-use cover change. Annual Review of Ecology and Systematics 23, 39–61.

Muñoz-Villers, L.E., Lopez-Blanco, J., 2008. Land use/cover changes using Landsat TM/ETM images in a tropical and biodiverse mountainous area of central-eastern Mexico. International Journal of Remote Sensing 29, 71–93.

Munro, R.N., Deckers, J., Haile, M., Grove, A.T., Poesen, J., Nyssen, J., 2008. Soil landscapes, land cover change and erosion features of the Central Plateau region of Tigrai, Ethiopia: photo-monitoring with an interval of 30 years. Catena 75, 55–64.

Nyssen, J., Haile, M., Naudts, J., Munro, N., Poesen, J., Moeyersons, J., Frankl, A., Deckers, J., Pankhurst, R., 2009a. Desertification? Northern Ethiopia rephotographed after 140 years. Science of the Total Environment 407, 2749–2755.

Nyssen, J., Munro, R.N., Haile, M., Poesen, J., Descheemaeker, K., Haregeweyn, N., Moeyersons, J., Govers, G., Deckers, J., 2007a. Understanding the environmental changes in Tigray: a photographic record over 30 years (vol. 3). VLIR - Mekelle University IUC Programme and Zala-Daget Project: Mekelle.

Nyssen, J., Poesen, J;, Deckers, J., 2009b. Land degradation and soil and water conservation in tropical highlands. Soil and Tillage Research 103, 197–202.

Nyssen, J., Poesen, J., Moeyersons, J., Deckers, J., Haile, M., Lang, A., 2004a. Human impact on the environment in the Ethiopian and Eritrean highlands—a state of the art. Earth-Science Reviews 64, 273–320.

Nyssen, J., Poesen, J., Moeyersons, J., Haile, M., Deckers, J., 2007b. Dynamics of soil erosion rates and controlling factors in the northern Ethiopian Highlands—towards a sediment budget. Earth Surface Processes and Landforms 33, 695–711.

Nyssen, J., Simegn, G., Taha, N., 2009c. An upland farming system under transformation: proximate causes of land use change in Bela-Welleh catchment (Wag, Northern Ethiopian Highlands). Soil & Tillage Research 103, 231–238.

Nyssen, J., Vandenreyken, H., Poesen, J., Moeyersons, J., Deckers, J., Haile, M., Salles, C., Govers, G., 2005. Rainfall erosivity and variability in the Northern Ethiopian Highlands. Journal of Hydrology 311, 172–187.

Nyssen, J., Veyret-Picot, M., Poesen, J., Moeyersons, J., Haile, M., Deckers, J., Govers, G., 2004b. The effectiveness of loose rock check dams for gully control in Tigray, northern Ethiopia. Soil Use and Management 20: 55–64.

Ojima, D.S., Galvin, K.A., Turner B.L., 1994. The global impact of land-use change. Bioscience 44, 300–304.

Petit, C., Lambin, E.F., 2002. Impact of data integration technique on historical land-use/land-cover change: comparing historical maps with remote sensing data in the Belgian Ardennes. Landscape Ecology 17, 117–132.

Petit, C., Scudder, T., Lambin, E., 2001. Quantifying processes of land-cover change by remote sensing: resettlement and rapid land-cover changes in south-eastern Zambia. International Journal of Remote Sensing 22, 3435–3456.

Rembold, F., Carnicelli, S., Nori, M., Ferrari, G.A., 2000. Use of aerial photographs, Landsat TM imagery and multidisciplinary field survey for land-cover change analysis in the lakes region (Ethiopia). International Journal of Applied Earth Observation and Geoinformation 2, 1056–1061.

Riaño, D., Chuvieco, E., Salas, J., Aguado, I., 2003. Assessment of different topographic corrections in Landsat-TM data for mapping vegetation types. IEEE Transactions on Geoscience and Remote Sensing 41, 1056–1061.

Rogerson, P.A., 2002. Change detection thresholds for remotely sensed images. Journal of Geographical Systems 4, 85–97.

Ruthenberg, H., 1980. Farming systems in the tropics. Clarendon Press, Oxford.

Serneels, S., Said, M.Y., Lambin, E.F., 2001. Land cover changes around a major east African wildlife reserve: the Mara Ecosystem (Kenya). International Journal of Remote Sensing 22, 3397–3420.

Singh, A., 1989. Digital change detection techniques using remotely-sensed data. International Journal of Remote Sensing 10, 989–1003.

Stehman, S.V., 1997. Selecting and interpreting measures of thematic classification accuracy. Remote Sensing of Environment 62, 77–89.

Swain, P.H., 1973. A result from studies of transformed divergence. Laboratory for Operations of Remote Sensing.

Taddesse, B., 1995. Deforestation and environmental degradation in Ethiopia: the case of Jam Jam province. Northeast African Studies 2, 139–156.

Tegene, B., 2002. Land-cover/land-use changes in the Derekolli catchment of the South Welo zone of Amhara region, Ethiopia. Eastern Africa Social Science Research Review XVIII: 1–20.

Tekle, K., Hedlund, L., 2000. Land cover changes between 1958 and 1986 in Kalu District, Southern Wello, Ethiopia. Mountain Research and Development 20, 42–51.

Thomlinson, J.R., Bolstad, P.V., Cohen, W.B., 1999. Coordinating methodologies for scaling landcover classifications from site-specific to global: steps toward validating global map products. Remote Sensing of Environment 70, 16–28.

Tiffen, M., Mortimore, M., Gichuki, F., 1994. More people less erosion: environmental recovery in Kenya. Wiley: Chichester.

Tra, N.T., Egashira, K., 2004. Land use effectiveness by farm households after land and forest allocation at Tran Yen district, Yen Bai province. Journal of the Faculty of Agriculture Kyushu University 49, 461–466.

Turner, B.L., Meyer, W.B., Skole, D.L., 1994. Global land-use and land-cover change—towards an integrated study. Ambio 23, 91–95.

UNDP, 2010. Human Development Report HDI rankings. United Nations Development Programme. Oxford University Press, Oxford.

Van de Wauw, J., Baert, G., Moeyersons, J., Nyssen, J., De Geyndt, K., Taha, N., Zenebe, A., Poesen, J., Deckers, J., 2008. Soil–landscape relationships in the basalt-dominated highlands of Tigray, Ethiopia. Catena 75, 117–127.

Vancampenhout, K., Nyssen, J., Gebremichael, D., Deckers, J., Poesen, J., Haile, M., Moeyersons, J., 2006. Stone bunds for soil conservation in the northern Ethiopian Highlands: impacts on soil fertility and crop yield. Soil and Tillage Research 90, 1–15.

Virgo, K.J., Munro, R.N., 1978. Soil and erosion features of the Central Plateau region of Tigrai, Ethiopia. Geoderma 20, 131–157.

Westphal, E., 1975. Agricultural systems in Ethiopia. Centre for Agricultural Publishing and Documentation, Wageningen.

Wilson, R.T., 1977. The vegetation of central Tigre, Ethiopia, in relation to its land use. Webbia 32, 235–270.

Wøien, H., 1995. Woody plant cover and farming compound distributionof the Mafud escarpment, Ethiopia: an aerial photo interpretation of changes, 1957–1986. Working Paper on Ethiopian Development, 9.

Zeleke, G., Hurni, H., 2001. Implications of land use and land cover dynamics for mountain resource degradation in the Northwestern Ethiopian Highlands. Mountain Research and Development 21, 184–191.

Chapter 7
Spatiotemporal covariability in rainfall, cropping systems, land cover by crops and gully dynamism

This chapter is modified from:

Frankl, A., Jacob, M., Mitiku Haile, Poesen, J., Deckers, J., Nyssen, J., 2012. Spatiotemporal covariability in rainfall, cropping systems, land cover by crops and gully dynamism in the Northern Ethiopian Highlands. Land degradation & Development, submitted.

Abstract

In the Northern Ethiopian Highlands, about 33% of the land consists of cropland. This land is mainly cultivated by smallholders who design their cropping system in accordance with spatiotemporal rainfall variability. In order to understand the linkages between rainfall variability and cropping systems, a field campaign was organized in the rainy season 2009, during which 118 farmers where interviewed at different locations which reflect the regional variability in environmental characteristics. This indicated that five cropping systems occur, each having a distinct cropping season length and crop association. Cropping systems having shorter cropping seasons were generally applied on the valley flanks whereas longer cropping took place in the valley bottoms; a gradient was also distinguished in which the length of the cropping season increased from north-northeast to south-southwest. Crop associations within cropping systems also varied with altitude. With interannual changes in precipitation, the cropping systems that were applied by farmers changed accordingly. This results in shifts of cropping systems at catchment scale and at the regional scale, with cropping systems having longer cropping seasons being applied as annual precipitation increases. Upscaling our results to the whole region was done by modeling the spatial distribution of cropping systems and linking it to the rainfall maps of Jacob et al. (2012), what allowed to produce cropping system maps at 8 x 8 km² resolution over the period 1996-2009. The large year-to-year variability in the duration of land cover by crops in Northern Ethiopia might be an important, generally overlooked, explanatory factor for understanding runoff coefficients, gully erosion and previous land degradation cycles.

Keywords: Cropping system, Land cover by crops, Northern Ethiopian Highlands, Rainfall variability.

7.1 Introduction

About 33% of the Northern Ethiopian Highlands consists of cropland (de Mûelenaere et al., 2012). Nearly all this land is cultivated by smallholders who cultivate lands totaling approximately one ha (Gebremedhin and Swinton, 2003), producing for their own subsistence or for the local market (Lanckriet et al., 2012). As a result of agricultural intensification and areal expansion, the total food production increased much over the past decades (Nyssen et al., 2004; FAO, 2012). However, with the rapid demographic expansion of the second half of the 20th century, the food production per capita increased much less, making a large part of the population dependent on food distribution programs (Segers et al., 2008; van der Veen and Gebrehiwot, 2011). This was especially the case during droughts as the mountainous landscape of Northern Ethiopia does not allow the widespread application of irrigation agriculture (FAO, 2012), making crop production primarily dependent on rainfall. Farmers will therefore optimize their cropping system to the expected amount of rainfall and its distribution over the rainy season, which is based on local tradition and the arrival of the first rains in the early rainy season.

The rainfall regime of Northern Ethiopia is characterized by an important spatiotemporal variability. Regarding the temporal variability, several studies investigated rainfall patterns since the 1960s and concluded that the occurrence of long runs of dry and wet years and important year-to-year variations characterize the rainfall regime, but that no long-term trends of increasing or decreasing yearly precipitation are apparent (Conway, 2000; Seleshi and Zanke, 2004; Nyssen et al., 2005; Segele and Lamb, 2005; Seleshi and Camberlin, 2006; Tilahun, 2006; Cheung et al., 2008). Besides the temporal variability, the importance of spatial variability in rainfall has also been acknowledged. This is related to the dominance of thunderstorms for the occurrence of rainfall, which are mostly the product of the convection of heated air, and which are typically only a few km in diameter (Krauer, 1988; Nyssen et al., 2005). Thunderstorms do not develop at random, but their occurrence is to some extent dictated by topographical factors as the slope orientation and the slope gradient over large distances (Nyssen et al., 2005). As a result, steep gradients may occur between areas that on average receive little rain and areas where rainfall peaks. On a regional scale, a north-northeast to south-southwest pattern of increasing rainfall occurs (Jacob et al., 2012) which is related to the movement of the Intertropical Convergence Zone over Northern Ethiopia (Robinson and Henderson-

Sellers, 1999). Jacob (2012) indicated that this gradient is persistent during dry and wet years.

This study aims at understanding the relation between the spatiotemporal variability in cropping systems and rainfall in Northern Ethiopia. Special attention is given to the length of the land cover by crops, as this has important implications for differences in the runoff response of the land and gully dynamism in dry or wet years.

7.2 Materials and Methods

7.2.1 Study area

The area of study is located in the Northern Ethiopian Highlands and covers around 10^4 km², situated between 12°30' – 14°10'N and 39° – 39°50'E. Eight study areas which are representative for the regional variability in environmental characteristics were selected to study the cropping systems in detail. From north to south these are Ablo, May Mekdan, May Ba'ati, May Tsimble, Atsela, Ayba, Seytan and Lake Ashenge (Figure 1.1), named after their corresponding catchments, and in total covering an area of 123 km². Additional observations were made near the settlements of Atsgeba, Tsabat, Munguda and Korem (Figure 1.1).

The Highlands of Northern Ethiopia developed as a result of their rapid uplift at the western margin of the East African Rift Valley over the past 25 million years (Williams and Williams, 1980). The exposure of subhorizontal layers of Palaeozoic and Mesozoic sandstone, Mesozoic limestone and Tertiary volcanics (Merla et al., 1979) and their differential resistance to erosion, gave the Highlands their stepped relief, dominated by flat-topped mountains. Elevations in the study areas range between 2000 and 3900 m a.s.l. The Ablo catchment exposes sandstone; May Mekdan and May Tsimble shale with limestone cliffs and occasionally dolerite at the summits; Atsela, Ayba, Seytan and Lake Ashenge expose volcanics and May Ba'ati exposes volcanics at higher elevations, while sandstone, limestone and shale occur at lower elevations.

The influence of parent material on soil characteristics is important in Ethiopia (Nyssen et al., 2002a; Moeyersons et al., 2006). On the two major lithological units limestone/shale and basalt, typical soil catenas occur (Nyssen et al., 2008). Along slopes on basalt, Leptosols, Skeletic Cumuli Regosols, Vertic Cambisols and Vertisols are typical. The typical succession in limestone/shale areas is Calcaric Regosols/Cambisols, Cumulicalcaric Regosols and Calcisols. Along these sequences, soil depth generally increases while rock fragment content decreases (Nyssen et al., 2002b; Nyssen et al., 2008). For the sandstone areas, common soils are Luvisols which can be found in the plains and on the plateaus, while Arenosols and Cambisols typically occur on the slopes (Kassa et al., 2011). Due to active geomorphological processes, most soils are young (Virgo and Munro, 1978).

The movement of the Intertropical Convergence Zone over the Highlands marks three distinct periods in the moisture regime of the region: the dry season (*bega*) from October until February, the spring rainy season (*belg*) from March until May and the summer rainy season (*kiremt*) from June until September (**Figure 7.1**; Seleshi and Zanke, 2004; Cheung et al., 2008). In the *belg* season, monthly rainfall depth is generally low and the occurrence of rainfall is highly unreliable (Nyssen et al., 2005). Rains that occur in March-April are very important for the crop production in Northern Ethiopia and, if persistent, are called *azmera* rains (Verdin et al., 2005). The *kiremt* season is the main rainy season and accounts for 65 to 95% of the annual precipitation, ending rather abruptly in September (Segele and Lamb, 2005). Average annual precipitation ranges from 500 to 900 mm y^{-1} and increases from north-northeast to south-southwest (Jacob et al., 2012).

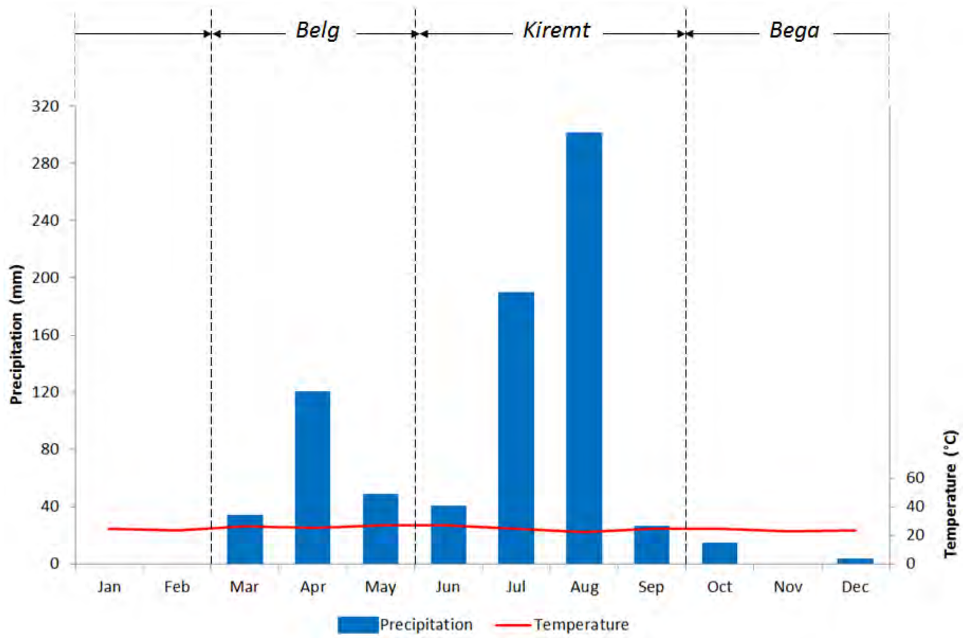

Figure 7.1 Ombrothermic diagram of 2006 for Mekele (Quiha). In the good rainfall year of 2006, the three seasons *bega*, *belg* and *kiremt* are well distinguished. The annual precipitation of 2006 was 755 mm, while the long-term average of this station is 611±148 mm (data from the National Meteorological Agency over the period 1960-2006).

The cropping system of our study area, defined in simple terms as farmers' map of their approach to their crop production (reformulated after http:// www.sarc.montana.edu/) has as most basic goal to increase food security of the household, especially in Northern

Ethiopia where many of the farming households suffer from food insecurity (van der Veen and Gebrehiwot, 2011). Here, the accent of the cropping system lies on cereals such as wheat (*Triticum aestivum*), barley (*Hordeum vulgare*) and the endemic fine-grained tef (*Eragrostis tef*) for the production of injera, the staple food of Ethiopia. If spring rains are good, sorghum (*Sorghum bicolor*) maize (*Zea mays*) and finger millet (*Eleusine coracana*) are increasingly being grown (Cheung et al., 2008; Slegers, 2008). Stews accompany the injera and, therefore, pulses like horse bean (*Vicia faba*), field pea (*Pisum sativum*), grass pea (*Lathyrus sativum*), fenugreek (*Trigonella foenum graecum*), lentil (*Lens culinaris*) and chickpea (*Cicer arientum*) are cultivated. Due to their ability to fix nitrogen, the pulses are applied in a crop rotation system. Fallow land is nearly absent (Nyssen et al., 2008) as a result of the agricultural intensification. Common is the mixture of crops like wheat-barley (called 'hanfets') and field pea-horse bean to avoid total crop failure in case of drought or disease. Fruit trees, green vegetables and tuber crops are nearly absent and mostly produced on very small plots near to the houses (Westphal, 1975; Nyssen et al., 2008). Livestock is also important in the agricultural system; especially oxen for ploughing but also sheep, goats, donkeys and mules are held (Nyssen et al., 2008). Since no forage crops are grown, a free grazing system is applied in which cattle are also allowed to graze stubble from fallow land and harvested land (Nyssen et al., 2008).

The agro-ecological belts of Northern Ethiopia reflect the differences in average annual temperature which mainly varies with altitude. Three belts can be distinguished in the study area: the *woina-dega* between 1500 and 2300 m a.s.l., the *dega* between 2300 and 3000 m a.s.l., and the *wurch* above 3000 m a.s.l. (Cheung et al., 2007; Tadesse et al., 2006). These agro-ecological belts have their typical crops which are wheat, tef, barley, maize, sorghum, finger millet and chickpea for the *woina-dega*; barley, wheat, tef, oilseeds and pulses for the *dega* and barley for the *wurch*.

As soil properties (depth, texture, fertility, water retention capacity, etc.) largely determine the crop productivity, these are also considered by farmers when applying cropping systems. Within a similar climate, soil characteristics are parallel to parent material and topographic position. Centuries of experience provided local communities with good insights into soil-crop relations (Nyssen et al., 2008) and an extensive nomenclature exists to denote soils of varying quality for cropping (Corbeels et al., 2000; Nyssen et al., 2008). In Northern Ethiopia, best soils for agriculture are found on basalt, where even shallow soils on steep slopes are being cultivated that can only be tilled by hoe. Soils derived from limestone are less intensively cultivated and more often used as range or grazing land (Van de Wauw et al., 2008).

7.2.2 Fieldwork

In order to investigate the cropping systems in the Northern Ethiopian Highlands, a field campaign was organized during July-September 2009. First, base maps were prepared of the different study areas on which land units were delineated. This was based on the stereoscopic interpretation of aerial photographs, field observations and information from interviews. A land unit was defined as an area having a distinct topography and lithology, where farmers usually apply the same cropping system. Second, in each of the land units, interviews with local key respondents were organized, as they have the best knowledge on how cropping systems are applied (Chambers, 1994). This aimed at understanding the variability in cropping systems and the relation with rainfall variability. Key informants were farmers older than 40 whom have been farming for many years in the land units. Semi-structured interviews were organized in the field or in nearby villages and included both specific and open-ended questions (Nyssen et al., 2006), allowing the respondents to put forward issues that otherwise would not have been addressed (Wengraf, 2001). Consistency was checked by selecting several key informants per land unit and by consulting the local office of the Bureau of Agriculture. In total, 118 interviews were held of approximately 45 minutes each.

The findings from the interviews were structured in a simple text analysis software (WinMax pro 98) by fragmenting the interviews according to keywords relevant to the study (Kuckartz, 1998). This allowed structuring the information gained from the interviews in a format that is easy to query.

7.2.3 Spatiotemporal rainfall variability maps

The rainfall maps prepared by Jacob et al. (2012) over the period 1996-2009 were used as an input to this study. These maps give the annual precipitation at a resolution of 8 x 8 km^2 for the Northern Ethiopian Highlands and are based upon the calibration with meteorological station data of NOAA’s Rainfall Estimates raster data (accessible from http://earlywarning.usgs.gov/).

7.2.4 Defining the cropping systems

Based upon the fieldwork, cropping calendars were created for each land unit. In contrast to the FAO format (e.g., Reynolds, 2006), the sowing and harvesting periods were not specified on the crop calendars. Instead, the period between the first moment of sowing and the last moment of harvesting was indicated, corresponding to the maximum period for which land cover by crops may occurs, considering that the crops need a few weeks to germinate (**Figure 7.2**). Cropping calendars were produced for dry, normal and wet rainfall years. Therefore, farmers were asked to recall dry, normal or wet rainfall years and to define the cropping system they had applied. As the farmers perception of dry, normal and wet may vary from place to place, farmers were asked to list a couple of years which they perceived as such. Consequently, the annual precipitation maps prepared by Jacob et al. (2012) could be used to define dry, normal and wet rainfall years in terms of the annual precipitation. The farmer perceptions on the rainy season are, however, not only based on the total yearly precipitation but also on the distribution of rainfall throughout the cropping season. As indicated by Jacob et al. (2012), there is a good correlation between the total yearly precipitation and the number of decades with precipitation above 10 mm (r = 0.62) or the occurrence of early rains in February-May (r = 0.52). Yearly precipitation thus largely reflects the characteristics of the rainy season and was therefore used to as a proxy of the applied cropping systems.

Based upon the length of the growing season of the dominant crops, cropping systems were defined, in consistency with short and long crop cycles defined in previous studies (Funk et al., 2003; Wubeneh et al., 2006; Reynolds, 2008), but were refined to match the complexity in the study area. Long crop cycles have a cropping season that starts in spring when *azmera* rains are good, while short crop cycles will rely solely on *kiremt* summer rains (Funk et al., 2003).

In order to understand shifts in cropping systems in the different land units as related to rainfall variability, maps displaying the cropping system applied in each land unit were prepared for dry, normal and wet rainfall years in ArcGIS® 9.2. On these maps, the bipolar yellow to green color gradient corresponds to the shift from short to long crop cycles and to an increase in land cover by crops.

7.2.5 Upscaling the cropping system patterns to the regional scale

The variability in cropping systems in the different land units and the relation with rainfall was upscaled to the Northern Ethiopian Highlands at the 8 x 8 km² raster of the rainfall maps of Jacob et al. (2012). Therefore, zones were delineated in the study area for which the same cropping system was applied in a dry, normal or wet rainfall year. As this zonation was different for upslope valley flanks (including structural flats) than for valley bottoms, these topographically distinct areas were considered separately. The zones were specified by defining Thiessen polygons between the studied land units. As a lower limit, the 2000 m a.s.l. contour line was used as the study did not consider areas below that altitude. As an upper limit, the 3000 m a.s.l. contour line defined the transition to the high-altitude mountain zones, which were represented by the study area of the Seytan catchment. The boundaries of the polygons were adjusted to match the raster of the rainfall maps and these boundaries corresponded to field observations of transition zones between areas with similar cropping systems.

In order to convert the annual rainfall maps of Jacob et al. (2012) to cropping system maps, dry, normal and wet rainfall years as perceived by farmers in each zone needed to be defined in terms of annual precipitation. Therefore, histograms of the average annual precipitation (25 mm interval) for the 14 years record of Jacob et al. (2012) were analyzed per zone. Thus, dry, normal and wet rainfall conditions were defined in each histogram.

Subsequently, each pixel on the rainfall maps of 1996-2009 could be classified into dry, normal and wet, corresponding to the perception of farmer and into cropping system maps. Regional maps at resolution of 8 x 8 km² were then created showing the variability in cropping systems and duration of the land cover by crops over the period 1996-2009.

7.3 Results

7.3.1 Variability in cropping systems as related to rainfall

Farmers will adapt their cropping calendar to the amount of rainfall expected in a year. Based on the timing of the moment when sufficient rain has fallen for sowing, farmers will design their cropping calendar so that for the selected crops, the length of the growing season reflects the expected rainfall. Such decisions take into account the very unreliable character of spring rains as compared to the more reliable summer rains (**Figure 7.1**; Nyssen et al., 2005). As the summer rains end rather abruptly in September, the selection of crops to sow is largely made at the beginning of the rainy season. For example, in the Lake Ashenge study area, early rains in the months April and May will motivate farmers to grow sorghum (*Sorghum bicolor*) in the valley bottoms as it has a long growing season (**Figure 7.2A**). In contrast, if rainfall amounts start only to be considerable for sowing as from July, the farmers will decide to grow barley (*Hordeum vulgare*) or wheat (*Triticum aestivum*). In May Mekdan, farmers will design their cropping calendar in a similar way as in the Lake Ashenge study area. In May Mekdan, the annual precipitation is however generally 200-300 mm lower so that cropping calendars are more compact and sowing is generally later (**Figure 7.2B**). In the valley bottoms, a normal rainy season will motivate farmers to start sowing wheat and tef (*Eragrostis tef*) in June/July, while harvesting occurs in November/December. Dry conditions delays the sowing to early August while wetter conditions allow sowing as from March/April

.

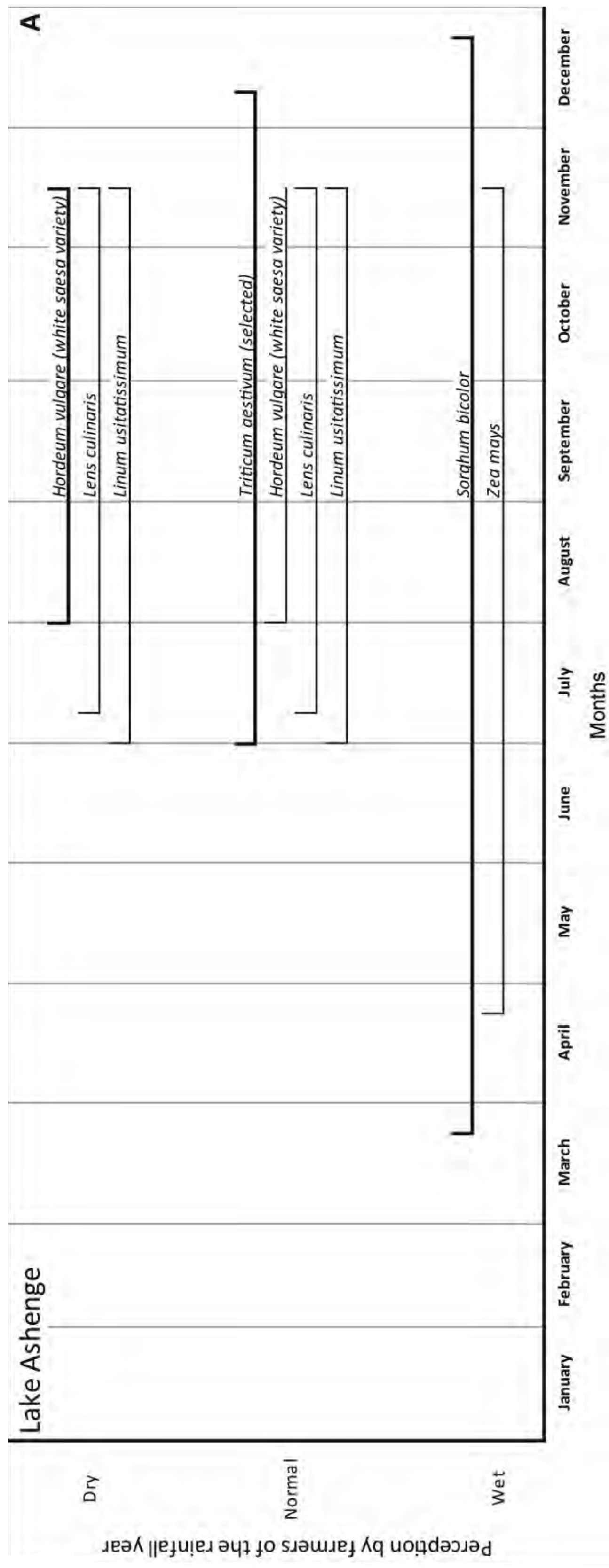
Lake Ashenge
A
Hordeum vulgare (white saesa variety)
Lens culinaris
Linum usitatissimum
Triticum aestivum (selected)
Hordeum vulgare (white saesa variety)
Lens culinaris
Linum usitatissimum
Sorghum bicolor
Zea mays
January
February
March
April
May
June
July
August
September
October
November
December
Months
Dry
Normal
Wet
Perception by farmers of the rainfall year

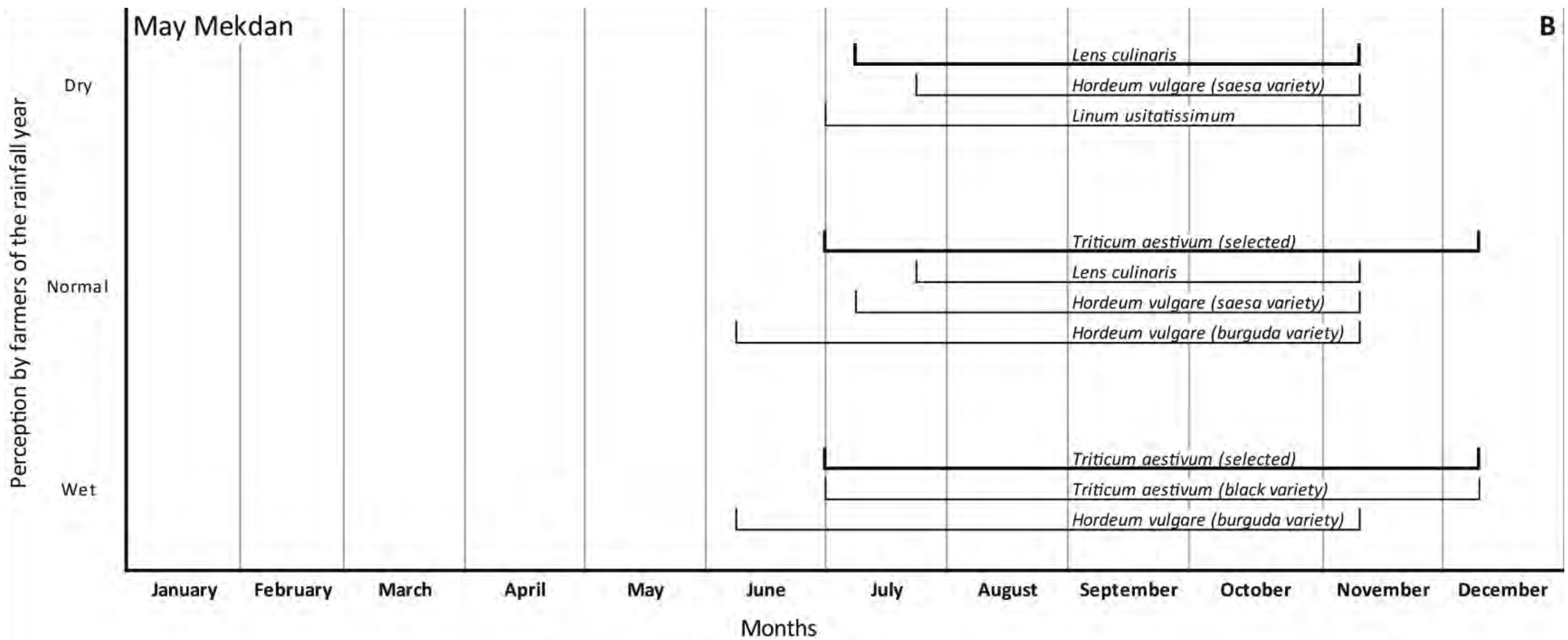

Figure 7.2 Cropping calendars in the valley bottoms of the study areas Lake Ashenge (A) and May Mekdan (B) in rainfall years perceived by farmers as dry, normal and wet. Major crops are indicated with a thicker line.

Considering all the studied land units, five types of cropping systems with distinct growing season lengths and typical plant associations could be defined: short crop cycle, short normal crop cycle, long normal crop cycle, long crop cycle and long two crop cycle. **Table 7.1** lists the most important crops and the length of the cropping season per cropping system. The short crop cycle (SC) crops had a grow period of maximum four months with sowing typically in July and harvesting in November. Barley and lentil (*Lens culinaris*) were the most important crops in this system. For the normal crop cycles, a distinction between short normal (SNC) and long normal (LNC) cycles was made, corresponding to grow periods of five or six months respectively. Sowing in these systems typically started in June and the major crops were barley, wheat and tef. Long crop cycles (LC) occur with good spring rains and the major crop sorghum may already be sown in March. If winter rains occur, a long two crop cycle (LTC) was applied in the southern part of the study area with sowing both in January/February and August and harvesting in July and November/December. Various crops were combined in the LTC system, with the exception of sorghum and maize (*Zea mays*) that have too long grow periods so that a second crop is not possible.

Table 7.1 Properties of the cropping systems in Northern Ethiopian Highlands.

Cropping system	Shortname	Duration of the land cover by crops (months)	Major crops
Short crop cycle	SC	4	Barley (*Hordeum vulgare, "white saesa"* variety) and lentil (*Lens culinaris*)
Short normal crop cycle	SNC	5	Wheat (*"selected"* variety) with barley (*"white saesa"* variety) or lentil
Long normal crop cycle	LNC	6	Barley (*"burguda"* variety), wheat (*"black" and "local"* variety) and/or tef (*Eragrostis tef "red"* variety)
Long crop cycle	LC	9	Sorghum (*Sorghum bicolor*)
Long two crop cycle	LTC	10	Two crops in one year

An analysis of the spatial variability in cropping systems for the 2009 situation, when rainfall was generally perceived as normal by farmers, indicated that three gradients occurred in the spatial distribution of cropping systems. Firstly, a gradient occurred at the catchment scale as a result of the topography-related soil and hydrological setting, with longer crop cycles being applied in the valley bottoms than on the valley flanks. For example, near Korem, farmers applied a LTC system in the valley bottom while a LC was applied on the valley flanks (**Figure 7.3**). Secondly, a latitudinal gradient was observed with a transition from shorter to longer cropping systems from north to south. This latitudinal gradient corresponds to the general north to south increase in precipitation in the region. Considering the cropping systems in the valley bottoms in 2009, while a LTC system was applied near Korem, LC systems were applied in the area of Lake Ashenge and LNC from Seytan to Ablo. Thirdly, an altitudinal gradient occurred related to decreasing temperature with altitude. This gradient especially considers the plant associations within a cropping system. For example, as leguminous crops, fenugreek will not be part of the crop rotation at high elevations but instead horse bean will be cultivated. Similarly, among the barley cultivars, *burguda* will not be part of the LNC at high elevations but instead *shewa* will be cultivated.

Figure 7.3 Cropping system variability at the catchment scale. In the cropping season of 2009, long two crop cycle system (LTC) was applied in the valley bottoms near to Korem, while a long crop cycle (LC) was applied on the valley flanks. The photograph taken on 17 July shows farmers harvesting the first crop and preparing the farmlands again for sowing the second crop in the valley bottom. On the valley flanks, mainly sorghum was cultivated that was only harvested in November/December.

As a result of the covariability between cropping systems and rainfall patterns, dry and wet anomalies in yearly precipitation will cause catchment-scale and latitudinal shifts in the cropping systems. At the catchment scale, switching from dry, normal to wet rainfall conditions will cause longer cropping systems to be applied, with the cropping system in the valley bottoms always retaining a longer cropping period as compared to the valley flanks. This is well illustrated for the Lake Ashenge study area (**Figure 7.4**). In the relatively dry year of 2004, a SNC was applied in the valley bottom while a SC occurred on the flanks. In 2009, when precipitation was perceived as normal by the local farmers, the valley bottom was under LC, while on the valley flanks a SNC was applied. Wet rainfall years, as was the case in 2006, allow two harvestings with the LTC system in the valley bottom, and a LC on the valley flanks.

The rainfall related patterns that occurred at the catchment scale were also reflected in north-south shifts of cropping systems at the regional scale. As compared to the situation

in normal years, cropping systems shifted southwards in dry years and northwards in wet years (**Figure 7.5A-D**). SC and SNC therefore became most widely applied in valley bottoms during dry years (e.g., 2004) while LC and LTC occurred during wet years (e.g., 2006). On the valley flanks, in SNC were mostly applied in normal rainfall years while SC occurred in dry years and LNC in wet years.

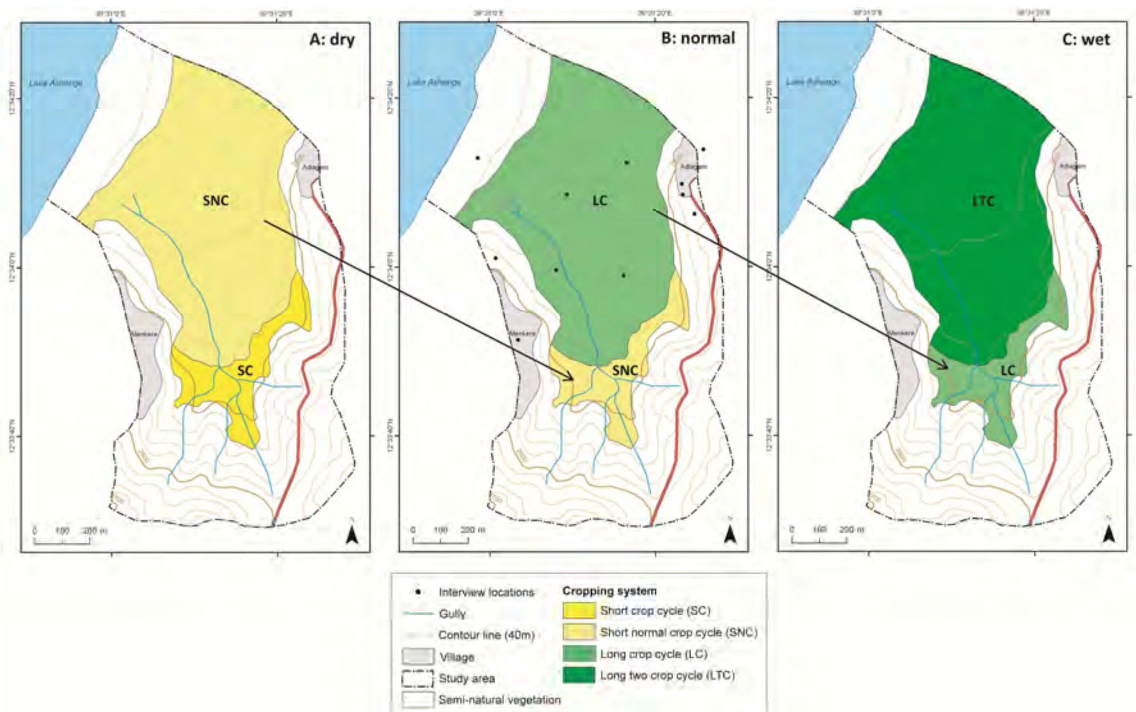

Figure 7.4 Cropping systems maps for the Lake Ashenge study area for rainfall years perceived as dry, normal and wet by farmers. **A**: dry year (e.g., 2004), **B**: normal year (e.g., 2009) and **C**: wet year (e.g., 2006). Switching from dry, normal to wet rainfall conditions causes longer cropping systems to be applied in the catchment, with the cropping system in the valley bottom always retaining a longer cropping period as compared to the valley flanks.

7.3.2 Regional cropping system maps (1996-2009)

Based upon the analysis of histograms that give the frequency of annual precipitation in classes of 25 mm over the period 1996-2009 per zone, dry-normal-wet perceptions on the rainfall year by farmers were defined in terms of annual precipitation. The transitions between dry/normal and normal/wet were defined for each zone and are given in **Table 7.2**. As can be observed, the transitions between dry/normal and normal/wet increase from north to south. This indicates that the perception of rainfall by farmers varied according to what is perceived as normal, which was also reflected by the latitudinal gradient in cropping systems. In the upper zone above the 3000 m a.s.l., the dry/normal and normal/wet transitions reflect the high precipitations at those altitudes.

Table 7.2 Transitions between dry, normal and wet rainfall years as perceived by farmers translated into annual precipitation for each zone.

Zone	dry/normal ($mm\ y^{-1}$)	normal/wet ($mm\ y^{-1}$)
Northern	350	575
Central	400	625
Southern	450	750
High-mountain	450	675

Consequently, the dry, normal and wet perceptions of the rainfall year by farmers could be transferred into cropping systems per zone. Applying this at a regional scale using pixel-based maps of annual precipitation (Jacob et al., 2012) allowed to produce maps displaying the cropping systems in the Northern Ethiopian Highlands over the period 1996-2009. Maps were prepared for valley bottoms and for valley flanks separately and allowed to investigate and to understand the spatiotemporal variability in cropping systems and the duration of the land cover by crops. **Figure 7.5A-D** shows from right to left cropping system maps for valley bottoms with increasing annual precipitation. The north to south increase in cropping season length explained in the previous section can clearly be observed on these maps. Furthermore, the maps indicate that this gradient is rather North-northeast to south-southwest. Additional observations and interviews at the sites of Atsgeba, Tsabet and Munguda (Figure 1.1) confirmed that indeed, cropping seasons length increased from east to west, but this to a lesser degree than from north to south. The map of 2004 (**Figure 7.5A**), which was generally perceived as a dry rainfall year by farmers, shows that only SC or SNC were applied in the valley bottoms. With only SC being applied on the valley flanks, the duration of land cover by crops is four to six months in a dry year. The maps of 2009 and 1999 show the situation in normal rainfall years, making a distinction between below-average and above-average normal rainfall years (**Figure 7.5B-C**). In general, LNC systems were applied in normal rainfall years, having a cropping season of six months. In the below-average normal rainfall year of 2009, SC were found in the north-northeastern driest part of the region while LC were found in the wetter southern part. Cropping season length in the valley bottoms therefore varied from four up to nine months. On the valley flanks, SC were most apparent, reducing the cropping season length to four months. In the above-average normal rainfall year (**Figure 7.5C**), SC did not occur in the valley bottoms and LTC systems occurred in the southern part of the region. Cropping calendars then varied between six and ten months. For the valley flanks SNC systems were widespread, which correspond to a cropping season length of five months. In an exceptionally wet year, like 2006 (**Figure 7.5D**), LC were most widely applied in the valley bottoms, with some LNC in the northeast and LTC in the south and at higher elevations. The cropping season therefore was generally nine months and varied between six and ten months. LNC systems were most important on the valley flanks.

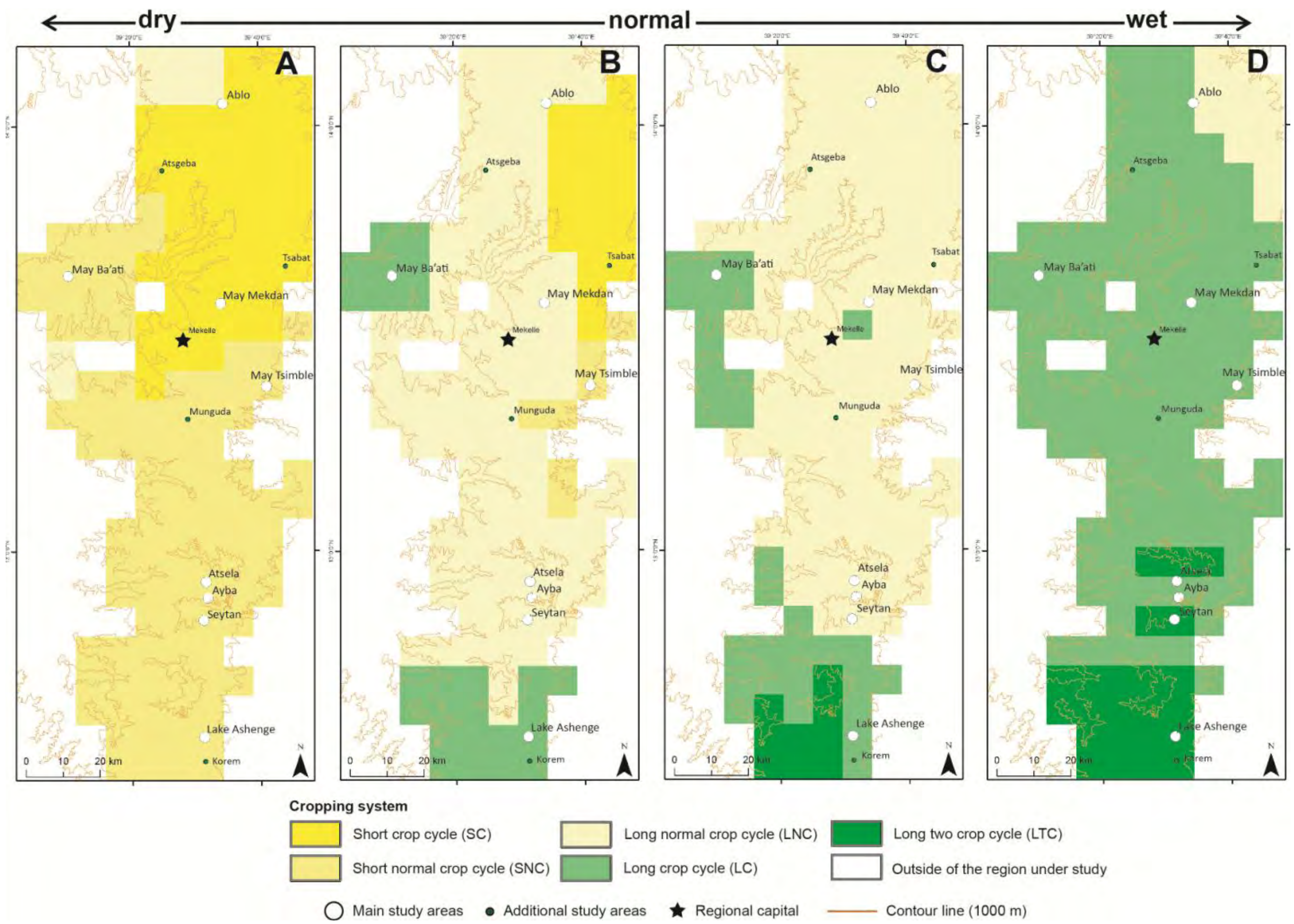

Figure 7.5 Cropping systems maps for valley bottoms in Northern Ethiopia as related to rainfall variability. Pixel size corresponds to that of the RFE maps. From right to left cropping system maps are shown with increasing total annual precipitation: A dry year (e.g., 2004), B below-average normal year (e.g., 2009), C above-average normal year (e.g., 1999), D wet year (e.g., 2006). The maps indicate a north-northeast to south-south-west shift in cropping systems having longer growing seasons with increasing annual precipitation.

7.4 Discussion: duration of land cover by crops and implications for land degradation and gully erosion

Successions of dry years, especially those of the 1970s and 1980s were associated with important land degradation by gullying in Northern Ethiopia (Virgo and Munro, 1978; Frankl et al., 2011, 2012). These dry years have increased the vulnerability of the land to water erosion processes by the rapid deterioration of the canopy and by adverse land use changes. On the steep valley flanks, where semi-natural ecosystems prevail, the runoff response of the land increased as a result of the decreased biomass production and the related increased impact of grazing. Moreover, the drop in land productivity during droughts forced farmers to cultivate marginal and steep land to maximize food production, aggravating the situation on the valley flanks (Frankl et al., 2011). This caused both the surface covered by cropland and bare ground to peak in the 1970s-1980s (de Mûelenaere et al., 2012), when extremely harsh droughts occurred. As a result, flash flood events became more severe during droughts which led to the development of dense gully networks (Frankl et al., 2012).

Crops intercept rainfall and can hence provide protection against water erosion processes (Styczen and Morgan, 1995; Dunne and Leopold, 1978). On the one hand, the above-ground biomass gives direct protection against splash erosion, decreases the kinetic energy of raindrops, and slows runoff velocities. On the other hand, the below-ground biomass physically binds the soil, decreasing the erodibility of the land, and enhances the soil permeability and soil structure. The combined effect of both the above- and below-ground biomass decrease soil losses by splash, sheet, rill and gully erosion (Gyssels et al., 2005; Knapen et al., 2007). After the harvesting, crop residues and dead roots remaining in the upper soil layer can still provide some protection against erosion (Gyssels et al., 2005).

With 33% of the land surface of Northern Ethiopian Highlands covered by cropland, the variability in the duration of land cover by crops might be important for understanding the severity of previous land degradation cycles. As indicated in this study, farmers apply short (SC) and short normal crop cycles (SNC) during dry years, limiting the cropping season to four or five months. This is in sharp contrast with the situation in a wet year, when long normal crop (LNC), long crop (LC) and long two crop (LTC) cycles are applied, increasing the land cover by crops to six-ten months. This implies that, during wet years, land benefits from a longer protection from erosion by crops, making it less vulnerable to the larger frequency of storms. In contrast, during dry years, the period for which the land benefits from the protection against erosion by crops shortens in the early rainy season. The croplands therefore become highly vulnerable to storms that occur in the early rainy season as they impact fallow land.

Several studies stressed the importance of crop cover characteristics throughout the rainy season in order to understand the temporal variability in soil losses. For example, in Zimbabwe seasonal runoff and soil losses prove to peak not when the rainfall was most severe, but rather in the early cropping season when the land cover by crops was highly variable (Elwell and Stocking, 1976). In the study area, Vanmaercke et al. (2010) showed that sediment concentration in rivers was highest in the beginning of the rainy season before crops could establish. Similar concerns were also put forward by Cyr et al. (1995) for Southern Quebec (Canada), who stressed that crops which rapidly develop a good land cover should be cultivated in rugged terrain in order to protect the slopes against high-erosive rains in the early cropping season. In erosion studies, in Ethiopia and elsewhere, the importance of crop cover characteristics on land degradation is however generally overlooked. For instance, in erosion models such as RUSLE (Renard et al., 1997), values for protection by crop cover are allotted to crop species, but not/or only partly to growth duration of cultivars or to cropping systems that could involve two subsequent crops. Regarding gully erosion in the Northern Ethiopian Highlands, Chapter 3 indicated that gully densities were generally higher for catchments in shale (Mekdan and May Tsimble) than for catchments in volcanics (Atsela, Ayba, Seytan and Lake Ashenge) (Table 3.4, Figure 3.4C), although the volcanics catchments receive on average 200-300 mm more yearly precipitation and expose steeper terrain. This can be related, to some extent, to the longer duration of land cover by crop cover in regions that are well endowed with rainfall and hence protect also better against erosion.

7.5 Conclusions

Farmers in the Northern Ethiopian Highlands have adopted flexible farming systems that optimally take into account local environmental conditions and largely adapt to interannual variations in rainfall. Five cropping systems could be identified with typical cropping season lengths: short crop cycle (four months), short normal crop cycle (five months), long normal crop cycle (six months), long crop cycle (nine months) and long two crop cycle (ten months). Each of these systems has a typical crop association (**Table 7.1**). At the catchment scale, cropping systems on valley flanks appeared to be of shorter duration than cropping systems in valley bottoms, which is the reflection of contrasting soil and hydrological characteristics in both topographical situations. At a regional scale, a north-northeast to south-southwest gradient of cropping systems occurs, with crop calendar lengths increasing towards the south-southwest, parallel to spatial variations in annual precipitation.

Depending of the period in which the first rains of the rainy season are good enough for sowing, farmers will apply a cropping system that matches the length of the rainy season. Therefore, shifts in cropping systems occur at the catchment and at the regional scale with temporal variations in annual precipitation. In a rainfall year percieved as normal by farmers, long normal crop cycles generally occurred in the valley bottoms while short (normal) crop cycles occurred on the valley flanks. When conditions were percieved as drier, and spring rains largely failed, short (normal) crop cycles were applied in the valley bottoms and short crop cycles on the valley flanks. When conditions were percieved as particularly wet, early spring cropping became possible and long (two) crop cycles generally occurred in valley bottoms while long normal crop cycles occurred on valley flanks.

With 33% of the land surface of Northern Ethiopian Highlands covered by cropland, the variability in the duration of land cover by crops is important for understanding previous land degradation cycles. As a result of the late sowing during relatively dry years, precipitation in the early rainy season impacts fallow land, and therefore, higher erosion rates are expected.

7.6 References

Chambers, R., 1994. The origins and practice of participatory rural appraisal. World Development 22, 953-969.

Cheung, W.H., Senay, G.B., Singh, A., 2008. Trends and spatial distribution of annual and seasonal rainfall in Ethiopia. International Journal of Climatology 28, 1723-1734.

Conway, D., 2000. Some aspects of climate variability in the North East Ethiopian Highlands - Wollo and Tigray. Sinet Ethiopian Journal of Science 23, 139–161.

Corbeels, M., Abebe Shiferaw, Mitiku Haile, 2000. Farmers' knowledge of soil fertility and local management strategies in Tigray, Ethiopia. In: Managing Africa's Soils, No. 10. IIED, London; 24.

Cyr, L., Bonn, F., Pesant, A., 1995. Vegetation indexes derived from remote-sensing for an estimation of soil protection against water erosion. Ecological Modelling 79, 277-285.

de Mûelenaere, S., Frankl, A., Mitiku Haile, Poesen, J., Deckers, J., Munro, N., Veraverbeke, S., Nyssen, J., 2012. Historical landscape photographs for calibration of LANDSAT land use/cover in the Northern Ethiopian Highlands. Land Degrad. Dev., Online Early View.

Dunne, T., Leopold, L., 1978. Water in Environmental Planning. Freeman, New York.

Elwell, H.A., Stocking, M.A., 1976. Vegetal cover to estimate soil erosion hazard in Rhodesia. Geoderma 15, 61-70.

FAO, 1995. FAO soils bulletin: Sustainable dryland cropping in relation to soil productivity. Accessed from http://www.fao.org/docrep/V9926E/V9926E00.htm on 24/05/2012.

FAO, 2012. FAO CountryStat for Ethiopia. Accessed from http://www.fao.org/ on 24/05/2012.

Frankl, A., Nyssen, J., De Dapper, M., Mitiku Haile, Billi, P., Munro, R.N., Deckers, J., Poesen, J., 2011. Linking long-term gully and river channel dynamics to environmental change using repeat photography (North Ethiopia). Geomorphology 129, 238-251.

Frankl, A., Poesen, J., Scholiers, N., Jacob, M., Mitiku Haile, Deckers, J., De Dapper, M., Nyssen, J., 2012. Assessment of decadal gully network and volume development in Northern Ethiopia using small-scale aerial photographs and high resolution satellite images. Earth Surface Processes and Landforms. Submitted.

Funk, C., Asfaw, A., Steffen, P., Senay, G., Rowland, J., Verdin, J., 2003. Estimating Meher crop production using rainfall in the 'Long Cycle' region of Ethiopia. Famine Early Warning System, Special Report C, 1-4.

Gebremedhin, B., Swinton, S.M., 2003. Investment in soil conservation in northern Ethiopia: the role of land tenure security and public programs. Agricultural Economics 29, 69-84.

Gyssels, G., Poesen, J., Bochet, E., Li, Y., 2005. Impact of plant roots on the resistance of soils to erosion by water: a review. Progress in Physical Geography 29, 189-217.

Jacob, M., Frankl, A., Haile, M., Nyssen, J., 2012. Assessing spatio-temporal rainfall variability in a tropical mountain area (Ethiopia) using Rainfall Estimates. In preparation.

Kassa Teka, Van Rompaey, A., Poesen, J., Van Bruyssel, S., Zenebe, A., Deckers, J., 2011. Land use and cover changes in Sinkata village. Excursion guide of the post-conference excursion: IAG/AIG regional conference, Ethiopian Association of Geomorphologists (EAG), 203-234.

Knapen, A., Poesen, J., Govers, G., Gyssels, G., Nachtergaele, J., 2007. Resistance of soils to concentrated flow erosion: A review. Earth-Science Reviews 80, 75-109.

Krauer, J., 1988. Rainfall, erosivity and isoerodent map of Ethiopia. Soil Conservation Research Project, Research Report 15, University of Berne, Switzerland. 132 pp.

Kuckartz, U., 1998. Winmax scientific text analysis for the social sciences user's guide. Udo Kuckartz, BSS, Berlin, 176 pp.

Lanckriet, S., Tesfay Araya, Derudder, B., Cornelis, W., Govaerts, B., Bauer, H., Deckers, J., Mitiku Haile, Naudts, J., Nyssen, J., 2012. Spatial diffusion and social acceptance of Conservation Agriculture in May Zeg-zeg (Ethiopia). Agronomy for Sustainable Development, in preparation.

Merla, G., Abbate, E., Azzaroli, A., Bruni, P., Canuti, P., Fazzuoli, M., Sagri, M., Tacconi, P., 1979. A geological map of Ethiopia and Somalia (1973) 1,2.000.000 and comment. University of Florence, Firenze.

Moeyersons, J., Nyssen, J., Poesen, J., Deckers, J., Mitiku Haile. 2006. On the origin of rock fragment pavements on Vertisol: A case study from the Ethiopian Highlands. Geomorphology 76, 411–429.

Nyssen, J., Moeyersons, J., Poesen, J., Deckers, J., Mitiku Haile. 2002a. The environmental significance of the remobilisation of ancient mass movements in the Atbara-Tekeze headwaters, Northern Ethiopia. Geomorphology 49: 303–322.

Nyssen J, Poesen J, Moeyersons J, Lavrysen E, Mitiku Haile, Deckers J. 2002b. Spatial distribution of rock fragments in cultivated soils in northern Ethiopia as affected by lateral and vertical displacement processes. Geomorphology 44: 1–16.

Nyssen, J., Poesen, J., Moeyersons, J., Deckers, J., Haile, M., Lang, A., 2004. Human impact on the environment in the Ethiopian and Eritrean highlands - a state of the art. Earth Sci. Rev. 64, 273-320.

Nyssen, J., Vandenreyken, H., Poesen, J., Moeyersons, J., Deckers, J., Mitiku Haile, Salles, C., Govers, G., 2005. Rainfall erosivity and variability in the Northern Ethiopian Highlands. J. Hydrol. 311, 172-187.

Nyssen, J., Poesen, J., Veyret-Picot, M., Moeyersons, J., Mitiku Haile, Deckers, J., Dewit, J., Naudts, J., Kassa Teka, Govers, G., 2006. Assessment of gully erosion rates through interviews and measurements: a case study from Northern Ethiopia. Earth Surf. Processes Landforms 31, 167-185.

Nyssen, J., Naudts, J., De Geyndt, K., Mitiku Haile, Poesen, J., Moeyersons, J., Deckers, J., 2008. Soils and land use in the Tigray highlands (Northern Ethiopia). Land Degrad. Dev. 19, 257-274.

Reynolds, C., 2006. Crop calendar of Ethiopia. USDA Foreign Agriculture Service. Accessed from http://www.pecad.fas.usda.gov on 7 October 2010.

Reynolds, C., 2008. Ethiopia 2008 crop assessment travel report. USDA Foreign Agriculture Service. Accessed from http://www.pecad.fas.usda.gov on 7 October 2010.

Segers, K., Dessein, J., Nyssen, J., Haile, M., Deckers, J., 2008. Developers and farmers intertwining interventions: the case of rainwater harvesting and food-for-work in Degua Temben, Tigray, Ethiopia. International Journal of Agricultural Sustainability 6, 173-182.

Segele, T.Z., Lamb, P.J., 2005. Characterization and variability of Kiremt rainy season over Ethiopia. Meteorology and Atmospheric Physics 89, 153-180.

Seleshi, Y., Camberlin, P., 2006. Recent changes in dry spell and extreme rainfall events in Ethiopia. Theoretical and Applied Climatology 83, 181-191.

Seleshi, Y., Zanke, U., 2004. Recent changes in rainfall and rainy days in Ethiopia. International Journal of Climatology 24, 973-983.

Slegers, F.W.M., 2008. Exploring farmers' perceptions of drought in Tanzania and Ethiopia. PhD thesis, Wageningen University and Research Centre, Netherlands, pp. 217.

Styczen, M.E., Morgan, R.P.C., 1995. Engineering properties of vegetation. in: Morgan, R.P.C., Rickson, R.J. (Eds.), Slope Stabilization and Erosion Control. Spon, London, pp. 5-58.

Renard, K.G., Foster, G.R., Weesies, G.A., McCool, D.K., Yoder, D.C., 1997. Predicting soil erosion by water: a guide to conservation planning with the Revised Universal Soil Loss Equation (RUSLE). Agriculture Handbook 703. United States Department of Agriculture, Washington.

Robinson, P.J., Henderson-Sellers, A., 1999. Contemporary Climatology. Pearson Education Ltd., Essex.

Tadesse, M., Betre, A., Gashaw, B., Tewodros, T., Jordan, C., Todd, B., 2006. Atlas of the Ethiopian rural economy. Ethiopian Development Research Institue.

Tilahun, K., 2006. Analysis of rainfall climate and evapo-transpiration in arid and semi-arid regions of Ethiopia using data over the last half a century. Journal of Arid Environments 64, 474-487.

Vanmaercke, M., Zenebe, A., Poesen, J., Nyssen, J., Verstraeten, G., Deckers, J., 2010. Sediment dynamics and the role of flash floods in sediment export from medium-sized catchments: a case study from the semi-arid tropical highlands in northern Ethiopia. J. Soils Sediments 10, 611-627.

Van de Wauw, J., Baert, G., Moeyersons, J., Nyssen, J., De Geyndt, K., Nurhussen Taha, Zenebe, A., Poesen, J. and Deckers, J., 2008. Soil-landscape relationships in the basalt-dominated highlands of Tigay, Ethiopia. Catena 75, 117-127.

van der Veen, A. and Gebrehiwot, T., 2011. Effect of Policy Interventions on Food Security in Tigray, Northern Ethiopia. Ecology and Society 16, 1-18.

Verdin, J., Funk, C., Senay, G., Choularton, R., 2005. Climate science and famine early warning. Philosophical Transactions of the Royal Society B 360, 2155-2168.

Virgo, K.J., Munro R.N., 1978. Soil and erosion features of the Central Plateau region of Tigrai, Ethiopia. Geoderma 20, 131-157.

Wengraf, T., 2001. Qualitative research interviewing: biographic narrative and semi-structered methods. SAGE publications, Londen,.

Westphal, E., 1975. Agricultural systems in Ethiopia. Wageningen: Centre for Agricultural Publishing and Documentation.

Williams, M., Williams, F., 1980. Evolution of the Nile basin. In, Williams, M., Faure, H. (Eds.), The Sahara and the Nile. Quaternary Environments and Prehistoric Occupation in Northern Africa. Balkema, Rotterdam, pp. 207-224.

Wubeneh, N.G., Sanders, J.H., 2006. Farm-level adaptation of Sorghum technologies in Tigray, Ethiopia. Agricultural Systems 91, 122-134.

Discussion and conclusions

Chapter 8
General discussion

This chapter is modified from:

Frankl, A., Nyssen, J., De Dapper, M., Mitiku Haile, Billi, P., Munro, R. N., Deckers, J., Poesen, J., 2011. Linking long-term gully and river channel dynamics to environmental change using repeat photography (Northern Ethiopia). Geomorphology 129, 238-251.

Abstract

Based on the results of Chapter 2 to 7, a conceptual hydrogeomorphic model was devised for the Northern Ethiopian Highlands. Three major phases could be distinguished in the hydrological regime of the region. In the first phase, between 1868 (or earlier) and ca. 1965, the relatively stable channels showed an oversized morphology inherited from a previous period when external forcing in environmental conditions had caused channel development. In the second phase (ca. 1965 – ca. 2000), increased aridity and continued vegetation clearance accelerated the channel dynamics of the gully and river system. The third phase (ca. 2000 – present) as a result of the wide implementation of soil and water conservation measures. In 2010, about one-fourth of the gully system was stabilizing. These hydrogeomorphic developments correspond to a gully cut-and-fill cycle in the second half of the 20th century, and they suggest that a pre-1868 cut-cycle took place.

Keywords: Gully, Hydrogeomorphologic model, Northern Ethiopia.

8.1 Hydrogeomorphic model

Changes in the hydrogeomorphology of the Northern Ethiopian Highlands and their gully systems are well correlated, which allows a better defining and understanding of the major phases of development in the hydrological regime of the region. To this end, the idealized fluvial system concept of Schumm (1977) was adapted to the findings of this thesis. According to Schumm (1977), the idealized fluvial system can be divided into three zones (**Figure 8.**). Zone I, the upper zone, consists of the headwaters, which form the sediment-source area. In Zone II, the transfer zone, input and output of sediment are equal. At the lower end of the fluvial system in Zone III, sediment is deposited in the sink area. In each zone, morphological attributes of the fluvial system (like channel width and depth) can be related to mean runoff discharge and sediment load, which, in turn, depend on external controls (Schumm, 2005).

Changes in external controls affect channel width and depth. On a timescale of 10^1 to 10^2 years, external controls that are expected to cause the channels to reshape are climatic oscillations and human-related activities (Graf, 1988, Knighton, 1998, Schumm, 2005). The influence of the climate lies in variations of precipitation and, specifically with regard to Ethiopia, in the effects of drought on the vegetation cover and runoff response of the land. Human activities affecting the fluvial system can be subdivided into direct modification of the channel (e.g., dam construction) and land use and land cover changes resulting from deforestation, agriculture, urbanization and infrastructure construction. The channel morphology adjustments do not depend only on the degree of change and the overtaking of thresholds, but are also related to reaction and relaxation times of the fluvial system, causing the channels to be possibly not in equilibrium with their control factors (Knighton, 1998). However, in semi-arid headwater basins, reaction times are expected to be short as a result of a high susceptibility to change and strong connectivity between hillsides and channels (Knighton, 1998).

In order to assess developments in mean runoff discharge and sediment load, the equations of Knighton (1998), which are based on the concept of Schumm (1977), were applied. These equations, where a + or – sign is used to denote an increase or decrease, relate the effects of changes in mean runoff discharge (Q) and sediment load (Q_s) to a response in channel depth (d), width (w) and width/depth ratio (w/d):

w^+, $(w/d)^+$	$\rightarrow$	Q^+ and/or Q_s^+	(7.1)
d^+	$\rightarrow$	Q^+ and/or Q_s^-	(7.2)
d^-	$\rightarrow$	Q^- and/or Q_s^+	(7.3)
w^-, $(w/d)^-$	$\rightarrow$	Q^- and/or Q_s^-	(7.4)

Increasing channel width can be related to an increase in mean runoff discharge and/or sediment load (Eq. 7.1), while a decrease in channel width suggests the opposite development in mean runoff discharge and/or sediment load (Eq. 7.4). Channel depth will respond to an increase in mean runoff discharge and/or a decrease in sediment load by degrading (Eq. 7.2), while an aggrading channel results from a decrease in mean runoff discharge and/or an increase in sediment load (Eq. 7.3).

Translated to changes in external forces, a transition to a more arid climate with related decrease in mean runoff discharge and increase in sediment load, is deemed to result in aggrading channels with widths that remain constant (Eq. 7.3). When mean runoff discharge remains equal or increases, and there is also a decrease in sediment load, channels will degrade (Eq. 7.2): this is the result of a clear water effect, often related to the construction of in-stream structures or the implementation of soil and water conservation measures (like terracing) on the hillsides of a basin (e.g., Boix-Fayos et al., 2007). Land use changes that result in increasing mean runoff discharge and sediment supply – such as deforestation – will cause the channels to widen (Eq. 7.1, e.g., Kondolf et al., 2002; Boix-Fayos et al., 2007).

Equations (7.1) to (7.4) can give merely an indication of the direction of change. They do not guarantee that the change in input conditions is proportional to the channel response and do not give the rates or magnitude of change (Knighton, 1998). This is especially the case in mountainous, semi-arid environments where flashy flow regimes dominate and channel form may be dictated by high-magnitude, low-frequency floods (Graf, 1988). Nevertheless, equations (7.1) to (7.4) provide us with general tendencies of channel response to catchment hydrology changes.

8.2 Hydrogeomorphic interpretation

Applying the hydrological model of Schumm (1977) to the Northern Ethiopian Highlands allowed us to distinguish three major phases in the hydrogeomorphic regime of the region (**Figure 8.1**). In phase I, from 1868 to ca. 1965, gullies were present in an already largely degraded environment, displaying a network similar to the present-day situation (Chapter

2 and 3, Appendix A and B). However, with low denudation rates on the slopes and sufficient obstacles to runoff, channels were low-active and had smooth cross-sections that supported vegetation. Mean runoff discharge and sediment load were relatively low, producing stable channels. The lower gully ends were fixed and a debris cone was either absent or very small. Phase I is detected on the majority of the photographs taken before 1961 and extends back to at least 1868 (Chapter 2). Exceptions of gullies that were highly dynamic were related to local conditions, as is the case with a photograph picturing the outskirts of Mekelle in 1895 and displaying a deeply incised gully with steep bank (Appendix A, photo-couple 29). In this example, supplying of the regional capital with wood, crop and livestock led to an early critical vegetation-cover decrease, resulting in accelerated gully erosion. The 1963-1965 gully networks and volumes quantified from aerial photographs also reflect phase I (Chapter 3, Appendix B), with the total drainage density (D_{total}), the drainage density of high-active gullies ($D_{high\text{-}active}$) and the area-specific gully volume (V_a) being on average 1.86 km km^{-2}, 0.89 km km^{-2} and 32.23 10^3 m^3 km^{-2} respectively.

The low-active gully networks present on a regional scale indicate that environmental vulnerability did not yet reach a critical point for large-scale channel extension and degradation to occur. There was still a relatively dense shrub cover on the hills and in the valley floors soil lynchets had good vegetation growth on their risers (e.g., Figure 2.8; **Figure 8.1**). However, quantifying land use and cover in five main study areas in the period 1868-1961 indicated that only 5% the surface was covered by forests and that many steep slopes were under degraded shrubland (Chapter 5). Villages comprised less than 1% of the surface. It seems that in the sparsely populated Northern Ethiopia, local communities did not invest in large-scale environment rehabilitation, apart from traditional measures, probably because negative effects of gully erosion remained limited and because gullies did not hamper agricultural activities. Considering the whole country, population size between 1868 and 1960 increased from approximately 6.6 to 25.9 million (Maddison, 2006; McEvedy and Jones, 1978).

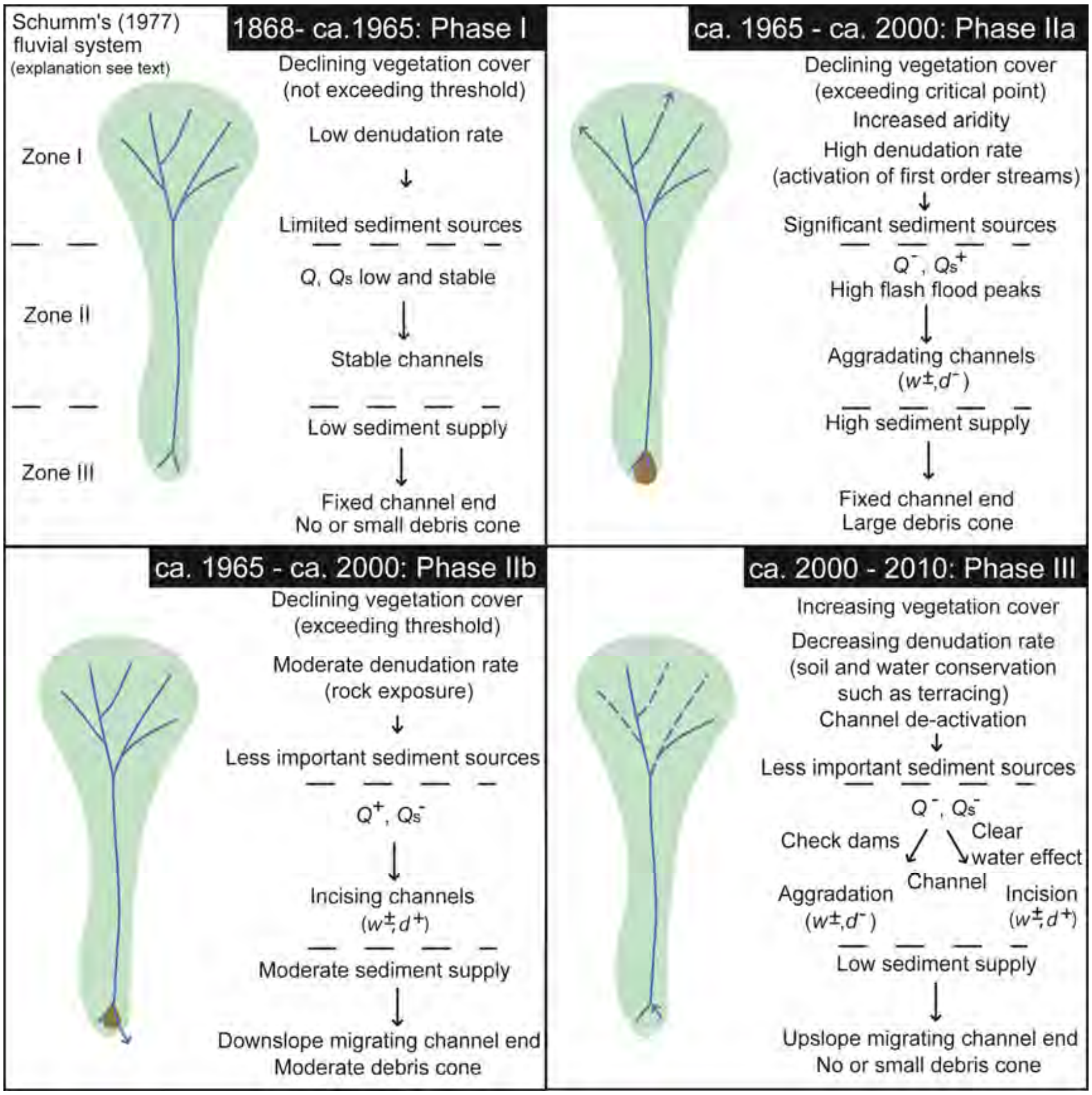

Figure 8.1 Conceptual model of changes in the hydrogeomorphology of the Northern Ethiopian highlands based on Schumm's (1977) fluvial system. The threshold refers to a critical reduction in vegetation cover resulting in runoff conditions triggering gully incision or network expansion.

Altough not used in this study, the 1935 Italian aerial photographs also reflect well phase I (**Figure 8.2**). In future research it will be increasingly possible to study the early 20th century environment of Northern Ethiopia, as aerial photographs of the 1930s are becoming available through a Memorandum of Understanding between the Ethiopian Mapping Agency, Ghent University and Mekelle University. As an illustration, one of the first availed, hence randomly selected 1935 Italian aerial photograph (left) evidences the past environmental and land management conditions. The interpreted aerial photograph covers around 1 km² in an area 30 km east-northeast of the town of Sinkata (Figure 1.1). As the first photographs of the 1930s could only be availed in April 2012, it was not possible to use them consistently in this study; yet the early 20th century historical aerial photographs tend to confirm our findings, indicating a late 19th century landscape where environmental degradation did not yet result in large-scale channel degradation. Terraces were less prominent in 1935 (**1**), but they had better vegetation growth on their risers and seem wider (**2**). The gullies (**3**, **4**) that are visible in 2005 were not yet developed in 1935, but instead vegetated shallow channels existed. Also, the ephemeral river (**5**) looks narrower in 1935 as compared to 2005. The circles indicate trees have lived through 70 years of environmental change.

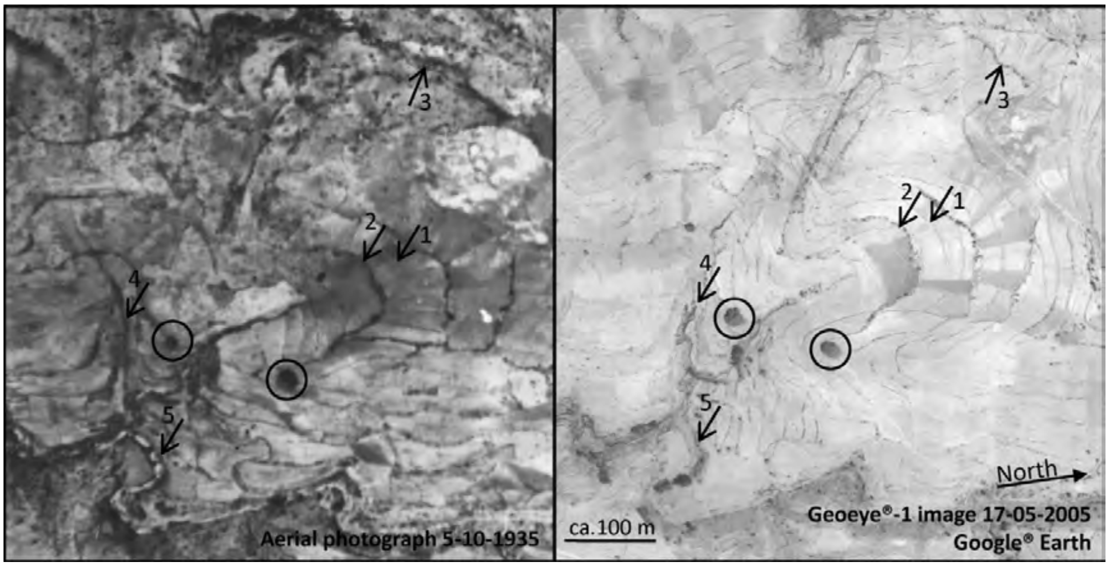

Figure 8.2 Aerial photographs of 1935 (left) as evidence of past environmental and land management conditions. Studying these photographs in further research and the comparison with high-resolution satellite images (right) will allow to quantify gullies in relation to their controlling factors in the 1930s over large areas. Location: 14°07’12’’ N, 39°17’36’’E, nearby the village of Nebelet. Approximate scale 1 : 50 000 (no orthorectification).

After ca. 1965, a second phase started in the hydrological regime of Northern Ethiopia, characterized by a marked transition from low- to high-active gullies (**Figure 8.1**). As quantified in Chapter 3, network density and gully volume strongly increased and reached a maximum in 1994, with averages for D_{total}, $D_{high\text{-}active}$ and V_a being 2.52 km km^{-2}, 2.35 km km^{-2} and 37.42 10^3 m^3 km^{-2} respectively. The 40 photographs portraying the landscape between 1970 and 1994 generally show gullies and river sections which are highly dynamic (Chapter 2), except for one (Appendix A, photo-couple 4), where smooth walls and good vegetation cover of a gully in a small catchment indicate that phase II had not started yet.

Phase II can be subdivided into two periods a and b, which may alternately exist in phase II. In phase IIa, the continued decline in vegetation cover resulted in a strong runoff response leading to high denudation rates on the hillsides and upslope migration of gully heads. As discussed in Chapter 4, medium- to long-term headcut retreat rates were high over the period 1963-2010 (average R_l = 3.8±4.7 m y^{-1}), and headcut retreat rates were larger during the early phases of gully development. Probably, arid pulses that frequently occurred during the 1970s and 1980s triggered phase IIa. Such arid pulses alter biomass production and force farmers to cultivate more steep and marginal land in order to ensure food production. Analyses of region-wide land use and cover in the 1970s and 1980s on the basis of Landsat imagery in Chapter 6 confirmed that in 1984/1986, the surface covered by bare ground was extensive and that the surface covered by cropland peaked. Analysis of land use and land cover on old terrestrial photographs in Chapter 5 also indicate a minimum in vegetation cover in the period 1940s-1990s. Chapter 7 showed that the length of the growing period decreases by two to four months with increasing drought in Northern Ethiopia, making croplands very vulnerable to high-intensive rainfall in the summer rainy season. The hydrogeomorphic changes of phase IIa are often still evident in the field and remain a vivid memory for older farmers (**Figure 8.3**).

Figure 8.3 Hydrogeomorphic changes in the second half of the 20th century in May Ba'ati as understood from interviews. According to a local respondent who cultivated the cropland on the foreground since many decades, increased runoff response of the land from the 1960s onwards resulted in strong flash floods that brought large amounts of rock fragments to his land (black arrows). In the early 1980s, the farmer tried to protect his farmland by diverting the water to the edge of the farmland. This resulted into the development of a gully (white arrow) which is at present starts to stabilize. Photograph by Amaury Frankl (2009).

As a result of the increased environmental vulnerability during droughts, the impact of sporadic rains increased. While mean runoff discharge decreased, the more flashy flood regime, with higher peaks, resulted in the activation of the channels. High sediment supply thus resulted in aggrading channels, while width increased due to the high flash flood peaks and lateral flow expansion, in turn due to the increase of flow resistance induced by the increased sedimentation. The gully lower end remained fixed, but the large quantities of debris transported by the channels produced large debris cones at the lower gully margin. At the end of phase IIa, gully head cuts were close to the divides with bedrock exposure increasing within the channels and in the adjacent land. As a result, the hillsides became less important sediment sources. Phase IIa is clearly discernible on photo-couples 27 and 28 (Appendix A), where the shallow gullies show very large top width/maximum depth ratios and carry large amounts of bedload, indicating that degradation rates on the surrounding hillsides were high and that strong flash floods could mobilize vast amounts of sediment. An active head cut can be seen on photo-couple 25 (Appendix A).

In phase IIb, aridity and denudation rates were decreasing. This was most probably related to an increase in mean runoff discharge, decrease in sediment supply and reduction of flash flood peaks flow. Channels therefore incised, and the lower gully end migrated rapidly downslope, which allowed the formation of only small debris cones. This was well evidenced in the catchment Lake Ashenge, where downslope migration of gully ends occurred at 14 m y^{-1} between 1965 and 1986. HTS (1976) and Virgo and Munro (1978) concluded for this phase an average downslope gully migration rate of 5 to 10 m y^{-1}. Phase IIb is well illustrated by the 1994 photographs taken in the May Mekdan catchment (Appendix A, photo-couples 9-17), where the deep gully incision led to over-steepened banks and forced gully width adjustment through mass failures. A similar event of gully network expansion by vegetation cover decline occurred in Senegal during the protracted drought that stroke the Sahel in the early 1970s (Poesen et al., 2003). River incision and widening as a result of the increased intensity and frequency of peak floods related to deforestation was also observed in Central Africa (D.R. Congo) in the second half of the 20th century (Moeyersons et al., 2010).

Since ca. 2000, the hydrogeomorphic regime of Northern Ethiopia entered a third phase in which the large-scale implementation of soil and water conservation measures started to yield positive effects on the environmental rehabilitation and on the stabilization of gullies. As a reaction to severe land degradation that stroke Northern Ethiopia in the 1970s and 1980s, environmental rehabilitation programs were launched with the aim of increasing the resilience of the land to the effects of droughts. Biophysical conservation measures that were implemented include (1) the establishment of exclosures in critical steep-sloped zones (Descheemaeker et al., 2006), (2) the introduction of stone bunds (Nyssen et al., 2008) and, (3) the construction of check dams in gullies (**Figure 8.4A**; Nyssen et al., 2004a). Important for the implementation of such measures was the availability of cheap or free labour, wherefore food-for-work programs proved to be very successful (Gebremedhin and Swinton, 2001). At present, exclosures cover 10% to 15% of the land surface, stone bunds are found at average densities of 57 km km^{-2} (Schumacher, 2012), and check dams are introduced on the majority of the first order gullies (Chapter 3). As shown in Chapter 5 and 6, this led to a greening of the landscape in which the surface covered by bushland, forest or Eucalypt plantation strongly increased. This greening is partly the result of the introduction of Eucalypt trees to support the growing need of construction wood in decades where population strongly increases. At a national level population size almost doubled, from 40 million in 1980 to 66.9 million in 2000 (Maddison, 2006; McEvedy and Jones, 1978). In Tigray, population size increased from 3.1 to 4.3 million from 1994 to 2007, accounting from 6% of the total population (CSA, 2008). Population density increased from 63 to 86 persons km^2.

As a result of the environmental rehabilitation, denudation rates decreased – although remaining fairly high in absolute terms – reducing the importance of the hillsides as sediment sources (**Figure 8.1**). Mean runoff discharge as well as sediment load and flash flood peaks decreased (cf. Moeyersons 1989, 1990), causing the gullies to deactivate and to fill partially, especially whenever check dams were present (**Figure 8.4A**). When proper land management is applied, gullies can even be transformed into a green oasis which benefits the ecological recovery of the area. Moreover, their resilience against the effects of drought or land use changes on the runoff response of the land increases (Figure 3.8). When mean runoff discharge remains too high and flow too strong to allow the construction of check dams, the drop in sediment load causes gullies to incise due to a clear-water effect. Such a situation occurred in the Lake Ashenge basin. Lower gully ends deactivated and migrated upslope.

Phase III is well evidenced by the results from Chapter 3 which indicate that average D_{total} decreased to 2.20 km km^{-2} and V_a to 48.96 10^3 m^3 km^{-2}. Even more important is the decrease in average $D_{high\text{-}active}$ to 1.65 km km^{-2}, indicating that 25% of the gully network had become low-active. These findings are also supported by the results of Chapter 2, indicating that in 2006-2009 about 23% (n = 8) of the sections were stabilizing and had cross-sectional characteristics similar to those of the gullies in phase I. Of the other 31 gullies and river sections studied from repeat photography, 44% were high-active, while 23% were in a transitional stage. Strong degradation can be the result of a clear-water effect, which causes the gullies in the valley bottoms to incise. This can be facilitated by the presence of thick, erodible soils in valley bottom position. However, strong degradation can also be the result of local factors, such as different slope/channel coupling, and connectivity or catchment scale, with large catchments having longer reaction times than small catchments; this explains why in this case their constituent channels did not evolve completely into phase III.

The reduced activity of the gully system is also apparent from the headcut retreat rates presented in Chapter 4. Present-day headcut retreat rates are much lower than on the medium- to long-term, with an average R_l of 0.34± 0.49 m y^{-1}. However, gullying in Vertisols remains very active as gully development is largely controlled by soil piping. In Vertisols present-day headcut retreat rates up to 1.93 m y^{-1} were registered and massive gabion check dams, which are cost and labour intensive, were sometimes by-passed in one rainy season, forcing the gully to expand laterally into the adjacent land (**Figure 8.4B**). Reducing gully expansion in Vertisols call for specific measures to reduce the severity of soil piping. As proposed in Chapter 3, introducing a subsurface geomembrane dam at gully heads can increase the water storage upslope of the dam, and thus, reduce soil piping.

The hydrogeomorphic changes discussed in this chapter indicate that the gully system developed through a cut-and-fill cycle in the second half of the 20th century. In 1868-1965, the quite extensive gully network merely consisted of low-active gullies which were inherited from a previous period. By 1974-1994, with a marked increase in high-active gullies, the gully network became highly erosive, with the expansion of the network and the increase in gully volume as a result. This corresponds to the gully cut-phase. Since ca. 2000, thanks to environmental rehabilitation, gully activity strongly decreased and the gully system developed into a fill-phase. The gully network shrunk, headcuts became less active and the total gully volume decreased. This cut-and-fill cycle can best be observed when considering the largest catchments, i.e. those of May Mekdan (44.7 km^2) and Ayba (37 km^2) (Figure 3.4).

Figure 8.4 Effectiveness of check dams as a measure to control gully erosion. **A**: Siltation behind gabion check dams caused the gullies to infill by approximately one-third of its depth in a catchment where the runoff response of the land decreased thanks to the implementation of

soil and water conservation measures. Note also that on the left gully bank pits are being prepared in order to plant trees. **B**: At another location, the presence of a Vertisol lens in the lower soil profile (white arrow) caused the gabion check dam to be by-passed in one rainy season, forcing the gully into the adjacent land. Photographs taken in May Ba'ati by Amaury Frankl in 2009 (A) and 2011 (B).

8.3 Pre-1868 erosion cycle

At a regional scale, in the late 19th to early 20th centuries, low-active gullies and rivers prevailed. Gullies, and to a lesser extent, rivers, could then be called 'dormant', meaning their morphology was not in equilibrium with the prevailing conditions, but was rather inherited from a previous period when external forcing of environmental conditions – i.e. changes in climate (precipitation and/or temperature) and land use – resulted in significant geomorphic change. Such dormant river sections were also observed on historical photographs elsewhere in the Highlands of Northern Ethiopia: near Hayk in Wollo in 1937 (Crummey, 1998), in the Mesheg valley on the Northern slopes of the Amba Alage and near Kulmesq on the Tekeze river in 1868 (both pictured in Nyssen et al., 2009). The well-preserved gully and river streambed morphology suggests that active gullying and floodplain shaping occurred long enough ago for bushy vegetation to regenerate, but not long enough for the gully to be infilled with sediment and/or to be totally smoothed out. However, under unique circumstances gullies can be preserved remarkably well in the landscape, as shown by Vanwalleghem et al. (2006), who related currently inactive gullies under forest in Belgium to incision periods during the Roman time (cal. y 46 BCE - 78 CE) and the Middle Bronze Age (ca. cal. yr 1750 -1500 BCE).

In the Highlands of Northern Ethiopia, the Mid-Holocene increase in aridity that struck tropical East Africa and surrounding areas (Thompson et al., 2002; Kiage and Liu, 2006) occurred at ca. 5000 yr BP (Nyssen et al., 2004b; Moeyersons et al., 2006; Marshall et al., 2009). This abrupt transition to a more arid climate is considered to have created an environment more vulnerable to erosion. Analogous to the present land degradation related to critical land clearance (Nyssen et al., 2004b), the onset of the accelerated soil erosion in the Northern Ethiopian Highlands can be related to forest clearance that started ca. 2000–3000 yr BP (Nyssen et al., 2004b and references therein). This is evidenced by metres-thick colluvial deposits on footslopes and by buried travertines and early Holocene soils in Tigray (Machado et al., 1998; Dramis et al., 2003; Moeyersons et al., 2006). Soil erosion rates increased in the first millennium AD in a period when land exploitation by the Axum civilization peaked (Butzer, 1981; Ciampalini et al., 2008; French et al., 2009). After the fall of the Axum civilization in the late 1st millennium AD and the consequent decline in population density, soil formation (Brancaccio et al., 1997) and related vegetation recovery suggest decreased soil erosion rates. This period of environmental recovery would have lasted approximately 500 years, until population growth and associated land clearance and arable intensification resulted in a new denudation phase that started around 300 to 500 years ago (Brancaccio et al., 1997; French et al., 2009). As indicated in this study, landscape denudation has not remained constant since then, and periods of relative landscape stability did exist. This study follows earlier work by Nyssen et al. (2008, 2009) in the assertion that the environment of the late 19th century in the Tigray Highlands was severely degraded and that degradation was continuous, eventually leading to the reactivation of the gully and river systems since the 1960–1970s. Strong environmental degradation before the late 19th century existed locally where population pressure was at its highest, as for the 19th century capital of Tigray, Hintalo (Antalo), which lay already in ruins in 1868 (Markham, 1868), but is unlikely to have existed at a regional scale. Climate must thus have triggered the erosion that led to reactivation of the late 19th century dormant gullies, in the sense that increased aridity – and hence decreased agricultural productivity – would have forced populations to reclaim land in order to ensure their subsistence. This in turn led to higher runoff responses of the land. Such circumstances occurred during the arid phases of the early 1970s and mid 1980s when pulses in land surface used as cropland and grassland was recorded by aerial photography (HTS, 1976) or satellite imagery (Chapter 6); these were also periods when gully erosion was very severe.

Concerning the reconstruction of the Little Ice Age (~ 1270–1850 CE) climate in the Tigray Highlands, information is scanty. In other parts of East Africa the Little Ice Age is considered to have been wetter and colder than the present (Thompson et al., 2002; Kiage and Liu, 2006). According to Bonnefille and Mohammed (1994), the southern Highlands of Ethiopia endured a cooling of 2°C at 560±120 yr. BP (= 1390 AD).

Regarding variations in precipitation in the Ethiopian Highlands, the scarce information available are historical records of droughts and famine. Pankhurst (1985) reports rain failure leading to famine and great mortality in 1835. Droughts recorded in East African lake sediments (e.g. Naivasha, Victoria, Turkana, Stephanie, Tanganyika, and other lakes) indicate that centurial-to-decadal arid surges occurred over East Africa (Verschuren, 2004). These data and other proxy data, for example Nile outflow (Hassan, 1981), indicate that droughts struck inter-tropical Africa frequently, and that drought was widespread in the late 17th and early 18th centuries. Numerous severe droughts are also recorded in the late 19th and early 20th centuries in the Northern Ethiopian Highlands during periods with low-active gullies and river channels: 1888–1892, 1895–1896, 1889–1900, 1913–1914, 1920–1922, and 1957 (Pankhurst, 1985; Webb et al., 1992).

8.4 References

Billi, 2008. Flash floods, sediment transport and bedforms in the ephemeral streams of Kobo basin, northern Ethiopia. Catena 75, 5-17.
Billi, P., Dramis, F., 2003. Geomorphological investigation on gully erosion in the Rift Valley and the Northern highlands of Ethiopia. Catena 50, 353-368.
Boardman, J., Parsons, A.J., Holland, R., Holmes, P.J., Washington, R., 2003. Development of badlands and gullies in the Sneeuberg, Great Karoo, South Africa. Catena 50, 165-184.
Boix-Fayos, C., Barbera, G.G., Lopez-Bermudez, F., Castillo, V.M., 2007. Effects of check dams, reforestation and land-use changes on river channel morphology, Case study of the Rogativa catchment (Murcia, Spain). Geomorphology 91, 103-123.
Bonnefille, R., Mohammed, U., 1994. Pollen-inferred climatic fluctuations in Ethiopia during the last 3000 years. Palaeogeogr. Palaeoclimatol. Palaeoecol. 109, 331-343.
Brancaccio, L., Calderoni, G., Coltorti, M., Dramis, F., 1997. Phases of soil erosion during the Holocene in the Highlands of Western Tigray (Northern Ethiopia), a preliminary report. In, Bard, K. (Ed.), The Environmental History and Human Ecology of Northern Ethiopia in the Late Holocene. Instituto Universitario Orientale, Napoli, pp. 30–48.
Bull, W.B., 1997. Discontinuous ephemeral streams. Geomorphology 19, 227-276.
Butzer, K.W., 1981. Rise and fall of Axum, Ethiopia – a geo-archeological interpretation. Am. Antiquity 46, 471-495.
Ciampalini, R., Billi, P., Ferrari, G., Borselli, L., 2008, Plough marks as a tool to asses soil erosion, a case study in Axum (Ethiopia), Catena 75, 18-27.
Crummey, D., 1998. Deforestation in Wollo, process or illusion? J. Ethiop. Stud. 32, 1-41.
CSA, 2008. Central Statistical Agency Federal Democratic Repuplic of Ethiopia population census commission. Summary and statistical report of the 2007 population and housing census.
Daba, S., Rieger, W., Strauss, P., 2003. Assessment of gully erosion in eastern Ethiopia using photogammetric techniques. Catena 50, 273-291.
Descheemaeker, K., Nyssen, J., Rossi, J., Poesen, J., Mitiku Haile, Moeyersons, J., Deckers, J., 2006. Sediment deposition and pedogenesis in exclosures in the Tigray Highlands, Ethiopia. Geoderma 132, 291-314.
Dramis, F., Umer, M., Calderoni, G. and Haile, M., 2003. Holocene climate phases from buried soils in Tigray (northern Ethiopia), comparison with lake level fluctuations in the Main Ethiopian Rift. Quat. Res. 60, 274-283.
Eitel, B., Eberle, J., Kuhn, R., 2002. Holocene environmental change in the Otjiwarongo thornbush savanna (Northern Namibia): evidence from soils and sediments. Catena 47, 43-62.
Felix-Henningsen, P., Morgan, R.P.C., Mushala, H.M., Rickson, R.J., Scholten, T., 1997. Soil erosion in Swaziland: A synthesis. Soil Technol. 11, 319-329.
French, C., Sulas, F., Madella, M., 2009. New geoarcheological investigations of the valley systems in the Aksum area of northern Ethiopia. Catena 78, 218-233.
Gebremedhin, B. and Swinton, S.M., 2001. Reconciling food-for-work project feasibility with food aid targeting in Tigray, Ethiopia. Food Policy, 26(1): 85-95.
Gobin, A.M., Campling, P., Deckers, J.A., Poesen, J., Feyen, J., 1999. Soil erosion assessment at the Udi-Nsukka Cuesta (southeastern Nigeria). Land Degrad. Dev. 10, 141-160.
Graf, W.L.,1988. Fluvial processes in dryland environments. The Blackburn Press.Caldwell, USA.
Hassan, F.A., 1981. Historical Nile floods and their implications for climate change. Science 212, 1142-1145.
Hauge, C., 1977. Soil erosion definitions. California Geology 30, 202– 203.

HTS, 1976. Tigrai Rural Development Study (TRDS). Hunting Technical Services Ltd. Government of Ethiopia and UK Ministry of Overseas Development,. Hunting Technical Services, Borehamwood.

Kassas, M., 1995. Desertification: a general review. J. Arid Environ. 30, 115-128.

Katsurada, Y., 2007. Regional scaled mapping of gully erosion sensitivity in Western Kenya. African J. Environ. Sc. Technol. 1, 049-052.

Kiage, L.M., Liu, K.B., 2006. Late Quaternary paleoenvironmental changes in East Africa, a review of multiproxy evidence from palynology, take sediments, and associated records. Prog. Phys. Geogr. 30, 633-658.

Knighton, D., 1998. Fluvial Forms and Processes – a New Perspective. Hodder Education, London.

Kondolf, G.M., Piegay, H., Landon, N., 2002. Channel response to increased and decreased bedload supply from land use change, contrasts between two catchments. Geomorphology 45, 35-51.

Leblanc, M.J., Favreau, G., Massuel, S., Tweed, S.O., Loireau, M., Cappelaere, B., 2008. Land clearance and hydrological change in the Sahel: SW Niger. Global Planet. Change 61, 135-150.

Machado, M.J., Perez-Gonzalez, A., Benito, G., 1998. Paleoenvironmental changes during the last 4000 yr in the Tigray, northern Ethiopia. Quat. Res. 49, 312-321.

Maddison A. The World Economy. Paris: OECD, DevelopmentCentre Studies; 2006. p. 660.

Markham, C.R., 1868. Geographical results of the Abyssinian expedition. J. R. Soc. Lond. 38, 12–49.

Marshall, M.H., Lamb, H.F., Davies, S.J., Leng, M.J., Kubsa, Z., Umer, M., Bryant, C., 2009. Climatic change in northern Ethiopia during the past 17,000 years, A diatom and stable isotope record from Lake Ashenge. Palaeogeogr. Palaeoclimatol. Palaeoecol. 279, 114-127.

Marzolff, I., Ries, J.B., 2007. Gully erosion monitoring in semi-arid landscapes. Z. Geomorph. 51, 405-425.

McEvedy C, Jones R. Atlas of World Population History. Middlesex: Penguin; 1978. p. 368.

Moeyersons, J., 1991. Ravine formation on steep slopes: Forward versus regressive erosion. Some case studies from Rwanda. Catena 18, 309-324.

Moeyersons, J., 1989. La nature de l'érosion des versants au Rwanda. Annales, Kon. Mus. Mid. Afr., Tervuren, Reeds Economische Wetenschappen, 19, pp. 396.

Moeyersons, J., 1990. Soil loss by rainwash: a case study from Rwanda. Z. Geomorph. 34, 385-408.

Moeyersons, J., Nyssen, J., Poesen, J., Deckers, J., Mitiku Haile, 2006. Age and backfill/overfill stratigraphy of two tufa dams, Tigray Highlands, Ethiopia, Evidence for Late Pleistocene and Holocene wet conditions. Palaeogeogr. Palaeoclimatol. Palaeoecol. 230, 165-181.

Moeyersons, J., Trefois, P., Nahimana, L., Ilunga, L., Vandecasteele, I., Byizigiro, V., Sadiki, S., River and landslide dynamics on the western Tanganyika rift border, Uvira, DR Congo: diachronic observations and a GIS inventory of traces of extreme geomorphologic activity. Natural Hazards 53, 291-311.

Moges, A., Holden, N.M., 2008. Estimating the rate and consequences of gully development, a case study of Umbulo catchment in southern Ethiopia. Land. Degrad. Develop. 19, 574-586.

Muhindo Sahani, 2011. Le contexte urbain et climatique des risques hydrologiques de la ville de Butembo (Nord-Kivu/RDC). Thèse présentée en vue de l'obtention du grade de Docteur en Sciences, Université de Liège, Collège de doctorat en géographie, pp. 273.

MU-IUC, 2007. IKONOS-2 satellite images. VLIR (Belgium) - Mekelle University Institutional University Cooperation Programme, Mekelle (Ethiopia) and Leuven (Belgium).

Munro, R.N., Deckers, J., Grove, A.T., Mitiku Haile, Poesen, J., Nyssen, J., 2008. Soil and erosion features of the Central Plateau region of Tigrai - Learning from photo monitoring with 30 years interval. Catena 75, 55-64.

Ndona, A., Truong, P., 2011. Community mobilization for the control of ravine erosion with vetiver technology in the Congo. http://www.vetiver.org/ICV4pdfs/DC04.pdf, last accessed on 28 August 2011.

Nyssen, J., Moeyersons, J., Deckers, J., Mitiku Haile, Poesen, J., 2000. Vertic movements and the development of stone covers and gullies, Tigray Highlands, Ethiopia. Z. Geomorph. 44, 145-164.

Nyssen, J., Poesen, J., Luyten, E., Veyret-Picot, M., Deckers, J., Mitiku Haile, Govers, G., 2002. Impact of road building on gully erosion risk: a case study from the Northern Ethiopian Highlands. Earth Surf. Process. Land. 27, 1267-1283.

Nyssen, J., Veyret-Picot, M., Poesen, J., Moeyersons, J., Mitiku Haile, Deckers, J., Govers, G., 2004a. The effectiveness of loose rock check dams for gully control in Tigray, Northern Ethiopia. Soil Use Manage. 20, 55-64.

Nyssen, J., Poesen, J., Moeyersons, J., Deckers, J., Haile, M., Lang, A., 2004b. Human impact on the environment in the Ethiopian and Eritrean highlands - a state of the art. Earth Sci. Rev. 64, 273-320.

Nyssen, J., Poesen, J., Veyret-Picot, M., Moeyersons, J., Mitiku Haile, Deckers, J., Dewit, J., Naudts, J., Kassa Teka and Govers, G., 2006. Assessment of gully erosion rates through interviews and measurements, a case study from Northern Ethiopia. Earth Surf. Process. Land. 31, 167-185.

Nyssen, J., Poesen, J., Descheemaeker, K., Haregeweyn, Nigussie, Haile, Mitiku, Moeyersons, J., Frankl, A., Govers, G., Munro, R.N., Deckers, J., 2008. Effects of region-wide soil and water conservation in semi-arid areas, the case of northern Ethiopia. Z. Geomorphol. 52, 291–315.

Nyssen, J., Haile, M., Naudts, J., Munro, N., Poesen, J., Moeyersons, J., Frankl, A., Deckers, J., Pankhurst, R., 2009. Desertification? Northern Ethiopia re-photographed after 140 years. Sci. Total Environ. 407, 2749-2755.

Nyssen, J., Frankl, A., Munro, R.N., Billi, P. Mitiku Haile, 2010. Digital photographic archives for environmental and historical studies: an example from Ethiopia. Scottish Geogr. J. 126, 185-207.

Oostwoud Wijdenes, D.J., Bryan, R., 2001. Gully-head erosion processes on a semi-arid valley floor in Kenya: A case study into temporal variation and sediment budgeting. Earth Surf. Process. Land. 26, 911-933.

Pankhurst, R., 1985. The history of famine and epidemics in Ethiopia. RRC, Addis Ababa.

Poesen, J., 1993. Gully typology and gully control measures in the European loess belt. In: Wicherek, S. (Ed.), Farm Land Erosion in Temperate Plains Environment and Hills. Elsevier, Amsterdam, pp. 221– 239.

Poesen, J., Vandaele, K., van Wesemael, B., 1996. Contribution of gully erosion to sediment production in cultivated lands and rangelands. International Association of Hydrological Sciences Publication 236, 251-266.

Poesen, J., Vandekerckhove, L., Nachtergaele, J., Oostwoud Wijdenes, D., Verstraeten, G., van Wesemael, B., 2002. Gully erosion in dryland environments. In: Bull, L.J., Kirkby, M.J. (Eds.), Dryland Rivers: Hydrology and Geomorphology of Semi-Arid Channels. Wiley, Chichester, UK, pp. 229–262.

Poesen, J., Nachtergaele, J., Verstraeten, G., Valentin, C., 2003. Gully erosion and environmental change, importance and research needs. Catena 50, 91-133.

Reubens, B., Poesen, J., Nyssen, J., Leduc, Y., Amanuel Zenebe, Sarah Tewoldeberhan, Bauer, H., Kindeya Gebrehiwot, Deckers, J., Muys, B., 2009. Establishment and management of woody seedlings in gullies in a semi-arid environment (Tigray, Ethiopia). Plant Soil 324, 131-156.

Schumacher, M., 2012. Recent trends in gully erosion as evidenced by repeat photography around Hagere Selam (Northern Ethiopia). Unpub. Master Thesis. Institute for Geography, Technical University of Dresden.

Schumm, S.A., 1977. The Fluvial System. John Wiley & Sons, New York.

Schumm S.A., 2005. River Variability and Complexity. Cambridge University Press, Cambridge.

Showers, K., 1996. Soil Erosion in the Kingdom of Lesotho and Development of Historical Environmental Impact Assessment. Ecological applications 6, 653-664.

Stocking, M.A., 1980. Examination of factors controlling gully growth. In De Boodt M, Gabriels D (eds)Assessment of Erosion. John Wiley & Sons, Chichester, 505–20.

Thompson, L.G., Mosley-Thompson, E., Davis, M.E., Henderson, K.A., Brecher, H.H., Zagorodnov, V.S., Mashiotta, T.A., Lin, P.N., Mikhalenko, V.N., Hardy, D.R., Beer, J., 2002. Kilimanjaro ice core records, Evidence of Holocene climate change in tropical Africa. Science 298, 589-593.

Thornthwaite, C.W., 1948. An approach toward a rational classification of climate. Geogr. Rev. 38, 55-94.

UN-DDD, 2012. United Nations Decade for Deserts and Fight Against Desertification (UNDDD). http://unddd.unccd.int/ (Accessed latest on 25/04/2012)

UNEP, 1994. United Nations Convention to Combat Desertification (UNCCD).

Valentin, C., Poesen, J., Li, Y., 2005. Gully erosion, impacts, factors and control. Catena 63, 132-153.

Vanwalleghem, T., Bork, H.R., Poesen, J., Dotterweich, M., Schmidtchen, G., Deckers, J., Scheers, S., Martens, M., 2006. Prehistoric and Roman gullying in the European loess belt, a case study from central Belgium. Holocene 16, 393-401.

Verschuren, D., 2004. Decadal and century-scale climate variability in tropical Africa during the past 2000 years. Past Climate Variability Through Europe and Africa 6, 139-158.

Virgo, K.J., Munro, R.N., 1978. Soil and erosion features of the Central Plateau region of Tigrai, Ethiopia. Geoderma 20, 131-157.

Webb, P., von Braun, J., Yohannes, Y., 1992. Famine in Ethiopia, policy implications of cropping failure at national and household levels, International food policy research institute, Washinton D.C.

Chapter 9
General conclusions

The main objective of this thesis was to understand gully development since the late 19th century at a regional scale in the Northern Ethiopian Highlands. In order to frame these developments within changes in the environmental controls, land use/cover changes and their relation to rainfall patterns were also analysed. Investigating historical and present-day gully erosion and land use/cover required to assemble a large dataset of terrestrial photographs, aerial photographs and satellite images. For each of these materials, appropriate methods of quantitative geomorphologic research were applied and fine-tuned with the aim of achieving the specific objectives (see Section 1.3). Key in this was the fieldwork which occurred during several campaigns in the period 2007-2011. The study mainly focused on eight catchments that are representative for the regional variability in environmental characteristics and which cover in total 123 km².

In order to compare the situation on the historical terrestrial photographs of the period 1868-1994 to the present, the photographs needed to be relocated in the field and repeated by the methods of repeat photography. Combining this with field measurements of gully morphology allowed to quantify historical gully cross-sections in Chapter 2. In Chapter 4, repeat photography methods were used to quantify headcut retreat rates. Accurate GPS measurements in the landscape portrayed by the terrestrial photographs allowed to prepare land use/cover maps of the situation in the late 19th – early 20th centuries (Chapter 5). The particularity of the historical terrestrial photographs is that they allowed to observe the environment in historical times, similar to the way we perceive landscapes in the field. Thus, with a large dataset of photographs at hand covering the regional variability in environmental characteristics, repeat photography demonstrated to be a powerful tool for assessing environmental change and channel response in historical times.

Studying gully development from aerial photographs of the period 1963-1994 (Chapter 3) required first to create orthophotographs. As it concerns aerial photographs of relatively poor quality (out of focus, low contrast) that cover a landscape which has undergone important changes and therefore difficult to survey, the geometric rectification of some aerial photographs was done by co-registration. With scales varying between 1 : 35 000 and 1 : 60 000, direct quantifications of the morphology of the gully were not possible. Only the gully networks could be delineated with sufficient accuracy. By establishing relations between the length of gully networks and their volume from field measurements, gully volumes from networks that were mapped on historical aerial photographs could be quantified. Such volume – length relations needed to account for the catchment lithology, varying proportions of high- and low-active gullies through time, and the implementation of check dams after 1994. Alternatively, the relationship between gully volume and catchment area and its average slope gradient was also explored. High-resolution satellite images (e.g., IKONOS) completed the time-series of aerial photographs for the most recent situation.

Low-resolution satellite images were found suitable to study land use/cover changes at a regional scale (Chapter 6). Land use/cover change analyses were performed from a conventional supervised classification of Landsat imagery of 1972, 1984/1986 and 2000. The use of historical terrestrial photographs to calibrate the images was also explored and yielded better results than the conventional methods (e.g., image differencing). As the different images had specific shortcomings and as they were recorded with different sensors, the images were subjected to an important pre-processing. NOAA Rainfall Estimates raster map that are derived from low-resolution satellite images were used to understand spatiotemporal variations in cropping systems in Chapter 7.

Fieldwork was an important component of this research, not only as essential part of the above mentioned methods, but also to characterize gullies and the environment. About two-month-long field campaigns were organized in the dry season of 2007 and in the rainy seasons of 2008, 2009 and 2010. Additionally, shorter visits occurred in 2011. Assessing the present-day variability in gully morphology and morphometry was done through measurements of 811 cross-sections. In addition, 57 photograph locations were visited in order to analyse historical changes in gully cross-sections. Gully network maps were validated and updated for recent changes. Furthermore, 24 headcuts were monitored during the rainy season of 2010 in the study area of May Ba'ati and an additional 18 headcuts were studied for long-term changes. In order to understand the spatiotemporal variability of gully morphology and changes therein, local environmental characteristics were studied in the field. Important was the characterization of the semi-natural vegetation and of the cropping systems. As farmers have good knowledge of past conditions, semi-structured interviews were organized with key informants. In total, about 170 local respondents were involved in this study.

Regarding the development of gully erosion, the main conclusion of this work is that over the past 140 years, three marked periods of gully activity could be distinguished. In a first period, from 1868 until ca. 1965, gullies were generally low active. Most gullies on historical photographs of that period show smooth and vegetated cross-sections. Their as their size and morphology suggest, the gullies were not in equilibrium with the prevailing conditions, but was rather inherited from a previous period when external forcing of environmental conditions caused significant geomorphic change.

Quantifying gully networks and volumes from aerial photographs of 1963-1965 indicated that the total gully drainage density (D_{total}) was 1.86 km km^{-2} and the area specific gully volume (V_a) 32.23 10³ m³ km^{-2}. 48% of the gully network was high-active. In this second period, from ca. 1965 until ca. 2000, gully erosion was very severe. Quantifying gully networks and volumes from aerial photographs of 1974, 1986 and 1994 indicated that D_{total} and V_a increase subsequently. By 1994 D_{total} was 2.52 km km^{-2} and V_a 59.59 10³ m³ km^{-2}, with 93% of the gully network being high-active. The terrestrial photographs of that period also show gullies which are very active, having clear-cut walls and transporting important amounts of debris. At the upper gully margins, headcuts incised upslope, while at the lower ends, debris fans were deposited and incised subsequently. Long- to medium-term linear headcut retreat rates (R_l) were on average 3.8±4.7 m y^{-1}.

Since ca. 2000, gully networks shrunk and decreased in volume, especially through the stabilization of first order gullies. In 2008-2010 D_{total} was 2.20 km km^{-2} and V_a 48.96 10³ m³ km^{-2}; 25% of the network was high-active. Present-day short-term headcut retreat rates decreased to an average R_l of 0.34± 0.49 m y^{-1}, with especially gullies in Vertisols remaining particularly active and calling for specific measures; currently being developed.

Regarding the most recent observations, the analysis of gully cross-sections in the field indicated that the median values for gully top width, depth and cross-sectional area were 6.34 m, 2.15 m and 10.1 m² respectively. Important factors that determined gully cross-sectional shape and size where the presence of check dams, gully activity and lithology. Gullies with check dams or that were low active had cross-sections that were 33.5% smaller than active gullies or gullies without check dams. Considering the effect of the lithology, median cross-sectional size increased from volcanics, sandstone to shale catchments. For the latter, the presence of incised travertine dams was considered as determent.

From these developments, the gully system appeared to experience a cut-and-fill cycle. Rapid gully development occurred between ca. 1965 and ca. 2000, while after ca. 2000, net gully infilling occurred. Expressed soil loss by gullying, soil loss rates of 17.6 ton ha^{-1} y^{-1} occurred between 1963-1965 and 1994. Between 1994 and 2008-2010, a net infilling of 8.3 ton ha^{-1} y^{-1} occurred. Large differences occurred between areas having contrasting lithologies, with soil losses by gullying in shales being about two times larger than in volcanics.

The gully erosion developments could be related to changes in land management (check dams, stone bunds), land use/cover and rainfall characteristics and were hence combined into a hydrogeomorphic model. In the first phase, from 1868 or earlier to ca. 1965, the predominance of low-active gullies was linked to an environment where the runoff response of the land was still low enough to prevent large-scale channel extension and degradation from occurring. Vegetation cover was however by no means abundant. The analysis of historical terrestrial photographs of ca. 12 km² revealed that only 5% of the surface was covered by forests and that many slopes were under degraded shrubland. After ca. 1965, the continued decline in vegetation cover resulted in a strong runoff response leading to high denudation rates on the hillsides and upslope migration of gully heads. Probably the marked arid surges of the 1970s and 1980s triggered the widespread activation of gully networks. During such droughts, biomass production was altered, vegetation was under increased grazing pressure and the surface cover by cropland increased to steep and marginal areas. In 1984/1986 the categories bare ground and cropland accounted for 52% of the surface in the Northern Ethiopian Highlands. Moreover, during dry years, farmers will generally apply cropping systems with reduced cropping seasons. As this increases the duration of the period for which fallow land occurs in the early rainy season, the vulnerability of the land to occasional rainfall events increases during dry years. Since ca. 2000, environmental rehabilitation programs stated to yield positive effects on the stabilization of gullies. Since the 1980s and especially the 1990s, widespread establishment of exclosures, introduction of stone bunds and building of gully check dams occurred. Surface cover by bare ground and cropland meanwhile decreased to 40%. A good example of how successful environmental rehabilitation can be, was found in the study area of Atsela, where a gully was transformed into a green oasis in the landscape as a result of well though land management.

This study validates previous research and indicates important land degradation by gullying in the second half of the 20th century in the Northern Ethiopian Highlands. In recent decades, local communities have however proven that with proper land management, this trend can be reversed. At a regional scale, gully networks are increasingly being stabilized and the landscape is greening. These developments have to be understood within a socio-economic environment of strong population growth and a low level of technological development, where most people rely on land resources for their livelihood, and where the fragility of the country's economy is frequently being emphasized, for example when climatic shocks such as drought cause severe food shortages and famine. Socio-economical developments and their relation to land degradation should therefore be monitored closely. With an annual population growth rate of 2.37% (period 2000-2010, CSA, 2008) and population size which is likely to double by 2050, the country faces immense challenges. Key is to rehabilitate land as a resource base for food security and ecosystem services, and to strengthen and diversify the rural economy in order to make local communities less dependent on land resources. Such challenges are embraced by many local, national and international programs, and should remain high on the agenda.

As to other dryland environments, this study emphasizes that fast land degradation may occur when improper land management is applied. Most dramatic is the development of extensive and deep gully networks, which export large quantities of sediment through the ephemeral gully and river system and therefore jeopardize in-situ agricultural production. Moreover, decreased agricultural production in the proximity of gullies can be expected as a result of the depressed water tables. With fast network expansion occurring, infrastructures may be damaged and costs related to future planning may be much higher than originally budgeted. Downstream effects are also important. Water pollution caused by sediment and urban wastewater threatens human health and decreases agricultural production. As a result of a stronger flash flood regime, rivers – even those that are located many km downstream of the gullies – may respond strongly and geomorphic changes may cause infrastructures to be damaged (e.g., Billi, 2008).

Scope for feature research

In order to understand more in detail the spatiotemporal variability in gully development and the relation with environmental controls, in Northern Ethiopia or in other dryland environments, feature research may be needed beyond the findings of this thesis.

Repeat photography proved to be very valuable to understand and to quantify historical gully development and land use and cover changes in the Northern Ethiopian Highlands. Besides qualitative observations, gully cross-sections (Chapter 2) and headcut retreat rates (Chapter 4) were quantified, land use and cover was mapped (Chapter 5) and observations from historical photographs served as a basis for Landsat image classification (Chapter 6). The elaborated methods can be of great value to understand past cycles of land degradation in other dryland environments, where historical terrestrial photographs are at hand. Better than any other data source, repeat photographs provide a view of the landscape and its geomorphic features much in the same way we perceive it ourselves. Detailed observations, interpretations and in some cases quantifications can thus be made for small areas which are covered by the historical photographs. As establishing trends in land degradation for large areas requires a large dataset of localized and repeated historical terrestrial photographs, the prerequisite for using repeat photography as a research basis is to assemble a large digital database of archival photographs (e.g., Nyssen et al., 2010).

As discussed in Section 8.3, historical terrestrial photographs of 1868-1960s show gully and river channels that appear as ‘dormant’, meaning that they were inherited from a previous period when external forcing in environmental conditions caused widespread geomorphic change. The well-preserved gully and river streambed morphology suggest that such events that caused the shaping of gullies and river channels occurred not long before those photographs were taken, as the gullies would have smoothed out totally otherwise. As it is unlikely that environmental degradation was more severe in the period preceding the 1868 situation than afterwards, it is suggested that severe droughts (like in

1835) lie at the basis of the development of gully networks. In order to clarify this, more research is needed on pre-1868 gully development and environmental conditions. Regarding the gully development, gully walls that were interpreted as remnants of pre-1965 stable gully sections could be analysed by OSL or ^{10}Be dating, which could provide chronologies of sedimentation. Similar studies can be done in old debris cones at the location of old gully ends. Past environmental conditions can be assessed by using for example pollen analysis as a proxy. These recommendations were already integrated in the PhD. research proposal of Sil Lanckriet (Geography Department, UGent).

When relating gully development to environmental conditions, this thesis mainly uses terrestrial or aerial photographs and satellite images to quantify the changes. Limited attention was given to the monitoring of present-day gully development in detail (Section 4.3.1). Such a monitoring is however important when addressing the rainfall and runoff conditions that control gully development, and the links with topography, lithology, soil, land use and land cover. Feature monitoring campaigns on gully headcut retreat or channel development therefore need to quantify changes in gully morphology in detail. This requires to use more sophisticated techniques (theodolite, terrestrial LiDAR) than a measuring tape, which are difficult to apply as the required equipments are not at hand locally or suffer from bad maintenance. Most promising is the use of 3D models prepared from photograph cameras to study gully erosion. Although never applied before in gully erosion studies, the participation to a workshop on gully measurement techniques (innovations in the evaluation and measurement of rills and gullies, CSIC, Cordoba, Spain, 9-20/05/2011) showed that 3D models from photograph cameras can be a rather inexpensive method for detailed understanding of gully erosion processes in mountainous landscape that is difficult to access. Expertise on 3D photograph models is available in the Department of Geography (Ghent University) which be applied to gullies in the near future.

The findings of Chapter 7 regarding the importance of cropping systems and land cover by crops give scope to further research as it tends to demonstrate that increased rain intensity goes in line with higher annual rainfall, hence better crop cover which may in turn annihilate or at least buffer the increase in rainfall erosivity. It would be very useful to verify this hypothesis in other areas of the world where crop growth is limited by water availability, and where cropping systems are flexible enough to adapt to spatiotemporal variability in rainfall.

Lastly, the linkages to the social system in which environmental changes occurred should be further elucidated. There is a strong hypothesis that the feudal land tenure system in most of the 20th century and before led to marginal farming on steep slopes (hence degradation and erosion), and that subrecent land distributions in the valley bottoms allowed to free parts of those slopes for vegetation recovery.

Recommendations for land managers

Gullies develop in size and morphology which reflect fluxes of water and sediment at a specific place and over a certain time, within the constraints given by local controls. Rehabilitating gullies should therefore primarily focus on reducing the runoff response of the land that drains to gullies. Any measure which focuses on the gully itself, like trapping sediment by check dams or stabilizing sections by planting woody vegetation, that is not accompanied with intense land management improvements will prove to be frustrating as gullies will continue to adapt their size and shape to (peak) discharge and sediment load properties. As shown in this thesis, soil and water conservation measures such as stone bunds, infiltration trenches/ ponds and exclosures can reduce the runoff response of the land and favour gully rehabilitation. Important is that implemented measures equally reduce runoff discharges as sediment loads, in order to prevent gully incision by the clear water effect. Soil and water conservation measures inside gullies proved to be especially successful when nearby land management was strongly improved. In other cases, in-channel measures like check dams were often rapidly destroyed by flash floods. In-channel measures and gully rehabilitation also proved to be better in upstream than in downstream areas, even when the implementation of soil and water conservation was equal throughout the catchments. This is the result of longer reaction times to land management improvements for downslope gully segments. Gullies located in headwater areas, close to the water divides, show strong links with the hillslopes, and changes in the runoff response of the land will rapidly be translated in channel response. More downstream, even with strongly reduced peak floods, the channels will continue to encounter important floods, which are related to the large catchment area. Downstream gullies will therefore only slowly react to changes in land management and in-channel measures like check dams should therefore be implemented in later phase.

In order to rehabilitate gullies in a cost-efficient way, a stepwise approach is suggested to land managers.

(i) In a first phase, soil and water conservation measures should focus on reducing the runoff response of the land and sediment trapping in the land that drains to gullies. This can include the implementation of stone bunds that are accompanied with infiltration trenches, the building of infiltration ponds, and the establishment of exclosures for vegetation recovery.

(ii) In a second phase, soil and water conservation measures should focus on the gully system in the headwater areas, i.e. those gullies in high landscape positions that are close to crestlines (cf. first/second order streams in the Horton-Strahler classification). Most common is the implementation of check dams in gullies, or the planting of trees on the gully walls, which can be of economic or ecologic value. Special care is required where soils occur that are vulnerable to soil piping. In such cases specific measures need to be applied, like subsurface geomembrane dams, as discussed in Section 4.4.3.

(iii) In a third phase, when check dams are filled and stable, trees have a good survival rate and gullies start to stabilize visibly in the headwaters, the lower gullies system may be treated with check dams or other in channel measures.

References from this chapter are listed in the Reference Section of Chapter 8.

Nederlandse samenvatting

De ontwikkeling en spatio-temporele variabiliteit van ravijnerosie sinds de late 19de eeuw in het Hoogland van Noord-Ethiopië

Hoofdstuk 1 – Algemene inleiding

Desertificatie, gedefinieerd door de *UN Convention to Combat Desertification* (UNCCD) als landdegradatie in aride, semi-aride en droog sub-humide gebieden, vormt wereldwijd een belangrijke bedreiging voor duurzame ontwikkeling in vele drooglanden. Ravijnerosie vormt een belangrijk proces waarbij landdegradatie in drooglanden plaatsvindt. In een overzichtstudie beoordeelde Poesen et al. (2002) dat ravijnerosie 50% tot 80% van de totale sedimentproductie bepaalt in drooglanden. Het verkrijgen van een grondig inzicht in het belang van historische en hedendaagse ravijnerosie is daarom cruciaal om de impact van toekomstige scenario's in landbeheer en van klimaatsverandering op landdegradatie te voorspellen (Poesen et al., 2003; Valentin et al., 2005). Weinig studies beschouwen echter het belang van ravijnerosie op landdegradatie, voornamelijk wanneer men zich beperkt tot sub-Saharisch Afrika. Kennisgevingen van ravijnerosie bestaan voor Burkina Faso (Marzolff en Ries, 2007), Democratische Republiek Congo (DRC; Ndona en Truong, 2011), Kenia (Oostwoud Wijdenes en Bryan, 2001; Katsurada, 2007), Lesotho (Showers, 1996); Namibië (Eitel et al., 2002), Niger (Leblanc et al., 2008), Nigeria (Gobin et al., 1999), Rwanda (Moeyersons, 1991), Senegal (Poesen et al., 2003), Zuid-Afrika (Boardman et al., 2003), Swaziland (Felix-Henningsen et al., 1997) en Zimbabwe (Stocking, 1980). Voor Ethiopië wordt het belang van ravijnerosie door talloze auteurs erkend (Virgo en Munro, 1978; Nyssen et al., 2000, 2002, 2004, 2006; Billi en Dramis, 2003; Daba et al., 2003; Moges en Holden, 2008; Munro et al., 2008; Reubens et al., 2009), doch is er onvoldoende inzicht in de kenmerken van ravijnen, de snelheden waarmee ravijnhoofden eroderen, de ontwikkeling van ravijnnetwerken, het belang van ravijnvolumes, en de link met omgevingsfactoren.

Ravijnerosie is een proces van watererosie waarbij oppervlakkig afstromend water accumuleert in lineaire kanalen die – over korte periodes – zich tot aanzienlijke dieptes ontwikkelen door het wegruimen van grond met het afstromende water (vrij vertaald uit Poesen et al., 2003). Talrijke oorzaken kunnen aan de basis liggen van het ontstaan van ravijnen, waarbij telkens een voorgaand stadium van evenwicht wordt verstoord en ertoe leidt dat de hoeveelheid water en sediment gebracht tot een plaats in het landschap verandert (Graf, 1988; Knighton, 1998). Oorzaken die meest relevant zijn voor de situatie in Noord-Ethiopië zijn: tektoniek, verlaging van het basisniveau, toenemende ariditeit of humiditeit, toenemende (piek) debieten, afnemende sedimentladingen, begrazing en vertrappeling, modificaties in stroomlijnen, urbanisatie en modificaties in infrastructuur (voor een exhaustief overzicht zie Schumm, 2005).

De primaire doelstelling van dit proefschrift is om de dynamiek van ravijnerosie te bevatten sinds de late 19de eeuw op een regionale schaal in het Hoogland van Noord-Ethiopië. Algemeen worden volgende doelstellen opgetekend:

- Het begrijpen van spatio-temporele variaties in ravijnmorfologie en –morfometrie,
- Het bevatten van spatio-temporele variaties in ravijnontwikkeling,
- Het begrijpen van spatio-temporele variaties in de factoren die ravijnerosie beïnvloeden,
- Het ontwikkelen van een hydrogeomorfologisch model die de dynamiek van ravijnerosie linkt met de omgevingsdynamiek.

Het studiegebied beslaat het Hoogland van Noord-Ethiopië. Acht hoofdstudiegebieden werden geselecteerd die representatief zijn voor de regionale variabiliteit in omgevingsfactoren. In totaal dekken deze gebieden 123 km². De keuze van focusgebieden werd mede bepaald door de beschikbaarheid van historische terrestrische foto’s, luchtfoto’s en satellietbeelden, die de studie van ravijnerosie mogelijk maken. De terrestrische foto’s gaan terug tot 1868 en vormen talloze puntobservaties tussenin de hoofdstudiegebieden. Luchtfoto’s beslaan de periode 1963-1994 en worden aangevuld met hoge resolutie satellietbeelden (IKONOS en Google® Earth beelden). Satellietbeelden van lage resolutie zijn voorhanden vanaf 1972.

Deel 1

In Deel 1 van dit proefschrift wordt in drie hoofdstukken de spatio-temporele variabiliteit in ravijnerosie besproken.

Hoofdstuk 2 – De dynamiek van ravijnerosie sinds de late 19de eeuw bestudeerd aan de hand van een diachrone analyse van terrestrische foto's

Over de voorbije 140 jaar leidde een weinig duurzaam landgebruik in het semi-aride gebergte van Noord-Ethiopië tot ernstige landdegradatie en de vorming van dichte ravijnnetwerken. Dit blijkt uit historische foto's die een landschap weergeven waar de toenemende landgebruikintensiteit en de afname van begroeiing resulteerde in erg dynamische ravijnen en rivierkanalen, voornamelijk sinds de jaren 1970. Om de dynamiek van ravijnen en rivierkanalen en de relatie met bepalende milieufactoren te begrijpen, zijn een set van 57 historische foto's (genomen tussen 1868 en 1994) precies herhaald tussen 2006 en 2009. De kwalitatieve en kwantitatieve analyses tonen aan dat 92,7% van de dwarssecties in oppervlakte zijn toegenomen. De gemiddelde jaarlijkse insnijding van de gekwantificeerde dwarssecties bedroeg 0,04 m $jaar^{-1}$, met een maximale waarde van 0,13 m $jaar^{-1}$. Dergelijke extreme waarden werden bekomen in Vertisolen, waar de maximale insnijding 4,49 m bedroeg over 35 jaar. Bij de laatste waarnemingen in 2009 bleek dat 23% van de ravijnen en rivierkanalen zich stabiliseren; dankzij de implementatie van bodem- en waterconserveringsmaatregelen sinds de jaren 1980.

Hoofdstuk 3 – Het kwantificeren van ravijnerosie sinds 1963 op basis van luchtfoto's en hoge resolutie satellietbeelden

Om een grondig inzicht te verkrijgen in de evolutie van ravijnerosie werden acht studiegebieden die representatief zijn voor de regionale variabiliteit in omgevingsfactoren geselecteerd. Door het gebruik van luchtfoto's en hoge resolutie satellietbeelden (o.a. geraadpleegt met Google® Earth) kon de evolutie van ravijnnetwerken en –volumes tussen 1963 en 2010 gekwantificeerd worden. Omdat enkel de lengte van de ravijnnetwerken met voldoende nauwkeurigheid kon bepaald worden, werden relaties tussen ravijnvolumes en ravijnlengtes opgesteld tijdens veldstudies. Deze studies geven aan dat de lithologie, de ravijnactiviteit en de aanwezigheid van weerdammen in ravijnen de belangrijkste factoren zijn die de variabiliteit in dwarssecties bepalen. Dwarssecties in mergels waren 36,7% groter dan in vulkanische gesteenten en weerdammen vulden de dwarssecties met 33,5%. De oppervlakte van de dwarssecties kon vrij goed gerelateerd worden aan de respectievelijke bekkengrootte. Uit de studie van de ravijnnetwerken en –volumes kon afgeleid worden dat het systeem een belangrijke insnijdingfase heeft ondergaan in de tweede helft van de 20ste eeuw, en dat er sinds recentelijk een opvullingfase geschiedt. In de periode 1965-1994 veranderde het ravijnsysteem van laagdynamisch naar hoogdynamisch, met een sterke uitbreiding van de totale ravijndensiteit (D_{total}) en het specifieke ravijnvolume (V_a) als gevolg. In 1994 was D_{total} = 2,52 km km^{-2} en V_a = 59,59 10^3 m^3 km^{-2}. Dit komt overeen met een sedimentexport door ravijnerosie van 17,6 ton ha^{-1} y^{-1} over de periode 1963/1965-1994. Door de grootschalige implementatie van bodem- en waterconserveringsmaatregelen in de voorbije decennia zijn D_{total} en V_a teruggevallen tot respectievelijk 2,20 km km^{-2} en 48,96 10^3 m^3 km^{-2}, met 25% van het ravijnnetwerk zijnde laagdynamisch. Voortbouwend op de bevindingen van Hoofdstuk 2 bevestigt deze studie de belangrijke landdegradatie in de tweede helft van de 20ste eeuw en toont aan dat het verbeterde landbeheer positieve effecten heeft op de rehabilitatie van ravijnen.

Hoofdstuk 4 – Ravijnhoofderosie

In Hoofdstuk 4 wordt een inzicht verschaft in de snelheden waarbij ravijnhoofden zich door regressieve erosie ontwikkelen. Hiervoor werd ravijnhoofderosie zowel op korte als op middellange tot lange termijn bestudeerd. Historische observaties van ravijnhoofden waren mogelijk dankzij het gebruik van terrestrische foto’s en luchtfoto’s. Het monitoren van ravijnhoofden in het regenseizoen van 2010, onthulde dat de huidige snelheden waarmee ravijnen eroderen vrij laag zijn. Gemiddelde waarden voor lineaire (R_l), oppervlakte (R_a), en volumetrische (V_e) ravijnhoofderosie zijn respectievelijk 0,34 m $jaar^{-1}$, 1,70 m^2 $jaar^{-1}$ en 5,2 m^3 $jaar^{-1}$. Dit reflecteert de positieve effecten van bodem- en waterconserveringsmaatregelen (voornamelijk geïmplementeerd sinds de tweede helft van de jaren 1990) op de stabilisatie van ravijnhoofden. Significant hogere terugschreidingssnelheden werden echter geregistreerd in Vertisolgebieden, met R_l-waarden tot 1.93 m $jaar^{-1}$. Het beschouwen van ravijnhoofderosie op middellange tot lange termijn gaf veel hogere erosiesnelheden, met R_l, R_a en V_e respectievelijk 3,8 m $jaar^{-1}$, 31,5 m^2 $jaar^{-1}$ en 47,7 m^3 $jaar^{-1}$. Ravijnhoofderosiesnelheden tot 10-maal hoger werden geregistreerd ten gevolge van recente wijzigingen in de weginfrastructuur. Op middellange tot lange termijn waren de terugschreidingssnelheden positief gecorreleerd met bekkengrootte (A). De machtsrelatie die dit voor V_e beschrijft is $V_e = 0.53\ A^{0.31}$ ($r^2 = 0.27$, $n = 18$). In vergelijking met andere gebieden wereldwijd zijn de snelheden waarmee ravijnhoofden zich ontwikkelden via regressieve erosie erg hoog. Dit is het gevolg van het gecombineerde effect van een steile topografie, erosieve regens, overbegrazing, agrarische intensivering en het voorkomen van Vertisolgebieden. In Vertisolgebieden wordt de uitbreiding van ravijnnetwerken gestuurd door pijperosie. Voor deze gebieden bestaan er tot op heden geen adequate technieken om ravijnhoofden te stabiliseren. Er is daarom nood aan alternatieve technieken. In deze studie wordt de introductie van een ondergrondse plastieken dam aan het ravijnhoofd uitgetest.

Deel 2

In Deel 2 van dit proefschrift worden variaties in landgebruik/bodembedekking en de invloed van neerslagpatronen hierop, besproken. Kennis hiervan is namelijk cruciaal om de patronen in de ontwikkeling van ravijnerosie te begrijpen. Dit deel bevat tevens drie hoofdstukken.

Hoofdstuk 5 – Veranderingen in landgebruik en bodembedekking sinds de late 19de eeuw op basis van terrestrische foto's

Terrestrische foto's bieden een zeldzame blik op de toestand van het leefmilieu in historische tijden. Om de toestand van landgebruik en bodembedekking in de late 19de en de vroege 20ste eeuw te bepalen, werden 10 foto's uit de periode 1868-1961 geselecteerd. Deze dekken ongeveer 12 km² terrein. Het kwantificeren van landgebruik en bodembedekking gebeurde door betreffende eenheden geïnterpreteerd op de foto's te herleiden naar het kaartvlak. Zodoende werden de geometrische vervormingen die gelinkt zijn aan het fotobeeld weggewerkt. Door de toestand uit de laat-19de en vroeg-20ste eeuw te vergelijken met de toestand in 2008, kon vastgesteld worden dat de bodembedekking door houtige vegetatie is toegenomen van 6,4% tot 10,9% over de voorbije 140 jaar in de studiegebieden. De acht tot tienvoudige toename in populatie over diezelfde periode wordt gereflecteerd in een toegenomen areaal aan bebouwde grond, van 0,8% tot 18,1%. Deze ontwikkelingen gebeurden voornamelijk ten koste van dekking door struikgewas, dat tussen 1868 en 2008 terugviel van 83,1% naar 15,3%. Over het algemeen werden landgebruikeenheden intenser gebruikt en desgevallend ook beter beheerd.

Hoofdstuk 6 – Veranderingen in landgebruik en bodembedekking sinds 1972, gebruikmakend van lage resolutie Landsat-beelden

Voor de recente decennia worden veranderingen in landgebruik en bodembedekking op regionale schaal optimaal bestudeerd met satellietbeelden. Gebruikmakend van *Landsat Multispectral Scanner* en *Landsat Thematic Mapper* beelden uit 1972, 1984/1986 en 2000, konden trends over een gebied van 8884 km² bestudeerd worden. Om de waarde van historische terrestrische foto's (uit 1974-1975) voor de kalibratie van satellietbeelden te evalueren, werd het Landsatbeeld uit 1972 op twee verschillende manier gekalibreerd. Ten eerste via een conventionele beelddifferentiatie en, ten tweede, via observaties gemaakt op de historische foto's. De resultaten hiervan tonen aan dat beeldklassificaties op basis van terrestrische foto's een betere nauwkeurigheid geven dan bij conventionele methodes. Dit wordt uitgedrukt door een toename in Kappa-coëfficiënt van 0,46 to 0,54. Inzake trends in landgebruik en bodembedekking tussen 1972 en 2000 konden verschillende vaststellingen gemaakt worden: (1) een graduele maar belangrijke afname in het areaal ingenomen door kale gronden, van 32% tot 8%; (2) een belangrijke toename in struikgewas (van 25% tot 43%) en bos (2,6% tot 6,3%; met inbegrip van Eucalyptusaanplanten) en (3) toename in het aantal waterreservoirs. Deze veranderingen gebeurden samen met een sterke toename in bevolkingsdichtheid, waarbij de zorg voor het leefmilieu (met in het bijzonder de implementatie van bodem- en waterconserveringsmaatregelen) verhoogde.

Hoofdstuk 7 – De realtie tussen de spatio-temporele variabiliteit in teeltsystemen, bodembedekking door gewassen, neerslag and ravijnerosie

Akkerland beslaat ongeveer 33% van de oppervlakte in het Hoogland van Noord-Ethiopië. Dit akkerland wordt voornamelijk bewerkt in een kleinschalig landbouwsysteem waarbij teeltsystemen grotendeels afgestemd worden op de neerslagvariabiliteit. Om het effect van die neerslagvariabiliteit op de teeltsystemen te bepalen, werden verschillende contrasterende gebieden bezocht in het Noord-Ethiopische Hoogland, en werden 118 boeren geïnterviewd. Hieruit bleek dat er 5 verschillende teeltsystemen toegepast worden, elk met specifieke teeltseizoenen en gewasassociaties. De duur van de teeltseizoenen varieerde van 4 tot 10 maand en de meest voorkomende gewassen waren graangewassen zoals tarwe, gerst, tef en sorghum of peulvruchten zoals linze en tuinboon. Door verschillen in bodemgesteldheid werden op de hellingflanken teeltsystemen toegepast die van kortere duur waren dan diegene in valleibodems. De toenemende gemiddelde jaarlijkse neerslag van noordwest naar zuidoost reflecteerde zich in teeltsystemen van langere duur naar het zuidoosten toe. De dalende gemiddelde temperatuur met de hoogte had voornamelijk een weerslag op de soortensamenstelling van de teeltsystemen. Het effect van veranderingen in jaarlijkse neerslag bestond erin dat teeltsystemen van langere duur werden toegepast met toenemende jaarlijkse neerslag. Dit gaf aanleiding tot verschuivingen van teeltsystemen zowel op bekkenschaal als op regionale schaal. Het opschalen van deze resultaten gebeurde door de neerslagkaarten van Jacob et al. (2012) te gebruiken, wat toeliet kaarten van teeltsystemen te produceren over de periode 1996-2009. Deze tonen een grote jaarlijkse variabiliteit in de duur van de bodembedekking door gewassen aan met veranderingen in jaarlijkse neerslaghoeveelheid. Deze variabiliteit wordt als een belangrijke, vaak over het hoofd geziene, verklarende factor beschouwd voor het begrijpen van vroegere cyclussen van landdegradatie.

Hoofdstuk 8 – Algemene discussie

Gebaseerd op de Hoofdstukken 2 tot 7 werd een conceptueel hydrogeomorfologisch model opgesteld voor het Noord-Ethiopische Hoogland. Drie voorname fases konden onderscheiden worden. In de eerst fase, van 1868 (of vroeger) tot ca. 1965, toonden de vrij stabiele ravijnen een morfologie die niet in relatie stond met het toenmalige landschap, maar eerder overgeërfd blijkt uit een vroegere meer erosieve periode. In de tweede fase, van ca. 1965 tot ca. 2000, nam de dynamiek van ravijnerosie sterk toe en vond een degradatiecyclus plaats. Dit kan gelinkt worden aan de belangrijke degradatie van de vegetatie en aan het voorkomen van droogtes in die periode. Vanaf ca. 2000 leidde de wijdverbreide toepassing van bodem- en waterconserveringsmaatregelen van de recente decennia tot een sterke daling in de dynamiek van de ravijnnetwerken. Met ongeveer een vierde van het ravijnnetwerk dat gestabiliseerd is in 2008-2010, bevindt het ravijnsysteem zich tegenwoordig in een opvullingsafe.

Hoofdstuk 9 – Algemeen besluit

Voor het bestuderen van de dynamiek van ravijnerosie in relatie tot de controlerende factoren, werd een grote dataset van terrestrische foto's, luchtfoto's en satellietbeelden samengesteld. Voor elk van deze materialen werden technieken van kwantitatieve geomorfologie verfijnd naar de specifieke doelstellingen. Belangrijk hierbij was het uitvoeren van veldwerk tijdens verschillende campagnes in 2007-2011. Acht studiegebieden die de regionale variabiliteit in omgevingsfactoren vertegenwoordigen vormden het focusgebied van dit onderzoek. De resultaten van deze studie tonen aan dat een belangrijke degradatiecyclus zich voorgedaan heeft in de tweede helft van de 20ste eeuw, waarbij ravijnnetwerk en –volumes sterk toegenomen zijn. Anno 2008-2010 kon de degradatiecyclus echter omgezet worden in een opvullingscyclus. Deze ontwikkelingen konden in een hydrogeomorfologisch model gelinkt worden aan veranderingen in omgevingsfactoren. Belangrijk voor het begrijpen van de degradatiecyclus zijn de landgebruik- en bodembedekkingveranderingen, in relatie met het voorkomen van droogtes, die aanleiding gaven aan een toenemende *runoff* respons van het land. De opvullingcyclus kan gelinkt worden aan verbeteringen van landbeheer en de grootschalige implementatie van bodem- en waterconserveringsmaatregelen over de voorbij decennia. Deze studie valideert vorige bevindingen van ernstige landdegradatie in de tweede helft van de 20ste eeuw en toont aan dat bodemverliezen door ravijnerosie aanzienlijk zijn. Locale, nationale en internationale actoren hebben in een samenbundeling van krachten deze degradatiecyclus reeds gedeeltelijk kunnen omkeren. Een van de grootste uitdagingen voor de toekomst is om deze trend van ravijnrehabilitatie en vergroening van het landschap verder te zetten in een gebied dat een sterke bevolkingsgroei kent en een laag niveau van technologische ontwikkeling.

Referentielijst zie Hoofdstuk 8.

Amaury Frankl (°1982, Ghent) specialized in Physical Geography at the Geography Department of Ghent University (Belgium). He started his PhD research in 2007 while working as a research and teaching assistant at the Geography Department. Based on months of fieldwork, the presented thesis focuses on gully development and its spatiotemporal variability in the Northern Ethiopian Highlands. Gully development and environmental controls were studied since 1868 using terrestrial photographs, aerial photographs and satellite images and were interrelated in a conceptual hydrogeomorphic model. Being a regional study that considers sub-Saharan Africa, the methods and findings of this work are of great value for understanding the links between land use, land management, climate variability and geomorphic response in dryland environments. Most of the ideas were presented at international conferences or publised in papers. Amaury Frankl (co-)authors 10 peer-reviewed international publications.

UNIVERSITEIT GENT